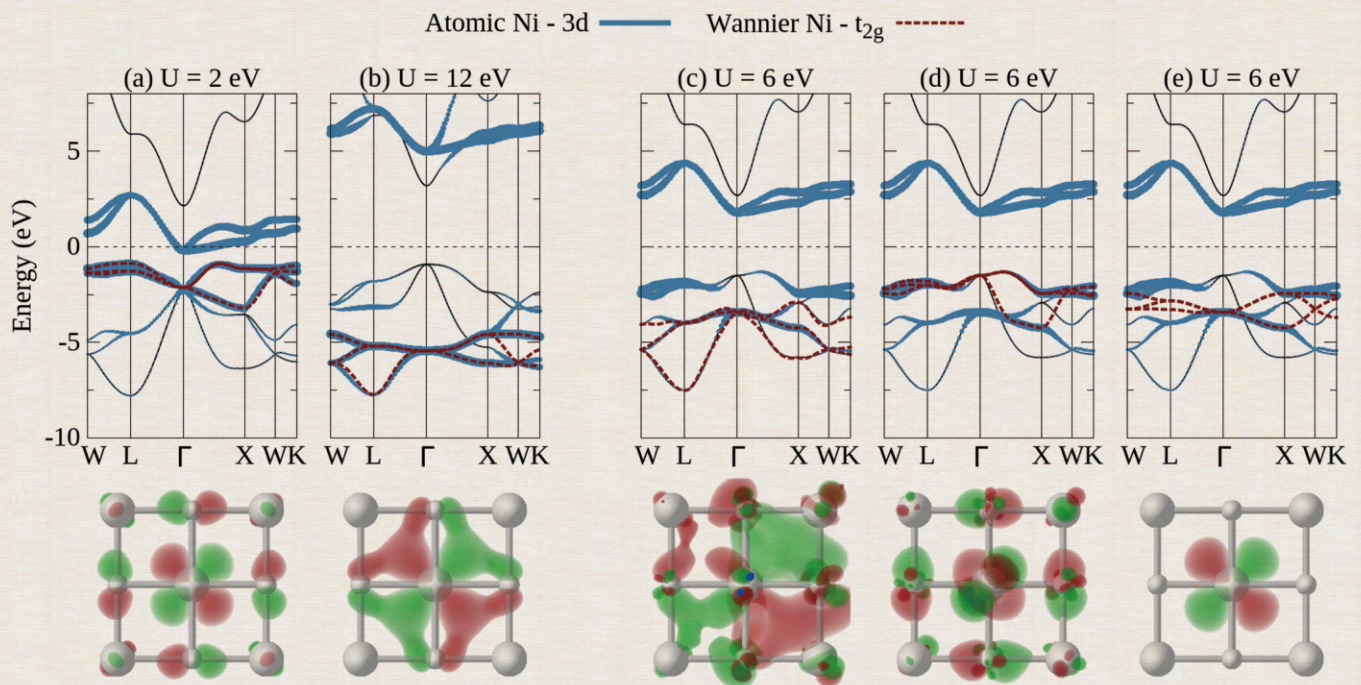


Journal of Modern Physics



Journal Editorial Board

ISSN: 2153-1196 (Print) ISSN: 2153-120X (Online)

<http://www.scirp.org/journal/jmp>

Editor-in-Chief

Prof. Yang-Hui He

City University, UK

Editorial Board

Prof. Nikolai A. Sobolev

Universidade de Aveiro, Portugal

Dr. Mohamed Abu-Shady

Menoufia University, Egypt

Dr. Hamid Alemohammad

Advanced Test and Automation Inc., Canada

Prof. Emad K. Al-Shakarchi

Al-Nahrain University, Iraq

Prof. Tsao Chang

Fudan University, China

Prof. Stephen Robert Cotanch

NC State University, USA

Prof. Peter Chin Wan Fung

University of Hong Kong, China

Prof. Ju Gao

The University of Hong Kong, China

Prof. Sachin Goyal

University of California, USA

Dr. Wei Guo

Florida State University, USA

Prof. Cosmin Ilie

Los Alamos National Laboratory, USA

Prof. Haikel Jelassi

National Center for Nuclear Science and Technology, Tunisia

Prof. Santosh Kumar Karn

Dr. APJ Abdul Kalam Technical University, India

Prof. Christophe J. Muller

University of Provence, France

Prof. Ambarish Nag

National Renewable Energy Laboratory, USA

Dr. Rada Novakovic

National Research Council, Italy

Prof. Tongfei Qi

University of Kentucky, USA

Prof. Mohammad Mehdi Rashidi

University of Birmingham, UK

Prof. Alejandro Crespo Sosa

Universidad Nacional Autónoma de México, Mexico

Dr. A. L. Roy Vellaisamy

City University of Hong Kong, China

Prof. Yuan Wang

University of California, Berkeley, USA

Prof. Fan Yang

Fermi National Accelerator Laboratory, USA

Prof. Peter H. Yoon

University of Maryland, USA

Prof. Meishan Zhao

University of Chicago, USA

Prof. Pavel Zhuravlev

University of Maryland at College Park, USA

Table of Contents

Volume 10 Number 8

July 2019

My C.G.S.I.S.A.H. Theory of Dark Matter

E. T. Tatum.....881

Expansion of a Y-Shaped Antenna Array and Optimization of the Future Antenna Array in Malaysia for Astronomical Applications

S. Kiehadrouinezhad, J.-F. Bousquet, M. Cada, C. I. Short, A. Shahabi, S. Kiehadrouinezhad.....888

Accurate, First-Principle Study of Electronic and Related Properties of the Ground State of Li₂Se

A. Goita, F. Gao, I. H. Nwigboji, Y. Malozovsky, L. Franklin, D. Bagayoko.....909

The World in an Equation: A Reappraisal of the Lemaître's Primeval Cosmic Rays

R. Bagdoo.....922

A Band Theory Perspective on Molecular Orbitals in Complex Oxides

K. Foyevtsova, G. A. Sawatzky.....953

Increased Temperature and Entropy Production in the Earth's Atmosphere: Effect on Wind, Precipitation, Chemical Reactions, Freezing and Melting of Ice and Electrical Activity

M. A. Pitt.....966

How the Dirac Sea Idea May Apply to a Spatially-Flat Universe Model (A Brief Review)

E. T. Tatum.....974

Calculation of the Mass of the Universe, the Radius of the Universe, the Age of the Universe and the Quantum of Speed

C. Mercier.....980

Topologically Stable States of the Anti-Centrifugal Potential

R. Dandolo.....1002

Explanation of Dark Matter, Dark Energy and Dark Space: Discovery of Invisible Universes

A. A. Antonov.....1006

Space-Time Universe versus Energy Driven Time Arrow Universe: Time-Neutrality Confronted with Fundamental Irreversibility

H. Tributsch.....1029

The figure on the front cover is from the article published in Journal of Modern Physics 2019, Vol. 10, No. 8, pp. 953-965 by Kateryna Foyevtsova, and George A. Sawatzky.

Journal of Modern Physics (JMP)

Journal Information

SUBSCRIPTIONS

The *Journal of Modern Physics* (Online at Scientific Research Publishing, www.SciRP.org) is published monthly by Scientific Research Publishing, Inc., USA.

Subscription rates:

Print: \$89 per issue.

To subscribe, please contact Journals Subscriptions Department, E-mail: sub@scirp.org

SERVICES

Advertisements

Advertisement Sales Department, E-mail: service@scirp.org

Reprints (minimum quantity 100 copies)

Reprints Co-ordinator, Scientific Research Publishing, Inc., USA.

E-mail: sub@scirp.org

COPYRIGHT

Copyright and reuse rights for the front matter of the journal:

Copyright © 2019 by Scientific Research Publishing Inc.

This work is licensed under the Creative Commons Attribution International License (CC BY).

<http://creativecommons.org/licenses/by/4.0/>

Copyright for individual papers of the journal:

Copyright © 2019 by author(s) and Scientific Research Publishing Inc.

Reuse rights for individual papers:

Note: At SCIRP authors can choose between CC BY and CC BY-NC. Please consult each paper for its reuse rights.

Disclaimer of liability

Statements and opinions expressed in the articles and communications are those of the individual contributors and not the statements and opinion of Scientific Research Publishing, Inc. We assume no responsibility or liability for any damage or injury to persons or property arising out of the use of any materials, instructions, methods or ideas contained herein. We expressly disclaim any implied warranties of merchantability or fitness for a particular purpose. If expert assistance is required, the services of a competent professional person should be sought.

PRODUCTION INFORMATION

For manuscripts that have been accepted for publication, please contact:

E-mail: jmp@scirp.org

My C.G.S.I.S.A.H. Theory of Dark Matter

Eugene Terry Tatum

Bowling Green, KY, USA

Email: ett@twc.com

How to cite this paper: Tatum, E.T. (2019)
My C.G.S.I.S.A.H. Theory of Dark Matter.
Journal of Modern Physics, 10, 881-887.
<https://doi.org/10.4236/jmp.2019.108058>

Received: June 10, 2019

Accepted: July 2, 2019

Published: July 5, 2019

Copyright © 2019 by author(s) and
Scientific Research Publishing Inc.
This work is licensed under the Creative
Commons Attribution International
License (CC BY 4.0).
<http://creativecommons.org/licenses/by/4.0/>



Open Access

Abstract

Theory and observations concerning the cosmic reionization epoch are briefly discussed in the context of recent observations attributed to dark matter. A case is made that cold ground state interstellar atomic hydrogen of average density of about one atom per cubic centimeter ($1.67 \times 10^{-21} \text{ kg}\cdot\text{m}^{-3}$ or $1.67 \times 10^{-24} \text{ g}\cdot\text{cm}^{-3}$) appears to be the most likely candidate to explain these observations.

Keywords

Dark Matter, Early Universe, Reionization Epoch, Dark Ages, Cosmology Observations, Galaxies: ISM, ISM: Atoms, Radio Lines: ISM

1. Introduction and Background

In May of 2019, I shared my C.G.S.I.S.A.H. theory of dark matter with colleagues at the dark matter workshop sponsored by the World Science Festival. What follows is a brief note concerning the new constraints on dark matter and a discussion of my conjecture and its observational predictions.

Convincing observational support for dark matter begins with the publication by Rubin and Ford [1] concerning unexpected galactic rotation curves. These observations, soon followed by others [2], provide strong support that an invisible (*i.e.*, “dark”) form of gravitationally attractive matter within the interstellar vacuum is contributing to galaxies approximately 5 - 10 times the total mass of the visible galactic matter (*i.e.*, stars, warm molecular gas clouds, and dust). By “invisible” it is meant that this matter is not emitting any detectable light.

It has subsequently become apparent that one can further observe the *effect* of this dark matter by its gravitational lensing properties. By these observations, there appears to be a roughly spherical cloud (*i.e.*, a “halo”) of dark matter gas or superfluid extending up to approximately 200 kpc from the observed galactic centers. Dark matter is also nearly collisionless due to a low scattering cross-section,

as deduced from Tucker's observations of the bullet cluster [3] and other colliding galaxy clusters. Furthermore, the Planck Collaboration report [4] of the cosmic microwave background (CMB) anisotropy indicates that dark matter was present at the time of the recombination/decoupling epoch. It is even postulated that dark matter has been the seeding structural scaffolding for the further formation of galaxies, galaxy clusters and filaments in the subsequent evolution of the universe.

In recent years, numerous theories and detection methods have been proposed for dark matter with the above properties. While it is not within the scope of this paper to review the many publications on this subject, three important publications in 2018 and two important publications in 2019 deserve special mention herein.

The first of these is Barkana's review [5] of the reionization epoch ("cosmic dawn") 21-cm observations. These observations constrain dark matter to a very slow-moving (*i.e.*, cold) particle with a mass-energy of no greater than 2 - 3 GeV. Furthermore, the graph on page 9 of the Barkana reference shows a very tight correlation between a dark matter particle of about 0.938 GeV and the minimum possible 21-cm brightness temperature T_{21} at redshift $z = 17$. Thus, *atomic hydrogen appears to be the only baryon not yet ruled out by these new tight constraints.*

The second reference of importance in 2018 is Posti and Helmi's analysis [6] of *Gaia* data extracted from a 20 kpc (65.2 thousand light-years) radius halo sphere centered at the Milky Way center. From their analysis one can deduce the ratio of dark matter to visible matter within this halo sphere to be approximately 1.37 to 0.54, or 2.54 to one. This ratio will be further addressed in the Results section to follow.

The third reference of importance in 2018 is physicist Stacy McGaugh's publication entitled, "Strong Hydrogen Absorption at Cosmic Dawn: The Signature of a Baryonic Universe" [7]. One should carefully read the McGaugh reference for the reasoning that *the cosmic dawn observations fit best for baryonic dark matter. Thus, nonbaryonic proposals for dark matter do not appear to be necessary.*

The first reference of importance in 2019 is the Read publication [8] which provides support for "dark matter heating" within active galactic centers. This process may explain why active galactic centers tend to have a somewhat shallower dark matter core. Thus, dark matter heating may be an important variable in understanding its perplexing spatial distribution, particularly with respect to the dark matter "cusp-core problem."

The second reference of importance in 2019 is the March online report [9] of the *Gaia*-Hubble Collaboration. Here, for the first time, one can have confidence that the "visible matter mass" of the Milky Way is approximately 250 billion M_{\odot} . Therefore, if one can assume that this visible matter mass is roughly confined to within the 20 kpc Posti and Helmi radius halo sphere, their 2.54 ratio would imply approximately 635 billion M_{\odot} of dark matter within 20 kpc of the

Milky Way center.

With all of the above observations concerning dark matter, one can now construct the following table (**Table 1**) of these features with the relevant references listed in the right-hand column.

Given these features characteristic of dark matter, it is useful to review what observations suggest about the evolution of the universe since the recombination/decoupling epoch. During the adiabatic cooling period of the cosmic “dark ages” the positive feedback of gravitational attraction is thought to have accentuated the anisotropy we now observe in the cosmic microwave background (CMB) by creating centripetal movements of the atomic hydrogen within the denser regions of the CMB map. In contrast to these collapsing and swirling clouds of the nascent stars and galaxies, the intervening atomic hydrogen within the minimum density regions of the CMB map is thought to have been relatively motionless (*i.e.*, colder). With the continuing cosmic expansion, this intervening atomic hydrogen, the primary matter in regions we now refer to as the intergalactic and interstellar vacuum, would have ultimately become so sparse as to be nearly collisionless and predominantly confined to the ground state (except where in close proximity to the nascent stars). At the beginning of the reionization epoch (*i.e.*, “cosmic dawn”) the Wouthuysen-Field effect of the Lyman-alpha radiation of the first stars should have reduced the spin temperature T_s of ground state interstellar atomic hydrogen to well below the CMB radiation temperature T_R [10]. Such a temporary decoupling from the CMB radiation temperature would have eventually resolved due to the increasing stellar black body radiation closing out the cosmic dawn epoch.

Astrophysical observations of the 21-cm absorption line in the redshift z range corresponding (in standard cosmology) to approximately 110 - 250 million years after the Big Bang show evidence of a process very much like this, as seen in **Figure 1** [11]. However, the conventional wisdom is that a mysterious nearly collisionless non-baryonic cold dark matter must have also been present in the interstellar vacuum, as a required intermediary in this process.

Table 1. Dark matter features and relevant references.

Dark Matter Features	References
Cold (<i>i.e.</i> , low velocity)	Barkana
No Emissions (<i>i.e.</i> , dark)	Rubin & Ford
Collisionless (<i>i.e.</i> , low cross-section)	Tucker
Baryon Expected	McGaugh
Mass-Energy less than 3 GeV	Barkana
Dark Matter M_{20kpc} 635 Billion M_{\odot}	Gaia/Posti & Helmi
Central DM Heating (“coring”)	Read
CMB Decoupling at Dawn	Astrobaki/McGaugh
Structural Scaffold	Planck
Existence at CMB Emission	Planck

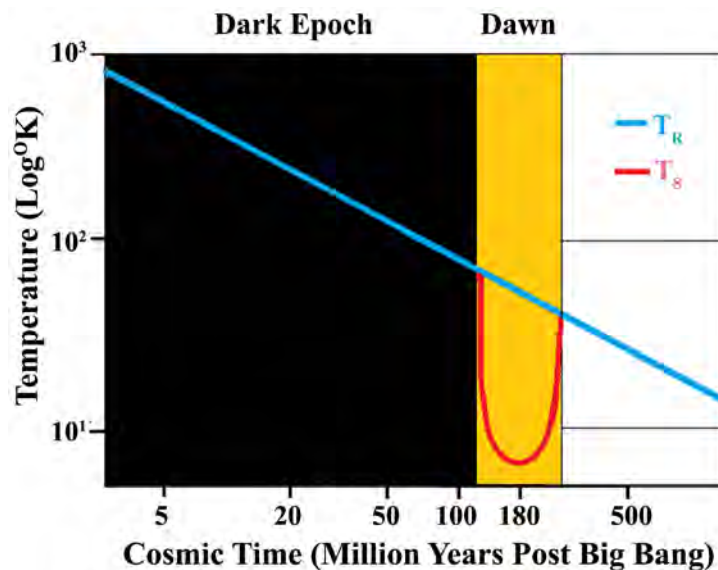


Figure 1. Radiation temperature (T_R) and spin temperature (T_S) vs time.

Unfortunately, the reasoning that such an intermediary nonbaryonic matter was required for this process is also somewhat mysterious, because a temporary decoupling from the CMB radiation temperature is to be expected in a purely baryonic universe (see McGaugh [7]).

Perhaps the ongoing search for exotic dark matter also reflects a misunderstanding about the current abundance of cold ground state interstellar atomic hydrogen in comparison to the constituents of the visible stars, warm molecular gas clouds and dust in our galaxy. It should be remembered that ground state interstellar atomic hydrogen coupled to the CMB radiation temperature (as was also undoubtedly present in great abundance during the “dark ages”) is essentially invisible to modern detectors, except where its characteristic 21-cm absorption line is “backlit” by distant starlight.

The Milky Way disc rotates with a period of approximately 250 million years [12]. Based upon the Baryonic Tully-Fisher relation [13] and the March 2019 *Gaia*-Hubble Collaboration report, the sum total mass of the visible stars, warm molecular gas clouds and dust in the Milky Way is reliably estimated to be 250 billion M_{\odot} . And yet, the calculated amount of ground state interstellar atomic hydrogen coupled to the CMB radiation temperature within a 20 kpc halo radius of the Milky Way center actually dwarfs this total visible matter mass estimate (see calculation below). This reflects the vastness of the interstellar vacuum in comparison to the visible matter.

2. Results

Line-of-sight measurements of the hyperfine 21-cm absorption line (within the light from distant stars of a known distance from the observer) allow one to estimate an average density of cold ground state interstellar atomic hydrogen of approximately one atom/cm³ (or 1.67×10^{-21} kg·m⁻³) [14] [15] [16].

One can now use this knowledge in the context of Posti and Helmi's recent Gaia survey analysis of the Milky Way (see reference [6]). They report the ratio of dark matter to visible matter within a 20 kpc spherical halo radius of the galactic center to be approximately 1.37 to 0.54. This simplifies to a ratio of approximately 2.54. If we assume the above current best estimate of the Milky Way visible matter mass (250 billion M_{\odot} is equal to 4.97×10^{41} kg) and divide that by the volume of a galactic halo sphere of 20 kpc radius (9.85×10^{62} m³), the average visible matter density within that galactic halo sphere is 5.05×10^{-22} kg·m⁻³, approximately one-third of the above-mentioned average density of cold ground state interstellar atomic hydrogen! Multiplying 1.67×10^{-21} kg·m⁻³ by a 0.83 correction factor (for the expected slightly lower ground state atomic hydrogen density in the halo sphere portion outside the galactic disk) times the 20 kpc radius galactic halo sphere volume gives an estimated mass of cold ground state interstellar atomic hydrogen of 1.37×10^{42} kg, in other words approximately 689 billion M_{\odot} , within that sphere. The corresponding 2.76 ratio (from dividing 689 billion M_{\odot} by 250 billion M_{\odot}) is well within the margin of error of Posti and Helmi's observed ratio of dark matter to visible matter for the same 20 kpc radius galactic halo sphere.

3. Discussion

The calculations made in the Results section suggest the strong possibility that cold ground state interstellar atomic hydrogen averaging approximately one atom/cm³ is what we currently refer to as cold dark matter (CDM). The following table (Table 2) compares the above-mentioned dark matter features with sparse interstellar atomic hydrogen coupled to the CMB temperature.

The origin of the C.G.S.I.S.A.H. acronym becomes apparent by reading down the letters in the right-hand column, which are abbreviations for the top five rows of the table. The abbreviation W-F effect stands for the Wouthuysen-Field effect on ground state neutral atomic hydrogen due to Lyman-alpha radiation

Table 2. Dark matter features vs. interstellar H features.

Dark Matter Features	Interstellar H at 1 atom/cm ³	CDM
Cold (<i>i.e.</i> , low velocity)	CMB Equilibrated	C
No Emissions (<i>i.e.</i> , dark)	Ground State	GS
Collisionless (<i>i.e.</i> , low cross-section)	Interstellar/Sparse	IS
Baryon Expected	Atomic Hydrogen	A
Mass-Energy less than 3 GeV	0.938 GeV Neutral H	H
Dark Matter $M_{20\text{kpc}}$ 635 Billion M_{\odot}	689 Billion M_{\odot}	
Central DM Heating ("coring")	Loses Ground State	
CMB Decoupling at Dawn	W-F Effect	
Structural Scaffold	Most Abundant Atom	
Existence at CMB Emission	Most Abundant Atom	

beginning with the first starlight of cosmic dawn. There is a nice discussion of this temporary CMB decoupling phenomenon in the AstroBaki reference. According to this reference, "...the W-F effect remains the dominant effect until reionization is complete." Once reionization was complete, the interstellar atomic hydrogen presumably became once again coupled to the CMB temperature, which is assumed to be the case at present.

As for future observable consequences of my dark matter conjecture presented herein, one can point to the ongoing refinement of observational constraints on the mass-energy of the dark matter particle. The studies to date appear to eliminate any baryonic particle much greater than about 1 GeV (see Barkana [5]). However, they do not yet exclude neutral atomic hydrogen, with its mass-energy of 0.938 GeV. I predict that these constraints will further tighten around a dark matter particle with a mass-energy of 0.938 GeV. Furthermore, the sophisticated dark matter/baryon interaction simulations being conducted at the Kavli Institute for Particle Astrophysics and Cosmology have not yet simulated the dark matter candidate in these interactions as cold ground state interstellar atomic hydrogen of average density of about $1.67 \times 10^{-21} \text{ kg}\cdot\text{m}^{-3}$ ($1.67 \times 10^{-24} \text{ g}\cdot\text{cm}^{-3}$) (R. Wechsler, Director, per verbal communication with this author on March 30, 2019). It is my prediction that such simulations will correlate nicely with dark matter observations, even to the extent of simulating central galactic coring (*i.e.*, relative dark matter depletion) due to "dark matter heating" within active galactic centers (see Read [8]). Thus, the previously unexplained galactic and peri-galactic dark matter spatial distribution may be best understood in terms of heating and other dynamic effects upon the distribution of cold ground state interstellar atomic hydrogen.

4. Conclusion

For the above theoretical and observational considerations, the distinct possibility that the dark matter candidate could ultimately prove to be the ubiquitous but incredibly sparse (and thus nearly collisionless) cold ground state interstellar atomic hydrogen must be seriously entertained.

Conflicts of Interest

The author declares no conflicts of interest regarding the publication of this paper.

References

- [1] Rubin, V. and Ford, W.K. (1970) *The Astrophysical Journal*, **159**, 379. <https://doi.org/10.1086/150317>
- [2] Rubin, V., *et al.* (1985) *The Astrophysical Journal*, **289**, 81. <https://doi.org/10.1086/162866>
- [3] Tucker, W. (2006) *AIP Conference Proceedings*, **801**, 21-30.
- [4] Aghanim, N., *et al.* (2018) Planck 2018 Results VI. Cosmological Parameters.

arXiv:1807.06209v1

- [5] Barkana, R. (2018) Cosmic Dawn as a Dark Matter Detector. <https://doi.org/10.1038/nature25791>
- [6] Posti, L. and Helmi, A. (2018) *Astronomy & Astrophysics*, **621**, A56. <https://doi.org/10.1051/0004-6361/201833355>
- [7] McGaugh, S.S. (2018) *Research Notes of the AAS*, **2**, 37. <https://doi.org/10.3847/2515-5172/aab497>
- [8] Read, J.I., *et al.* (2019) *Monthly Notices of the Royal Astronomical Society*, **484**, 1401-1420. <https://doi.org/10.1093/mnras/sty3404>
- [9] Gaia-Hubble Collaboration (2019). <http://sci.esa.int/hubble/61198-hubble-and-gaia-accurately-weigh-the-milky-way-hic1905>
- [10] AstroBaki (2017). https://casper.ssl.berkeley.edu/astrobaki/index.php/Wouthuysen_Field_effect
- [11] Bowman, J.D. (2018) *Nature*, **555**, 67. <https://doi.org/10.1038/nature25792>
- [12] Morris, M. (2002) The Milky Way. *The World Book Encyclopedia*, 551.
- [13] Torres-Flores, S., *et al.* (2011) *Monthly Notices of the Royal Astronomical Society*, **416**, 1936-1948. <https://doi.org/10.1111/j.1365-2966.2011.19169.x>
- [14] Pananides, N.A. and Thomas, A. (1979) *Introduction to Astronomy*. Second Edition, Wiley & Sons, New York, 293.
- [15] Chaisson, E. and McMillan, S. (1993) *Astronomy Today*. Prentice Hall, New York, 418.
- [16] Mammana, D.L. (2000) *Interstellar Space*. Popular Science, New York, 220.

Expansion of a Y-Shaped Antenna Array and Optimization of the Future Antenna Array in Malaysia for Astronomical Applications

Shahideh Kiehadrouinezhad¹, Jean-François Bousquet¹, Michael Cada¹, C. Ian Short², Adib Shahabi^{1*}, Samiramis Kiehadrouinezhad^{3,4}

¹Department of Electrical and Computer Engineering, Faculty of Engineering, Dalhousie University, Halifax, Canada

²Department of Astronomy and Physics, Saint Mary's University, Halifax, Canada

³Department of Physics, Eberhard-Karls-Universität Tübingen, Tübingen, Germany

⁴Department of Astronomy, Institute of Astronomy and Astrophysics, Tübingen, Germany

Email: *adib.shahabi@dal.ca

How to cite this paper: Kiehadrouinezhad, S., Bousquet, J.-F., Cada, M., Short, C.I., Shahabi, A. and Kiehadrouinezhad, S. (2019) Expansion of a Y-Shaped Antenna Array and Optimization of the Future Antenna Array in Malaysia for Astronomical Applications. *Journal of Modern Physics*, 10, 888-908.

<https://doi.org/10.4236/jmp.2019.108059>

Received: May 26, 2019

Accepted: July 2, 2019

Published: July 5, 2019

Copyright © 2019 by author(s) and Scientific Research Publishing Inc.

This work is licensed under the Creative Commons Attribution International License (CC BY 4.0).

<http://creativecommons.org/licenses/by/4.0/>



Open Access

Abstract

To achieve high quality images from the sky by extending an existing interferometric array, in this work, the Geometrical Method (GM), Genetic Algorithm (GA), and Division Algorithm (DA) are compared. These methods are each applied independently to an interferometer array starting from the same initial conditions. Using the GM method, the spiral configuration is suggested as an optimum arrangement that provides the desired u - v coverage with low side lobe levels (SLLs). Using the GA method, as the number of generations is increased, the unsampled cells are reduced, enhancing the imaging quality. As such, the algorithm improves the overlapped samples as it works with a greater number of generations. Moreover, the GA is able to suppress the SLL. Finally, the DA is applied to such an array. Results show that the DA is able to process the sampled data with less overlapping of the data in the snapshot observations, in comparison to the other discussed configurations in this paper; effectively the DA reduces the overlapped samples, such that it is more efficient than the GA. The configuration of antennas that arrives by applying the DA method can achieve a certain image quality with less overlapping, as compared to the configuration arriving by applying the GA method. The calculated SLLs for the DA configuration are used to demonstrate that the efficiency of the DA is potentially better than that of the GA. Moreover, the GA and DA algorithms discussed in this study are applied to an array of 10 antennas with coordinates that represent the antennas deployed in Malaysia. Results show that the DA can reduce the overlapping of the samples more efficiently than the GA for a 6-hour tracking observation and in terms of unsampled cells the DA has the same efficiency of the GA.

Keywords

Interferometers, Telescopes, Genetic Algorithm, Array of Antennas

1. Introduction

In order to measure with fine angular detail in the radio frequency range from the sky, two-element radio interferometers, or alternatively synthesis arrays can be used. The angular resolution of a single telescope does not provide sufficient information for astronomy applications; therefore, a synthesis array or radio interferometer is used to fulfill the aim of the end user. On the other hand, the light waves from very distant stars or galaxies take a long time to travel through space to our telescopes; therefore, it limits the astronomers to visually observe light waves that occurred a very long time ago.

The time lag to observe events has led astronomers to build more powerful telescopes to study the first stars and galaxies formed. One of the most powerful arrays is the Giant Meterwave Radio Telescope (*GMRT*). To get higher resolution than what the current *GMRT* array can provide, additional antennas were added to the array. To improve existing correlator antenna arrays like the Giant Metrewave Radio Telescope (*GMRT*), an expansion of the array is required to obtain higher resolution. A project called the Square Kilometre Array (*SKA*), which involves more than ten countries worldwide, will be the most powerful radio telescopes array. It allows observation of the sky and it can produce images from radio waves with very high resolution. However, the location of the telescope limits the image quality and has a direct effect on the side lobe levels (*SLLs*) [1].

In the design of an array for astronomy applications, the choice of each antenna's localization in the array is key. An ideal arrangement must ensure optimal configuration to capture a clear image of a radio source by either decreasing the side lobe level (*SLL*) in the l - m domain or increasing the sampled data in the spatial frequency domain, which is referred to as u - v plane coverage [2].

In this work, we focus on the comparison of different methods: the Geometrical Method (*GM*), the Genetic Algorithm (*GA*), and the Division Algorithm (*DA*) [1] [2] [3] and [4]. These techniques and methods for assisted interferometry and how they can be implemented in a correlator antenna array, particularly applied to the *SKA* are described. The ability of the proposed receiver to suppress the severe *SLL* effect, to increase the u - v plane coverage, and to smoothen the linear ridges in the u - v plane coverage at a low number of snapshots or low duration of observation will be demonstrated through simulations, using Matlab.

The first method (*GM*) uses the optimization of the array configuration problem with various changes of coordinates in a specific area with the *GMRT*'s arms as an illustrative example. The results show that spiral configurations give very

good improvement in both u - v plane coverage and reduction of side lobe levels.

For the second technique, the proposed GA presented in [2] is used to optimize a correlator array of antennas. The algorithm is able to distribute the u - v plane more efficiently than $GMRT$ with 49.77% overlapped samples. The configuration arrived at with this algorithm is able to sample the u - v plan more efficiently than the current $GMRT$ configuration.

The third method is the new proposed algorithm named Division Algorithm (DA) that has been recently presented in [3] to solve optimization problems.

The above methods are used to yield the optimum configuration for an extended interferometric array, and effectively to investigate the feasibility of extending the interferometric array using 10 antennas that would be deployed in Malaysia.

This paper is organized as such; Section 2 introduces the material and methods for expanding a Y -shape array and to represent the antenna array in Malaysia. Section 3 presents the simulation results. Finally, Section 4 and 5 cover the discussion and conclusions, respectively.

2. Material and Methods

2.1. Expanded Y -Shape

To extend the $GMRT$, it is proposed to add 15 antennas for cost-effectiveness and to realize the scientific goals. In order to add the antennas to the current array, the position of each antenna using rectangular coordinates (x , y , z) is calculated using:

$$\begin{aligned} X &= R \times \sin \theta \times \cos \varphi \\ Y &= R \times \sin \theta \times \sin \varphi \\ Z &= R \times \cos \theta \end{aligned} \quad (1)$$

where R , θ , and φ are the latitude, longitude, and radial distance R (equal to about 6378.1 km, the value of earth's radius), respectively. The extended configuration is placed at 110 km along the arms of the $GMRT$. The declination of the radio frequency source of interest for all configurations is the same (and is equal to 45°). Spiral configurations follow the theory of a logarithmic spiral [1].

Results in [1] show that the spiral antenna array configuration provides low SLL and good u - v coverages and therefore achieves high image resolution. Therefore, the following equations are used to calculate the gridded cells in u - v domain:

$$N_{\text{grid}} = \sqrt{\left(\frac{A_r}{A}\right)} \times (\text{nosmp}) \quad (2)$$

$$\Delta u = \frac{u_{\text{max}} - u_{\text{min}}}{N_{\text{grid}}} \quad (3)$$

$$\Delta v = \frac{v_{\text{max}} - v_{\text{min}}}{N_{\text{grid}}} \quad (4)$$

where nosmp , A_r , A , and N_{grid} are the number of samples in the snapshot or hour tracking observation, the total desired area, the covered area by the current configuration, and the number of gridded cells, respectively.

And Δu , Δv , u_{max} , u_{min} , v_{max} , v_{min} and N_{grid} are the dimension of the cell in the u direction, the dimension of the cell in the v direction, the maximum value of u in the spatial frequency domain, the minimum value of u in the spatial frequency domain, the maximum value of v in the spatial frequency domain, the minimum value of v in the spatial frequency domain and the number of gridded cells as defined in Equation (2), respectively [1].

Also, results in [2] show the good performance of the *GA* configuration in terms of *SLL* and sampling. The algorithm provides an optimum solution for both a snapshot observation and a 6-hour tracking observation with minimum values of overlapping. This happens due to the discrete grid locations of the plane as defined in:

$$N_{\text{grid}} = \text{nearest} \sqrt{(n \times (n-1) \times A_{\text{total}} / A_{\text{first}})} \quad (5)$$

where n is the number of antennas, A_{total} is the total area, A_{first} is the first calculated area of tracking observation from the first random population, and nearest rounds N_{grid} to the nearest integer. This selection helps distribute the samples in the u - v plane with less overlapping in both snapshot and hour tracking simultaneously [1].

The new algorithm (*DA*), explained in [3], shows good results in optimizing an interferometric array. Therefore, these three methods are used in this section to investigate an optimum configuration, in order to extend an interferometric array.

To evaluate the position of each antenna using *GA* and *DA* methods, the fitness function elaborated in [2] is used:

$$\text{fitness}(k) = -\frac{ol_{\text{sam}}(k)}{\max(ol)} - \frac{D(k)}{R} - \frac{(A_{\text{tofsam}} - A_{\text{sam}}(k))}{A_{\text{tofsam}}} \quad (6)$$

where: $\text{fitness}(k)$ is the fitness value of k^{th} baseline in n^{th} generation. $ol_{\text{sam}}(k)$ indicates the number of overlapped samples generated by k^{th} baseline in n^{th} generation. $\text{Max}(ol)$ provides the maximum value of overlapping that is in n^{th} generation. $D(k)$ is the sample distance from the grid center. R is the gridded cell radius. $A_{\text{sam}}(k)$ is the calculated area generated by k^{th} baseline's samples in n^{th} generation. A_{tofsam} is the total area generated by n^{th} generation [2].

Finally, the mean *SLL* for all the aforementioned methods are calculated using the following equation [1]:

$$\text{mean } SLL = -\text{mean}(\text{first } SLL + \text{second } SLL + \text{third } SLL) \quad (7)$$

2.2. Antenna Array in Malaysia

Malaysia has started to fund major research astronomy projects recently with two telescopes. In this work, we apply the proposed theory of localization using

an array of antennas for astronomy applications to suppress the *SLLs* and/or increase the number of samples in the *u-v* plane coverage for the future array configuration in Malaysia.

We expect that the proposed methods can optimize the number of data samples and minimize the side lobe levels in the angular domain to enhance the image quality as much as possible. The methods discussed in this study are applied to 10 antennas which will be placed at the coordinates of the antennas in Malaysia.

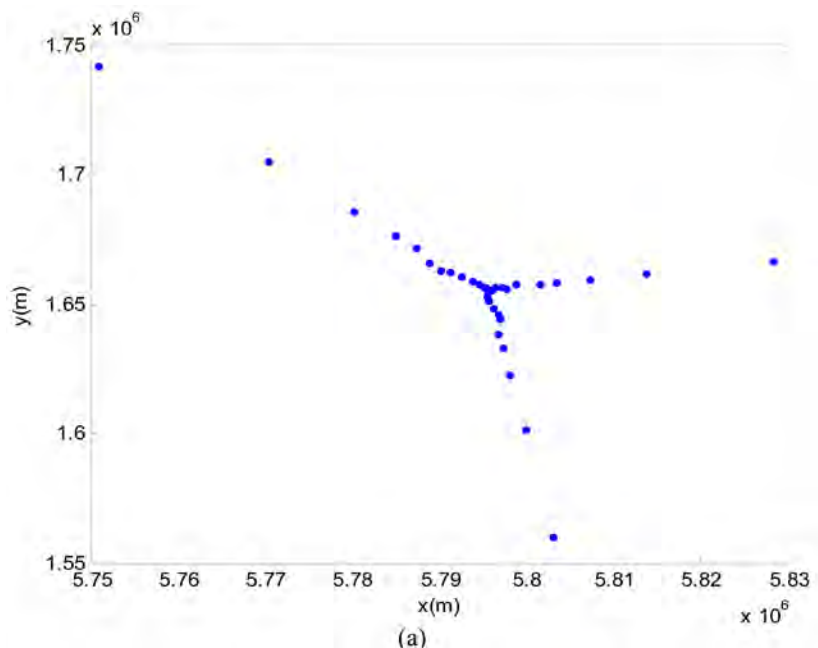
The materials and methods used in this section are taken from [2] [3]. Here, the *GA* and *DA* algorithms are used to investigate the optimum solutions for ten antennas in Malaysia.

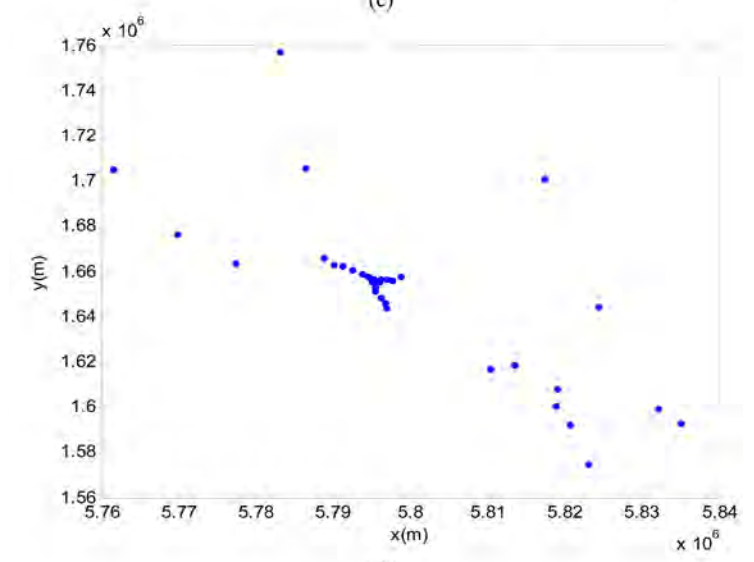
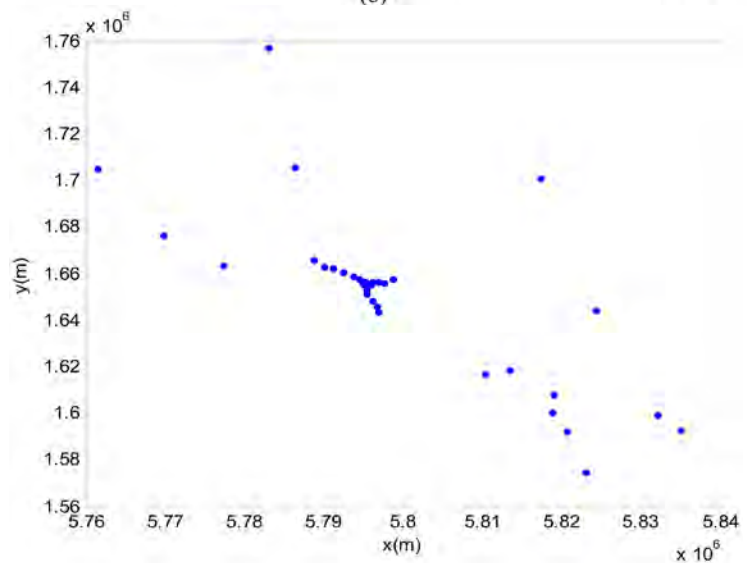
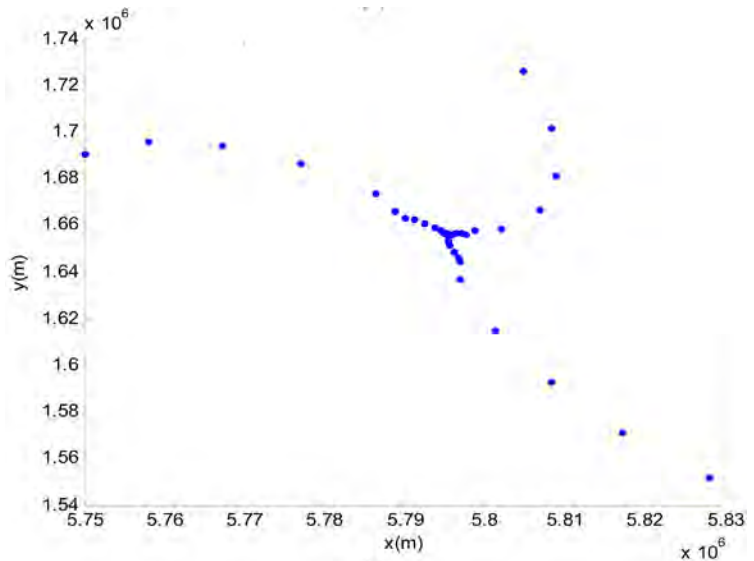
3. Results

3.1. Expanded Y-Shape

To expand the existing array, 15 antennas are added for the following configurations: 1) extended *Y*-shaped; 2) spiral; 3) 25th generation using *GA*; 4) 150th generation using *GA*; and 5) *DA*. **Figure 1** shows the different configurations. The *u-v* plane coverage achieved from these different configurations are shown in **Figure 2** and **Figure 3** for the snapshot and 6-hour tracking observations, respectively. The results are summarized in **Figures 1-3**, and **Table 1** & **Table 2**.

In the first step, extension of the *Y*-shaped array is investigated. In this configuration, 15 antennas are located along the three arms of the *GMRT*. Five antennas are added in each arm and broadened around to 110 km. This array gets a *Y*-shape to investigate the effect of extending the arms in the original *Y*-shape. This new arrangement, its snapshot observation, and 6-hour image synthesis are shown in **Figure 1(a)**, **Figure 2(a)**, and **Figure 3(a)**, respectively.





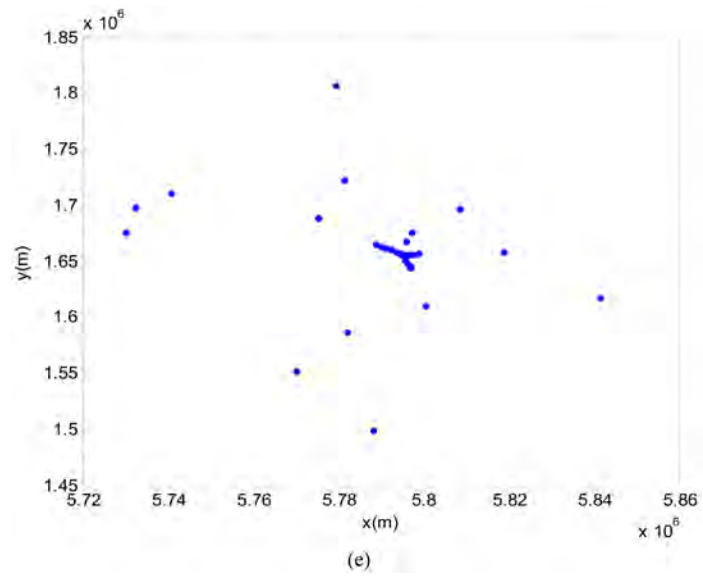
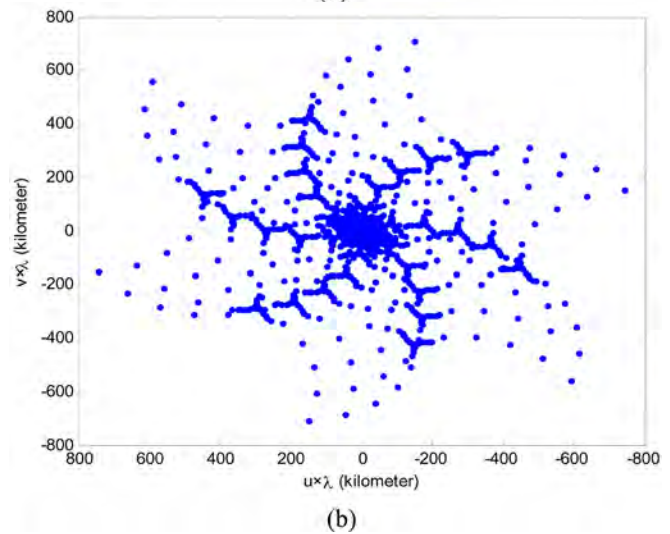
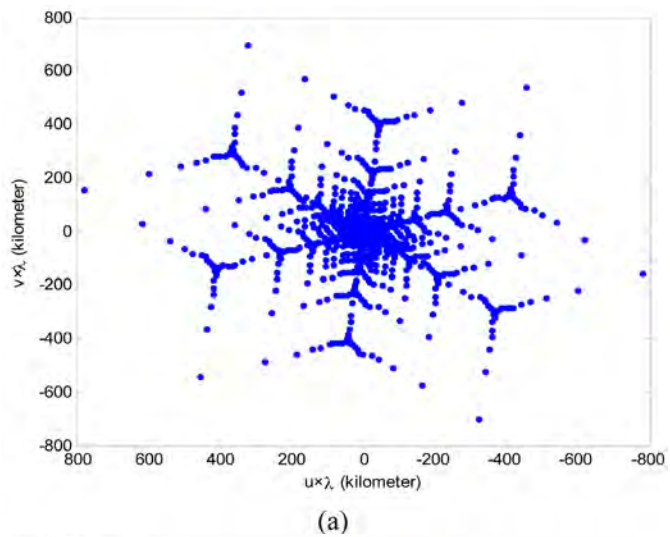


Figure 1. Configuration for (a) extended *GMRT*, (b) spiral, (c) twenty-five generations, (d) one hundred fifty generations using Genetic Algorithm and (e) Division Algorithm.



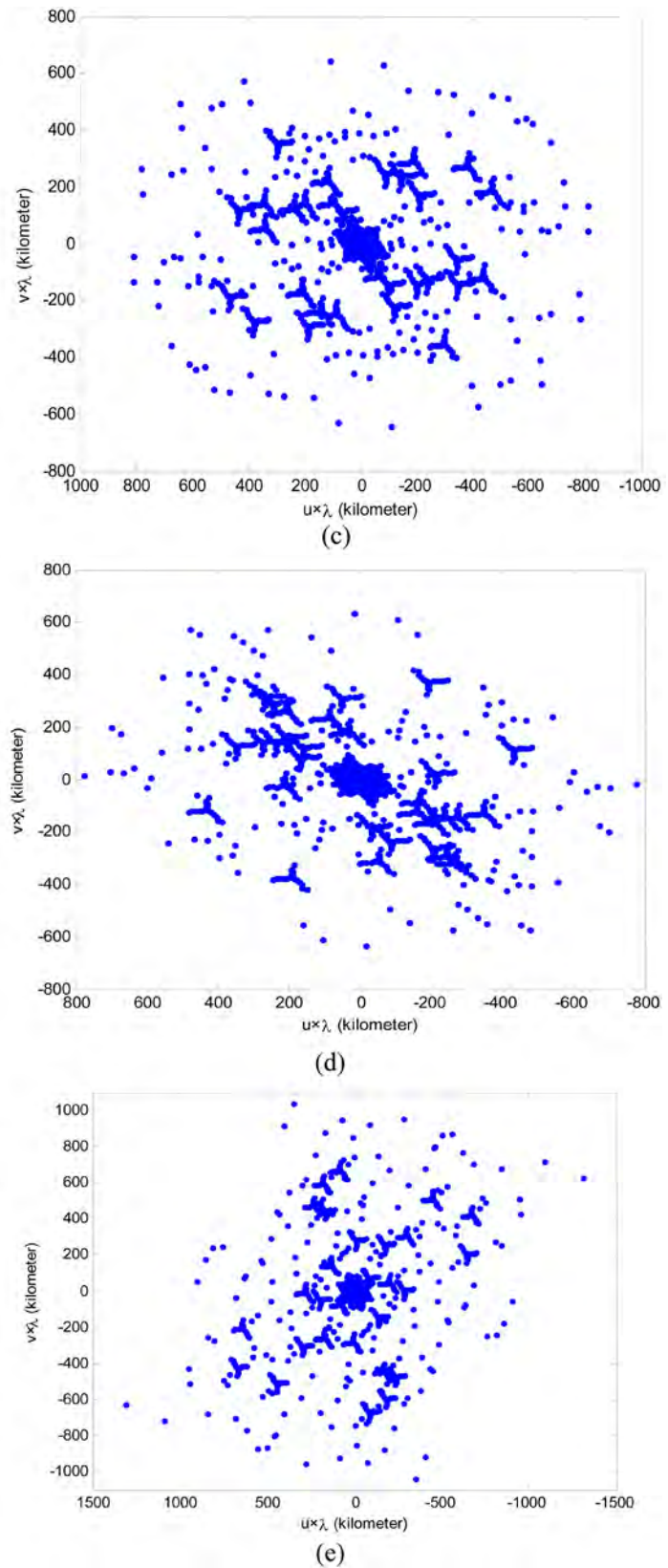
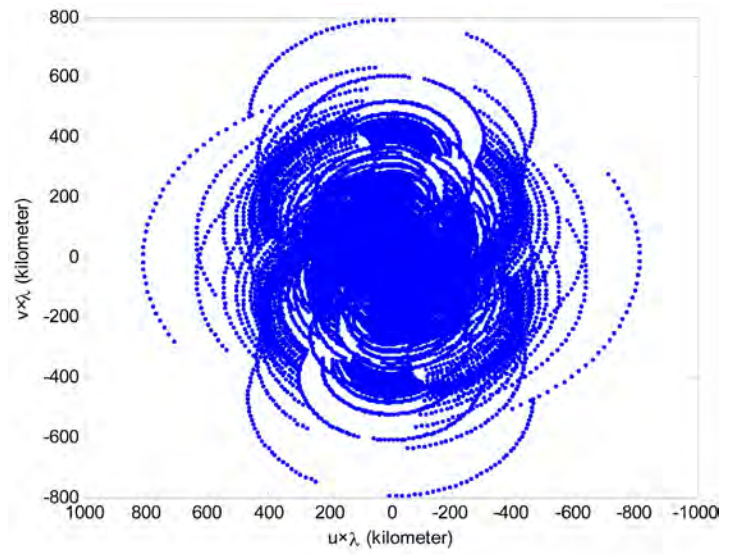
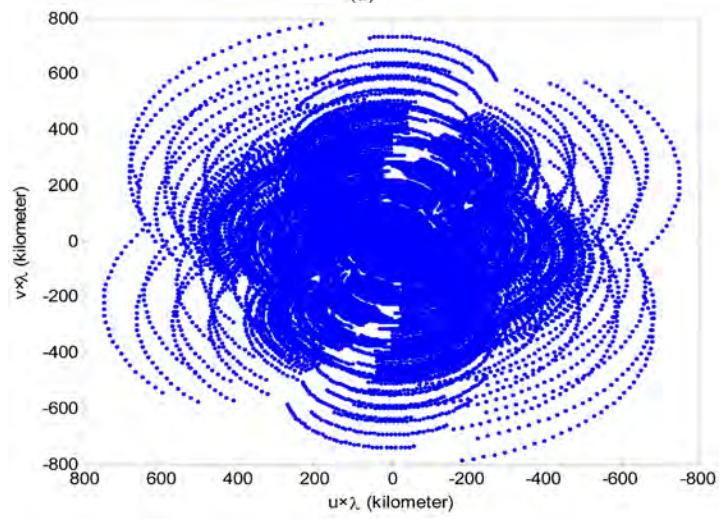


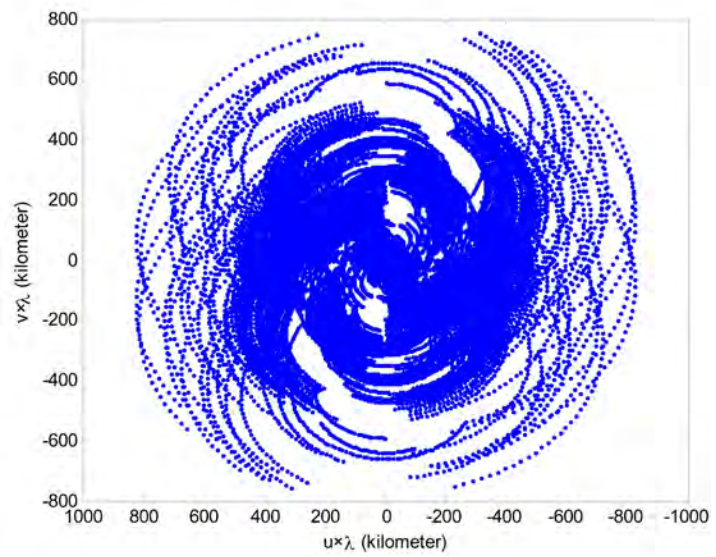
Figure 2. Snapshot u - v plane coverage for (a) extended $GMRT$, (b) configuration of spiral, (c) GA using 25 generations, (d) GA using 150 generations and (e) Division Algorithm.



(a)



(b)



(c)

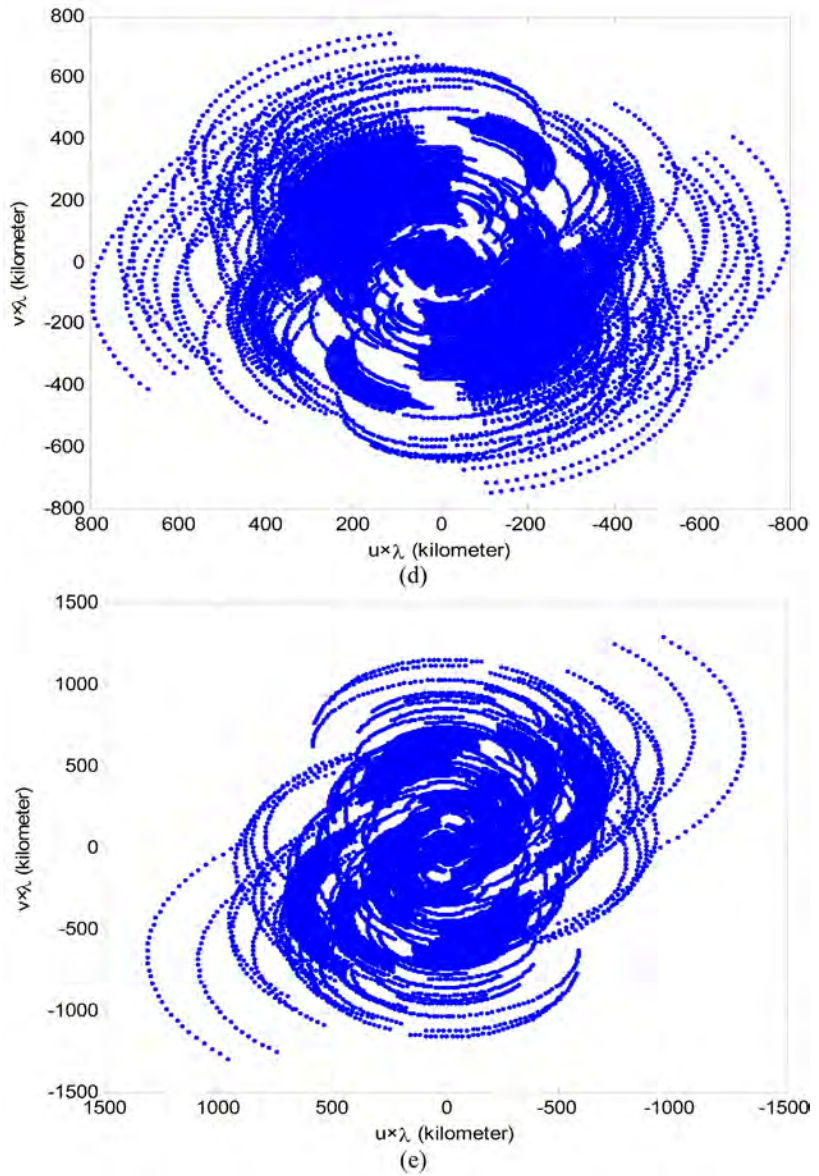


Figure 3. Spatial frequency coverage for a 6-hour tracking observation $u-v$ plane coverage for configuration of (a) extended *GMRT*, (b) spiral, (c) twenty-five generations, (d) one hundred fifty generations using Genetic Algorithm and (e) Division Algorithm.

Table 1. Comparison of different configurations.

Configuration	Overlapped samples% (Snapshot)	Overlapped samples% (Hour tracking)	Unsampled cells% (Snapshot)	Unsampled cells% (Hour tracking)
Extended <i>GMRT</i>	89.19	88.89	78.67	75.19
Spiral	86.77	85.51	72.56	67.59
25th generation	85.91	86.58	76.34	70.74
150th generation1	85.05	84.76	74.56	66.65
DA array	79.45	83.87	72.00	63.76

Notes: 6-hour is used in hour tracking synthesise.

Table 2. Comparison of *GMRT*'s *SLL* and different configurations' *SLL*.

Configuration	First <i>SLL</i> (dB) (Hour tracking)	mean <i>SLL</i> (dB) (Hour tracking)	Peak <i>SLL</i> (dB) (Hour tracking)
Extended <i>GMRT</i>	-11.18	-11.97	-10.59
Spiral	-11.25	-12.46	-10.86
25th generation	-11.88	-13.85	-12.55
150th generation1	-12.04	-13.88	-13.75
<i>DA</i> array	-19.30	-16.86	-14.80

Notes: 6-hour is used in hour tracking synthesise.

Table 1 shows the number of overlapped samples using snapshot as well as for a 6-hour tracking observation. This parameter is valued at 89.19% using the snapshot and 88.89% for a 6-hour tracking observation. The unsampled cells ratio achieved with this configuration (expanded *GMRT*) are 78.67% using the snapshot observation and 75.19% for a 6-hour tracking observation.

As shown in **Figure 2(a)**, for the u - v plane coverage using the snapshot observation, the linear ridges are not smooth, and this configuration provides a poor sensitivity and consequently a poor signal to noise ratio [1]. Therefore, the linear ridges need to be smoothened. In order to perform this requirement, the arms are curved in the next arrangement as is shown in **Figure 2(b)**.

Arms in the spiral configuration cover the angular position of 60 to 96, 180 to 216 and 300 to 336 degrees. The angular positions of five added antennas in each arm are 62 to 70, 182 to 190 and 302 to 310 degrees. The overlapped sample ratio is equal to 86.77% for the spiral using the snapshot observation. Similarly, it is equal to 85.51% for a 6-hour tracking observation. The unsampled cells ratio from the u - v coverage indicate the percentage of the cells without any sample. This ratio is equal to 72.56% using the snapshot (see **Figure 2(b)**) and 67.59% for a 6-hour tracking observation (see **Figure 3(b)** and **Table 1**). This means the spiral configuration is able to sample the Fourier space of the image better than the extended Y-shape. In comparison to the extended *GMRT*, the lower ratios of overlapped samples and unsampled cells resulting from the spiral suggest that this configuration provides more information about the source due to a greater number of samples in the u - v plane. Therefore, the configuration of the spiral provides a better u - v plane coverage in both types of observations in comparison to the extended *GMRT*'s as shown in **Figure 2(b)** and **Figure 3(b)**.

In the next step, the *GA* is applied to this extended interferometric array, to investigate the effect of the algorithm.

From the results achieved using the previous configurations (see **Figure 1(a)** and **Figure 1(b)**), the data in the spatial frequency domain needs to be spread out to get less overlapping. Therefore, the *GA* is applied to work on sampled data using the snapshot to provide the desired resolution.

For the *GA*, the optimum ratio values of mutation and crossover (25% mutation ratio and 25% crossover ratio) are used in the proposed algorithm. The

number of antennas (chromosomes) is set to 45 and for each the diameter is equal to 45 m to assess the efficiency of the algorithm. To distribute the sampled data in u - v plane coverage more smoothly, the algorithm works on 150 generations to optimize the image resolution.

The position of the antennas (chromosomes) in the array for the 25th, and the 150th generations using the *GA* are shown in **Figure 1(c)** and **Figure 1(d)**, respectively. The snapshot in the u - v plane coverage for the 25th, and the 150th generations that are shown in **Figure 2(c)** and **Figure 2(d)**. These illustrate how the sampled data distribution are from the results using the extended *GMRT*. As can be observed qualitatively, the data in the 150th generation improves the distribution of the data somewhat more evenly. The calculated ratios shown in **Table 1** summarize the ability of the *GA* (when using snapshot) in distributing the samples and obtaining more samples rather than the extended *GMRT*.

The calculated ratios in **Table 1** show that the *GA* can sample data with less overlapped data using the snapshot observation. Specifically, for the 150th generation the ratio is equal to (85.05%), in comparison to 89.19% for the extended *GMRT*. This indicates that as the algorithm works with more generations, it distributes sampled data in the u - v plane coverage more efficiently than extended *Y*-shaped.

The calculated ratio of overlapped samples for a 6-hour tracking is shown in **Table 1**. From the results, this value is improved from 88.89% to 86.58%, and then to 84.76% using the extended *GMRT*, the 25th, and the 150th generation configurations, respectively. It means the algorithm improves the ratio of overlapped samples since it works with a greater number of generations.

When the number of generations goes up, the number of unsampled cells is lower; specifically, this percentage is 78.67% using the extended *GMRT* configuration and becomes 76.34%, and 74.56% values using the 25th, and 150th generations using the snapshot, respectively. This ratio is equal to 75.19% using the extended *GMRT* observation and is equal to 70.74% and 66.65% values using the 25th, and the 150th generations for 6-hour tracking observations, respectively.

In the last step, the *DA* is applied to this extended interferometric array, to investigate the effect of the algorithm. The algorithm provides an optimum solution for both the snapshot and for the hour-tracking observations with minimum ratios of overlapping.

The position of the antennas, u - v coverages at snapshot and 6-hour tracking observations in the array using *DA* are shown in **Figure 1(e)**, **Figure 2(e)**, and **Figure 3(e)**, respectively. The calculated parameters shown in **Table 1** express the ability of the *DA* in distributing the samples and obtaining more samples rather than the extended *GMRT*'s at the snapshot.

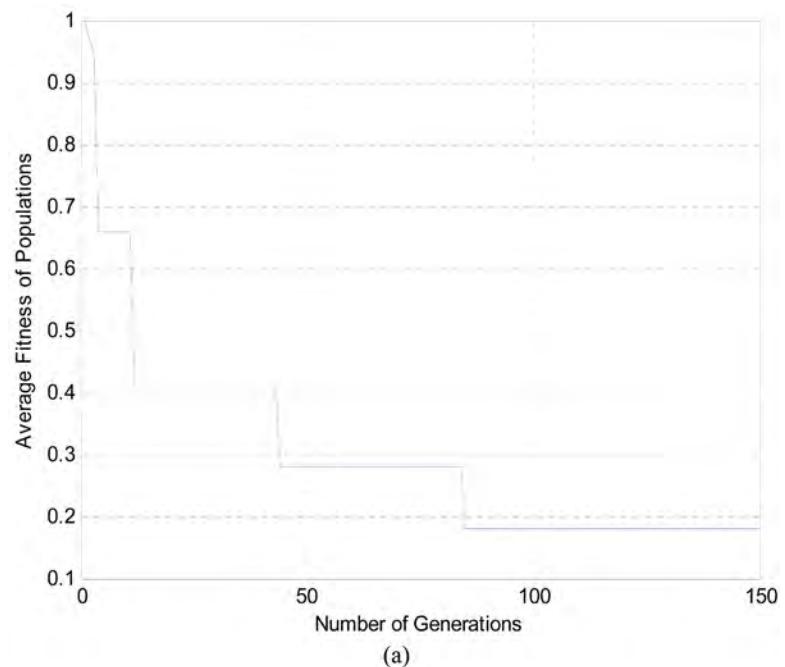
The results calculated in **Table 1** show that the *DA* can achieve the sampled data with less overlapped data at snapshot observation among all discussed configurations in this study (79.45%). The calculated overlapped samples ratio for a 6-hour tracking is shown in **Table 1**. From the results, this value is equal to 83.87%. It means the algorithm improves the overlapped number of samples

more efficiently than *GA*. When the number of generations goes up, the unsampled cells get reduced; specifically, this percentage is 72% at snapshot and 63.76% for a 6-hour tracking observation.

The calculated *first SLL*, mean of the first three *SLL* (*mean SLL*), and the worst *SLL* defined as the *peak SLL* are shown in **Table 2**. The calculated *SLLs* show that the spiral geometry has lower side lobes (*SLL* = -11.25 dB and *mean SLL* = -12.46 dB, and *peak SLL* = -10.86 dB) than the extended *GMRT* (*SLL* = -11.18 dB and *mean SLL* = -11.97 dB, and *peak SLL* = -10.59 dB) and the linear ridges using the snapshot is also smoother than for the extended *GMRT* (see **Figure 2(b)**). As such, the spiral configuration smoothens the linear ridges.

The first and the mean values of the first three *SLLs* of 25th and 150th generation using *GA* are also calculated **Table 2**. The *first SLL* is -11.18 dB in extended *GMRT* and -11.88 dB, and -12.04 dB for the 25th, and the 150th generation configurations, respectively. The calculated mean value of the first *SLL* shown in **Table 2** depicts that the configurations have the *mean SLL* of -13.85 dB and -13.88 dB at the 25th, and the 150th generation, respectively (this ratio is valued at -11.97 dB using the extended *GMRT*). The algorithm is also able to decrease the level of the *peak SLL* as the number of generations goes up (this ratio is -12.55 dB and -13.75 dB using 25th and 150th generation configurations, respectively). The calculated *first SLL*, *mean SLL*, and *peak SLL* values of *DA* configuration are -19.3 dB, -16.86 dB, and -14.8 dB, respectively. These values show the better efficiency of the *DA* in comparison to the *GA*.

The evolution of the average fitness in each generation for the *u-v* plane coverage using the snapshot observation and *SLL* reduction are shown in **Figure 4**. As shown in **Figure 4(a)**, the optimum solution occurred at the 47th generation for the first 50 generations, and the optimum value in the range of 82th to 150th



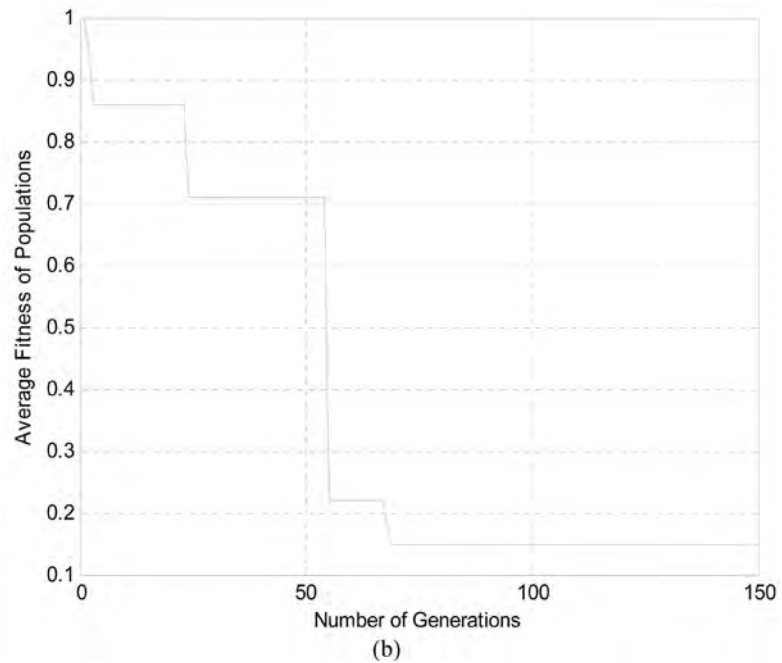


Figure 4. The evolution of average fitness in each generation in (a) the spatial frequency domain and (b) the l-m domain.

generation remains constant. The fitness value for the first 50 generations in **Figure 4(b)** obtains the optimum solution at 23rd generation. Since the algorithm seeks the solutions randomly, it provides different solutions each time. The aim of this study is to demonstrate optimum solutions for an extended interferometric array. It is not written for any specific constraints for astronomy applications; however, it can work with different constraints.

From the results obtained from the different configurations in this study, a spiral shape suggests good results in the angular domain as well as in the u - v domain and the GA and DA provide improved $SLLs$, and u - v plane coverages.

3.2. Antenna Array in Malaysia

The simulated source declination is 45 degrees. The duration for the fully synthesized observation is a 6-hour tracking with 10 minutes time interval between each two samples.

As a first step, the GA is applied to an interferometric array, to investigate the effect of the algorithm.

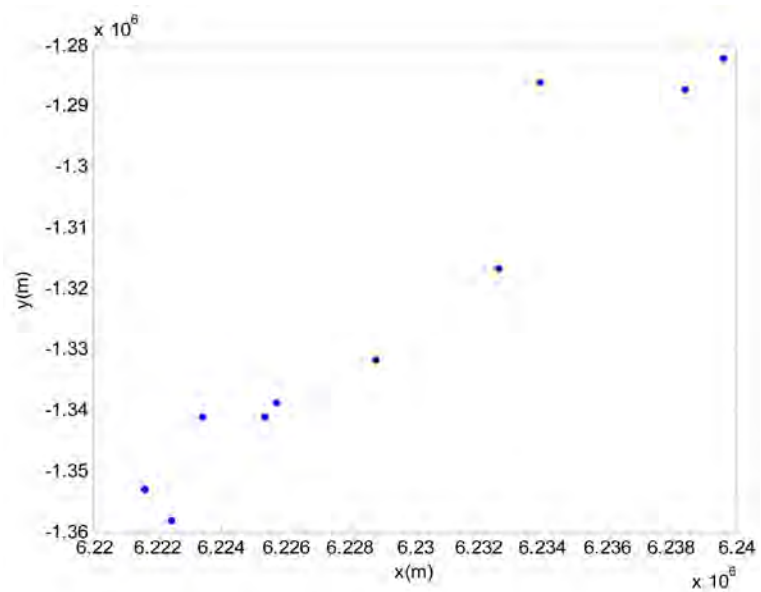
The algorithm provides an optimum solution for both the snapshot and the hour-tracking observations with minimum values of overlapping (this happens due to the grounding of the plane as defined in (2) and (3)).

The optimum ratio values of mutation and crossover (25% mutation ratio and 25% crossover ratio) are used in the algorithm. The number of antennas (chromosomes) is fixed to 10. To distribute the sampled data in u - v plane coverage more smoothly, the u - v plane is gridded with the dimension of $D_u \times D_v$ as defined in (3) and the algorithm works on 150 generations to optimize the resolu-

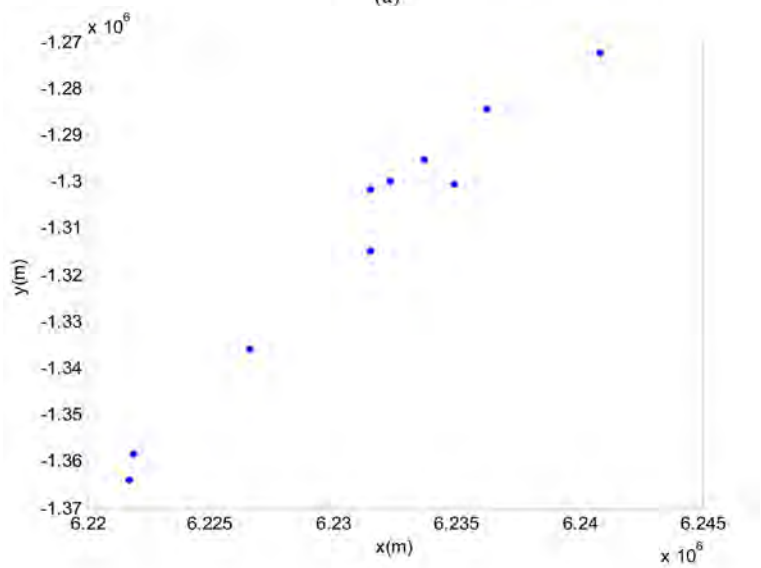
tion of the image.

The positions of the antennas (chromosomes) in the array of the 25th and 150th generations using the *GA* are shown in **Figure 5(a)** and **Figure 5(b)**, respectively. Using the snapshot, the *u-v* plane coverages for the 25th, and 150th generations in **Figure 6(a)** and **Figure 6(b)** and 6-hour tracking in **Figure 7(a)** and **Figure 7(b)** show how the sampled data is distributed using 25th generation gradually to 150th generation.

The calculated parameters shown in **Table 3** express the ability of the *GA* to distribute the samples and obtaining more samples as the number of generations goes up at the snapshot. The calculated results summarized in **Table 3** show that the *GA* achieves the sampled data with less overlapped data at snapshot observation from the 25th generation (12%) to the 150th generation (2%). This indicates



(a)



(b)

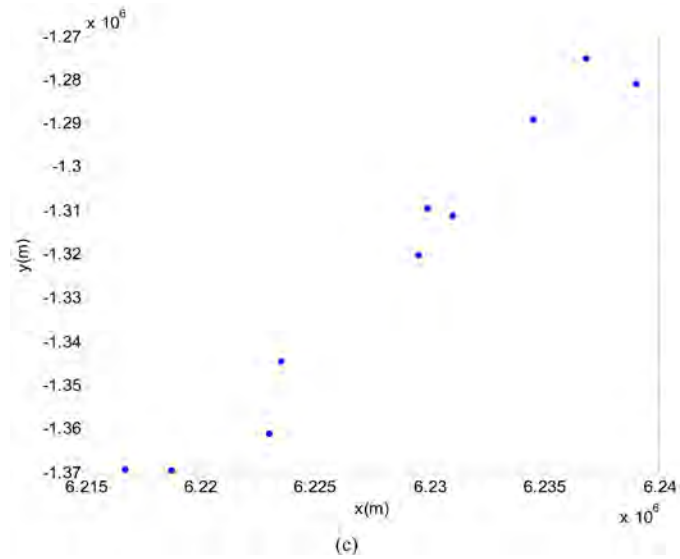
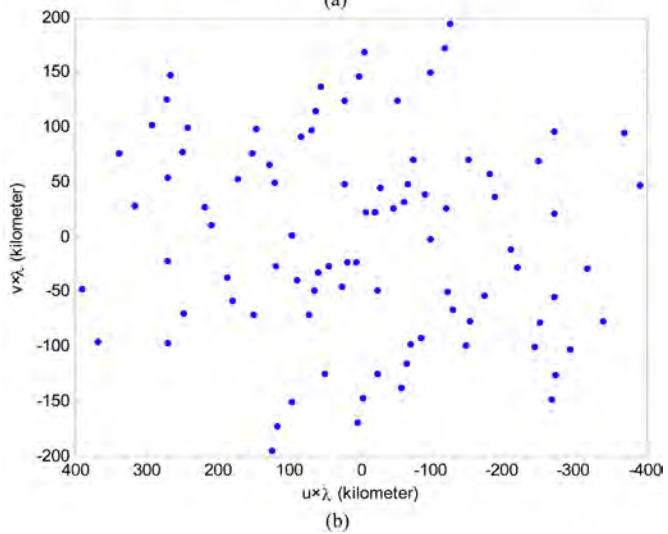
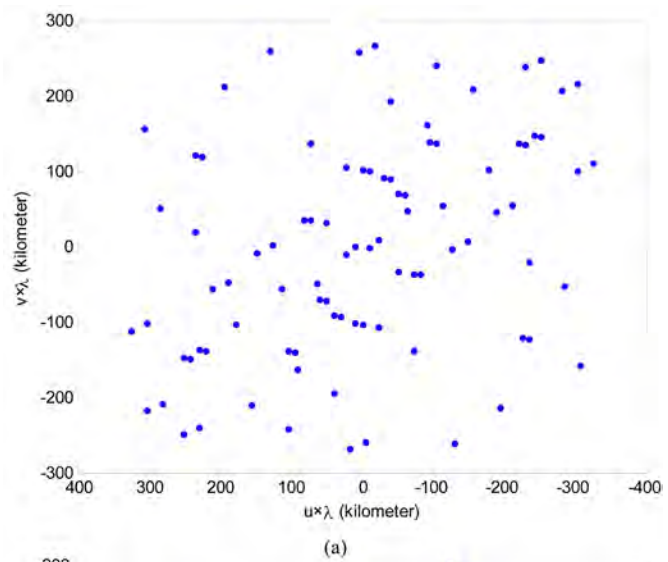


Figure 5. Configuration for (a) twenty-five generations, (b) one hundred fifty generations using Genetic Algorithm and (c) Division Algorithm.



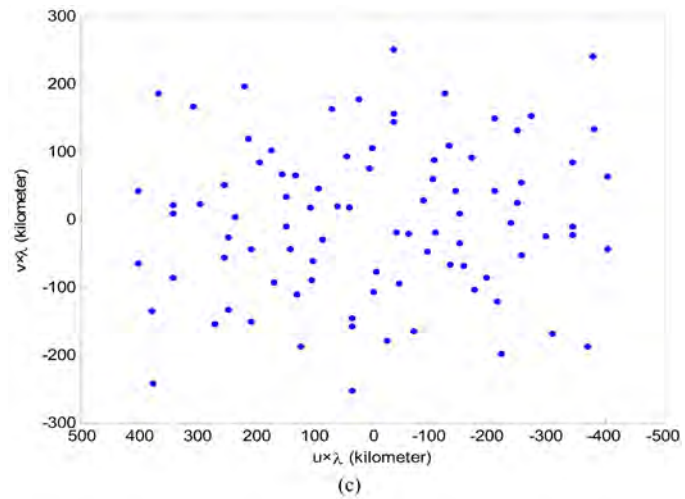
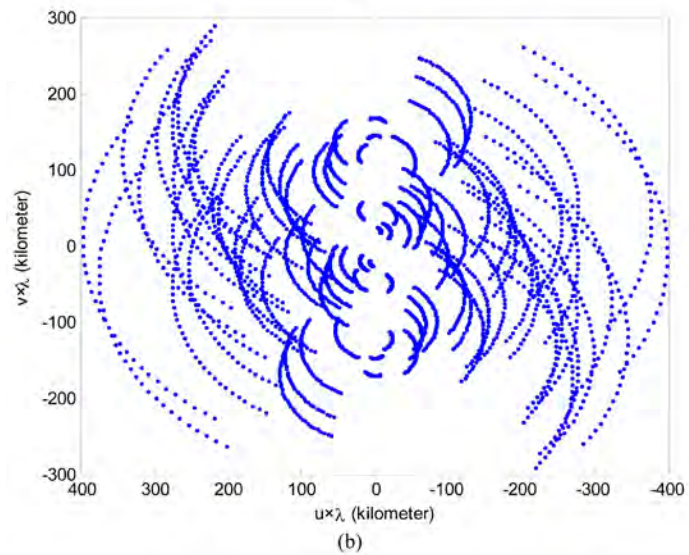
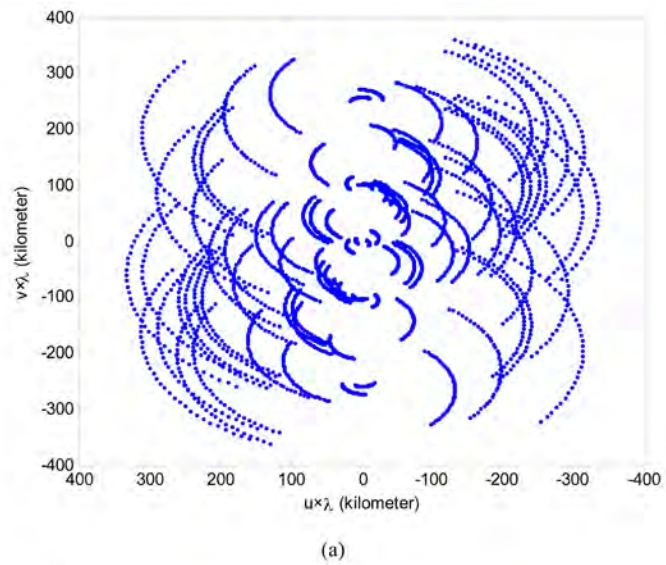


Figure 6. Snapshot u - v plane coverage for (a) twenty-five generations, (b) one hundred fifty generations using Genetic Algorithm and (c) Division Algorithm.



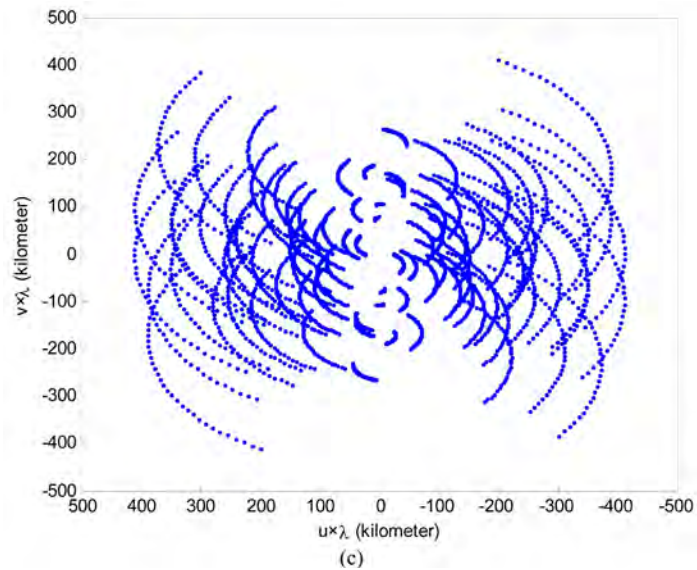


Figure 7. Spatial frequency coverage for a 6-hour tracking observation $u-v$ plane coverage for (a) twenty five generations, (b) one hundred fifty generations using Genetic Algorithm and (c) Division Algorithm.

Table 3. Comparing of different parameters of DA to the GA .

Configuration	Overlapped samples% (Snapshot)	Overlapped samples% (Hour tracking)	Unsampled cells% (Snapshot)	Unsampled cells% (Hour tracking)
25th generation	13.34	25.23	94.89	93.23
150th generation1	2.23	24.45	94.00	92.49
DA array	0.00	22.28	91.56	92.16

Notes: 6-hour is used in hour tracking synthesise.

that as the algorithm works with more generations, it can distribute sampled data in the $u-v$ plane coverage more efficiently.

The calculated overlapped samples ratio for a 6-hour tracking is shown in **Table 3**. From the results, this value is varied from 13.34% to 2.23% using the 25th and the 150th generation configurations, respectively. It means the algorithm improves the overlapped samples as it works with more numbers of generations.

Since the number of generations goes up, the number of unsampled cells are decreased; specifically, the ratio is 94.89% using the 25th generation observation and becomes 94.00% using the 150th generations at the snapshot. This ratio is equal to 93.23% using the 25th generation observation and becomes 92.49% using the 150th generation for a 6-hour tracking observation.

Finally, the DA is applied to the extended interferometric array, to investigate the effect of the algorithm. The algorithm provides an optimum solution for both the snapshot and the hour-tracking observations with minimum values of overlapping (this happens due to the gridding of the plane as defined in (2) and (3)).

The position of the antennas, the $u-v$ coverage for the snapshot observation and for a 6-hour tracking observation in the array using the DA are shown in

Figure 6(c), Figure 7(c), and Figure 8(c), respectively. The calculated ratios shown in Table 3 express the ability of the *DA* in distributing the samples and obtaining more samples rather than the *GA* for the snapshot.

The calculated results that are summarized in Table 3 show that the *DA* can achieve the sampled data with the same efficiency as the *GA* for the snapshot observation. The calculated overlapped samples ratio for a 6-hour tracking is shown in Table 3. From the results, this ratio is valued at 22.28%. It means the algorithm improves the overlapped samples more efficiently than *GA* for a 6-hour tracking observation.

Since the number of generations goes up, the number of unsampled cells is reduced; specifically, this percentage is 91.56% at snapshot and 92.16% for a 6-hour tracking observation, which show the same efficiency of the *GA*.

The calculated *first SLL*, mean values of the first three *SLLs* (*mean SLL*), and the worst *SLL* defined as the *peak SLL* are shown in Table 4. The values of the

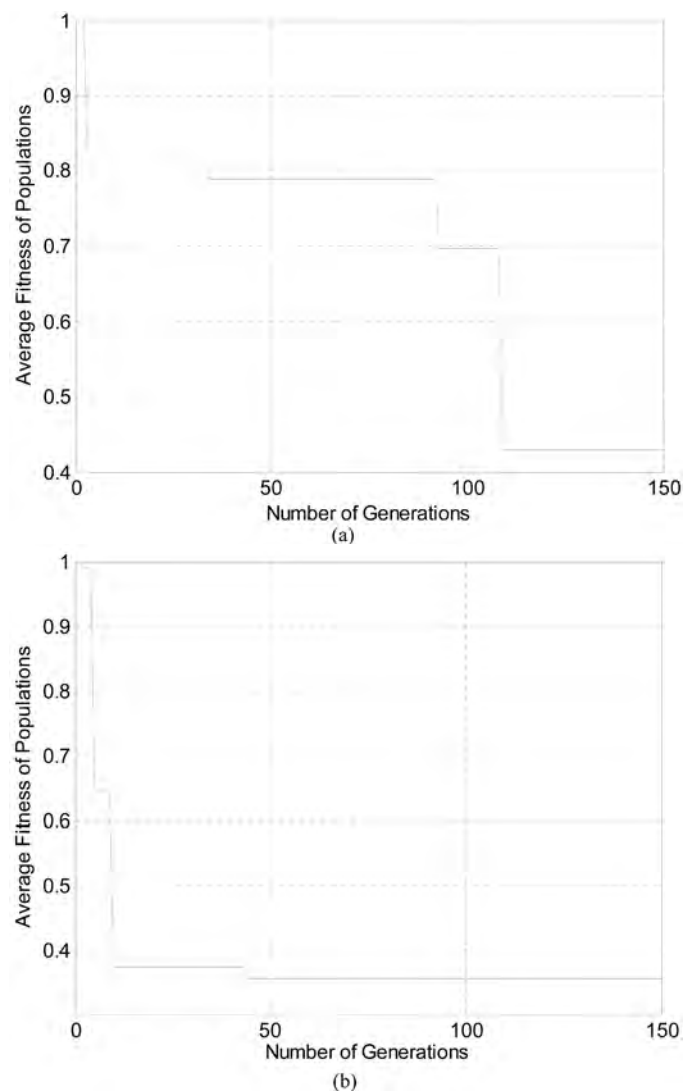


Figure 8. The evolution of average fitness in each generation in (a) the spatial frequency domain and (b) the l-m domain.

Table 4. Comparison of different configurations.

Configuration	First <i>SLL</i> (dB) (Hour tracking)	mean <i>SLL</i> (dB) (Hour tracking)	Peak <i>SLL</i> (dB) (Hour tracking)
25th generation	-6.99	-6.75	-3.03
150th generation1	-5.23	-8.45	-5.20
<i>DA</i> array	-10.00	-9.86	-5.88

Notes: 6-hour is used in hour tracking synthesize.

first SLL, *mean SLL*, and *peak SLL* are -6.99 dB, -6.75 dB, and -3.03 using the 25th generation, -5.23 dB, -8.45 dB, and -5.2 dB using the 150th generation, and -10 dB, -9.86 dB, and -5.88 dB for the *DA* array, respectively. It shows that even though the *GA* decreases the *SLL*, the *DA* gains reasonable *SLL* and optimum ratios in the spatial frequency domain, with the same population.

The evolution of the average fitness in each generation for the *u-v* plane coverage at the snapshot and *SLL* reduction is shown in **Figure 8**. As shown in **Figure 8(a)**, for the first 50 generations, the optimum solution is reached at the 38th generation. In contrast, for a total of 150 generations, a better solution is obtained at the 112th generation. Similarly, the fitness value for the first 50 generations in **Figure 8(b)** obtains the optimum solution at 43th generation. Since, the algorithm seeks for the solutions randomly; it provides different solutions for each generation.

4. Discussion

Astronomical observations benefit from arrays that can achieve high resolution with low *SLLs*, smooth linear ridges, and good *u-v* plane coverage. The aim of the study was to extend such an array to optimize the configuration. Therefore, the principal aim of the present simulation was to compare different extended configurations. Based on the results shown in **Table 1**, the spiral configuration or curved arm achieves good results in *l-m* domain and *u-v* domain. Also, it was found that the curvature smoothens the linear ridges for a low duration observation. Finally, the *GA* was able to provide good results for all the desired requirements.

Malaysia has started to get involved in astronomy project recently with two telescopes. As such, the second part of this study has investigated an optimum solution for the future correlator array antennas in Malaysia. Based on the results, it has been shown that the *DA* is able to obtain a configuration that provides almost all desired requirements in both spatial frequency domain and angular domain.

5. Conclusions

In conclusion, the aim of this study was to investigate different solutions to extend an interferometric array and the future array in Malaysia. For expanding the existing array, initially, the expansion along the three arms configuration was

studied and then the effect of expanding it to a spiral shape was evaluated. The results have shown that the spiral could provide better $u-v$ plane coverage in a 6-hour tracking synthesized observations (in an aperture synthesis observation of six hours duration) with the lowest levels of the SLL . Then, the GA was applied to the interferometric array. From the results (different results of $u-v$ plane coverage) shown in this paper, the extended curved arms have better $u-v$ coverage results than the extended Y -shaped. It also suppressed the $SLLs$. As such, the algorithm improves the number of overlapped samples, as the number of generations increases. Finally, the DA was applied to such an array. Calculated results in **Table 1** show that the DA method can sample the data more efficiency for the snapshot observation compared to the other configurations discussed in this paper.

Then, the GA and DA were applied to 10 antennas. Calculated results show that the DA can achieve the sampled data with the same efficiency as the GA for the snapshot observation. The calculated overlapped samples ratios for a 6-hour tracking are discussed. It is shown that the DA improves the overlapped samples ratio more efficiently than the GA for a 6-hour tracking observation.

Conflicts of Interest

The authors declare no conflicts of interest regarding the publication of this paper.

References

- [1] Shahideh, K., Cada, M., Chen, Z., Shahabi, A., Short, C.I., Abidin, Z.Z. and Samiramis, K. (2018) *Astronomical Journal*, **156**, 177.
- [2] Shahideh, K., Noordin, N.K., Sali, A. and Zamri, Z.A. (2014) *Astronomical Journal*, **147**, 147.
- [3] Shahideh, K., Valente, D., Cada, M., Noordin, N.K. and Shahabi, A. (2017) *Astronomical Journal*, **154**, 167.
- [4] Shahideh, K., Kyun, Ng.C. and Noordin, N.K. (2013) Expansion of a Y-Shaped Array Antennas for Radio Astronomy. 2013 *IEEE International Conference on Space Science and Communication (IconSpace)*, Melaka, 1-3 July 2013, 39.

Accurate, First-Principle Study of Electronic and Related Properties of the Ground State of Li_2Se

Abdoulaye Goita, Feng Gao, Ifeanyi H. Nwigboji, Yuriy Malozovsky, Lashounda Franklin, Diola Bagayoko*

Department of Physics, Southern University and A&M College, Baton Rouge, LA, USA

Email: *Diola_Bagayoko@subr.edu

How to cite this paper: Goita, A., Gao, F., Nwigboji, I.H., Malozovsky, Y., Franklin, L. and Bagayoko, D. (2019) Accurate, First-Principle Study of Electronic and Related Properties of the Ground State of Li_2Se . *Journal of Modern Physics*, 10, 909-921.

<https://doi.org/10.4236/jmp.2019.108060>

Received: May 13, 2019

Accepted: July 6, 2019

Published: July 9, 2019

Copyright © 2019 by author(s) and Scientific Research Publishing Inc.

This work is licensed under the Creative Commons Attribution International License (CC BY 4.0).

<http://creativecommons.org/licenses/by/4.0/>



Open Access

Abstract

We present results from ab-initio, self-consistent calculations of electronic and related properties for the ground state of cubic lithium selenide (Li_2Se). We employed a local density approximation (LDA) potential and performed computations following the Bagayoko, Zhao, and Williams (BZW) method, as enhanced by Ekuma and Franklin (BZW-EF). This method verifiably leads to the ground state of materials without employing over-complete basis sets. We present the calculated electronic energies, total and partial densities of states, effective masses, and the bulk modulus. The present calculated band structures show clearly that cubic Li_2Se has a direct fundamental energy band gap of 4.065 eV at the Γ point for the room temperature experimental lattice constant of 6.017 Å. This result is different from findings of previous density functional theory (DFT) calculations that uniformly reported an indirect band gap, from Γ to X_1 for Li_2Se . We predicted a direct band gap of 4.363 eV, at the computationally determined equilibrium lattice constant of 5.882 Å, and a bulk modulus of 35.4 GPa. For the first time known to us, we report calculated electron and hole effective masses for Li_2Se . The experimental confirmation of the large, direct gap we found will point to a potential importance of this material for ultraviolet technologies and applications. Due to a lack of experimental results, most of our calculated ones in this paper are predictions for Li_2Se .

Keywords

Density Functional Theory, BZW-EF Method, Electronic Properties, Bulk Modulus

1. Introduction

Alkali metal chalcogenides (X_2Ch , $\text{X} = \text{Li}, \text{Na}, \text{K}$; $\text{Ch} = \text{O}, \text{S}, \text{Se}, \text{Te}$) have high

ionic conductivity and large fundamental energy band gaps, leading to their promising applications in power sources, fuel cells, solid state gas-detectors, ultraviolet space technology devices and photocatalysis [1] [2] [3] [4]. Compared to the extensive studies on the alkali metals oxides and sulfides, the alkali metal selenides have received much less attention. Recently, several research works have focused on lithium selenide (Li_2Se) for its superionic (SI) properties. The fast Li^{1+} -ion transport of the SI Li_2Se solid makes it a prime candidate for solid-state electrolytes in next generation lithium battery technologies [5]. Up until now, however, experimental studies of electronic and related properties of Li_2Se are very few. As far as we know, most of the research work on Li_2Se has been confined to studies of its structural properties. No experimental measurements regarding the electronic and related properties of Li_2Se are available. Theoretically, only the following three research groups have performed first-principle calculations of electronic band structures of Li_2Se . We summarized their findings in **Table 1** below. Eithiraj *et al.* calculated the electronic structure of Li_2Se , using a Tight-Binding and Linear Muffin-Tin Orbital (TB-LMTO) method [6] [7] and the local density approximation (LDA) potential of von Barth and Hedin [8] [9]. Their results show that Li_2Se is an indirect band gap semiconductor, with a gap of 2.748 eV, from Γ to X . Alay-e-Abbas *et al.* calculated the band structures of Li_2Se using the Full Potential Linearized Augmented Plane Wave (FP-LAPW) method, as implemented in the WIEN2K program package [10], and density functional theory (DFT) potentials [11] [12]. Specifically, these authors employed a local density approximation (LDA), the Perdew-Burke-Ernzerhof [13] generalized gradient approximation (PBE-GGA), the Wu and Cohen [14] GGA (WU-GGA), which entails fourth-order gradient expansion of exchange energy function, and the Engel and Vosko [15] GGA (EV-GGA) potentials. The band structures calculated within the LDA, PBE-GGA, WC-GGA and EV-GGA potentials exhibit Γ to X indirect band gap values of 2.78 eV, 2.93 eV, 2.82 eV, and 4.08 eV, respectively.

Table 1. Previously calculated band gaps of Li_2Se . The computational approaches and the utilized DFT potentials are respectively in Columns I and II, while the two lowest, calculated gaps are in Columns III and IV.

Calculation Methods	Exchange-Correlation	Energy Band Gap, E_g (eV)	
		Direct (Γ - Γ)	Indirect (Γ - X)
FP-LAPW	LDA	3.23 [11]	2.78 [11]
FP-LAPW	PBE-GGA	3.45 [11]	2.93 [11]
FP-LAPW	WC-GGA	3.18 [11]	2.82 [11]
FP-LAPW	EV-GGA	4.73 [11]	4.08 [11]
FP-LAPW	WC-GGA	-	2.80 [15]
FP-LAPW	EV-GGA	-	4.12 [15]
FP-LAPW	mBJ	-	4.19 [15]
TB-LMTO	LDA	3.457 [8]	2.748 [8]

Ali *et al.* carried out first-principle DFT calculations of electronic properties of Li_2Se , using the FP-LAPW method and the WC-GGA as well as the EV-GGA potentials [16]. In their work, they utilized the recently modified Becke and Johnson (mBJ) potential [17], which is a “hybrid” potential whose amount of “exact exchange” is controlled by a parameter c , to improve the calculated, electronic band structure. The first-principles WC-GGA, EV-GGA and mBJ calculations by Ali *et al.* show that Li_2Se has a Γ to X indirect band gap of 2.80 eV, 4.12 eV, and 4.19 eV, respectively [16].

Our motivation for this work partly stems from current and potential applications of Li_2Se for the next generation of battery technologies. Accurate, calculated electronic and related properties are important in informing and in guiding the development of new applications. While previous DFT calculations agreed on the indirect nature of the band gap, the resulting numerical values range from 2.748 eV to 4.19 eV. Such a wide range points to the need for further theoretical studies of electronic and related properties of lithium selenide. The current lack of experimental studies of electronic and related properties of Li_2Se is an added motivation for this work. With our distinctive computational method, we have correctly described and predicted electronic and related properties of more than 30 semiconductors [18]. These past successes portend an accurate DFT description of this material, using our BZW-EF method. We describe below, in Section 2, the general computational approach and our distinctive method. We subsequently present our findings in Section 3. We then provide discussions and a conclusion in Sections 4 and 5, respectively.

2. Computational Method

In ambient conditions, Li_2Se crystallizes in a stable face center cubic (FCC) anti-fluorite (anti- CaF_2 -type) structure [19] (Space group $O_h^5 - Fm\bar{3}m$, No. 225), with the Li atoms located at $\pm (0.25, 0.25, 0.25)$ and the Se atoms at $(0, 0, 0)$ Wyckoff positions. In this work, we performed first-principle full-potential DFT calculations for the electronic properties of Li_2Se , using the experimental lattice constant of 6.017 Å from Zintl *et al.* [19] and our predicted, equilibrium lattice constant. We utilized a linear combination of atomic orbitals (LACO) formalism and the BZW-EF method, which has been extensively described in several of our previous publications [18] [20] [21] [22] [23]. Our first-principle LCAO package is from the Ames laboratory of the US Department of Energy, in Ames, Iowa [24] [25]. We began the calculations with self-consistent computations for the atomic wave functions for Li^{1+} and Se^{2-} atoms. The radial parts of the atomic wave functions were expanded in terms of Gaussian functions. The s , p orbitals for the cation Li^+ were described with 16 even-tempered Gaussian functions with respective minimum and maximum exponents of 0.2400 and 0.90×10^5 for the atomic potential and 0.1200 and 0.90×10^5 for the atomic wave functions. The self-consistent calculations for Li^+ led to the total charge of 2.0009, which is also the valence charge. For Se^{2-} the s , p and d orbitals were described with 24 even-tempered Gaussian functions with respective minimum and maximum

Gaussian exponents of 0.2300 and 0.220×10^6 for the atomic potential and 0.1350 and 0.240×10^6 for the atomic functions, respectively. These Gaussian exponents led to the convergence of the atomic calculations. We utilized the Ceperley and Alder local density approximation (LDA) potential. In the iterations for self-consistency, we used a mesh of 60 k -points with proper weights in the irreducible Brillouin zone. We reached convergence for a given self-consistent calculation after 90 iterations; the criterion for convergence was that then, the difference between the potentials from the last two consecutive iterations was 10^{-4} or less. Further, for the production of the final, self-consistent electronic band structures, we used a total of 81 k points in the Brillouin zone, with the same computational errors as for the self-consistent potential calculations. Based on the above points, our computational approach is the same as those of other DFT calculations. We underscore below the critically important, distinctive feature of our computational method, with multiple, self-consistent calculations with basis sets of different sizes.

Our *ab initio* self-consistent calculations for the solid, with the BZW-EF method, began with a small basis set containing the minimum basis set, which is the smallest one accounting for all the electrons in the system under study, *i.e.*, Li_2Se . Following this Calculation I, we augmented the basis set with one orbital representing an excited state and performed Calculation II. We graphically and numerically compared the occupied energies from Calculations I and II, with the Fermi levels set to zero. After augmenting the basis set of Calculation II with one orbital, we carried out Calculation III and compared the resulting occupied energies with those from Calculation II. In both of the preceding comparisons of occupied energies, at least some of the ones obtained with the larger basis set were lower than corresponding ones from the immediately preceding calculation (with a smaller basis set). We continued this process of augmenting the basis set and of performing self-consistent calculations until three consecutive ones led to the same occupied energies. The perfect superposition of these occupied energies is the criterion or proof that these calculations produced the absolute minima of the occupied energies, *i.e.*, the ground state of the system.

Let N be the number of the first of these three calculations to reach the ground state. We dubbed the basis set of this calculation as the *optimal basis set*, *i.e.*, the *smallest basis set that leads to the ground state upon the attainment of self-consistency*. Calculations $(N + 1)$, $(N + 2)$ and other with larger, augmented basis sets produced (a) the same charge density, (b) the same Hamiltonian, and (c) the same occupied energies as respectively obtained with Calculation N . We distinguish the Hamiltonian from the Hamiltonian matrix that changes with the size of the basis set. Despite (a) through (c) above, some unoccupied energies from calculations $(N + 1)$, $(N + 2)$ and others with larger, augmented basis sets, were generally lower than corresponding ones obtained in Calculation N . Given that the Hamiltonian did not change from that of Calculation N , any eigenvalues that deviate from (*i.e.*, are lower than) their corresponding values resulting from Calculation N are clearly unphysical. Another proof of this assertion stems from

the second corollary¹⁸ of the first DFT theorem: According to it, the spectrum of the ground state Hamiltonian is a unique functional of the ground state charge density. Hence, if an eigenvalue from Calculation (N + 1) or higher is different (lower than) its corresponding value obtained in Calculation N, then the new value no longer belongs to the spectrum of the Hamiltonian—as the charge density did not change. In summary, Calculation N is the only one providing the true DFT description of the material; the resulting eigenvalues possess the full physical content of the DFT, unlike eigenvalues resulting from self-consistent iterations with a single basis set. These iterations produce stationary solutions among an infinite number of such solutions. Our generalized minimization of the energy functional of the Hamiltonian, using successive, self-consistent calculations, verifiably reaches the true ground state of the system—instead of an arbitrary, stationary solution unwittingly confused with the ground state.

3. Results

Table 2 shows the successive calculations inherent to the implementation of the BZW-EF method. Calculation III-V were the first ones to reach the ground state of the system, as explained above in the method section. As per the explanations in this method section, Calculation III is the one providing the DFT description of Li₂Se. **Table 2** also shows the specific orbitals for the two ionic species, the total number of valence functions (with the number of orbitals for Li⁺ counted twice for Li₂Se), and the calculated band gaps at the Γ point, from Γ to X, and from Γ to K. The superscript of zero for an orbital signifies that it represents an unoccupied state, *i.e.*, an excited state.

Figure 1 shows the calculated, electronic band structures of Li₂Se along high symmetry k points in the irreducible Brillouin zone, as obtained in Calculations III and IV of the BZW-EF method.

Table 2. Successive, self-consistent calculations in the implementation of the BZW-EF method of the generalized minimization of the energy. The band gaps are in the last three columns, in eV. For the total number of valence functions, the number of orbitals on Li⁺ is counted twice. The smallest band gap is direct, for Calculations I-V, it is indirect for Calculation VI. Calculation III provides the DFT description of Li₂Se; it is the first of three consecutive ones leading to the same absolute minima of the occupied energies (*i.e.*, the ground state, with a direct band gap of 4.065 eV at Γ).

Cal. No.	Orbitals for Li ⁺	Orbitals for valence state of Se ²⁻	No. of Valence Functions	Gap (at Γ) in eV	Gap (Γ -X) in eV	Gap (Γ -K) in eV
I	1s ² 2s ⁰ 2p ⁰	3s ² 3p ⁶ 3d ¹⁰ 4s ² 4p ⁶	46	4.111	4.551	5.427
II	1s ² 2s ⁰ 2p ⁰	3s ² 3p ⁶ 3d ¹⁰ 4s ² 4p ⁶ 4d⁰	56	4.096	4.536	5.412
III	1s ² 2s ⁰ 2p ⁰ 3p⁰	3s ² 3p ⁶ 3d ¹⁰ 4s ² 4p ⁶ 4d ⁰	68	4.065	4.395	5.195
IV	1s ² 2s ⁰ 2p ⁰ 3p ⁰ 3s⁰	3s ² 3p ⁶ 3d ¹⁰ 4s ² 4p ⁶ 4d ⁰	72	4.023	4.394	5.172
V	1s ² 2s ⁰ 2p ⁰ 3p ⁰ 3s ⁰	3s ² 3p ⁶ 3d ¹⁰ 4s ² 4p ⁶ 4d ⁰ 5p⁰	78	3.940	4.221	4.967
VI	1s ² 2s ⁰ 2p ⁰ 3p ⁰ 3s ⁰	3s ² 3p ⁶ 3d ¹⁰ 4s ² 4p ⁶ 4d ⁰ 5p⁰5s⁰	80	3.923	3.900	4.883

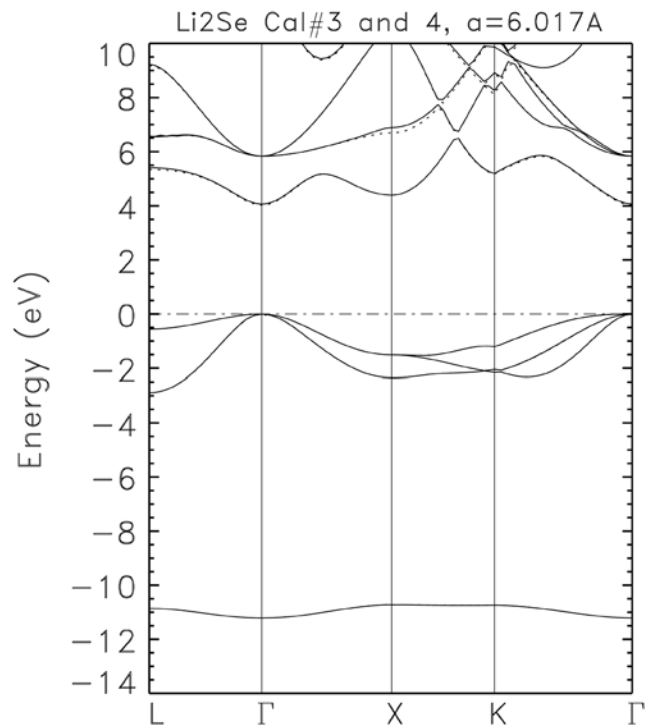


Figure 1. Calculated band structure of Li_2Se , as obtained in Calculations III and IV of the BZW-EF method. The occupied energies from the two calculations are perfectly superimposed. No calculations with basis sets resulting from augmenting that of Calculation III produce occupied energies lower than their corresponding values from Calculation III.

From this figure and the content of **Table 2** above, we conclude that Li_2Se is a direct band gap semiconductor; this result is in stark disagreement with the previously reported DFT band gaps, in **Table 1**, that are uniformly given that all of these previous gaps are indirect. The top of the valence band and the bottom of the conduction bands are both at the Γ point. From the results of Calculation III, performed with the optimal basis sets, the calculated DFT band gaps of the material are 4.065 eV (at Γ), 4.395 (Γ -X) and 5.195 eV (Γ -K), respectively.

In **Table 3**, we list illustrative, calculated, electronic energies for Li_2Se at high symmetry points (Γ , X, K, and L) in the Brillouin zone. These energies are expected to be useful in comparisons of our findings with future, experimental results. Such results include direct, optical transition energies and various X-ray and ultraviolet (UV) spectroscopic measurements.

Figure 2 shows the total electronic density of states (DOS) derived from the bands produced in Calculation 3, with the optimal basis set. The inset presents the magnified DOS in the vicinity of the band gap. This inset suggests a relatively sharp absorption edge starting around 4 eV. The total valence bandwidth is about 11.22 eV, from the DOS figure, and 11.21 eV, from the above table of eigenvalues. From the DOS figure, the width of the lowest lying valence band is 0.456 eV, while that of the group of upper valence bands is about 2.93 eV. The peaks in the DOS for the conduction band are at 5.74 eV, 6.653 eV, 8.86 eV, and 9.47 eV, according to **Figure 2**.

Table 3. At the room temperature lattice constant of 6.017 Å, the calculated eigenvalues (in eV), along high symmetry points, for rock salt Li_2Se are shown below. They resulted from Calculation III, the first to reach the ground state of the system.

Γ -point	X-point	K-point	L-point
14.367	15.494	14.907	13.690
12.251	12.993	13.748	13.109
12.251	12.993	10.588	11.760
12.251	11.615	10.353	11.760
5.836	10.509	9.875	9.221
5.836	10.509	8.918	6.573
5.836	6.889	8.264	6.548
4.065	4.395	5.194	14.907
0.000	-1.509	-1.207	-0.557
-0.003	-1.509	-2.041	-0.557
-0.003	-2.347	-2.142	-2.889
-11.211	-10.724	-10.739	-10.857

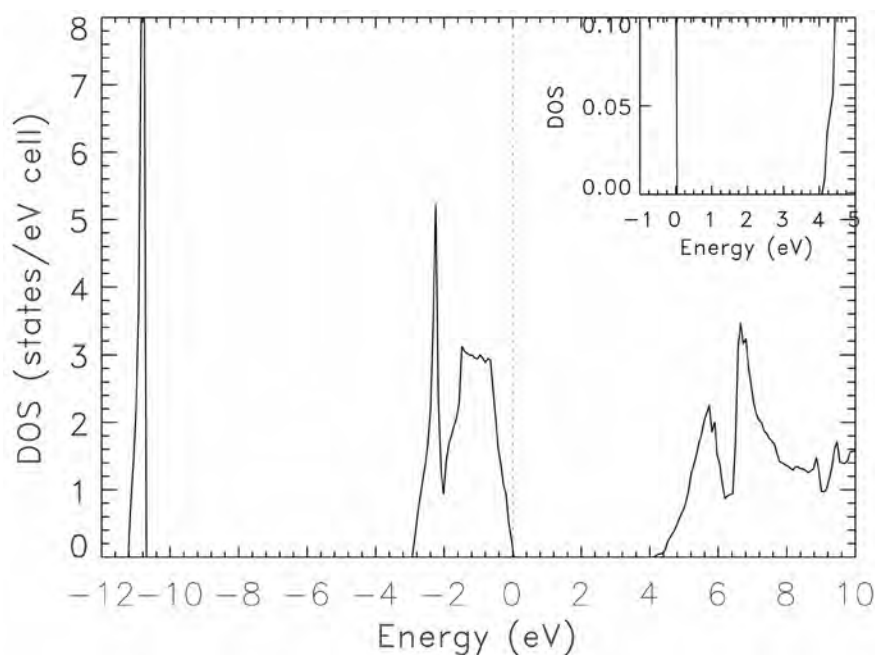


Figure 2. Calculated, total density of states (DOS) for Li_2Se , as derived from the bands resulting from Calculation III, the first to reach the ground state. The vertical line at zero indicates the position of the Fermi level. The inset suggests a relatively sharp absorption edge in the vicinity of 4 eV.

We present the electronic, partial DOS (pDOS) in **Figure 3**. These densities are also derived from the bands obtained with the optimal basis set. From the pDOS, we see that the valence band of Li_2Se is almost exclusively composed of Se s and p states. In other words, these bands are described by the s and p atomic

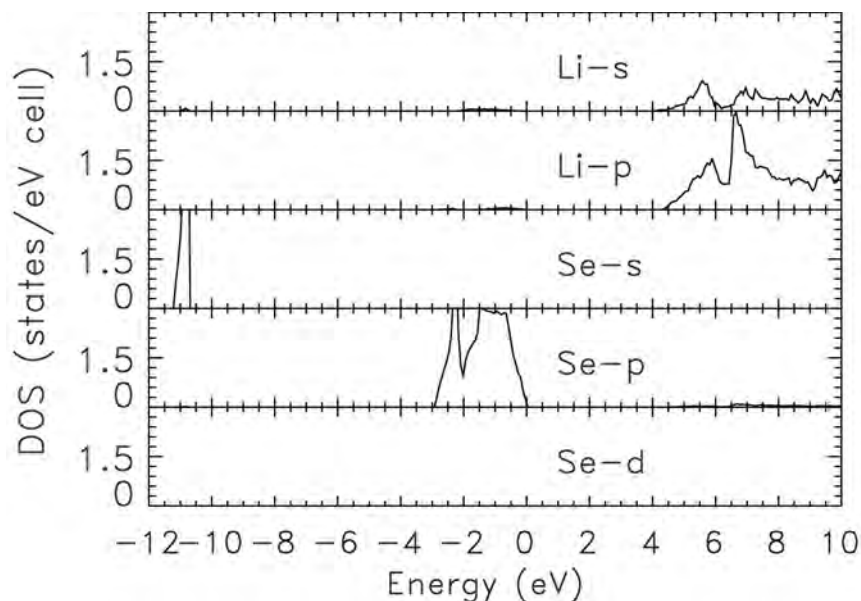


Figure 3. Calculated, partial densities of states (pDOS) for Li_2Se , as derived from the band resulting from Calculation, the first one to reach the ground state of the system. Zero on the horizontal axis indicates the position of the Fermi level.

orbitals on Se. More specifically, the lowest laying valence band is dominated by Se s state, with a feint contribution from Li-s. The uppermost group of valence bands is from Se p state. The conduction bands are mainly from the hybridization of Li p and s, with the domination of the former. Se d (3d), even though treated as valence states in the calculations, turned out to belong to the core states. The pDOS figure shows that Se 4d contributes to much higher, excited states. The above features of the band structure can be measured in various X-ray and UV spectroscopic investigations, as was the case for our calculations of electronic and related properties of wurtzite aluminum nitride [26].

The electrical conductivities, and transport and other related properties of materials require an accurate and detailed knowledge of effective masses. As per the content of **Table 4**, we have performed calculations of electron effective masses around the minimum of the conduction band, at the Γ point, and around the next, lowest conduction band minimum at the X-point. We have calculated the effective masses of the light and the two heavy holes at the top of the valence band, at the Γ -point. We list these calculated, effective masses in **Table 4** below, for various directions, in units of the mass of the electron (m_0). The effective masses of heavy Hole 1 and heavy Hole 2 are equal, except in the $(\Gamma\text{-K})_{110}$ direction. Their difference in that direction is due to the splitting of the bands in the $(\Gamma\text{-K})_{110}$ direction by the Coulomb crystal field. The hole effective masses are much more anisotropic than those for the electron. The calculated electron effective mass for antifluorite Li_2Se , in the vicinity of the Γ point, is nearly isotropic and is equal to $0.352 m_0$. The electron effective masses at the X point are essentially anisotropic, with the longitudinal electron effective mass of $0.647 m_0$ in the X to Γ direction, with the transverse electron effective mass of $0.413 m_0$ in

the X to K direction, and of $0.464 m_0$ in the X to U direction. The value of the heavy Hole 1 effective mass is $2.33 m_0$ in the Γ to L direction $(\Gamma-L)_{111}$, $1.17 m_0$ in the Γ to X direction $(\Gamma-X)_{100}$, and $1.53 m_0$ in the Γ to K direction $(\Gamma-K)_{110}$. This hole effective mass is strongly anisotropic. The heavy Hole 2 effective mass in the $(\Gamma-K)_{110}$ direction is $0.989 m_0$. The effective masses of light Hole are $0.292 m_0$ in the $(\Gamma-L)_{111}$ direction, $0.515 m_0$ in the $(\Gamma-X)_{100}$ direction, and $0.343 m_0$ in the $(\Gamma-K)_{110}$ direction. We found no experimental values for these effective masses. We expect future measurements to confirm our predictions in **Table 4**.

The graph of the total energy versus the lattice constant is shown in **Figure 4**

Table 4. Calculated, effective masses for antiferroite Li_2Se , in units of free electron mass (m_0). M_e indicates an electron effective mass at Γ or at X.; M_{hh} and M_{lh} denote the heavy and light hole effective masses, respectively.

Types and Directions of Effective Masses	Values of Effective Masses (m_0)
M_e	0.352
M_e (X- Γ) Longitudinal	0.647
M_e (X-K) Transverse	0.413
M_e (X-U) Transverse	0.464
M_{hh1} (Γ -L) ₁₁₁	2.33
M_{hh1} (Γ -X) ₁₀₀	1.17
M_{hh1} (Γ -K) ₁₁₀	1.53
M_{hh2} (Γ -K) ₁₁₀	0.989
M_{lh} (Γ -L) ₁₁₁	0.292
M_{lh} (Γ -X) ₁₀₀	0.515
M_{lh} (Γ -K) ₁₁₀	0.343

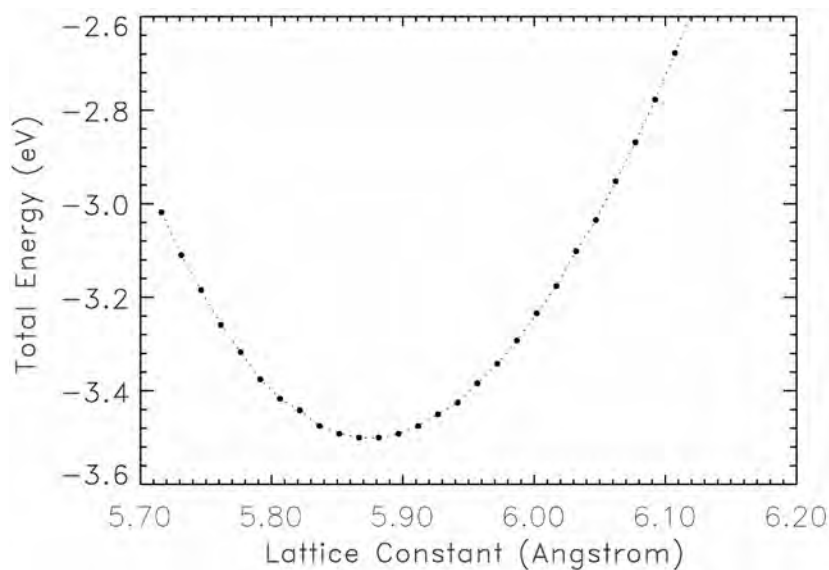


Figure 4. The total energy per unit cell, for Li_2Se . The minimum of the curve occurs at $a = 5.882 \text{ \AA}$. The predicted, direct, band gap (Γ - Γ) at this lattice constant is 4.363 eV .

below. The range of the lattice constant in which our total energy values were obtained is 5.70 to 6.20 Å. The minimum of the total energy curve is at 5.882 Å, which is our predicted equilibrium lattice constant. With this lattice constant, we predicted at zero temperature band gap of 4.363 eV at the Γ point, larger than the room temperature value by 0.298 eV. Our calculated bulk modulus is 35.4 GPa; it is the same as the finding of Ali *et al.* [16] and is slightly larger than the calculated result of 34.72 GPa of Alay-e-Abbas [11] [12]. No experimental measurements for the bulk modulus of Li_2Se are available for comparison.

4. Discussion

The following discussion is guided by the fact that our calculations, as explained in the section on our method, 1) verifiably attained the ground state of the system 2) while avoiding over-complete basis sets. The latter feature guarantees that spuriously low, unoccupied energies are not in the spectrum of the ground state Hamiltonian. The two features further guarantee that the eigenvalues obtained with the optimal basis set, defined earlier, possess the full, physical content of DFT. The claim in the literature that DFT eigenvalues do not have any particular physical meaning does not apply to our findings that are true ground state results.

As shown in **Table 1**, all previous DFT calculations produced indirect band gaps for Li_2Se , in stark contrast to our calculated, direct (Γ - Γ) band gaps of 4.065 eV and 4.363 eV, respectively, obtained with room temperature and the equilibrium lattice constants. Additionally, while three of the previous GGA results (4.08 - 4.19 eV) are numerically close to ours, the latter is larger by 1.135 or more than five (5) GGA and LDA results in **Table 1**. The excellent agreement between our previous results and corresponding, experimental ones [8] portends a future, experimental confirmation of our findings. Such a confirmation will point to extensive, potential importance of Li_2Se in various ultraviolet technologies and applications.

Most DFT calculations in the literature perform self-consistent iterations with a single basis set to produce results that are assumed to describe the ground state of the system. Such a single basis is deliberately chosen to be large, more often than not. This choice is to avoid possibilities for the basis set to be incomplete, *i.e.*, not large enough in size (number of functions) or not rich enough in radial and angular features to accommodate the redistribution of the charge density in the formation of the system under study. As explained in our method section, large basis sets that contain the optimal one can lower some unoccupied energies; the larger the basis set, the larger the lowering is.

Hence, we should expect single basis set calculations by different authors to produce different underestimates of the band gap of a semiconductor, even if they employ the same DFT potential and similar computational approaches. The outcomes of our Calculation VI illustrate the point. Let us first recall that calculations with large basis sets resulting from an augmentation of the optimal basis set do not lower any occupied energies from their value obtained with the op-

timal basis set. Additionally, if such basis sets are not significantly larger than the optimal one, they also reproduce low lying, unoccupied energies obtained with the optimal basis set. The content of **Figure 1** shows that the low lying, unoccupied energies produced by Calculation IV are the same as those from Calculation III, up to +6 eV. The values of the band gaps resulting from Calculation VI, whose basis set contains 12 more functions than the optimal one, illustrate the point. This calculation not only reduced the band gaps from their values obtained in Calculation III, but also it resulted in an indirect (Γ -X) band gap. The latter feature is in qualitative agreement with the findings of the previous DFT calculations shown in **Table 1**; we presume that these single basis set calculations most likely utilized relatively large basis sets.

5. Conclusion

In summary, we performed first principle, self-consistent calculations of electronic, transport, and bulk properties of cubic antiferroelectric lithium selenide (Li_2Se), using a local density approximation (LDA) potential. As per the BZW-EF method, our implementation of the linear combination of atomic orbitals entailed the performance of successive, self-consistent calculations with increasingly large basis sets. We obtain the basis set of a calculation, except for the first one that has a small basis set, by augmenting the basis set of the immediately preceding calculation with one orbital. This generalized minimization of the energy not only reached the ground state, but also does so without employing over-complete basis sets that tend to lower, unphysically, some unoccupied energies. This fact suggests that the widespread underestimation of the band gaps of semiconductors and insulators, by DFT calculations, may be due to this spurious lowering of unoccupied energies. Our calculated, indirect band gap of Li_2Se , at room temperature, is 4.065 eV. This result is in stark contrast with those from previous DFT calculations that found an indirect band gap. The accurate results we obtained for more than 30 semiconductors are the basis for us to expect a future, experimental confirmation of our results for the energy bands, the densities of states, effective masses, and the bulk modulus of Li_2Se .

Acknowledgements

This research work was funded in part by the US Department of Energy (DOE), National Nuclear Security Administration (NNSA) (Award No. DE-NA0003679), the National Science Foundation (NSF, Award no, 1503226DE), LaSPACE, and LONI-SUBR.

Conflicts of Interest

The authors declare no conflicts of interest regarding the publication of this paper.

References

- [1] Minami, T., Hayashi, A. and Tatsumisago, M. (2000) *Solid State Ionics*, **136-137**,

- 1015-1023. [https://doi.org/10.1016/S0167-2738\(00\)00555-5](https://doi.org/10.1016/S0167-2738(00)00555-5)
- [2] Bisero, D., Oerle, B.M.V., Ernst, G.J., Verschuur, J.W.J. and Witteman, W.J. (1996) *Applied Physics Letters*, **69**, 3641. <https://doi.org/10.1063/1.117009>
- [3] Bisero, D., Oerle, B.M.V., Ernst, G.J., Verschuur, J.W.J. and Witteman, W.J. (1997) *Journal of Applied Physics*, **82**, 1384. <https://doi.org/10.1063/1.365915>
- [4] Hull, S., Farley, T.W.D., Hayes, W. and Hutchings, M.T. (1988) *Journal of Nuclear Materials*, **160**, 125. [https://doi.org/10.1016/0022-3115\(88\)90039-6](https://doi.org/10.1016/0022-3115(88)90039-6)
- [5] Dumett Torres, D. and Jain, P.K. (2018) *The Journal of Physical Chemistry Letters*, **9**, 1200. <https://doi.org/10.1021/acs.jpcclett.8b00236>
- [6] Andersen, O.K. (1975) *Physical Review B*, **12**, 3060. <https://doi.org/10.1103/PhysRevB.12.3060>
- [7] Andersen, O.K. and Jepsen, O. (1984) *Physical Review Letters*, **53**, 2571. <https://doi.org/10.1103/PhysRevLett.53.2571>
- [8] Eithiraj, R.D., Jaiganesh, G. and Kalpana, G. (2009) *International Journal of Modern Physics B*, **23**, 5027-5037. <https://doi.org/10.1142/S0217979209052418>
- [9] Barth, U.V. and Hedin, L. (1972) *Journal of Physics C: Solid State Physics*, **5**, 1629-1642. <https://doi.org/10.1088/0022-3719/5/13/012>
- [10] Blaha, P., Schwarz, K., Madsen, G.K.H., Kvasnicka, D. and Luitz, J. (2001) WIEN2K: An Augmented Plane Wave + Local Orbitals Program for Calculating Crystal Properties. Karlheinz Schwarz, Techn. Universität Wien, Wien.
- [11] Alay-e-Abbas, S.M., Sabir, N., Saeed, Y. and Shaukat, A. (2010) *Journal of Alloys and Compounds*, **503**, 10-18. <https://doi.org/10.1016/j.jallcom.2010.05.014>
- [12] Alay-e-Abbas, S.M., Sabir, N., Saeed, Y. and Shaukat, A. (2011) *International Journal of Modern Physics B*, **25**, 3911-3925. <https://doi.org/10.1142/S02179792110093X>
- [13] Perdew, J.P., Burke, K. and Ernzerhof, M. (1996) *Physical Review Letters*, **77**, 3865-3868. <https://doi.org/10.1103/PhysRevLett.77.3865>
- [14] Wu, Z. and Cohen, R.E. (2006) *Physical Review B*, **73**, Article ID: 235116.
- [15] Engel, E. and Vosko, S.H. (1993) *Physical Review B*, **47**, Article ID: 13164. <https://doi.org/10.1103/PhysRevB.47.13164>
- [16] Ali, R., Khanata, R., Amin, B., Murtaza, G. and Bin Omran, S. (2013) *International Journal of Modern Physics B*, **27**, Article ID: 1350170. <https://doi.org/10.1142/S0217979213501701>
- [17] Becke, A.D. and Johnson, E.R. (2006) *The Journal of Chemical Physics*, **124**, Article ID: 221101. <https://doi.org/10.1063/1.2213970>
- [18] Bagayoko, D. (2014) *AIP Advances*, **4**, Article ID: 127104. <https://doi.org/10.1063/1.4903408>
- [19] Zintl, E., Harder, A. and Dauth, B. (1934) *Zeitschrift für Elektrochemie und angewandte physikalische Chemie*, **40**, 588-593.
- [20] Bagayoko, D., Zhao, G.L., Fan, J.D. and Wang, J.T. (1998) *Journal of Physics: Condensed Matter*, **10**, 5645-5655. <https://doi.org/10.1088/0953-8984/10/25/014>
- [21] Zhao, G.L., Bagayoko, D. and Williams, T.D. (1999) *Physical Review B*, **60**, 1563. <https://doi.org/10.1103/PhysRevB.60.1563>
- [22] Franklin, L., Ekuma, C.E., Zhao, G.L. and Bagayoko, D. (2013) *Journal of Physics and Chemistry of Solids*, **74**, 729-736. <https://doi.org/10.1016/j.jpccs.2013.01.013>
- [23] Chinedu, E.E. and Diola, B. (2011) *Japanese Journal of Applied Physics*, **50**, Article

ID: 101103.

- [24] Feibelman, P.J., Appelbaum, J.A. and Hamann, D.R. (1979) *Physical Review B*, **20**, 1433-1443. <https://doi.org/10.1103/PhysRevB.20.1433>
- [25] Harmon, B.N., Weber, W. and Hamann, D.R. (1982) *Physical Review B*, **25**, 1109. <https://doi.org/10.1103/PhysRevB.25.1109>
- [26] Nwigboji, I.H., Ejembi, J.I., Malozovsky, Y., Khamala, B., Franklin, L., Zhao, G., Ekuma, C.E. and Bagayoko, D. (2015) *Materials Chemistry and Physics*, **157**, 80-86. <https://doi.org/10.1016/j.matchemphys.2015.03.019>

The World in an Equation: A Reappraisal of the Lemaître's Primeval Cosmic Rays

Russell Bagdoo

Independent Searcher, Saint-Bruno, Quebec, Canada

Email: rbagdoo@gmail.com, rbagdoo@yahoo.ca

How to cite this paper: Bagdoo, R. (2019) The World in an Equation: A Reappraisal of the Lemaître's Primeval Cosmic Rays. *Journal of Modern Physics*, 10, 922-952. <https://doi.org/10.4236/jmp.2019.108061>

Received: May 29, 2019

Accepted: July 6, 2019

Published: July 9, 2019

Copyright © 2019 by author(s) and Scientific Research Publishing Inc. This work is licensed under the Creative Commons Attribution International License (CC BY 4.0). <http://creativecommons.org/licenses/by/4.0/>



Open Access

Abstract

Based on radioactive phenomena (weak force), Georges Lemaître conceives, as soon as 1927, the primeval universe as a “unique super-dense quantum”, whose disintegration gave birth to all the current components of the universe [1] [2]. Using quantum mechanics, he proposes to explain the origins of the world from the point of view of quantum theory. He believes to find in the cosmic rays the manifestation of the initial fragmentation. However, regardless of the adopted cosmology, the hypothesis of the primeval atom (cold big bang) had no equation to support it and was not retained. Like all other cosmologists, he fell back on the Friedmann-Einstein equation with a repulsive cosmological constant which, according to supernova observations at the end of the millennium, propels expansion towards infinity. We juxtapose our equation of “quantum cosmology” to this equation of relativistic cosmology. We have already proposed this equation in an earlier paper [3], which has its source in quantum mechanics and fits Lemaître's hypothesis of the “primeval atom”. It's an equation in which the concept of matter-space-time is mathematically connected; gravitation and electromagnetism are also bound by space-time. A mechanism is described showing how velocity, time, distance, matter and energy, are correlated. We are led to ascertain that gravity and electricity are two distinct manifestations of a single underlying process: electrogravitation. For the first time, the cosmological time, considered as a real physical object, is integrated into a “cosmological equation” which makes coherent what we know regarding the time (its origin, its flow...), the matter and the space. Moreover, the equation indicates a constantly decelerated expansion. The concentration of the material medium and the importance of the decreasing energy of the vacuum contribute to the progressive increase of the positive pressure which becomes responsible for the increasing deceleration of the expansion. Does this mean that our equation leads us inevitably to the hypothesis of the primeval atom for the whole cosmos? Certainly not, since our model includes both the hot Gamow model and the cold Lemaître

model. The term “dynamic evolution” (used in the beginning by specialists for big bang models) is appropriate for our model since there is both an explosive origin and, throughout the expansion, a disintegration of a hyper-dense matter. The discovery of cosmic microwave background radiation has confirmed the hot big bang model that Gamow and his team have achieved. The predicted light prevailed over the primitive cosmic rays (particles) suggested by Lemaitre. Nevertheless, we think that Lemaitre was also right. The so-called big bang theory (singular cataclysmic explosion), in addition to not meeting basic criteria of science, is contradicted by several observations that are ignored. For example, the work of Armenian astronomers has convinced us that the origin of cosmic particles results not only from supernova explosions, but also from the partition of radio galaxies, not only from the death of the world, but also from their birth.

Keywords

Theory of Relation, Irreversible Cosmological Time, π , Deceleration, New Variable, Quantum Cosmology, Primeval Atom, Cosmic Rays

1. Introduction

The standard model of the big bang theory, in its main features, is widely distributed in the general public, at the risk of doing that the history of the universe is from now on an acquired knowledge. To describe our universe, the cosmological model relies on fundamental laws supposed to describe all the phenomena of nature, which it extrapolates to cosmic scales. But, in order for this model to be in agreement with all the astronomical observations (the acceleration of the expansion of the universe highlighted in 1998), it was necessary to introduce a dark energy of which no physical theory explains the origin.

If general relativity describes gravitation at cosmological scales, then the expansion of the universe can be accelerated only under one condition: the matter that dictates the dynamics of the universe today must be such that the sum its energy density and of three times its pressure is negative. For this, a repulsive black energy has been inserted in the Einsteinian equations. This new material component incorporated in the model in the form of a cosmological constant would be only a manifestation of the quantum fluctuations of the vacuum. The calculations lead to a value between 10^{60} and 10^{120} times greater than that deduced from cosmological observations. Which is a real disaster!

But this does not end here. When, in 1998, cosmologists announced that, based on a study of 21 Type-1A supernovae, the very fabric of space was expanding, they concluded that they were a proof of a positive cosmological constant and a hitherto unsuspected dark energy that accelerated the expansion of space [4]. In our view, it was a botched and biased study to preserve the construction of the standard cosmological model. In a previous article about the Pioneer effect, we said the deceleration of the probe in distant spaces where the

wavelength of space-time grows is in itself an experimental proof of a world in deceleration [5]. In another article on the positive cosmological constant starting from type Ia supernovae observations, we showed that its official accreditation in 1998 was premature and misinterpreted [6].

Subsequently, by adding type Ia supernovae, astronomical teams confirmed these data, others revealed systematic uncertainties, and no clear evidence was found for a possible evolution of the slope (beta) of the color-luminosity relation with the redshift [7], direct evidence of dark energy rather weak [8], serious doubts about the acceleration of the universe [9], statistical analysis of supernovae data-set that leaves much to be desired [10], results consistent with a cosmological constant that give only weak constraints on a w that varies with redshift [11], etc. Despite serious reservations, three astronomers received the Nobel Prize in Physics in 2011 for their discovery that the universe was growing at an accelerated rate.

In 2016, an international team of physicists, approaching the problem with a fresh look, questioned the acceleration of the expansion of the universe [12]. As Subir Sarkar, a researcher at Oxford University, reports: “We analysed the latest catalogue of 740 Type Ia supernovae—over 10 times bigger than the original samples on which the discovery claim was based—and found that the evidence for accelerated expansion is, at most, what physicists call ‘3 sigma’. This criterion is far short of the ‘5 sigma’ standard required to claim a discovery of fundamental significance.” Instead of finding evidence to support the accelerated expansion of the universe, Sarkar and his team say it looks like the universe is expanding at a constant rate [13].

If expansion is constant, drawing new physics with dark energy is not necessary. Does this also mean that the fundamental principles of the standard cosmological model do not have to be questioned? They must be called into question because, despite the consolidations for the big bang theory and the setting of the fundamental parameter values for thirty years, it is a model “weaken” by the theory of inflation in effect. Recall that the satellite XMM-Newton of Agency’s European Space X-ray observatory (ESA) [14], has returned data about the nature of the universe indicating that the universe must be a high-density environment, in clear contradiction to the “concordance model” (according to which the universe is today composed of about 73% of dark energy) linked to the theory of inflation (whose origin is unknown). In a survey of distant clusters of galaxies, the results of XMM-Newton revealed that today’s clusters of galaxies are superior to those present in the universe around seven thousand million years ago. Such a measure also goes toward a decelerated expansion [15].

The acceleration of the universe and the repulsive dark energy are the two components of the inflation theory, which was supposed to be the miracle cure for the pathology of the causality of the standard model. It seems that the remedy is worse than the disease. There is no convincing theoretical explanation for the existence of dark energy, its nature or its magnitude. The so-called accelera-

tion of the universe only further demonstrates that the theories of fundamental particles and gravity are incorrect or incomplete. Most experts believe that it will take nothing less than a revolution in our understanding of fundamental physics to achieve a complete understanding of cosmic expansion. For these reasons, we propose our quantum cosmological model.

It contains an equation, developed in an earlier work [3], which is doubly hybrid: quantum and relativistic by its construction, revealing and embarrassing because of its consequences. If it elegantly gives a natural place to cosmological time, it reveals objects that are hated: negative energies. The purpose of this paper, besides the exposure of this equation, is to present the hypothesis of the primitive atom of Georges Lemaitre at the origin of the concepts of expanding universe and big bang. Lemaitre had anticipated the fundamental role played by quantum mechanics, vacuum energy and the existence of a fossil radiation. In the absence of an equation to support his vision, he adopted the Einstein-Friedmann equation, which led to the current acceleration of expansion. We think that our equation is the one that Lemaître was missing from the start.

This paper is divided into four parts, intended to be complementary. In 2.1 and 2.3 the equation of the theory of Relation presents the universe as an expanding super-atom. In 2.2 we emphasize the importance of pi in the equation. In 2.4 expansion... and yet it decelerates! In 3.1 we discuss the hypothesis of the primeval atom of Georges Lemaitre. In 3.2 some features of the history of the standard big bang. In 3.3 the hypothesis of the primeval atom of Lemaitre is confronted with that of the primitive atom of Gamow. In 3.4 we discuss about Lemaître's primeval cosmic rays. In 3.5 we discuss to find out if Lemaitre's cold model is as true as Gamow's hot model. In 4.1 we show how the cosmological time in our equation links the physics of the infinitely large to that of the infinitely small. In 4.2 we browse Planck's units through our equation. In 4.3 we present M_{vp}^2 , the new essential parameter. In 5 we list the advantages of this quantum cosmological model and its equation which gives the same results as those obtained with the classical models which refer to the Einstein-Friedmann equation. Nature of our universe: everything happens as if there were two universes in one; the expansion would have been preceded by a period of contraction and it would not have occurred at the same time for all matter. We emphasize that the standard big bang theory refuses to take into account the existence of negative energy particles, thus denying half of our universe. It is also contradicted by several observations left aside, for example the works of Armenian astronomers whose observations have confirmed the hypothesis of the formation of stars according to which evolution was made of hyper-dense bodies to less dense bodies. These astronomers have furthermore validated that the birth-places of the new galaxies were the centers of the old galaxies, as well as the theory of the division of galaxies. In 6 we conclude that this equation is the one which gets closer most to the equation which missed to Lemaître to defend his "hypothesis of the primeval atom" and his prediction of fossil cosmic rays.

2. Equation of the Theory of Relation

2.1. The Equation of the Theory of Relation

Historically, Newton's discovery of the law of gravitation can be appreciated as the first "unification", combining the laws of heaven and earth. The next great leap took place in the mid-1860's with Maxwell's theory of electromagnetism uniting electricity and magnetism. In 1905, Einstein created the special theory of relativity connecting space and time and associating the concepts of matter and energy. In 1915, he proposed general relativity, which explained gravitation as the marriage of space-time and matter-energy. In the 1960's, the works of S. Weinberg, A. Salam and S. Glashow led to the unification of the electromagnetic interaction and the weak nuclear interaction. The next step, namely the unification of the electroweak and strong interactions, drove to the electronuclear theory (GUT) whose predictions were the object of no conclusive result. As for the ultimate synthesis—the unification of gravitation and GUT—, it has defied all attempts [16].

More than seventy years ago, Paul Dirac suggested that more than a coincidence was at work between the age of the universe in atomic time units and the ratio of the electric force between an electron and a proton to the gravitational force between the two $\left[ke^2 / (GM_p M_{e^-}) = 10^{40} \right]$ [17] [18]. The most fundamental unit of time would be one associated with atomic processes, because it would depend only on basic natural constants, such as the electric charge (e), the mass of the electron (M_{e^-}), or the speed of light (c). This time unit, which appears throughout physics as the basic time scale for atomic and nuclear processes, is roughly the time required for light to travel the electron radius: $10^{-15} \text{ m} / 10^8 \text{ s} = 10^{-23} \text{ s}$. Thus the evaluated age of the universe (10^{17} s) in atomic time units is $10^{17} \text{ s} / 10^{-23} \text{ s} = 10^{40}$. Dirac postulated that the near equality of these two numbers was a manifestation of some as yet the unknown deeper law of nature that required them to be nearly equal for all time.

The problem is that the age of the universe is increasing. If the quantity between the two 10^{40} is to be maintained, then one of the other numbers must change with time. For many physicists, the gravitational constant (G) seems the only plausible candidate which can vary in spite of general relativity, which states that G is a physical constant whose numerical value is fixed.

Let us compare the electrostatic and the gravitational forces between two protons in the same nucleus, with a distance of 0.2 nanometers [19]. We will use the MKS system which has the advantage of incorporating the constants of the permittivity of free space and of permeability of free space. The value of the Coulomb constant k is $1/4\pi\epsilon_0 = 8.9875 \times 10^9 \text{ N} \cdot \text{m}^2 / \text{coul}^2$. The value of the constant ϵ_0 , called permittivity of free space, is $8.8542 \times 10^{-12} \text{ coul}^2 / \text{N} \cdot \text{m}^2$. According to Coulomb's law, the electrostatic repulsive force is

$$F_e = q^2 / (4\pi\epsilon_0 R^2) = 5.775 \times 10^9 \text{ N}; \quad e^2 / \left[4\pi(8.8541878 \times 10^{-12})(0.2 \times 10^{-9})^2 \right].$$

The attractive Newtonian force is $GM_{op}^2 / R^2 = 4.666 \times 10^{-45} \text{ N}$. The ratio is

$$F_e/F_g = ke^2/GM_p^2 = 1.23 \times 10^{36}.$$

Let us pursue Dirac's suggestion on the time, and replace the ratio by a universal time factor with the constants G and c : $F_e/F_g = t_o c/G$; $F_e = F_g t_o c/G$. And suppose we relativize the masses of the protons, in accordance with special relativity, as if they were moved with a speed of 200,000 km/s, we would obtain

$$\begin{aligned} & ke^2 / \left[R_o \left(1 - v^2/c^2 \right)^{1/2} \right]^2 \\ &= G \left[M_{op} / \left(1 - v^2/c^2 \right)^{1/2} \right]^2 / \left[R_o \left(1 - v^2/c^2 \right)^{1/2} \right]^2 \left[t_o c/G \right], \end{aligned} \tag{1}$$

thus we would have

$$ke^2 = M_{vp}^2 t_o c. \tag{2}$$

[M_{op} is rest-mass; $M_{op} \left(1 / \left(1 - v^2/c^2 \right)^{1/2} \right)$ gives M_{vp} , *i.e.*, rest-mass + kinetic energy (T); $v = 200000$ km/s = $2/3c$].

Particles come in pairs, each with a counterpart antiparticle

$$\pm ke^2 = \pm \left[M_{op} / \left(1 - v^2/c^2 \right)^{1/2} \right]^2 t_o c \tag{3}$$

$$2.3 \times 10^{-28} \text{ kg} \cdot \text{m}^3 \cdot \text{s}^{-2} = \left(2.2439 \times 10^{-27} \text{ kg} \right)^2 \left(1.528 \times 10^{17} \text{ s} \right) \left(3 \times 10^8 \right).$$

We ascertain that the link between the charge squared and the relativized proton's mass squared confers a universal time of 1.5283×10^{17} s multiplied by c . That time gives 4.84 billion years $\left[\left(1.5283 \times 10^{17} \right) / \left(365.24 \times 24 \times 60 \times 60 \right) \right]$.

2.2. The Importance of pi

We have already talked about pi in a previous article [3]. We considered that pi made an essential difference between a linear time in accordance with a longitudinal wave and a circular time which refers to a transverse wave. A particle that travels 4.84 billion years in the metric of a straight-line space will travel the same Euclidean distance in 15.21 billion years using the metric of a space with constant curvature. We imagined that a wave rolled up around the radial line A-Z would travel it in the 5.21 billion years, which is linear time multiplied by π . It fits a transverse electromagnetic wave

$$ke^2 = M_{vp}^2 (\pi) t_o c. \tag{4}$$

Of this expression, one must keep in mind that π is used for winding the particle spirally around the radial length $t_o c$. It could be a transverse electromagnetic wave but it could also be a transverse gravitational wave. Mathematically, the equation should be

$$(\pi) ke^2 = M_{vp}^2 (\pi) t_o c. \tag{5}$$

This way of seeing predicts the existence of transverse and longitudinal electromagnetic waves, as well as transverse and longitudinal gravitational waves. The particles that may be associated with longitudinal electromagnetic waves

and longitudinal gravitational waves could be the neutrino and the graviton. The longitudinal electromagnetic wave already exists. The gravitational wave, which has always been considered to be transverse, would have been captured in 2015. This does not exclude the existence of a longitudinal gravitational wave.

This article describes π in another way. The reason is that it makes it possible to obtain other forecasts. We find that the case of a transverse wave in relation to a longitudinal wave is very similar to that of the light propagating on the circumference of a circle, or on the surface of a sphere, whose π makes it possible to determine its radius. Although the two descriptions seem to be very different from each other, there is a mathematical equivalence between them [$\alpha = \pi R = \pi t_o c$; α can represent a semicircle, a transverse path, a transverse wave; R can represent a radius, a radial path, a longitudinal wave].

When Einstein's geometric theory of gravitation is applied to the entire universe, space is curved on a global scale. This curvature results in geodesics and the light ray (or photon) is the ideal tracer of geodesics. The curvature of the universe on a cosmic scale is manifested by the fact that the real mutual distance between two galaxies located at the antipodes of each other will be equal to the product of π by the radius R : $\alpha = \pi R$. What fixes the scale of the curvature is the inner radius of the universe because we consider the universe as a sphere having a volume and not only a surface. This "geometric" way of representing π makes it possible to obtain a central point, an origin, a privileged direction. While the Einsteinians can assert that a point on the surface of the universe is everywhere a center of the universe, we can say that any point on the surface of the universe has the same center of the universe. The center of the sphere becomes a unique, privileged direction.

With the theory of Relation, the radius R of the universe gives on the center of the universe, towards the original point of our universe. This model considers our universe to be spherical, expanding, with a surface that is curved, finite, and boundless [20]. It gives its approximate age, its past and future history starting from microscopic units based on atomic data. The model of the theory of Relation follows the cosmological principle of homogeneity and isotropy and the law of raisin cake. In a cake of raisins that swells while cooking, the raisins move away from each other not because they move in the dough but because it increases in volume and at the same time grows the mutual distance between any two raisins. It is the space between the raisins which increases, it is not them who move in the dough. The term $t_o c$ in the equation represents the dough of the cake being inflated, it is the radius of the universe which grows and remains unobservable, it is a cosmological dark energy whose wavelength follows the size of the space. The wavelength of this energy-radiation propagating through the space-time it creates varies as the size of the universe and is expressed by the cosmological redshift. What is observable are the galaxies, that is to say the raisins. It is not the galaxies that are in motion, it is the space between the galaxies

that is expanding [21].

It can be said that with expansion, galaxies are at the edge of the universe. We are part of a galaxy and we measure the universe through light from other galaxies. If we leave the edge of the universe, what we call its surface and go straight away, as a light ray would do, along a geodesic, we would eventually reach the farthest point, which we call the anti-center.

This point is situated at a certain distance α , and the elementary geometry teaches us that the distance α from one pole to the other is equal to the product π by the radius R

$$\alpha = \pi R. \quad (6)$$

In the opposite direction, if we do not know what the radius R is, it suffices to divide the distance α between a pole and the opposite pole, that is to say the point which is the furthest away, by the number π . This definition is applicable to our universe. This internal radius will be

$$R = \alpha/\pi. \quad (7)$$

We consider the universe as a finite object without limits. The circumference of a circle and the surface of a sphere are examples of one- and two-dimensional spaces that are finite but have no beginning or end. One can imagine a four-dimensional mathematical sphere, a hypersphere, of which the three-dimensional universe constitutes the surface, or rather the hypersurface. Just as the circle and the sphere are equidistant from a fixed point of the space called the center, so the hypersphere is made of a three-dimensional distribution of points, all situated at the same distance from the center [22]. The three-dimensional volume of the hypersphere is: $2\pi^2 R^3$ [Volume = area (πR^2) \times circumference ($2\pi R$) = $2\pi^2 R^3$].

By moving on the surface of a sphere (along a meridian, for example) the light would eventually return to its starting point, having traveled the distance $2\pi R$. The distance α from one pole to the other, a half circumference, is equal to the product π by the radius R (which is $t_o c$ in our equation). The radius R is $\alpha/\pi = t_o c$. If one admits an explosive origin, the ray starts from the center of the sphere in all directions, looping the 360 degrees of the surface. There is a simultaneity of time between the ray which reaches the point which forms the surface and that surface which is formed, since the ray comes everywhere from the same origin. In the expression $\alpha = \pi R = \pi t_o c$, the time is the same to obtain R and α , but the distances are different, which suggests a curved electromagnetic distance for α and a longitudinal radial distance for R .

We measure the universe thanks to the light that comes from the stars. This light follows a geodesic to reach us. The estimated age of the universe is about 15 billion light-years and its radius is 10^{26} meters. This geodesic ray (α) of 15 billion light-years has an internal radius (α/π) with a time of 4.5 billion light-years.

For the Einsteinians, the universe-sphere is a false image that seeks to impose

itself on our mind and the radius of the universe in relation to the big bang is not the radius of a ball. They seem to know only the universal space of the surface that surrounds the solid globe, and which constitutes the three-dimensional universe on which we could go where we want and visit all of its galaxies. Everywhere the space would be the same, we would never meet any edge opening on an outside. This universe is finite but without borders. It has no exterior, and even less interior. It is their truth, but their very truth that carries its nonsense by wanting to consider the universe only for the surface that surrounds it. The universe must be considered for itself in its volume. We can measure its size using its internal radius, understood as the distance from a point of the surface to its anti-point divided by π .

2.3. Return to the Equation of the Theory of Relation

Equation (4) establishes a clear mathematical link between electromagnetism and gravitation. It takes into account π , as if $t_o c$ was a transverse space-time wave. Equation (3), in the form

$$\pm k e^2 = \pm M_{vp}^2 t_o c, \quad (8)$$

does not take account of π , as if $t_o c$ was longitudinal. We will not take into consideration π for relativistic expressions of the rest of the paper.

In the right-hand side, matter (M_{vp}^2), space ($t_o c$), and time are linked into one whole. The radius of the universe is represented by " $t_o c$ ". We can see in relation (1) that the term $G \left[M_{op} / (1 - v^2/c^2)^{1/2} \right]^2 / \left[R_o (1 - v^2/c^2)^{1/2} \right]^2$ links the gravitational Newtonian force and special relativity. We obtain a relativized Newtonian gravitation [23], which means, on the one hand, that gravitation is a reality everywhere and, on the other hand, that special relativity is neither only a mathematical tool nor a simple Galilean reference without gravity. Both are linear theories applied to a linear three-dimensional Euclidean geometry with flat space-time. Let's add that electromagnetism is also a linear theory.

According to the theory of Relation, gravity is not a distinct force, but an aspect of electromagnetism. The two forces are connected by space-time in four dimensions. In fact, gravity is electromagnetic dissolution in space-time. Basically, electric and gravitational forces are part of a common super-force: electrogravitation. As magnetism and electricity are both sides of electromagnetism [24]. In the physics of subatomic particles, electrogravitation takes the appearance of the electrostatic force, and the gravitational force, 10^{36} weaker, plays no apparent role in it. When the pair of particles with its two positive electric charges repel and move away at a speed close to light, creating the "space-time" between them, electromagnetism decreases with distance and becomes the vacuum energy. Its lost energy has turned into attractive energy, that of gravitation that grows with space-time. On a large scale, electrogravity has become gravity. On a large scale, electrogravitation becomes gravity. We are led to think that attractive gravitational forces are electromagnetic forces with attractive charges

acting in space-time rather than in the subatomic world. The expansive driving force, caused by the initial explosion, would be the electromagnetic forces of the repulsive forces operating in the universe.

According to Newton's theory of gravitation, the force GMm/r^2 instantaneously transmits energy or a signal. Newton was unhappy with an instantaneous phenomenon, or a "remote action," associated with gravity. Poincaré (1904), Minkowski (1908), and de Sitter (1911) agreed that gravity must propagate at the speed of light. Indeed, according to special relativity nothing moves faster than light, not even gravity. None of the several theories of gravity—even Einstein's, which were compatible with special relativity in that the speed of propagation of gravity is the speed of light, was satisfactory. The combination of the Lorentz transformation and t_0/c , ensures that the speed of light or gravity does not go faster than the speed of the universal constant c .

However, the gravitational constant G disappears in the equation, which implies that the classical gravitational mass of matter at the beginning is in the form of a minimum potential while the energy is at its maximum [25]. This goes against Paul Dirac who, in papers published in *Nature* in 1937 and in the *Proceedings of the Royal Society* in 1938, described a cosmology with a changing gravitational constant. He postulated that G varies like the inverse age of the universe, so as the universe expanded from the big bang, the gravitational constant, or force, became weaker and weaker as time passed until today, when we experience the present very weak force of gravity [26]. With the theory of Relation, Newton's gravitational constant G does not vary, just as in general relativity. On the other hand, potential energy-mass increases with cosmic time [27].

The equation of the theory of Relation is in phase with the Englert-Brout-Higgs proposition allowing to reconcile the equations of the standard model with the empirical data. It consisted in postulating the existence of a quantum field filling the whole space, with which the elementary particles, effectively without mass, interact more or less strongly, which has the effect of slowing down their movements in the same way as if they had a mass. Everything happens as if the elementary particles were massless objects at the beginning of the expansion, moving on an electromagnetic field (or an electromagnetic space-time wave—amalgamated with the vacuum energy, at the cosmological constant [6] and dark energy) that loses energy over time. This lost energy is recovered by the particles that move more and more with friction, so at a speed less than that of light and their mass is non-zero. In the equation, the mass then appears as a measure of the velocity decrease of the matter (v of v^2/c^2 which decreases throughout the expansion), the inertia, the resistance to movement, mass.

The equation is remarkably that of expansion. Imagine that the proton masses of our equation that we have relativized above, as if they were moving at a speed of 200,000 km/s, are galaxies moving away at $2/3c$, we then obtain "a cosmological equation" which establishes the age and distance of the universe in relation to the speed of recession of galaxies. The farther the galaxy is from the earth, the

greater the velocity of recession, and the younger the age of universe. Velocity, age and distance are correlated. A speeding away of the galaxies at $2/3c$, taking account of π , is tantamount to 15 billion years. These two numbers are roughly fitting with the actual valuations of science.

If we admit that the universe is a kind of expanding super-atom:

$$ke^2 \rightarrow M_{vp}^2 t_o c, \quad (9)$$

giving the age of the universe, we have an arrow toward the future being the same as at least 3 arrows of time that do distinguish the past from the future: thermodynamic (disorder increases); cosmological (universe expands rather than contracts); psychological (we remember the past, not the future) [28].

2.4. Two-Edged Reasoning

The distant supernovae serve as luminous standards for surveying the universe on a large scale. The gigantic explosion of a voracious white dwarf makes visible an intense light that persists for several days. Their curves of light are similar. It has been deduced that any difference between two curves of light can only come from distance: the further away the supernova is, the weaker the received light. The results obtained showed that the light of distant supernovae was 25% fainter than expected in case of deceleration. The majority of astrophysicists have therefore concluded that the expansion of the universe has been accelerating for several billion years and that a repulsive dark energy plays the role of accelerator [29].

A contrario, if we assume a deceleration of the expansion, this means that the transformations accelerate towards the past and that the intrinsic luminosity can no longer be theoretically always the same and that we cannot be satisfied with measure their apparent luminosity to deduce their distance. The physical conditions change by going as far as possible, the speed rating of chemical, atomic and nuclear reactions had to be faster. The explosions of these stars were to occur when they reached a critical mass different from the supernovae that are close. They release a different amount of energy, their radiations are modified. They emit less luminosity because the mechanisms are too fast or skip steps. It can be assumed that the peak of brightness may last less and the subsequent weakening. As for the apparent luminosity, one can conjecture its degradation by the galactic dust, in particular the iron needles produced by condensation of the iron rejected by preceding generations of supernovae [30].

Whatever the current scientific consensus, the fact remains that the same results obtained (pallor greater than expected) show that these supernovae are no more distant than those predicted by classical cosmological models. They show that the explosion of the universe, contrary to what has been imagined since 1998, has been in a deceleration phase since the Planck era [6]. Which is consistent with the equation of the theory of Relation.

What does it mean for the dark energy that must play a role of accelerator as if a sort of antigravity forced the universe to constantly increase the speed of its expansion? It exists but differently. It is nothing else but the gigantic kinetic

energy of the universe when it started in a “cosmic fireball”. It has become today the vacuum energy [31]. The logic of this cosmological adventure revolves around an essential property: the progressive de-excitation of the quantum field by the decelerated expansion of space [32]. There is a snowball process. The deceleration of space precipitates the rate of condensation of the matter energy, which reduces the influence of the vacuum energy, which dilutes and decreases, in return, the rate of expansion, which leads to a universe in which clusters of matter become very dense. In the context where dark energy and dark matter do exist, we believe that their proportion to constitute matter must be reassessed. We expect, by keeping the ordinary visible matter at about 4%, that the dark matter would be about 45% and that the dark energy, which was diluted with the expansion of the universe, is about 50%. (consistent with the hypothetical $2/3c$ velocity of our equation and with a constant rate of expansion [12]).

3. The Hypothesis of the Primeval Atom of Georges Lemaitre

3.1. The Primeval Atom of Georges Lemaitre

The term M_{vp}^2 dovetails with Georges Lemaitre’s hypothesis that the universe comes from a kind of gigantic atomic nucleus containing all the nucleons of the universe, a nucleus whose decay would have initiated the expansion of the universe [33]. Lemaitre believes that the cosmic rays, which are endowed with energy of several billion electrons-volts, are the manifestation of initial fragmentation.

Although Lemaitre’s idea of explaining the expansion of the universe as being due to an initial explosion is still relevant, his theory that the entire universe was originally contained in a single atom that has disintegrated is now relegated to oblivion. He had wished to give an experimental basis to his hypothesis of the primitive atom, and he believed find in the cosmic rays the relics of the primitive universe. He had deepened the question with collaborators such as Odon Godart (1913-1996) and Manuel Sandoval Vallarta, but the failure of their explanation will not favor the credibility of the model of the primeval atom [2].

Physicists are now leaning towards a sort of cloud of elementary particles (quarks and leptons) that have condensed gradually, which has released energy and given the universe its initial impetus. They recognise the existence of fossil radiation, a trace of the initial explosion, but which no longer comes, as Lemaitre thought, from a drag of particles propelled by the disintegration of the original atom but from electromagnetic radiation [34]. It was therefore concluded that Lemaitre was mistaken. In light of the developments that followed, one can question, without excluding it, his model of the primitive atom. But we believe he was not mistaken about cosmic rays: fossil cosmic rays from the beginning exist just as much as fossil light. But to claim it, it is necessary to revisit the history of standard big bang.

3.2. Some Features of the History of the Standard Big Bang

In 1929, Edwin Hubble discovered the law of recession of galaxies thanks to the

telescope placed on Mount Wilson: they move away from each other at a speed that is greater as their distance is greater, proof that the universe is expanding and not static. Until then, Einstein believed in a static universe. In 1922, Friedmann, by dynamically interpreting Einstein's equations, had provided the first expanding universe model with positive curvature and density, a nonzero cosmological constant, and zero pressure. Regardless of Friedmann, Lemaître in 1927 suggested, with calculations of general relativity in support, that the universe was expanding: he gave the first interpretation of the redshifts related to the expansion of the universe and predicted the linear relation distance-shift to red. Friedmann and Lemaître had put forward this hypothesis before it was confirmed by the observations of redshift of galaxies and the Hubble law. Contrary to what Hubble himself imagined, it is not the galaxies that move, but the space itself that extends, taking with it the galaxies. Hubble experimentally establishes the linear relationship distance-redshift, but has not linked it to expansion. Einstein, Friedmann, Lemaître and Hubble were the pioneers of relativistic cosmology. The latter is essentially based on the Friedmann-Einstein equation.

In 1931, Lemaître distinguished himself by proposing a quantum origin of the universe. He proposed his initially singular universe model, the primitive atom, in which a phase of stagnation allows the formation of galaxies. He suggested that cosmic rays could come from radiation produced during decays during the first expansion period. This hypothesis, prefiguration of big bang models, left physicists very skeptical. Einstein and others blamed this hypothesis for having been inspired by the Christian dogma of creation. Lemaître often expressed that the physical beginning of the world was quite different from the metaphysical notion of creation. The irony is that in the same year Einstein published an article in which he admits that the observations establish without any doubt that the universe is expanding. The whole scientific community ranked behind the models describing an expanding universe only in 1964, the year in which they received a start of confirmation thanks to the discovery of the cosmic microwave background [2] [34].

3.3. The Hypothesis of the Primitive Atom of Lemaître Confronted with That of the Primitive Atom of Gamow

In 1945, Lemaître assembled his cosmological work in "*The hypothesis of the primeval atom*" [35]. It is a cosmogonic hypothesis according to which the present world has resulted from the radioactive decay of an atom. He was led to formulate it by being guided by thermodynamic considerations that sought to interpret the law of energy degradation in the context of quantum theories. The discovery of radioactivity and the establishment of the corpuscular nature of cosmic rays have made plausible its hypothesis that assigned a radioactive origin to these rays as well as to all existing matter.

This hypothesis had to compete with that of George Gamow. The latter also tackled the fundamental problem of the origin of our universe. He wondered

why our universe was in a state of such high compression and what triggered the expansion? His answer: The great compression that occurred at the beginning of the history of our universe resulted from a collapse which had taken place in an even older time, and that the current expansion is simply an “elastic” rebound that began as soon as the density corresponding to the maximum possible compression was reached. We can presume over the pre-compression era, but we can say that as soon as the density of the universe reached its maximum value, the direction of motion reversed (which is why the negative energy belongs to before the big compression and the positive energy to after) and expansion began, so that the very high densities probably existed for a very short time. The theory of Relation shares this cyclical vision [36].

In fact, it is especially with regard to the nuclear forces that the two hypotheses opposed: weak nuclear for Lemaître and strong nuclear for Gamow. Radioactivity, that is to say the spontaneous emission of radiation by matter, was discovered in 1896 by Henri Becquerel. As early as 1931, Lemaître proposed his initially singular model of universe, the primitive atom, which, unstable, exists only for a moment, breaks up into pieces that break in turn and give rise to all the present components of the universe. He suggests that cosmic rays are the relics of the primitive universe. He advances a quantum origin of the universe, he introduces the idea of a cold big bang, that is to say an expansion resulting from the radioactive decay of an atom-universe. He first had a slowly evolving model related to the intensity of the weak force, responsible for the disintegration, then, based on the new knowledge of atomic physics, he turned towards a faster cosmology, with an explosive origin. He gives his cosmology a more structured version in 1933, published in French under the title “L’Univers en expansion” in the *Annales de la Société scientifique de Bruxelles*. In this text, Lemaître demonstrates, among other things, the occurrence of singularities in the homogeneous relativistic cosmological models [2].

In return, Gamow proposes in 1946 the cosmological nucleosynthesis. In 1948, Alpher, Bethe and Gamow calculate the abundances of the elements formed in the primitive universe. The same year, Alpher and Herman predicted cosmic background radiation in the form of a black body at a temperature of 5 K. In 1952, Baade revises the extragalactic distance scale, which increases the cosmic time scale by a factor of 2.6. In 1965, Penzias and Wilson discovered the background radiation at a temperature of 3 K. Dicke, Peebles, Roll and Wilkinson gave the cosmological interpretation of it in the framework of big bang models [2]. In essence, it can be said that the discovery of cosmic background radiation is due to the hot big bang model that Gamow and his team have achieved.

It’s important to note that there is no direct succession between the work of Lemaître and that of Gamow. Nuclear physics was Gamow’s inspiration here—not at first the influence of the prior mathematical work of Lemaître or even Gamow’s first teacher, Friedmann. Gamow had read Lemaître’s, de Sitter’s,

and Eddington's papers on expanding models, but initially he did not apply them to his physics of the early universe. At the end of 1946, Gamow and Alpher decided to develop the rather abbreviated ideas that Gamow had issued during the year on primordial nucleosynthesis at the beginning of an expanding universe. Specifically, this meant working out hydrogen and helium could be developed out of the decaying neutron gas of the early phase of the universe. This led to Alpher and Gamow's 1948 paper, also known as the $\alpha\beta\gamma$ paper, a paper that has become a milestone in big bang history—and one that, like Lemaître's and Friedmann's important papers, was almost entirely overlooked at the time. It was only in 1948, with the $\alpha\beta\gamma$ paper, that Gamow and Alpher and Herman realized that the model they wanted needed to originate in the Lemaître model—and more importantly, it had to originate in a hot state, not in a cold nucleus as Lemaître had envisaged. Only a hot state of millions of degrees, they reasoned, could allow nucleosynthesis to “cook” elements like hydrogen, helium, and heavier elements [37].

Gamow, in other words, took Lemaître's primeval atom and turned it into the big bang model that remains the base of the standard model to this day. One immediate consequence of such a hot big bang model, Gamow and his team realized, is that radiation from the primeval fireball should still remain, albeit at very attenuated wavelengths in the radio end of the electromagnetic spectrum. Where Lemaître's atom model led him to examine cosmic rays as candidates for the leftover fireworks, Gamow's model more simply suggested a low hum of microwaves in the background of the universe.

3.4. Theory of the Origin of Lemaître's Cosmic Rays

In 1965, Penzias and Wilson discover the fossil radiation at the temperature of 3 K, thus realizing the predictions of Gamow, Alpher and Herman on the primitive light. It has since been said that Lemaître was not far from predicting the existence of cosmological black body radiation, photons emitted at a temperature of about 3000 K and cooled by a factor of 1000 by expansion, but that he will make the confusion with massive particles in cosmic rays [2]. It is now believed that most cosmic rays come from a number of sources such as the Sun, some stars, supernovae and their remains, neutron stars, and black holes. Does this mean that Lemaître's suggestion that cosmic rays (massive particles) are relics of the early universe is false? We think, like Lemaître, that cosmic radiation could have been created at the beginning of the world because these rays are endowed with energy of several billion electrons-volts and that we do not know any phenomenon currently taking place that is capable of such effects. What these rays might look like the most, are the rays that would be produced during decays of super-radioactive origin. They appear as the memory of the great initial transformations of the universe.

Lemaître's thought on the origin of cosmic rays can be schematized by the following lines. The total energy of cosmic rays can be estimated at 10^{-34} grams

per cm^3 . This value is based on the evaluation of the energy of the cosmic radiation falling on the Earth per square centimeter of surface and the transformation of this energy in mass by the relation $E = mc^2$. This energetic value, fairly secure in its order of magnitude, is a “density of equivalent mass”. It should be compared with the density of matter, that is to say, what would be obtained if all the nebulae were vaporized and this matter was distributed uniformly in space. An order of magnitude of 10^{-30} grams per cm^3 is found. Cosmic rays, assuming them uniformly distributed in space, have a considerable intensity since they are of the order of ten thousandth of all existing energy. It seems impossible to explain such energy, which represents one in ten thousand of all existing energy, if these rays have not been produced by a process that has brought into play all existing matter [38].

Imagine then ideal spheres that would be the neutral zones of attraction between neighboring nebulae. These spheres are expanding, since the whole system of the universe is expanding, the nebulae in each sphere are separating more and more. Cosmic radiation crosses these spheres, but, as the whole is symmetrical, we can imagine it bouncing on the surface of these spheres. With this image, we understand that the cosmic radiation must lose energy since it bounces on a body that flees. The calculation shows that this energy varies inversely with the radius of the sphere. So, assuming that cosmic rays occurred when the radius of the sphere was one-tenth of what it is now, then the energy of cosmic radiation would have reached not the ten thousandth, but the thousandth of the energy total of the universe. What assumes that cosmic rays come from far away and are not due to a nova or a small number of nearby stars. No satisfactory explanation is given for cosmic rays, which are 100 billion times more energetic than the others, and strike every km^2 of the earth’s surface about once every century. Models have already invoked ultra-energetic cosmic rays stemming from big bang, saying that Lemaitre would not totally have been wrong on this question. Our model also plans ultra-energetic cosmic rays from the big bang. We believe that the hypothesis of fossil cosmic rays is just as true as the existence of cosmic black body radiation.

3.5. Is Lemaitre’s Cold Model as True as Gamow’s Hot Model?

We are then confronted with this other question: if we argue that Lemaitre’s idea of fossil cosmic rays is just as truthful as the cosmic background radiation, does that mean that Lemaitre’s universe model of a single cold quantum is just as true as Gamow’s model of hot radiative universe?

At this point, it must be said that the first big bang models took into account only one force of nature, gravitation, described using the formalism of general relativity. Gravitation, attractive and of infinite scope, dominates on a large scale but is incapable of describing the physical conditions of the small-scale matter that prevailed at the beginning of the universe. General relativity constitutes a specific theory of gravitation, consequently incomplete. His equations lose all

validity when the particles present in the primordial universe, endowed with gigantic energies, undergo other interactions than gravitation [33].

Lemaître opposed, the first one, a “quantum cosmology” to this “relativistic cosmology”. In 1934, he made the link between the cosmological constant and the vacuum energy of which he was the first to calculate the energy and to associate a negative pressure. However, he had no equation to explain the hypothesis of the single quantum. As for Gamow, he thought that some chemical elements had been produced during the first few minutes of the big bang and that the remaining radiation should be omnipresent. As a consequence of cosmic expansion, this original radiation must have cooled to a temperature of 5° above absolute zero [25]. Just like Lemaître, he didn’t have any equation for its “Ylem”, this great Compression in a state of complete disaggregation from which the components had to emerge. They noted, Lemaître first, the close correlation between observed expansion phenomena and certain mathematical consequences of Einstein’s theory of general relativity. They had to fall back on the Friedmann-Einstein equation, and thus on the inadequacies of general relativity.

At the time of Penzias and Wilson’s discovery in 1965 of background fossil radiation, the hypothesis of the primeval atom became, under the media name of big bang, a physical theory in its own right. The irony of history is that the radical novelty introduced by Lemaitre and Gamow, which consists in linking the structure of the universe on a large scale to the intimate nature of atoms, swims more than ever in the midst of speculation. Misunderstanding will persist as long as quantum mechanics remains irreconcilable with general relativity. The first can account for the quantum fluctuations that presided over the birth of the universe. It is the Planck era where the characteristic times of the phenomena are 10^{-43} s. In contrast, Edwin Hubble’s observations on the escape of galaxies can only be explained in the context of general relativity. The duration to take into account is the age of the universe, that is to say 15 billion years, or 10^{17} s. There is therefore a factor 10^{60} between the two scales! The real is a ditch of 60 orders of magnitude that no theory currently can decrypt except the theory of Relation.

4. A fundamental Equation

4.1. An Equation That Says Where Does the Time Come from

We have said that Lemaitre had made the connection between the cosmological constant and the vacuum energy. The theory of the Relation, for its part, argues that vacuum energy, cosmological constant, dark energy and cosmological space-time wave constitute a single entity. They have the same flavor, color and smell, so that one can certify that they merge through cosmological time [33].

The cosmological time of this space-time is the key to the theory of Relation. The time t_o of the term $t_o c$ of the equation comes from M_{Vp}^2 which represents the energy-matter. It emerges from the kinetic energy in dilation of protons, that is to say of a quantum cosmology. It is a physical time consubstantial with

the universe which is born and an indicator of an energy propagated at the speed of light. The term “ t_0c ” refers to a radius from the center point of a sphere created by the large initial boom (in this case, the Planck length of the Planck sphere, but it may shrink towards the absolute zero point). The image of the big bang as a cosmic explosion ejecting the material contents of the universe like shrapnel from an exploding bomb is a useful and non-misleading representation as long as these splinters make space-time instead of being in it. The big bang would be an eruption of compressed space-time-matter, whose deployment, like a shock wave, would still transport matter and energy [39].

This radial move is an electromagnetic wave. We can say that the radius of space-time belongs to the family of electromagnetic waves: the wavelength is the radius ($\sim 10^{26}$ m) of the universe and the period ($\sim 10^{17}$ s) is his age. Just like Maxwell’s electromagnetic theory of light, the space-time wave is an oscillation wave of the electric and magnetic fields that propagate in space. We can call it electrogravitational wave or electromagnetic wave of space-time. It carries energy and momentum. In fact, it is the electromagnetic standing wave [40], the “radiation” at 2.7 K, or the vacuum energy.

The equation gives a negative cosmological constant which prints a deceleration of the expansion of the universe. Its positive pressure exerts an attractive force. Does this deceleration of the universe affect the course of time? Physics formally distinguishes the course of time from the arrow of time. The course of time indicates to the fact that time passes and that by passing it produces duration. It generates the succession of events and is causal, because time goes in one direction without backtracking. The arrow of time presupposes the existence of a well-established course of time within which certain phenomena are themselves temporally oriented, that is to say irreversible: once accomplished, it is impossible to cancel the effects they produced. In the context of expansion, it seems that the course of time and the arrow of time ultimately proceed from one and the same reality.

Can we claim, with this relation where the time stemming from the energy-matter M_{vp}^2 links the physics of the infinitely large to that of the infinitely small, to explain the emergence of the irreversibility observed at the macroscopic scale from physical laws that ignore it at the microscopic scale?

We know that according to the equations of current physics, all the phenomena taking place at the microscopic level are reversible, they can unfold in one direction as well as in the other. The dynamics of the phenomena do not depend on the orientation of the course of time. We could call past what we call future, and vice versa, without affecting the physical process in which they participate. On the other hand, at our scale, we observe only irreversible phenomena, arrowed phenomena. The oldest explanation is based on the second principle of thermodynamics, according to which any physical system evolves in general without returning to its initial configuration: lukewarm water never becomes hot water on one side, cold water of the other. However, it seems convincing that if

the universe, after its expansion, entered the contraction phase, it would imply a reversal, not of the course of time, but of the arrow of time. The irreversibility of expansion would only be in fact, not in principle [41].

What is the true origin of cosmological time? Our equation, as well as the equations of traditional cosmology (derived from the Friedmann-Lemaître equation), allow us to go back to the Planck scale, where, below, the usual representations of space and time lose all meaning. Admittedly, the theory of the cyclic universe makes it possible to envisage a “pre-time” different from the usual (reversible) physical time, but this notion only moves a link in the chain of causality that goes back in time, a chain that either has no beginning, or ends in a first cause. We can call “zero time” this first moment which corresponds to a situation where the equations begin to be valid. This first moment is not quite one, in the sense that corresponds in no way to the “absolute zero instant” of the origin of the universe.

How did cosmological time begin? The expansion of the universe becomes the real engine of time. Our model of mathematized cosmos is unambiguous: the universe decelerates. This deceleration of the expansion goes against the phenomenon of acceleration endowed with a positive cosmological constant which gives rise to a universal repulsive force with a density of the energy of the vacuum which remains the same—what seems absurd to us—, while ordinary matter is diluted and ends up being unable to slow down [42]. It seems certain that this is not the case in the theory of Relation. What is revolutionary in the latter is that in the process of expansion, the energy of the vacuum at the beginning was to be 10^{120} times higher than today where the density of the cosmological constant is almost equal to zero. It dilutes and ends up slowing expansion. We have a negative cosmological constant which gives rise to a universal attractive force [6]. On the other hand, ordinary matter (which is the potential energy of our equation) had to have a gravitational mass almost zero at the beginning, it strengthens with expansion and its attractive effect always increases.

Neither general relativity, nor quantum physics, nor a possible synthesis of the two, can today describe the apparition of the universe as a physical event. How could they do it when they consider that the passage of time is an illusion? The reality defined by the special relativity is a four-dimensional space-time block where it is impossible to define a “now”. General relativity says that this block is actually a space-time-force-matter block where the force-matter content is nested in the space-time container that it distorts by its presence. Quantum theory says this block is multiple.

The notions of universal time and the oneness of the reality do not exist for these theories while they are at the heart of the theory of Relation. The conceptual leap was to introduce the notion of temporal flow and that of temporal orientation (or temporal arrow). This temporal arrow implies privileged strata that correspond to the idea of a “stratum of the now” that would move towards the future as if a projector successively illuminated the “strata of density” of

space-time [43]. The course of time, as well as the arrow of time, would result from the fundamental cosmic temporal irreversibility of expansion and would correspond to emerging properties of quantum cosmology [44].

The universe erupted from a singular energetic event, which gave birth to all space and all matter. Our equation goes back to that “zero instant” from which cosmological time emerges. This zero instant corresponds to the 10^{-43} s which followed the big bang, known as Planck time where the temperature is estimated at 10^{32} Kelvin degrees. It also coincides with the maximum increase in quantum mass obtained by relativization, or the transformation of Lorentz, from v^2 to c^2 . If the expansion decelerates, that is to say if the engine of time decreases, its speed, the speed goes from c^2 to v^2 , and the course of time should itself “decelerate”.

Energy spreads by creating space-time, and cools. We can see this freeze in the formula in two ways, because there are two speeds. First, a drop in the speed of “ M_{vp}^2 ” caused a gradual drop in temperature and a slowing of the rate of expansion, and a concomitant increase in gravity. The fermions, a priori in the state of radiation, maintained their maximum speed until about 300,000 years and the decoupling of the matter from the radiation took place when the speed passed under c . The arrow of time, which refers to the possibility that things have of knowing over time of irreversible changes or transformations, is in our equation a property of material phenomena since it originates from M_{vp}^2 . Secondly, the velocity c of the electromagnetic wavelength of space-time: when the universe became that of today, the kinetic energy and the density of the radiation diminished. The space-time line “ $t_o c$ ” conveys a field of less and less energetic bosons that propagates at the speed of light. Each second contains less energy-event, and the universe-as a whole-no longer changes significantly over the seconds.

4.2. Planck Units; Wall of Planck

At Planck time, that is during the oldest period of the universe which our only equations manage to conceive, the universe was nervous and dry, tiny and full of energy, and its space-time had a weird structure. The Planck wall is expressed in the form of a time, a length and a characteristic energy. Planck’s wall refers to circumstances in which the quantum and gravitational phenomena begin to really overlap. His description must involve together the constant of the gravitation G , the speed of the light c and the constant of Planck h . Their combination leads to the following results:

Planck energy is given by the expression $(hc^5/G)^{1/2}$. It is worth ten billion billion times the mass energy of a proton, or 10^{19} . Matter at that time was furiously agitated.

Planck length is given by the expression $(hG/c^3)^{1/2}$. It is about 10^{-35} meters, which is seventeen orders of magnitude less than the size of a quark or an electron. It is interpreted as saying that below this scale of distance, the notion of

space as we describe it in our physical theories no longer makes sense. Planck time is given by the expression $(hG/c^5)^{1/2}$. It is worth about 10^{-43} s. Planck wall applies to the universe as it was 10^{-43} s after the big bang [33]. The time t_o used at the Planck scale is a time during which the nascent universe was governed by quantum effects, a time during which the quantum and relativistic gravitational effects of Planck's units simultaneously become comparable. This suggests that the correct description of space-time-matter in the primordial universe requires a theory combining relativistic gravitation and quantum mechanics [45].

The theory of Relation offers an equation that integrates the two theories. We wrote it in (2) above [$ke^2 = M_{vp}^2 t_o c$, where M_{op} is rest-mass; $M_{op} \left(1/\left(1-v^2/c^2\right)^{1/2}\right)$, or M_{vp} , is rest-mass + kinetic energy (T)]. Particles come in pairs, each with a counterpart antiparticle:

$$\pm ke^2 = \pm \left[M_{op} / \left(1 - v^2/c^2\right)^{1/2} \right]^2 t_o c.$$

In our time ($v = 2/3c$), it becomes

$$2.3 \times 10^{-28} \text{ kg} \cdot \text{m}^3 \cdot \text{s}^{-2} = \left(2.2439 \times 10^{-27} \text{ kg}\right)^2 \left(1.528 \times 10^{17} \text{ s}\right) \left(3 \times 10^8\right).$$

But at the time of Planck's values, the antagonism between the two theories is appeased and they are brought together for the first time. If we apply

$$\pm ke^2 = \pm M_{vp}^2 t_o c = \pm M_{vp}^2 h/m_o c = \pm M_{vp}^2 2GM^o/c^2, \tag{10}$$

the mass of the "baryon-proton" M_{vp} will be

$$1.479 \times 10^3 \text{ kg} \left(2.3069 \times 10^{-28} = M_{vp}^2 3.51 \times 10^{-43} c\right).$$

The wavelength

$$\lambda = t_o c = R = h/(2\pi m_o c) = \hbar/(m_o c) = 1.05458 \times 10^{-34} \text{ m}.$$

We use \hbar with the Planck time (\hbar/c) and the Planck length: this is consistent with $t_o c$, which is linear, not circular. [It may seem odd to say that wavelength 1.05458×10^{-34} m numerically equals the value of \hbar in J sec (1.05458×10^{-34}). We explain it from the relation $Et = h$; $Et = 2\pi\hbar$; $(m_o c/2\pi)t_o c = \hbar$. Planck's mass [$ke^2 = M_{vp}^2 h/(m_o c)$; $2.3069 \times 10^{-28} = 2.1874 \times 10^6 h/(m_o c)$; $m_o = 2.0958 \times 10^{-8}$], in the expression $(m_o c/2\pi)$ gives 1, hence $t_o c = \hbar$.]

With the de Broglie wave that travels at the speed of light as that of the particle m_o , the boson m_o gives $2.09 \times 10^{-8} \text{ kg} (ke^2 = M_{vp}^2 h/m_o c)$. We employ $h/m_o c$ because quantum mechanics describes a particle, not a radius. Everything happens as if the light consisted of grains, and each grain of light had an energy proportional to the frequency ν of the light: $E = h\nu$. We write $\varepsilon = \hbar\omega = 2\pi\hbar\nu = h\nu$ (ω is the pulsation while ν is the frequency; $\omega = 2\pi\nu$). We have just equated \hbar with a wavelength, a distance, a radius, it goes without saying that $2\pi\hbar = h$ represents the circumference of a "quantum" of radiation energy, which constitutes a particle, hence the use of $h/m_o c$.

With $ke^2 = M_{vp}^2 2\pi GM^o/c^2$, general relativity determines the mass of the universe at Planck time, $M^o = 2.26 \times 10^{-8} \text{ kg}$. We utilize $2\pi GM^o/c^2$ (not

GM^o/c^2), considering that the term describes a mass with a circumference, not a radius.

Instead of having $M_{\text{Planck}} = (hc/2\pi G)^{1/2} = 2.1768 \times 10^{-8} \text{ kg}$, which seems to be one of two similar masses, we have $M^o m_o = hc/2\pi G$, which are two different masses: $m_o = 2.09 \times 10^{-8} \text{ kg}$ of quantum theory and $M^o = 2.26 \times 10^{-8} \text{ kg}$ of general relativity. The Planck mass $2.1768 \times 10^{-8} \text{ kg}$ is actually the average of these two distinct masses $(M^o m_o)^{1/2}$. Their numerical value corresponds to Planck mass $[(\hbar c/G)^{1/2} = 2.17682 \times 10^{-8} \text{ kg}]$ and they are reminiscent of the famous hidden variables.

4.3. The New Variable: M_{VP}^2

The new parameter M_{VP}^2 , or $[M_{op}/(1-v^2/c^2)^{1/2}]^2$, is an essential element. Its value changes throughout the expansion. The Lorentz transformation of this variable [12] inscribes the equation in a relativistic cosmology (although our mathematical model is central and global whereas general relativity is above all peripheral and local). The velocity v of this transformation, starting from the speed of light and moving towards 0 (it would be about $2/3c$ today), constitutes a variable velocity of light. Thus the limit of a signal it was thought up till now to be that first measured with the light waves was much greater at the beginning of the history of the universe.

The value of M_{VP}^2 (two protons relativized with a speed close to light) at Planck time is confused with the “isotope of the neutron” (also called “unique quantum”) of Lemaître or with the primitive atom of Gamow. A gigantic kinetic energy is stored in this very dense and very hot atom in the form of an electromagnetic mass. When all this energy is released, it appears in the universe in two forms: on the one hand the energy of the electromagnetic radiations, without mass; on the other hand, energy brought into play by mass movements, kinetic energy.

In our equation, $t_o c$ represents the emission of electromagnetic radiation, without mass. During the 380,000 years that followed the big bang, light could not propagate freely in space: the density of matter was such that photons never ceased to interact with particles of matter, so that the universe was an opaque medium to its own light. Its continuous cooling, however, eventually caused a phase change after 380,000 years of expansion, when the temperature of the universe was only 3000 Kelvins: the electrons were captured by nuclei, forming electrically neutral atoms. Since photons interact little with atoms, they can propagate freely in the universe, without encountering obstacles at every step. This radiation, which has been liberated from matter, now constitutes what is called the “cosmic microwave background” (detected in 1964 by Arno Penzias and Robert Wilson). It is the light predicted by the hot atom of George Gamow. It is the light predicts by George Gamow’s hot atom [33].

In the equation $ke^2 = M_{VP}^2 2\pi GM^o/c^2$ at Planck time, M_{VP}^2 represents the

kinetic energy of the universe while M^o of $2\pi GM^o/c^2$ represents its potential energy. During the initial explosion, the first stage of the big bang, M_{VP}^2 releases the extraordinary mass of inertia (due to resistance to movement, resistance to acceleration) that it contained. In the minutes following the big bang, some nuclear reactions occurred. Helium was then synthesized. The first stages of the expansion consisted of a rapid expansion determined by the energy-matter of the entire universe condensed in the initial quantum of Lemaitre, roughly equal to the mass of the universe. If we admit that cosmic radiation was emitted during the first fragmentations of the universe, it would correspond to transformations of the kind that accompany the radioactive phenomena that we know, but with a considerably greater generality. Often, during the same phenomenon, radioactivity manifests itself in the form of disintegration, α endowed with mass, on the other hand in the form of electromagnetic energy, the emission of a ray γ , without mass. The ratio between the wavelength of space-time and the wavelength of cosmic gamma rays is $(10^{26} \text{ m}/10^{-14} \text{ m}) \approx 10^{40}$.

Thus the cosmic rays would be the witnesses of the primitive activity of the cosmos, and it would have preserved, for billions of years, in the empty space, the memory of the super-radioactive age. We endorse Lemaitre's hypothesis, and it is probable that it will eventually be verified.

5. Discussion on the Model of the Theory of Relation and That of the Classic Big Bang Theory

All the models proposed by Lemaitre, and consolidated by Gamow, concerning the expansion of space refer to the Einstein-Friedmann equation. The relativistic cosmology that emerges is at the origin of the standard cosmology of the big bang which succeeds in giving the approximate age of the expanding universe, its previous and future history, as well as, in our view, the irrational drift of the acceleration of the expansion. However, the first big bang models only take into account gravitation, described using the formalism of general relativity. They have nothing to do with quanta and electromagnetic interactions, strong nuclear and weak, which determine the behavior of the matter at the beginning [33].

The equation that we propose, developed in a previous work [3], although it has nothing to do with the equation of Einstein-Friedmann, gives results of the same order on the age of the universe, as well as with the results obtained by Hubble or by the analysis of the cosmic microwave background. It is truly suitable for "quantum cosmology": it has its source in quantum mechanics and also relies on relativistic cosmology derived from the theory of general relativity. It brings a different theoretical background on the quantum origin of the universe, integrates an irreversible cosmological time, gives a new light on the cosmological constant, the energy of the vacuum and the dark energy. It has the advantage of being able to teach us a lot about the internal structure of the universe, since this structure is included in the model. It reveals the fundamental role played by the energy of the quantum vacuum, both in the birth process of the universe and

in the expansion phase resulting from it. It introduces negative energy. It predicts an expanding universe in constant deceleration and contradicts the accelerated expansion phase that currently appears to be in effect.

The quantum cosmology of the theory of Relation aims to describe the evolution of the universe as a whole from a quantum point of view through a “space-time wave function of the universe”, but does not necessarily imply the quantification of gravitation. It must be recognized that quantum cosmology is not a theory of quantum gravity. The latter seeks to describe phenomena on a very small scale and does not necessarily imply the description of the universe as a whole. Several hypotheses are candidates for quantum gravity, although we aspire to a unique, coherent and conceptually satisfactory theory, of which quantum mechanics and general relativity are only valid approximations in their respective domains [45].

In an article in the journal *Astrophysical Journal* [46], a team of astronomers led by Fred Hoyle asserted that it is possible to design a cosmology without resorting to the classical big bang theory. Already in the fifties, Fred Hoyle had supported a theory opposed to that of the big bang, known as the theory of “stationary state” or “continuous creation”. He came back, more than forty years later, with a model partly identical to the one he had to abandon. With a difference in size however: if the idea of continuous creation is saved, it no longer occurs anywhere in space but in privileged places. And there would not have been an initial explosion but infinity of mini-big-bang. And here is transgressed the taboo theory of the big bang by astronomers who claim that there was not a unique and creative big bang but repetitive mini big bang that make the history of the universe an eternal re-beginning [47].

In a very broad way, our model considers the universe as a fragment of multiverse, which is like a soup pot boiling perpetually; continually forming new bubbles. These eventually grow and burst, but the soup jar is eternal. Each of them is a universe started by a big bang. Often these bubbles-big bang come from internal bubbles of the pot which ended in big crush. The latter becomes the big bang of a universe like ours. Thus can be explained the contradictory duality of our universe. Our universe was given birth by another universe which continues its childbirth by disintegrating in our universe.

Everything happens as the two universes coexisted, as if there were two universes in one, ours which is formed on the account of a universe that never stops disintegrating [5]. Because of the inversion of the arrow of cosmological time, based on the laws of the thermodynamics, the energy of the world which contracted is negative in relation to the positive energy of our expanding world. Yet, on the grounds that the existence of particles of negative energy would not be in accordance with the observable reality, it is half of our universe that is denied [48].

The existence of particles of negative energy has been scratched by a stroke of pen by most physicists. It is nevertheless part of the results obtained by Dirac in

his formulation of the equations of quantum mechanics [49]. These equations, which remain the foundation of quantum theory, reveal a continuum of states of negative energy. If we consider the binding energy of a hydrogen atom, the equations describe a whole series of possible energies, with a minimal state of energy. Below this state of minimum positive energy, the energy becomes zero over a very long vacuum interval, then reappears in negative form, and develops in the other direction with infinity of states. From a conventional point of view, these states of negative energy are considered supernumerary and superfluous, but for Dirac, these states had a reality. It is by calculating from these states of negative energy that he predicts the existence of the positron. The experiment gave him reason. This arbitrary decision by physicists to discard this type of particle of negative energy, explicitly provided by the Dirac equations, today distorts all the reasoning of cosmological physics. This question was the subject of two previous articles [32] [50].

Astrophysicists would do well to question the basis of their creed. Besides starting from a beginning of which we know nothing, whether by observation or experimentation, that it does not meet the basic criteria of science, the standard big bang theory is contradicted by several current observations, which are ignored. For example, the subtle observations made by astronomers at the Bura-kan Observatory (of the Armenian Academy of Sciences), of which Viktor Am-bartsumian was the director, have been left aside. The work of Armenian astro-nomers confirmed the new hypothesis of star formation according to which the evolution was from condensation to rarefaction, from hyperdense bodies to less dense bodies. They further confirmed that the birthplaces of the new galaxies were the centers of the old galaxies. The latter swell, from time to time, show a tendency to divide and eject powerful gas clouds containing free electrons that explain the powerful radio-ray emission. Rapid protons give birth to cosmic par-ticles. They confirmed the theory of the division of galaxies: they noticed that in some cases, from the center of a giant galaxy escaped a jet that ended in a dwarf galaxy whose color, unlike the “old galaxies”, yellow and red, was blue. It was a birth of a small galaxy by a big one. Over time, the jet binding—a kind of “um-bilical cord”—should disappear, giving the “offspring” the opportunity to start an independent life. Such dwarf galaxies were discovered near many supergalax-ies [51] [52].

Because standard theory cannot explain certain phenomena, its advocates have developed an ability to systematically ignore these facts [53]. Observations show, contrary to the Lemaître-Gamow postulate, that stars and galaxies have not structured in one go and that their age can be very different. Does this mean that we must, however, invalidate the hypothesis of the primitive atom for the entire cosmos? Certainly not.

We believe that our universe undergoes both processes. This would be ex-plaind as follows: About 15 billion years ago (at the Planck scale, and not at ab-solute zero), the primary matter, then dense and hot, began its expansion. The

expansion would have been preceded by a period of contraction and it would not have occurred at the same time for all the matter. In the world in contraction, some of the matter has contracted faster than the other, giving the big crush which is for us the big bang. The first process would be that the kinetic energy of the primordial explosion that spawned the expansion would be counterbalanced by the gravitational attraction that caused in the early days of the universe the formation of much of the condensed objects (atoms, molecules, stars...). The sequence density variation-gravitational collapse-accretion would be the prerogative of the standard model. The second process concerns isolated pieces of material from the pre-universe that contracted and that would have been delayed in their appearance and development. These would be pre-existing hyperdense material nuclei as a starting point for galactic or stellar formations. These phenomena are observed and localized in time and space. They would come from the latent matter which, at the end of a certain time, appears, expands in turn, begins to interact with the surrounding environment, generating the hotspots of intense radiation and violent patterns that we are currently seeing. The violent explosive effect of a strong negative pressure within a localized region where an important mechanism of creation has occurred, for example active galactic nuclei, produces an ejection from this region.

Photos taken by specialists have shown the phenomenon of ejection. Examples have been provided. There are a large number of objects whose figures give examples of direct evidence that discrete objects—galaxies or quasars—with a strong redshift are ejected from low redshift galactic nuclei. Standard theory offers no explanation for this type of phenomenon, which its defenders have continued to ignore. Yet these are real facts.

Even if we accept with caution the hypothesis of Ambartzoumian, according to which these stellar formations would have for origin a prior concentration of hyperdense matter (nuclear plasma) in proto-stars, it is nevertheless true that, often, everything takes place, not as if stars clustered into galaxies, but rather as if the stars were formed somehow from a galactic core (itself hyperdense) since the galaxies, composed of billions of stars, then develop in the aspect that we know them, with their own rotational movement. Physicist Milne has already tried to reconcile the thesis of the primitive atom with the continuous formation of stars or galaxies and with their evolution. While retaining the idea of an initial explosion of all matter concentrated “somewhere” at the instant “zero”—explosion causing by molecular dispersion the creation of a space in constant expansion over time, Milne admitted, however, that the particles were grouped progressively to form stars then stellar systems. Subsequent observations have shown that stars are born in groups within galaxies, and then separate from each other.

The above development would seem to imply—if we accept Ambartzoumian’s conception of the prior existence of proto-stars—that hyperdense nuclei have themselves preceded the formation of galaxies. The proto-stars could be only fragments of these nuclei, which, by splitting themselves primitively, could have

given rise to the formation in groups (or at least in pairs) of galaxies. This, which is no longer a simple view of the mind, concurs, in a certain way, with Lemaître's cosmogonic hypothesis in 1931 according to which the present world has resulted from the radioactive decay of an atom. Guided by thermodynamic considerations that sought to interpret the law of the degradation of energy within the framework of quantum theories, the discovery of the universality of radioactivity, since then, makes more plausible its suggestion which assigned a radioactive origin to all the existing cosmic matter as well as the most powerful cosmic rays that would be the relics of the primitive universe.

6. Conclusions

The year 1998 is that of a spectacular twist: the experimental discovery of the acceleration of the expansion of the universe. Astrophysicists have observed several distant supernovae of type 1a acting as luminous stallions. The results indicate that they seem more distant than expected. Their position suggests that the expansion of the universe would have been accelerating for at least six billion years. On the other hand, the very distant galaxies in which the type 1a supernovae explode show a slowing of their recession velocity, sign that the expansion of the universe has been slowed down in the first billions of years. They concluded overnight without discussion that the acceleration of distant supernovae would result from a dark, hypothetical and invisible energy, which could be a quantum vacuum energy in the form of a positive cosmological constant. The problem is that the value of the quantum vacuum energy deduced from astronomy, which seems to be 10^{120} times too high compared to what the observations indicate and to the value calculated by the theoretical physicists. Explicitly and approximately, the vacuum energy density proposed by quantum field theory is about 10^{121} GeV/m³, which corresponds to about 10^{121} protons/m³. The value of the current cosmological medium is 10 GeV/m³ or about 10 protons/m³. The gigantic gap between the two is what is called the vacuum catastrophe [31] [33].

In our view, we are witnessing a farce of official science. First, the technique of measuring astrophysical distances using supernovae cannot be trusted. Astronomers assume that the intrinsic brightness of the supernovae is the same for all, independent of the particular object being measured. This hypothesis, impossible to prove, is free. The chemical composition of the first supernovae was necessary of a composition different from that of now since the generations of stars had not yet succeeded one another to make the heavy elements. Then, considering what physicists know about radioactivity and cosmic radiation, the researchers thought they were right that the cosmological constant should be several orders of magnitude larger than the density of ordinary matter. It was enough to introduce into the equations a simple parameter, dark antigravitational energy appeared and it is done. The fact is that cosmological observations indicate a low vacuum energy and a cosmological constant with a near zero density [21].

The problem of the cosmological constant (or the vacuum energy) constitutes

the greatest challenge of contemporary theoretical physics. Many theoreticians sense that the resolution of this major conflict could perhaps lead to the unification of gravity and quantum theory. For more than half a century, two tracks have been followed to quantify gravitation. The string theory which favors the geometric approach of general relativity and the theory of loops which prioritizes the quantum approach of fields. Whatever may be said about these two promising theories, and other approaches, these have not yet yielded results in terms of prediction or experimentation. Moreover, they lack a basic, coherent and unique equation, which translates simple laws leading to unification.

We claim to have such an equation whose master key is time. If the mathematical story told by the standard model springs from a mathematical singularity, the equation presents a non-singular physical beginning in the form of a “fireball” which represents the physical birth certificate of the universe. This material content that cools when expanding gives birth to space-time. The time t_o of the expression $t_o c$ makes impasse on the question of the genesis (initial singularity) to concern itself only with the immediately subsequent cosmological events (Planck era). The equation of theory of Relation therefore presents a universe governed by the laws of mathematical physics that incorporates a time that becomes a unit of measurement, which gives a thermal history and legitimacy to the existence of things. It bridges the gap of 10^{60} orders of magnitude separating the quantum mechanics of the subatomic world from the astronomical scale of general relativity by a cosmological time that extends between a time of 10^{-43} s and a time of 10^{17} s. It is proof that both quantum theory and general relativity are wrong about the nature of time that constitutes cosmological history [31] [54].

This cosmological time which defines the notions of space and time between this beginning of space-time and now gives meaning to the laws of physics as we know it. It merges with the vacuum energy, or a dark energy, that empties the universe by never ceasing to dilute itself in favor of ordinary matter. The model of the theory of Relation also attempts to reconcile the dynamic aspects of the big bang theory with the eternal nature of continuous creation. It strives to create a bridge between the competing cosmological models: the idealistic models that presuppose the creation of an incredible density nucleus containing all the matter and the energy of the universe, which nucleus would have disintegrated once for all, and the materialistic models that conceive pre-existing hyperdense nuclei as a starting point for galactic or stellar formations.

We believe that this equation, which contrasts with the current popular view of cosmology and cosmogony, is closest to the equation that Lemaître lacked to defend his “primeval atom hypothesis” and his prediction of fossil cosmic rays, witnesses of the primitive activity of the cosmos.

Conflicts of Interest

The author declares no conflicts of interest regarding the publication of this paper.

References

- [1] Lemaître, G. (1931) *Monthly Notices of the Royal Astronomical Society*, **91**, 490-501. <https://doi.org/10.1093/mnras/91.5.490>
- [2] Luminet, J.-P. (2004) *L'invention du Big Bang*. Éditions du Seuil, Paris, 111-126, 151, 159, 163, 194, 196, 203, 210.
- [3] Bagdoo, R. (2019) *Journal of Modern Physics*, **10**, 310-343. <https://doi.org/10.4236/jmp.2019.103022>
- [4] Stein, J.D. (2011) *Cosmic Numbers*. Basic Books, New York, 199-201.
- [5] Bagdoo, R. (2008) The Pioneer Effect: A New Theory with a New Principle. <http://vixra.org/abs/0812.0005>
<https://www.academia.edu/5535864>
- [6] Bagdoo, R. (2011) Cosmological Inconstant, Supernovæ 1a and Decelerating Expansion. <https://www.academia.edu/5539777>
<http://vixra.org/abs/1304.0169>
- [7] Guy, J., *et al.* (2010) *Astronomy & Astrophysics*, **523**, A7. <https://doi.org/10.1051/0004-6361/201014468>
- [8] Blanchard, A. (2005) Cosmological Interpretation from High Redshift Clusters Observed within the XMM-Newton Ω -Project. *Proceedings of the International Conference DARK2004*, College Station, 3-9 October 2004, 34-46.
- [9] Vishwakarma, R.G. (2003) *Monthly Notices of the Royal Astronomical Society*, **345**, 545-551. <https://doi.org/10.1046/j.1365-8711.2003.06960.x>
- [10] Vishwakarma, R.G. and Narlikar, J.V. (2010) *Research in Astronomy and Astrophysics*, **10**, 1195-1198. <https://doi.org/10.1088/1674-4527/10/12/001>
- [11] Kowalski, M., *et al.* (2008) *The Astrophysical Journal*, **686**, 749-778.
- [12] Nielsen, J.T., Guffanti, A. and Sarkar, S. (2016) *Scientific Reports*, **6**, Article No. 35596. <https://doi.org/10.1038/srep35596>
- [13] Crew, B. (2016) No, The Universe Is Not Expanding at an Accelerated Rate, Say Physicists, 24 Oct. <https://www.sciencealert.com>
- [14] European Space Agency News Release (2003) Has XMM-Newton Cast Doubt over Dark Energy?
- [15] Hubble, E. and Tolman, R.C. (1935) *Astrophysical Journal*, **82**, 302. <https://doi.org/10.1086/143682>
- [16] Kaku, M. and Trainer, J. (1987) *Beyond Einstein*. Bantam New Age, New York, 10-20-1, 30-1, 35.
- [17] Will, C.M. (1986) *Was Einstein Right?* Basic Books Inc., New York, 153, 166-167.
- [18] Gamow, G. (1963) *La Gravitation*. Payot, Paris, 134-139.
- [19] Bramand, P., Faye, P. and Thomassier, G. (1980) *Physique, Terminale C*, E. Eurin-Hachette, Paris, 52-55.
- [20] Nottale, L. (1997) *L'Univers et la lumière*, Champs. Flammarion, Paris, 141.
- [21] Magnan, C. (2011) *Le théorème du jardin*. amds édition, 127, 160-1, 168-9, 247-8, 263.
- [22] Narlikar, J.V. (1986) *Une gravitation sans gravité*. Payot, Paris, 175.
- [23] Orear, J. (1967) *Fundamental Physics*. John Wiley & Sons, Inc., New York, 87, 100, 156, 284-287.
- [24] Davies, P.C.W. and Brown, J. (1988) *Superspring*. Cambridge University Press,

- Cambridge, 5, 26, 27, 47.
- [25] Silk, J. (1997) *Le Big Bang*. Éditions Odile Jacob, Paris, 10.
- [26] Moffat, J.W. (2009) *Reinventing Gravity*. Thomas Allens Publishers, Toronto, 121, 122, 162, 206-208.
- [27] Michaud, A. (2017) *Electromagnetic Mechanics of Elementary Particles*. 2nd Edition, Scholars' Press, Berlin, 205-223.
- [28] Hawking, S.W. (1988) *Physics Today*, **41**, 115. <https://doi.org/10.1063/1.2811637>
- [29] Klein, É. (2018) *Les secrets de la matière*. Édition j'ai lu, Paris, 83-84.
- [30] Narlikar, *et al.* (2002) *PASP*, **114**, 1092. <https://doi.org/10.1086/342374>
- [31] Gunzig, E. (2008) *Que faisiez-vous avant le big-bang?* Odile Jacob, Paris, 162, 200, 218, 218, 219.
- [32] Bagdoo, R. (2019) *Journal of Modern Physics*, **10**, 163-175. <https://doi.org/10.4236/jmp.2019.102013>
- [33] Klein, É. (2010) *Discours sur l'origine de l'univers*. Champs Sciences, Paris, 34-36, 46, 57-59, 65, 66, 116-118.
- [34] Landa, P. (2016) *Georges Lemaître: The Big Bang Theory and the Origins of Our Universe*. 50Minutes.com, USA Columbia, SC, 16-18.
- [35] Lemaître, G. (1945) *L'hypothèse de l'atome primitif*, Actes de la Société Helvétique des sciences naturelles. 77-96.
- [36] Gamow, G. (1961) *La création de l'univers*. Dunod, Paris, 30-36.
- [37] Farrell, J. (2010) *The Day without Yesterday*. Basic Books, New York, 135, 136.
- [38] Leprince-Ringuet, L. (1948) *Les rayons cosmiques*. Albin Michel, Paris, 349, 350.
- [39] Greene, B. (1999) *The Elegant Universe*. Vintage Books, Random House, Inc., New York, 83.
- [40] Pagels, H.R. (1982) *The Cosmic Code*. Bantam New Age Book, New York, 5, 9, 237-243.
- [41] Klein, É. (2009) *Le facteur temps ne sonne jamais deux fois*. Flammarion Champs Sciences, Paris, 41, 164, 165. <https://doi.org/10.14375/NP.9782081220225>
- [42] Susskind, L. (2007) *Le paysage cosmique, folio essais*. 235, 251, 252.
- [43] Damour, T. (2016) *Si Einstein m'était conté...* Flammarion, Champs, Paris, 153, 252, 277, 278.
- [44] Klein, É. (2009) *Les tactiques de Chronos*. Flammarion, Champs essais, Paris, 43, 126, 128, 153, 177, 178
- [45] Luminet, J.-P. (2006) *Le Destin de l'Univers II*. Librairie Arthème Fayard, Paris, 561, 563-568.
- [46] Hoyle, F., Burbidge, G. and Narlikar, J.V. (1993) *The Astrophysical Journal*, **410**, 437-457. <https://doi.org/10.1086/172761>
- [47] Andrillat, H. (1994) *Science & Vie*, No. 916, 33-35.
- [48] Petit, J.-P. (1997) *On a perdu la moitié de l'univers*. Edition Albin Michel, S.A., Paris, 10, 11.
- [49] Davies, P. (1988) *The Forces of Nature*. Cambridge University Press, Cambridge, 53-58.
- [50] Bagdoo, R. (2013) *The Energy in Virtue of the Principle of Compensation*. <http://vixra.org/abs/1301.0180>
<https://www.academia.edu/5539802>

- [51] Hoyle, F., Burbidge, G. and Narlikar, J.V. (1998) Le big bang, une conception bien fumeuse. In: *La Recherche*, Hors Série Cosmologie No. 1, 104-108.
- [52] Radounskaïa, I. (1972) Les idées "folles". Editions Mir, U.R.S.S., Moscow, 145, 366-374.
- [53] Cuny, H. (1961) *Astronomie d'aujourd'hui*. Editions La Farandole, Paris, 62-68.
- [54] Smolin, L. (2006) *The Trouble with Physics*. Mariner Books, Wilmington, 256.

A Band Theory Perspective on Molecular Orbitals in Complex Oxides

Kateryna Foyevtsova^{1,2}, George A. Sawatzky^{1,2}

¹Department of Physics & Astronomy, University of British Columbia, Vancouver, BC, Canada

²Stewart Blusson Quantum Matter Institute, University of British Columbia, Vancouver, BC, Canada

Email: foyevtsova@phas.ubc.ca

How to cite this paper: Foyevtsova, K. and Sawatzky, G.A. (2019) A Band Theory Perspective on Molecular Orbitals in Complex Oxides. *Journal of Modern Physics*, 10, 953-965.

<https://doi.org/10.4236/jmp.2019.108062>

Received: May 20, 2019

Accepted: July 6, 2019

Published: July 9, 2019

Copyright © 2019 by author(s) and Scientific Research Publishing Inc.

This work is licensed under the Creative Commons Attribution International License (CC BY 4.0).

<http://creativecommons.org/licenses/by/4.0/>



Open Access

Abstract

In view of the growing interest in molecular orbitals (MOs) encountered in certain complex oxides, we review some of their properties from the band theory perspective and provide detailed examples based on real materials. Our discussion includes some technical aspects of identifying MOs in electronic structure calculations and considers cases when MOs can be both orthogonal and non-orthogonal. We also describe orthonormalization of MOs, a procedure converting them into Wannier functions, and discuss the problem of Wannier functions possibly being rather spatially extended and how using MO, rather than atomic orbital, based effective Hamiltonians might be a better choice in describing certain strongly correlated systems as well as systems with strong electron-phonon coupling. Furthermore, we address the problem of strongly correlated MOs and how it can be treated in band theory calculations.

Keywords

Electronic Structure of Solids, Molecular Orbitals, Complex Oxides, Negative Charge-Transfer Insulators

1. Introduction

Ligand molecular orbitals (MOs) have been recognized as important players in the physics of transition-metal compounds since the introduction of the Zhang-Rice singlet back in 1988 [1]. They have recently gained a renewed interest after the concept of oxygen MOs strongly coupled to lattice degrees of freedom in a polaronic way was used to describe rare-earth nickelates [2] [3] and superconducting bismuthates [4] [5] [6]. Ligand MOs are particularly important in negative charge-transfer and hole-doped charge-transfer insulators, where of-

ten they are the orbitals that end up being occupied by the (self-)doped holes and therefore have a direct impact on the system's low-energy properties [7]. Among this important class of materials are such vigorously discussed but still controversial systems as superconducting cuprates [8] [9] and bismuthates [10] [11] [12], rare-earth nickelates [13], and transition-metal oxide based Li-ion battery cathode materials [14] [15]. Since this topic is expected to generate only more interest in the future, the current paper will present a band theory perspective on some important aspects of MOs in complex oxides, including the mathematical construction of MO-based basis sets (Section 2), the non-orthogonality problem (Section 3), their usage in effective models in the presence of strong electron-phonon coupling (Section 4), as well as the problem of a proper treatment of strong local correlations on MOs (Section 5); conclusions will be given in Section 6. Each part of the discussion will include a detailed example of a real material.

2. Projecting Electronic States onto Molecular Orbitals (NaNiO₂ as an Example)

Let us consider the prototypical negative charge-transfer insulator NaNiO₂ as our first example. Its monoclinic $C2/m$ crystal structure consists of triangular layers of edge-sharing cooperatively elongated NiO₆ octahedra intercalated with Na⁺ ions, with one formula unit per primitive unit cell [16]. Although here Ni has a formal valency of 3+, spectroscopic studies clearly show the abundant presence of oxygen holes which suggest an actual electronic configuration of Ni²⁺ \underline{L} , where \underline{L} is an oxygen hole [17]. This three-hole state has a net spin of ½ and would formally correspond to Ni³⁺ (e_g^3) with spin 1/2, which is quite contrary to what one would expect from Hund's rules if it really were Ni³⁺. Due to the strong hybridization between the Ni- e_g orbitals and the oxygen MOs of respective symmetry, the oxygen holes select to occupy the O- (x^2-y^2) MOs, one hole per oxygen octahedron, and form a Zhang-Rice-like spin singlet state with the hole in the Ni- (x^2-y^2) orbital. This selective occupation of the (x^2-y^2) MOs by the holes, which results in the mentioned cooperative elongation of the NiO₆ octahedra, constitutes a molecular orbital (or band) Jahn-Teller effect.

A way of verifying and visualizing this picture using band theory is to perform a projection of the NaNiO₂ electronic structure on a MO-based basis set. We note, however, that band theory is unable to fully capture the multi-determinant character of the spin singlet state in question and will underestimate the energy of the singlet as $\frac{1}{4}J_{pd}$ rather than $\frac{3}{4}J_{pd}$, where J_{pd} is the spin exchange coupling between interacting atomic d and molecular p states. Still, it provides a fair description of on-site symmetries and spin densities, worth exploring with the projection technique.

Figure 1(a) shows the calculated NaNiO₂ density of states (DOS) projected onto the Ni- $3d$ orbitals (left) and the oxygen molecular orbitals (right) for the majority and minority spin channels. This is a spin-polarized local density

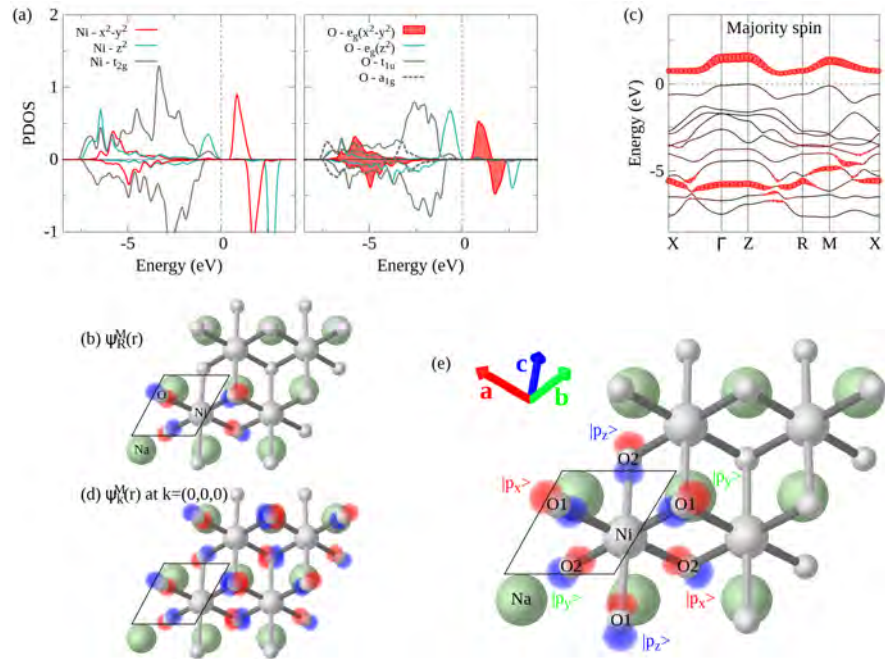


Figure 1. Oxygen molecular orbitals in NaNiO_2 . (a) Projected densities of states (PDOS) per formula unit for the Ni— $3d$ atomic orbitals and the oxygen MOs. (b) An isolated oxygen— (x^2-y^2) MO $\psi_R^M(\mathbf{r})$. The primitive cell comprising a single formula unit is marked with black lines. The short Ni—O bonds in the elongated octahedra are colored in a darker grey color than the long ones. (c) The majority spin band structure with the oxygen— (x^2-y^2) character highlighted in red. (d) An oxygen— (x^2-y^2) Bloch function $\psi_R^M(\mathbf{r})$ at the Γ point. In (a) and (c) the Fermi level is set to zero and marked with a dashed line. (e) Oxygen— p_o orbitals are in fact the $|p_x\rangle$, $|p_y\rangle$, and $|p_z\rangle$ orbitals of the two inequivalent oxygens O1 and O2 in a unit cell, but each coming from an oxygen belonging to a different unit cell.

approximation + U (LDA + U) [18] [19] calculation (on-site Coulomb repulsion $U = 6$ eV, Hund's exchange interaction $J_H = 1$ eV for Ni— $3d$ electrons [20]) performed, like the rest of the calculations presented in this paper, using the linearized augmented plane waves method implemented in the Wien2k package [21]. A ferromagnetic order of Ni magnetic moments, both within and between the Ni planes, is assumed for simplicity. The majority spin hole has a mixed character of the Ni— (x^2-y^2) atomic orbital and the oxygen— (x^2-y^2) molecular orbital, which is a result of strong hybridization between these orbitals. This hole state is the anti-bonding combination of the two orbitals pushed up in energy above the Fermi level, while the bonding combination lands at about -5 eV below the Fermi level. An isolated oxygen— (x^2-y^2) molecular orbital $\psi_R^M(\mathbf{r})$ centered at a Ni site \mathbf{R} is shown in **Figure 1(b)**, but the actual projection of the DOS [**Figure 1(a)**] or the \mathbf{k} -resolved projection of the band structure [**Figure 1(c)**] are performed onto the Bloch functions $\psi_k^M(\mathbf{r})$ constructed from $\psi_R^M(\mathbf{r})$:

$$\psi_k^M(\mathbf{r}) = \sum_{\mathbf{R}} \psi_R^M(\mathbf{r}) e^{-i\mathbf{k}\mathbf{R}}, \quad (1)$$

where M indicates an MO character of the wave function and \mathbf{k} is the crystal

wave vector. To give a visual example, we show the oxygen— (x^2-y^2) MO Bloch function at the Γ point [$\mathbf{k} = (0, 0, 0)$] in **Figure 1(d)**.

Generally speaking, MO Bloch functions $\psi_{\mathbf{k}}^{M_i}(\mathbf{r})$ can be obtained from the atomic orbital Bloch functions $\psi_{\mathbf{k}}^{a_j}(\mathbf{r})$ via a unitary transformation $\mathcal{U}(\mathbf{k})$:

$$\psi_{\mathbf{k}}^{M_i}(\mathbf{r}) = \sum_j U_{ij}(\mathbf{k}) \psi_{\mathbf{k}}^{a_j}(\mathbf{r}). \quad (2)$$

Allowing for the \mathbf{k} -dependence of the transformation matrix elements $U_{ij}(\mathbf{k})$ reflects the fact that an MO can be built from atomic orbitals nominally belonging to different unit cells. This is, for instance, the case for the oxygen— (x^2-y^2) MO shown in **Figure 1(b)**, where the oxygen— p_σ orbitals to the left of the Ni atom and those to its right belong to different unit cells. **Figure 1(e)** explains in further detail that the six oxygen p_σ orbitals on a given NiO_6 octahedron are in fact the $|p_x\rangle$, $|p_y\rangle$, and $|p_z\rangle$ orbitals of the two inequivalent oxygens O1 and O2 in a unit cell, but each coming from an oxygen belonging to a different unit cell. In a way, using a \mathbf{k} -dependent unitary transformation matrix $\mathcal{U}(\mathbf{k})$ broadens the technical definition of a unit cell as used in band-structure calculations for the purpose of setting up a Bloch basis set, where now atomic orbitals from the same atom can belong to different unit cells as in the case of NaNiO_2 .

Let us also note that if a MO character of an electronic state shows very little variation with \mathbf{k} -vector this should be regarded as a sign of the robustness of the molecular nature of this state in real space. As one can see in **Figure 1(c)**, this is the case for our example of NaNiO_2 , where indeed the majority spin hole state has a strong oxygen— (x^2-y^2) character at every \mathbf{k} -vector.

Although in the charge- and negative charge-transfer systems it is very typical for the ligand holes to occupy MOs of the same symmetry as that of the cation atomic orbitals that they hybridize with [like the oxygen— (x^2-y^2) MO and the Ni— (x^2-y^2) atomic orbital in NaNiO_2], there are a number of notable exceptions. For example, in the iron disulfide FeS_2 (pyrite structure) and the recently discussed iron dioxide FeO_2 [22], the ligand holes reside on the MOs formed on sulfur/oxygen dimers owing to strong intra-dimer hybridization between the sulfur/oxygen— p_σ orbitals. The same is the case in the superoxides like KO_2 , where oxygen dimers have a net spin of 1/2 and which order magnetically below the ordering temperature.

As a final technical remark for this section, our MO projections are performed using atomic-like functions $|u_i^{\alpha,\sigma}(E_{ll})Y_m^l\rangle$, which are the solutions of the Schrödinger equation within the muffin-tin sphere of atom α at the linearization energy E_{ll} and where $|Y_m^l\rangle$ are spherical harmonics, to construct molecular orbitals. This is in some contrast with the approach adopted in Wien2k, where atomic orbital projections are done onto the spherical harmonics $|Y_m^l\rangle$ inside muffin-tin spheres. In practice, the two approaches give very similar results for the projected DOS, but having also the radial part $u_i^{\alpha,\sigma}(E_{ll}, r)$ means that projections are being done on a true atomic-like orbital (or molecular orbital combination), which, in particular, enables their visualization in real space.

3. Non-Orthogonality (BaBiO₃ as an Example)

For certain lattice structures—including those of the cuprates, with their characteristic two-dimensional square CuO₂ planes, as well as of the bismuth and nickel perovskites—construction of MOs may also require their proper orthonormalization performed on top of the unitary basis transformation discussed above. In this regard, let us consider the example of the barium bismuth perovskite BaBiO₃. In a perovskite lattice structure of the ABO₃ type [Figure 2(a)], neighboring BO₆ octahedra share their corners such that the O-B-O angle is equal or close to 180°. As a result, the oxygen-*p*_σ orbitals, typically involved in the formation of MOs, have to be shared between neighboring B cations. In the case of BaBiO₃, the MO of most importance is oxygen-*a*_{1g}, shown in Figure 2(a), due to its strong hybridization with the Bi-6*s* atomic orbital. However, because of the problem of a common oxygen-*p*_σ orbital, neighboring oxygen-*a*_{1g} MOs are *non-orthogonal* to each other. If no orthonormalization is done to such MOs, the Bloch functions constructed out of them will have a *k*-vector dependent overlap integral, $\langle \psi_{\mathbf{k}}^M | \psi_{\mathbf{k}}^M \rangle$, and may even completely vanish at certain *k*-points. As demonstrated pictorially in Figure 2(c) & Figure 2(d) and also shown in the LDA band structure calculation in Figure 2(b), this is the case for the oxygen-*a*_{1g} MO in BaBiO₃ at the Γ point.

In order to be suitable for use in effective models, MOs of this kind need to be orthonormalized first. As was originally shown by Zhang and Rice [1], the *k*-vector dependent normalization factor $\beta_{\mathbf{k}}$,

$$|\beta_{\mathbf{k}}|^2 \langle \psi_{\mathbf{k}}^M | \psi_{\mathbf{k}}^M \rangle = 1, \quad (3)$$

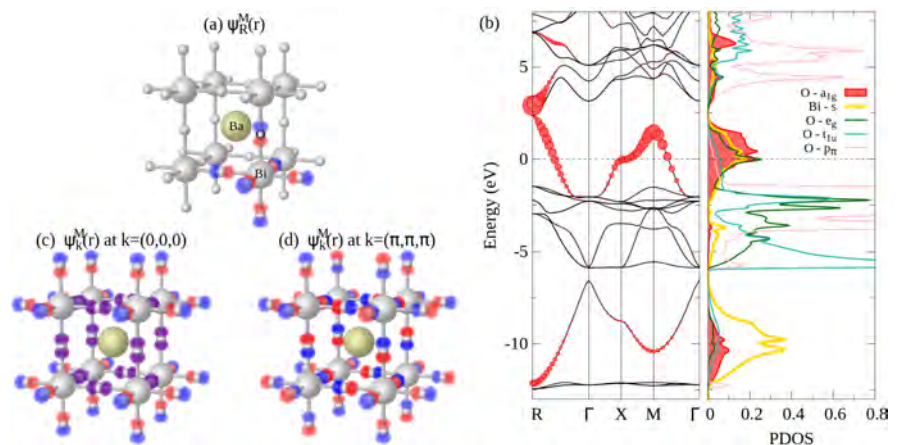


Figure 2. Oxygen molecular orbitals in BaBiO₃. (a) An idealized (e.g., without octahedra's rotations or bond disproportionation) cubic perovskite crystal structure of BaBiO₃, with one formula unit per unit cell, featuring also an isolated oxygen-*a*_{1g} MO $\psi_{\mathbf{R}}^M(\mathbf{r})$. (b) Projection of the BaBiO₃ electronic states onto oxygen MOs; the Fermi level is marked with a dashed line. (c) and (d) show oxygen-*a*_{1g} MO Bloch functions at the Γ [$\mathbf{k} = (0, 0, 0)$] and R [$\mathbf{k} = (\pi, \pi, \pi)$] points, respectively. Note that at the Γ point the individual $\psi_{\mathbf{R}}^M(\mathbf{r})$ contributions completely cancel out due to their non-orthogonality, which results in vanishing oxygen-*a*_{1g} MO weight at this *k*-vector in (b).

may be ill-defined at certain \mathbf{k} -points. For the oxygen— a_{1g} MO in BaBiO₃, for example, it diverges at the Γ point:

$$\beta_{\mathbf{k}} = \left[1 - \frac{1}{3} (\cos k_x + \cos k_y + \cos k_z) \right]^{-1/2}, \quad (4)$$

as obtained using the oxygen— a_{1g} MO given by

$$|\psi_{\mathbf{k}}^{a_{1g}}\rangle = \frac{1}{\sqrt{6}} \left[|p_{\mathbf{k}}^x\rangle (1 - e^{-iak_x}) + |p_{\mathbf{k}}^y\rangle (1 - e^{-iak_y}) + |p_{\mathbf{k}}^z\rangle (1 - e^{-iak_z}) \right], \quad (5)$$

where $|p_{\mathbf{k}}^i\rangle$, $i = x, y, z$, are the Bloch functions of orthonormal oxygen— p_{σ} orbitals and a is the cubic lattice constant. Let us note that an MO with contributions from both the oxygen— a_{1g} MO and the Bi— $6s$ atomic orbital $|s_{\mathbf{k}}\rangle$,

$$|\psi_{\mathbf{k}}^{s-a_{1g}}\rangle = \frac{1}{\sqrt{\alpha^2 + \beta^2}} \left(\alpha |s_{\mathbf{k}}\rangle \pm \beta |\psi_{\mathbf{k}}^{a_{1g}}\rangle \right), \quad (6)$$

which was used by us and our co-authors in [5] for analyzing the BaBiO₃ effective hopping parameters, does not have this divergence problem.

4. Comparison with Wannier Functions and Usage in Effective Models

It is important to recognize the fact that orthonormalization of a molecular orbital $\psi_{\mathbf{R}}^M(\mathbf{r})$ of any kind via multiplication of its corresponding Bloch function $\psi_{\mathbf{k}}^M(\mathbf{r})$ by $\beta_{\mathbf{k}}$ converts this molecular orbital into a Wannier function [23]. The same, of course, applies to atomic orbitals. It is also a common practice to adjust Wannier functions such that their corresponding eigenvalues match a selected set of bands obtained from an LDA(+U) calculation, which can be achieved through the following expansion in terms of self-consistently obtained Bloch eigenstates $|\Psi_{\mathbf{k},\nu}\rangle$:

$$|w_{\mathbf{k}}\rangle = \sum_{n < \nu < m} \langle \Psi_{\mathbf{k},\nu} | \psi_{\mathbf{k}} \rangle |\Psi_{\mathbf{k},\nu}\rangle. \quad (7)$$

Here, $|\psi_{\mathbf{k}}\rangle$ can be either an atomic or a molecular orbital Bloch function and ν is a band index running from band n to band m . On top of this construction, one may also apply the maximal localization [23] and the disentanglement [24] procedures. This is finalized by orthonormalization [Equation (3)] to determine $\beta_{\mathbf{k}}$. The resulting Wannier functions $|w_{\mathbf{k}}\rangle$ are convenient to use in effective models since the basis set size can be kept minimal but at the same time the LDA(+U) bands would remain well reproduced by the model's eigenstates. This approach is, for example, often used in regard to transition metal oxides in order to eliminate oxygen— p orbitals and derive a transition metal— d only based effective model. However, depending on how large and how strongly \mathbf{k} -vector dependent $\beta_{\mathbf{k}}$ is, such Wannier functions can be quite extended objects in real space with orbital contributions from many atomic shells. One disadvantage of using the Wannier functions $|w_{\mathbf{k}}\rangle$ [Equation (7)] in effective models is that most often it is not possible to fully control the degree of their spatial extension, even when attempts to optimize them through “maximal localization” have been made. This is a well-known problem for strongly localized

atomic orbitals, like transition metal— $3d$, in Hubbard-type models where electron interactions are supposed to be strictly local. There, the Wannier functions $|w_k\rangle$ [Equation (7)] would be very different for the occupied and the unoccupied states, especially for a charge-transfer gap insulator where the occupied d^{n-1} state is inside the O— $2p$ band while the unoccupied d^{n+1} state is very well above. In this situation, there would be no easy way to define properly the Hubbard interaction parameter U .

As an example of how much spatial extension a nominally maximally localized atomic Wannier function $|w_k\rangle$ can have and how strongly it can be affected by covalence effects, let us consider Ni— $3d$ orbitals in the charge-transfer gap insulator NiO. **Figure 3** shows the NiO minority spin band structure calculated for ferromagnetically aligned Ni magnetic moments using LDA + U with $J_H = 1$ eV and $U = 2$ eV [panel (a)], $U = 12$ eV [panel (b)], and $U = 6$ eV [panels (c)-(e)] applied to Ni— $3d$ electrons. Fat bands indicate the strength of the Ni— $3d$ character, while the dashed lines are the eigenvalues of an effective Hamiltonian in the basis of maximally localized Ni— t_{2g} Wannier functions obtained using the Wannier90 package [25]. For the very small U value of 2 eV and the very large U value of 12 eV, the Ni— t_{2g} bands lie either above or below the oxygen— $2p$ bands, respectively, which reduces their hybridization and makes it possible to obtain a reasonable effective Hamiltonian with eigenvalues closely matching the LDA + U bands. However, the resulting Wannier functions in real space (shown below the corresponding band-structure plots in **Figure 3**) look quite different in the two cases and, in particular, have different degrees of spatial extension. In the most realistic case of $U = 6$ eV, the Ni— t_{2g} and oxygen— $2p$ bands are

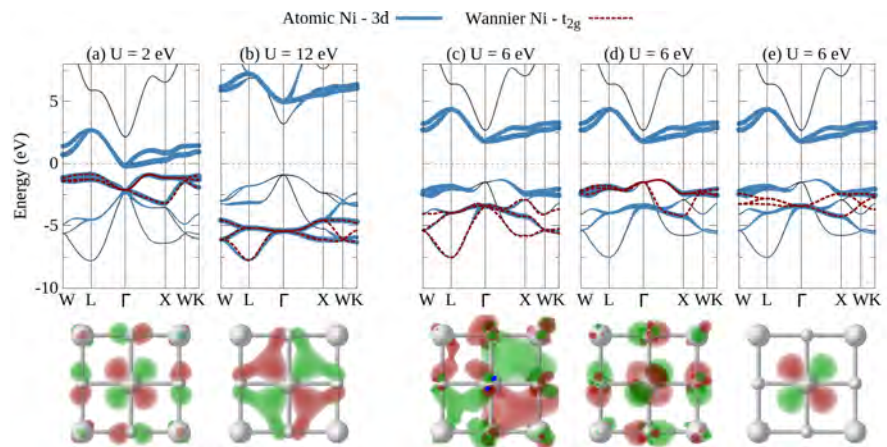


Figure 3. Maximally localized Ni— t_{2g} Wannier functions in NiO. At the top shown are the NiO spin minority band structures, with fat bands indicating the Ni— $3d$ orbital character, as well as the eigenvalues of the Ni— t_{2g} maximally localized Wannier functions based effective Hamiltonians. The Fermi level is set to zero and marked with a dashed black line. One of the Ni— t_{2g} Wannier functions in real space is shown below each corresponding band-structure plot. The band-structure results were obtained in LDA + U with (a) $U = 2$ eV, (b) $U = 12$ eV, and (c)-(e) $U = 6$ eV. In (c)-(e), the effective Hamiltonian's eigenvalues were constrained during wannierization to match (c) the lowest, (d) the highest, or (e) no LDA + U bands in the occupied manifold.

energetically very close and so get strongly hybridized. As a result, wannierization may give even more ambiguous results in this case. Depending on whether certain constraints are applied [Figure 3(c) and Figure 3(d)] or not [Figure 3(e)], one can obtain either very extended and ill-shaped or very well-localized Wannier functions. In the latter case, however, the effective Hamiltonian's eigenvalues are a poor match to the LDA + U bands.

The cuprates are another good example where we can define the upper Hubbard band very well because it is well separated from the oxygen— $2p$ band, while the lower Hubbard band, involving also all kinds of multiplets spread out over about 8 eV, is for a large part inside the oxygen— $2p$ band. Also, the lowest energy d^8 state without the hybridization switched on is a triplet F state and not a singlet state, as one assumes in a Hubbard model. In fact, the singlet $A_{1g}d^8$ state hybridizes so strongly that it pushes out the Zhang-Rice singlet state from the top of the O band and this state has more oxygen— $2p$ than Cu— $3d$ character in it. This is very similar to the BaBiO₃ “bound two-hole state” pushed up above the Fermi level that we discussed in Section 3. If the Zhang-Rice state is well enough pushed out of the top of the O band, then we could actually define a single site Wannier function for this but it would have more density on O than on Cu.

In this case of correlated oxides where transition metal— d orbitals are strongly localized yet also subject to hybridization with oxygen— p orbitals, a way to improve on the localization of Wannier functions would be to also include oxygen— $2p$ orbitals into the Wannier basis. This, however, may significantly increase the size of the Hilbert space required in model calculations. On the other hand, the increase can be much less dramatic if only the most important molecular combinations of oxygen— p orbitals are considered, such as the oxygen— (x^2-y^2) or oxygen— a_{1g} in our earlier examples of NaNiO₂ and BaBiO₃. Recently, this promising MO based approach has been successfully applied to calculate resonant X-ray spectral responses in rare-earth nickelates [3]. Another useful application would be to study systems with strong electron-phonon coupling, especially of the kind that strongly affects hybridization between cation and oxygen orbitals. There is, for example, a strong electron-phonon coupling of this kind in BaBiO₃ where the A_{1g} —symmetric (so-called “breathing”) oxygen phonon mode is coupled to the hybridization strength between the Bi-6s atomic orbital and the oxygen— a_{1g} MO. The role of this coupling in the bismuthates' superconductivity has recently been a subject of intense theoretical research, both at the band theory [4] [5] [6] and also model Hamiltonians levels, the latter including conventional atomic orbital based models [26] as well as MO based ones [27].

5. Strongly Correlated Molecular Orbitals (Na₂IrO₃ as an Example)

Since molecular orbitals are localized objects, electrons or holes occupying them may be subject to strong on-site Coulomb repulsion, where a site can now be a molecular orbital one and technically comprise more than one atomic site. From

the band theory point of view, it would be very desirable to have a mean-field method, perhaps similar to the conventional LDA + U, in order to describe local correlations in systems with dominant MO character of the valence bands. Interestingly, application of the conventional LDA + U method to such systems may have an unphysically detrimental effect on their MO nature.

As an illustration, let us consider sodium iridium oxide Na_2IrO_3 , a famous candidate Kitaev system [28], with an unusual property that its Ir—5*d* orbitals hybridize in a way such as to form MOs on Ir hexagons [29] [30]. It is worth emphasizing that, in contrast with our previous examples, here MOs are formed out of cation instead of oxygen orbitals, which makes this case rather special. This becomes possible thanks to the larger spatial extent of the 5*d* orbitals, compared to that of the 3*d* ones, which leads to their larger nearest-neighbor hybridization, and also thanks to the peculiar geometrical arrangement of the IrO_6 octahedra. **Figure 4(a)** shows the Na_2IrO_3 DOS projected onto Ir—5*d* MOs, as obtained from a generalized gradient approximation [31] (GGA) calculation. Here, we would like to focus on the MO aspects of the Na_2IrO_3 electronic structure and therefore neglect spin-orbit coupling effects, which one would otherwise need to also take into account. In this calculation, we assume a zig-zag order of Ir magnetic moments, shown in **Figure 4(b)**, since it is experimentally found to be the ground magnetic state for Na_2IrO_3 [32]. As one can see from the GGA calculations, this magnetic order can be well described in terms of on-hexagon molecular orbitals. In particular, near the Fermi level we find a completely filled $A_{1g} + E_{2u}$ MO and slightly filled $A_{1g} - E_{2u}$ MO in one spin channel and an opposite situation in the other spin channel, with $A_{1g} \pm E_{2u}$ standing for linear combinations of MOs with the A_{1g} and E_{2g} symmetries. The connection between the zig-zag magnetic order and such peculiar MO occupations becomes

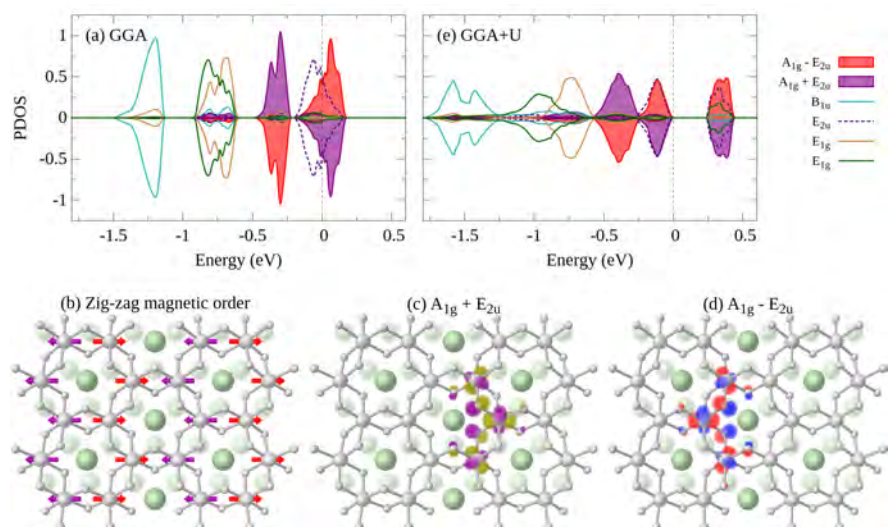


Figure 4. Ir molecular orbitals in Na_2IrO_3 . (a) and (e) show Ir MO projected DOS of Na_2IrO_3 calculated using GGA and GGA + U, respectively. (b) The zig-zag order of Ir magnetic moments within a hexagonal Ir layer. (c) and (d) show, respectively, the isolated $A_{1g} + E_{2u}$ and $A_{1g} - E_{2u}$ Ir MOs.

clear if one inspects the shapes of these two MOs in real space. Indeed, as shown in **Figure 4(c)** and **Figure 4(d)**, one of these MOs is located on the right side of an Ir hexagon while the other MO is located on its left side, and this exactly produces the zig-zag order if the two MOs are occupied by holes of opposite spins. Now, there is one more MO at the Fermi level, namely, E_{2p} which is slightly empty in both spin channels. If a method like GGA + U but designed to act in the basis of MOs were applied to Na_2IrO_3 , it would push up in energy and completely empty the $A_{1g} - E_{2u}$ and $A_{1g} + E_{2u}$ MO states and would push down and completely fill the E_{2g} MO states. This is not what happens when the conventional GGA + U method ($U = 2.7$ eV and $J_H = 0.7$ eV on Ir-5d orbitals) is applied [**Figure 4(e)**]. Although it does open a charge gap of 0.25 eV, but in a way that splits and mixes the $A_{1g} - E_{2p}$, $A_{1g} + E_{2p}$, and E_{2u} MO states, thus destroying the MO nature of the Na_2IrO_3 valence bands. Similar damage is also done to the lower-lying B_{1u} and E_{1g} MOs.

For the local MO correlations to be treated properly (at least, in a mean-field sense), two approaches seem to be in place. In the first approach, one can first construct MOs via the unitary basis transformation of Equation (2) and then use the conventional LDA + U expressions for total energy and potential but written in the basis of MOs. We see three problems associated with this approach. First, it is not always obvious in which way MOs should be constructed. Second, this approach is intrinsically rotationally non-invariant, *i.e.*, would produce different results depending on the choice of the basis. Third, calculation of the Coulomb and exchange interaction matrix elements $U_{M_i M_j}$ and $J_{M_i M_j}$, with M_i and M_j denoting MOs, may pose a serious challenge.

The second and, as we believe, more promising approach consists in extending the atomic orbital LDA + U method by additionally taking into account Coulomb interactions between different atomic sites. Also referred to as extended DFT + U + V, this approach was first discussed by Campo and Cococcioni in [33]. It can be shown that if all important inter-site interaction terms are taken into account, this approach can capture the same MO physics as the more intuitive first approach discussed above. Whether the inter-site interaction terms that the authors of [33] chose to keep in their interaction Hamiltonian are sufficient in doing so is an open question, and further investigations into this matter would be of great value. By the way, recognizing the importance of inter-site interactions explains why GGA + U fails in the case of Na_2IrO_3 . Indeed, although GGA suffers from the self-interaction problem, it at least treats both on-site and inter-site interactions on the same footing. This allows GGA to capture qualitatively all MO energy splittings in Na_2IrO_3 [**Figure 4(a)**]. On the other hand, in GGA + U the on-site interactions are unphysically exaggerated in comparison with the inter-site ones, which apparently must be similarly strong.

6. Conclusion

In summary, we presented our band theory perspective on some important as-

pects of molecular orbitals in complex oxides. In particular, we first discussed technical issues related with the implementation of MO-based projection of electronic states, using NaNiO_2 as an example. Then, this discussion was extended by considering non-orthogonal MOs, as observed in BaBiO_3 , and the way of performing their orthonormalization. This led us to the concept of atomic and molecular orbital Wannier functions, where we discussed the problem of the Wannier functions being typically rather extended in real space and how this property may restrict their usage as basis functions in model Hamiltonians, using NiO as an example. A suggestion was then made that MO based model Hamiltonians might be a good approach to describing correlated transition metal systems with strong cation-anion orbital hybridization and also systems with strong electron-phonon coupling. Our final point concerned the problem of a proper band theory treatment of strong correlations between electrons or holes occupying molecular rather than atomic orbitals. In this context, we discussed the failure of the conventional atomic LDA + U method to capture the MO nature of the electronic states in Na_2IrO_3 , and outlined possible pathways towards a more adequate band theory based description. As the interest in better understanding of the role of molecular orbitals in complex oxides is growing, we expect that our current review will provide a useful reference for future studies.

Acknowledgements

This work was supported by NSERC, CIFAR, and the Max Planck—UBC Stewart Blusson Quantum Matter Institute.

Conflicts of Interest

The authors declare no conflicts of interest regarding the publication of this paper.

References

- [1] Zhang, F.C. and Rice, T.M. (1988) *Physical Review B: Condensed Matter*, **37**, 3759-3761. <https://doi.org/10.1103/PhysRevB.37.3759>
- [2] Johnston, S., Mukherjee, A., Elfimov, I., Berciu, M. and Sawatzky, G.A. (2014) *Physical Review Letters*, **112**, Article ID: 106404. <https://doi.org/10.1103/PhysRevLett.112.106404>
- [3] Green, R.J., Haverkort, M.W. and Sawatzky, G.A. (2016) *Physical Review B: Condensed Matter*, **94**, Article ID: 195127. <https://doi.org/10.1103/PhysRevB.94.195127>
- [4] Foyevtsova, K., Khazraie, A., Elfimov, I. and Sawatzky, G.A. (2015) *Physical Review B: Condensed Matter*, **91**, Article ID: 121114. <https://doi.org/10.1103/PhysRevB.91.121114>
- [5] Khazraie, A., Foyevtsova, K., Elfimov, I. and Sawatzky, G.A. (2018) *Physical Review B: Condensed Matter*, **97**, Article ID: 075103. <https://doi.org/10.1103/PhysRevB.97.075103>
- [6] Khazraie, A., Foyevtsova, K., Elfimov, I. and Sawatzky, G.A. (2018) *Physical Review B: Condensed Matter*, **98**, Article ID: 205104. <https://doi.org/10.1103/PhysRevB.98.205104>

- [7] Zaanen, J., Sawatzky, G.A. and Allen, J.W. (1985) *Physical Review Letters*, **55**, 418-421. <https://doi.org/10.1103/PhysRevLett.55.418>
- [8] Bednorz, J.G. and Müller, K.A. (1986) *Zeitschrift für Physik B*, **64**, 189-193. https://doi.org/10.1007/978-94-011-1622-0_32
- [9] Leggett, A.J. (2006) *Nature Physics*, **2**, 134-136. <https://doi.org/10.1038/nphys254>
- [10] Cava, R.J., *et al.* (1988) *Nature*, **332**, 814-816. <https://doi.org/10.1038/332814a0>
- [11] Sleight, A.W., Gillson, J.L. and Bierstedt, P.E. (1975) *Solid State Communications*, **17**, 27-28. [https://doi.org/10.1016/0038-1098\(75\)90327-0](https://doi.org/10.1016/0038-1098(75)90327-0)
- [12] Sleight, A.W. (2015) *Physica C: Superconductivity and Its Applications*, **514**, 152-165. <https://doi.org/10.1016/j.physc.2015.02.012>
- [13] Medarde, M.L. (1997) *Journal of Physics: Condensed Matter*, **9**, 1679-1707. <https://doi.org/10.1088/0953-8984/9/8/003>
- [14] Liu, W., *et al.* (2015) *Angewandte Chemie International Edition in English*, **54**, 4440-4457. <https://doi.org/10.1002/anie.201409262>
- [15] Okubo, M. and Yamada, A. (2017) *ACS Applied Materials & Interfaces*, **9**, 36463-36472. <https://doi.org/10.1021/acsami.7b09835>
- [16] Dyer, L.D., Borie, B.S. and Pedro Smith, G. (1954) *Journal of the American Chemical Society*, **76**, 1499-1503. <https://doi.org/10.1021/ja01635a012>
- [17] Kuiper, P., Kruizinga, G., Ghijsen, J., Sawatzky, G.A. and Verweij, H. (1989) *Physical Review Letters*, **62**, 221-224. <https://doi.org/10.1103/PhysRevLett.62.221>
- [18] Perdew, J.P. and Wang, Y. (1992) *Physical Review B: Condensed Matter*, **45**, 13244-13249. <https://doi.org/10.1103/PhysRevB.45.13244>
- [19] Liechtenstein, A.I., Anisimov, V.I. and Zaanen, J. (1995) *Physical Review B: Condensed Matter*, **52**, R5467-R5470. <https://doi.org/10.1103/PhysRevB.52.R5467>
- [20] Anisimov, V.I., Zaanen, J. and Andersen, O.K. (1991) *Physical Review B: Condensed Matter*, **44**, 943-954. <https://doi.org/10.1103/PhysRevB.44.943>
- [21] Schwarz, K., Blaha, P. and Madsen, G.K.H. (2002) *Computer Physics Communications*, **147**, 71-76. [https://doi.org/10.1016/S0010-4655\(02\)00206-0](https://doi.org/10.1016/S0010-4655(02)00206-0)
- [22] Streltsov, S.S., Shorikov, A.O., Skorniyakov, S.L., Poteryaev, A.I. and Khomskii, D.I. (2017) *Scientific Reports*, **7**, Article No. 13005. <https://doi.org/10.1038/s41598-017-13312-4>
- [23] Marzari, N. and Vanderbilt, D. (1997) *Physical Review B*, **56**, 12847-12865. <https://doi.org/10.1103/PhysRevB.56.12847>
- [24] Souza, I., Marzari, N. and Vanderbilt, D. (2001) *Physical Review B: Condensed Matter*, **65**, 9028. <https://doi.org/10.1103/PhysRevB.65.035109>
- [25] Mostofi, A.A., *et al.* (2014) *Computer Physics Communications*, **185**, 2309-2310. <https://doi.org/10.1016/j.cpc.2014.05.003>
- [26] Li, S. and Johnston, S. (2019) Quantum Monte Carlo Study of Lattice Polarons in the Two-Dimensional Multi-Orbital Su-Schrieffer-Heeger Model.
- [27] Yam, Y.-C., Berciu, M. and Sawatzky, G.A. to be published.
- [28] Chaloupka, J., Jackeli, G. and Khaliullin, G. (2010) *Physical Review Letters*, **105**, Article ID: 027204. <https://doi.org/10.1103/PhysRevLett.105.027204>
- [29] Mazin, I.I., Jeschke, H.O., Foyevtsova, K., Valentí, R. and Khomskii, D.I. (2012) *Physical Review Letters*, **109**, Article ID: 197201. <https://doi.org/10.1103/PhysRevLett.109.197201>
- [30] Foyevtsova, K., Jeschke, H.O., Mazin, I.I., Khomskii, D.I. and Valentí, R. (2013)

Physical Review B: Condensed Matter, **88**, Article ID: 035107.

<https://doi.org/10.1103/PhysRevB.88.035107>

- [31] Perdew, J.P., Burke, K. and Ernzerhof, M. (1996) *Physical Review Letters*, **77**, 3865-3868. <https://doi.org/10.1103/PhysRevLett.77.3865>
- [32] Choi, S.K., *et al.* (2012) *Physical Review Letters*, **108**, Article ID: 127204. <https://doi.org/10.1103/PhysRevLett.108.127204>
- [33] Campo, V.L. and Cococcioni, M. (2010) *Journal of Physics: Condensed Matter*, **22**, Article ID: 055602. <https://doi.org/10.1088/0953-8984/22/5/055602>

Increased Temperature and Entropy Production in the Earth's Atmosphere: Effect on Wind, Precipitation, Chemical Reactions, Freezing and Melting of Ice and Electrical Activity

Michael A. Pitt

Paraparaumu, New Zealand

Email: pitt@xtra.co.nz

How to cite this paper: Pitt, M.A. (2019) Increased Temperature and Entropy Production in the Earth's Atmosphere: Effect on Wind, Precipitation, Chemical Reactions, Freezing and Melting of Ice and Electrical Activity. *Journal of Modern Physics*, 10, 966-973.

<https://doi.org/10.4236/jmp.2019.108063>

Received: May 28, 2019

Accepted: July 6, 2019

Published: July 9, 2019

Copyright © 2019 by author(s) and Scientific Research Publishing Inc. This work is licensed under the Creative Commons Attribution International License (CC BY 4.0).

<http://creativecommons.org/licenses/by/4.0/>



Open Access

Abstract

Since the late nineteenth century, until the present time, there has been an increase in the earth's global mean surface temperature (GMST). This temperature increase has been calculated at 0.85°C over the period 1880-2012. The causes of this temperature increase include increased levels of greenhouse gases (GHG's), variations in solar irradiance and changes in absorption and re-radiation of heat. Volcanic activity and orbital cycles work to cool the earth's surface. A thermodynamic analysis is presented of the earth's atmosphere. The analysis demonstrates an increase in entropy production as a result of increased GMST. An equation is derived expressing entropy production in the atmosphere based on atmospheric processes (wind, precipitation, chemical reactions, electrical activity and heat transfer). The effects of increased entropy production on wind, precipitation, freezing and melting of ice, chemical reactions and electrical activity are given showing an increase in the combination of the above phenomena.

Keywords

Temperature, Entropy, Earth's Atmosphere

1. Introduction

Since the late nineteenth century, until the present time, there has been an increase in the earth's global mean surface temperature (GMST) [1]. This temperature increase has been calculated at 0.85°C over the period 1880-2012 [1]. The

period 1880 to 2012 is arbitrary. Any period of time from the present (or near present) to a time in the recent past will suffice, provided there is an increase in GMST. ([1]—Chapter 2 provides detailed evidence for global warming). The causes of this temperature increase include increased levels of greenhouse gases (GHG's), variations in solar irradiance and changes in absorption and re-radiation of heat [1]. Volcanic activity and orbital cycles work to cool the earth's surface.

In this paper, a thermodynamic analysis is presented of the earth's atmosphere. This analysis consists of three parts: 1) Derivation of excess entropy produced in the atmosphere due to increased temperature; 2) Derivation of an equation expressing entropy production (in the atmosphere) based on atmospheric processes (wind, precipitation, lightning, chemical reactions and heat transfer); and 3) Proof that there must be an increase in a combination of these atmospheric processes due to increased temperature.

Thus, the aim of this paper is to gain an understanding of the production of entropy in the atmosphere by atmospheric processes, the effect of global warming on that entropy production and, in turn, the effect of global warming on those atmospheric processes.

2. Methods

The thermodynamic analysis of the earth's atmosphere developed in this paper uses theory from the following sources:

- The Clausius inequality ([2], p86)
- The equation for entropy changes dS as the sum of interior entropy change ($d_i S$) and external entropy change ($d_e S$) ([2], p88)
- The equation for local entropy production ([2], p336)
- The equation for entropy production in terms of heat conduction, electrical conduction and chemical reactions and the equation for entropy production in a bilinear form *. ([2], p346)
- The acceleration of a compressible fluid in an inertial frame—the Navier-Stokes equation ([3], pp 97-101)
- The acceleration of a compressible fluid in a rotating frame ([3], p104)
- The viscous force acting on rain (hail) ([3], p51)
- The Theorem of minimum entropy production ([2], p392)
- Air resistance to snow ([4])

*The entropy produced by rain (hail) or snow and wind is derived from the entropy production in a bilinear form ([2], p346)

$$\sigma = \sum_{\alpha} F_{\alpha} J_{\alpha} \quad (1)$$

3. Results and Discussion

The higher GMST at the present time (T_2) compared to the late nineteenth century (T_1) is maintained by more heat from solar irradiance being retained in the atmosphere.

That is:

$$\frac{dQ_2}{dt} > \frac{dQ_1}{dt} \tag{2}$$

Q_2 = Heat absorbed from solar irradiance at the present time
 Q_1 = Heat absorbed from solar irradiance in the late 19th century
 t = Time

Thus, excess heat production ($\frac{dQ^*}{dt}$) occurs at the present time compared to the late nineteenth century, and is given by

$$\frac{dQ^*}{dt} = \frac{dQ_2}{dt} - \frac{dQ_1}{dt} \tag{3}$$

The Clausius inequality states that

$$dS \geq \frac{dQ}{T} \tag{4}$$

S is entropy and T is temperature in Kelvins and, therefore,

$$\frac{dS}{dt} > \frac{dQ/dt}{T} \tag{5}$$

Thus: $\frac{dS^*}{dt}$ is the excess entropy produced in the atmosphere at the present time compared to the late nineteenth century.

The entropy produced in the atmosphere is given by

$$\sigma = \sum_{\alpha} F_{\alpha} J_{\alpha} \tag{1}$$

$$\frac{d_i S}{dt} = \int_v \sigma dV = \int_v \sum_{\alpha} F_{\alpha} J_{\alpha} dV \tag{6}$$

where:

$$\sigma \equiv \frac{d_i S}{dt} = \text{local entropy production [2]}$$

F_{α} = forces

J_{α} = flows

$$\begin{aligned} \frac{d_i S}{dt} = & \int_v \left[\overbrace{\left(\frac{1}{\rho V} \left(-\frac{1}{\rho} \nabla p - g\mathbf{k} + \mathbf{F}_{visc} \right) \right)}^2 \overbrace{\left(\frac{\rho V \mathbf{k}}{t} \right)}^3 \right] dV \\ & + \int_v \frac{4}{t} \left[\overbrace{(mg\mathbf{k} - 6\pi\eta r\mathbf{v})}^5 + \overbrace{\rho V \left(-\frac{1}{\rho} \nabla p - g\mathbf{k} + \mathbf{F}_{visc} \right)}^6 + \overbrace{\left(mg\mathbf{k} - \frac{1}{2} \rho C A v^2 \right)}^7 \right] dV \tag{7} \\ & + \int_v \left[\overbrace{\frac{8}{T} \mathbf{I}_K \cdot \mathbf{E}}^8 + \overbrace{\frac{9}{T} \mathbf{J}_u \cdot \nabla 1}^9 + \overbrace{\sum_j \frac{10}{T} A_{2j} v_{2j}}^{10} \right] dV \end{aligned}$$

In Equation (7):

ρ is air density
 p is air pressure
 g is acceleration due to gravity
 \mathbf{k} is unit vector

$$\mathbf{F}_{visc} = \frac{\delta \mathbf{F}_{visc}}{\delta V} \quad (8)$$

and

$$\delta \mathbf{F}_{visc} = \delta V \eta \left[\nabla^2 \mathbf{u} + \frac{1}{3} \nabla (\nabla \cdot \mathbf{u}) \right] \quad (9)$$

\mathbf{u} is air velocity
 η is the dynamic viscosity of air
 m is the mass of rain (hail) drops or snow
 \mathbf{v} is the rain (hail) or snow velocity
 \mathbf{E} is the Electric field Strength
 \mathbf{I} is the ion current density
 \mathbf{J}_u is the heat flow
 T is the temperature in kelvins
 A_{2j} is the affinity of the j th reaction
 v_{2j} is the rate of the j th reaction
 t is time
 r is the radius of a rain (hail) drop
 V is volume
 C is the drag coefficient on snow
 A is cross section of the snowflake
1 is the mass of air
2 is the acceleration of a blob of air—the Navier-Stokes Equation
3 is the flow of air
4 is the flow of rain (hail) or snow
5 is the force exerted on rain (hail)
6 is the force exerted by wind on rain (hail) or snow
7 is the force exerted on snow
8 is the entropy produced by lightning
9 is the entropy produced by freezing or thawing of surface ice and precipitation
10 is the entropy produced by chemical reactions

In Equation (7) acceleration

$$\mathbf{a} = -\frac{1}{\rho} \nabla p - g\mathbf{k} + \mathbf{F}_{visc} \quad (10)$$

gives the acceleration of wind in the inertial frame. To obtain acceleration in the rotating frame

$$\mathbf{a} = -\frac{1}{\rho} \nabla p - 2\boldsymbol{\Omega} \times \mathbf{u}_R - \boldsymbol{\Omega} \times (\boldsymbol{\Omega} \times \mathbf{r}) - g\mathbf{k} + \mathbf{F}_{visc} \quad (11)$$

where

$$-2\boldsymbol{\Omega} \times \mathbf{u}_R$$

Is the Coriolis Force

and

$$-\boldsymbol{\Omega} \times (\boldsymbol{\Omega} \times \mathbf{r})$$

Is the Centrifugal Force

where

$\boldsymbol{\Omega}$ is angular velocity of the rotating frame

u_R is velocity in the rotating frame

\mathbf{r} is distance

And in Equation (7) the acceleration of wind [3] should be replaced by the right-hand side Equation (11).

Entropy produced at temperature T_2 and T_1 is

$$\left(\frac{d_i S}{dt}\right)_{T_2} \text{ and } \left(\frac{d_i S}{dt}\right)_{T_1} \text{ respectively.}$$

And the excess entropy produced due to increased temperature from T_1 to T_2 is

$$\frac{d_i S^*}{dt} = \left(\frac{d_i S}{dt}\right)_{T_2} - \left(\frac{d_i S}{dt}\right)_{T_1} \tag{12}$$

Using Equation (7)

The excess entropy production must be manifested by a combination of increased wind, precipitation, electrical activity, rates of chemical reactions and freezing and melting of ice. The more global mean surface temperature increases, the more there will be an increase in the combination of wind, precipitation, electrical activity, rates of chemical reactions and freezing and melting of surface ice.

Notes:

- 1) It is expected that an increase in GMST will result in:
 - a) Melting of surface ice to predominate over freezing of surface ice
 - b) Less freezing of precipitation
- 2) There is increased water holding capacity of air with increased temperature
- 3) In this paper no account is taken for wind of vorticity or wave motion

In the present work, entropy production (σ) for atmospheric processes are expressed in the bilinear form of forces (\mathbf{F}_α) and flows (\mathbf{J}_α)

$$\sigma = \sum_{\alpha} \mathbf{F}_\alpha \mathbf{J}_\alpha \tag{1}$$

As stated in the Methods Section, entropy production for heat conduction, electrical conduction and chemical reactions are given in Reference ([2], p346) of the Methods Section. In the case of wind and the effect of wind on rain (hail) or snow, the force acting on these processes is derived from the acceleration of a compressible fluid as given in References ([3], pp 97-101) & ([3], p104) of the Methods Section and the mass of fluid. The flow is given by the mass of fluid and

the rate of flowing per time. The force acting on rain (hail) or snow is given by the acceleration due to gravity and the mass of rain (hail) or snow. The flow of rain (hail) or snow is the rate of falling of these substances.

The change of entropy may be expressed as the sum of two parts. $dS = d_i S + d_e S$ (refer to Methods). Where $d_e S$ is the entropy change, due to exchange of matter and energy with the exterior and $d_i S$ is the entropy produced by irreversible processes in the interior of the earth's atmosphere. The production of entropy by electromagnetic radiation is not considered as this radiation originates from outside the atmosphere, only interior entropy production in the atmosphere is considered in this paper.

The present study defines entropy production in the atmosphere in terms of atmospheric processes, namely wind, rain, heat transfer, lightning and chemical reactions.

There have been many studies of entropy production in the atmosphere. Nicolis and Nicolis [5] show that decreasing and increasing values of entropy production are possible in the earth's atmosphere. Paillard and Herbert [6] suggest the maximum entropy production principle, generally assumed to be applicable only for stationary systems, could be extended to time-varying climatic problems, provided the internal time scales are small compared to the speed of external changes**.

Paltridge [7] discusses that small-scale convective heat transfer processes (where the preferred steady state mode is one of maximum entropy production) may be applied to the larger earth atmospheric system**. A system of minimum entropy exchange can accurately predict meridional distribution of temperature, cloud cover and energy flux [8]. Other studies postulate maximum entropy production in the atmosphere [9]. There is much debate on the application of maximum entropy production to the earth's atmosphere. [10] [11]. Bannon [12] discusses entropy production and climate efficiency using two representations of climate efficiency. Kleidon, [13] reviews the earth's atmospheric operating far from thermodynamic equilibrium and considers three different case of maximum entropy production. Liu *et al.* [14] have reviewed the concept of entropy and the principle of maximum entropy production in meteorology. Sura [15] considers the earth's atmosphere far from equilibrium, maximum entropy production and non-Gaussian variability about the mean of meridional heat flux and meridional temperature gradient. Marini-Bettolo [16] has described chemical reactions in the atmosphere.

***Minimum entropy production would occur if the atmosphere was in a stationary state. ([2], p392).*

In the current study, heat conduction includes formation of ice, thawing of ice and formation of hail from rain droplets. Also included in heat conduction is heat generated by forest fires, and the burning of fossil fuels and geothermal and volcanic activity.

The present study postulates neither minimum nor maximum entropy production. Rather it calculates entropy production based on atmospheric processes

using the bilinear relation.

$$\sigma = \sum_{\alpha} F_{\alpha} J_{\alpha} \quad (1)$$

However, it does postulate increased entropy production as a result of increased global mean surface temperature.

The study undertaken here is analogous to a thermodynamic study of cancer [17]. In that study cancerous tumours are hotter than surrounding normal tissue. Because of the increased temperature of cancerous tumours, there is an increase in entropy production in the cancer, compared to surrounding normal tissue. In the thermodynamic study of cancer [17] the increased temperature and entropy production in cancer are spatial compared to surrounding normal tissue. In the present atmosphere study, the increased temperature and entropy production are temporal.

This paper breaks new ground by deriving expressions for entropy production by wind and rain (hail) or snow based on the bilinear relation:

$$\sigma = \sum_{\alpha} F_{\alpha} J_{\alpha} \quad (1)$$

It also proves that global warming must result in a combination of more severe weather patterns.

The increases in atmospheric processes, postulated in this paper, have been confirmed by observations of more severe weather patterns at present compared with past years [1].

4. Conclusions

In this paper the following theories are developed:

- 1) The concept of excess entropy production in the atmosphere $\frac{d_i S^*}{dt}$ due to temperature increases over a period of time.
- 2) An equation (Equation (7)) is developed describing entropy production in the atmosphere $\frac{d_i S}{dt}$ due to wind, precipitation and the effect of wind on precipitation, lightning, heat transfer and chemical reactions.
- 3) Proof that, as a consequence of excess entropy production, there must be an increase in a combination of wind, precipitation, lightning, chemical reactions and heat transfer.

A comparison of the increased entropy production of the earth's atmosphere is made with increased entropy production in cancer [17].

Conflicts of Interest

The author, Dr Michael A Pitt, states that there is no actual, potential or perceived conflict of interest in regard to the manuscript submitted for review.

References

- [1] IPCC (2014) Climate Change 2013: The Physical Science Basis. Cambridge Univer-

- sity Press, New York.
- [2] Kondepudi, D. and Prigogine, I. (1998) *Modern Thermodynamics. From Heat Engines to Dissipative Structures*. John Wiley & Sons, Chichester.
 - [3] Andrews, D.G. (2010) *An Introduction to Atmospheric Physics*. 2nd Edition, Cambridge University Press, Cambridge.
 - [4] Newman, D. ffden-2.phys.uaf.edu.
 - [5] Nicolis, G. and Nicolis, C. (1980) *Quarterly Journal of the Royal Meteorological Society*, **106**, 691-706. <https://doi.org/10.1002/qj.49710645003>
 - [6] Paillard, D. and Herbert, C. (2013) *Entropy*, **15**, 2846-2860. <https://doi.org/10.3390/e15072846>
 - [7] Paltridge, G.W. (1978) *Quarterly Journal of the Royal Meteorological Society*, **104**, 927-945. <https://doi.org/10.1256/smsqj.44205>
 - [8] Paltridge, G.W. (1975) *Quarterly Journal of the Royal Meteorological Society*, **101**, 475-484. <https://doi.org/10.1002/qj.49710142906>
 - [9] Ozawa, H., Ohmura, A., Lorenz, R.D. and Pujol, T. (2003) *Reviews of Geophysics*, **41**, 1-24. <https://doi.org/10.1029/2002RG000113>
 - [10] Goody, R. (2007) *Journal of the Atmospheric Sciences*, **64**, 2735-2739. <https://doi.org/10.1175/JAS3967.1>
 - [11] Volk, T. and Pauluis (2010) *Philosophical Transactions of the Royal Society B*, **365**, 1317-1322. <https://doi.org/10.1098/rstb.2010.0019>
 - [12] Bannon, P.R. (2015) *Journal of the Atmospheric Sciences*, **72**, 3268-3280. <https://doi.org/10.1175/JAS-D-14-0361.1>
 - [13] Kleidon, A. (2010) *Philosophical Transactions of the Royal Society*, **365**, 1303-1315. <https://doi.org/10.1098/rstb.2009.0310>
 - [14] Liu, Y., Liu, C. and Wang, D. (2011) *Entropy*, **13**, 211-240. <https://doi.org/10.3390/e13010211>
 - [15] Sura, P. (2016) Maximum Entropy Production and Non-Gaussian Climate Variability. arXiv:1603.05260v1 [physics.ao-ph]
 - [16] Marini-Bettolo, G.B. (1986) *Studies in Environmental Science*, **26**, 607-617. [https://doi.org/10.1016/S0166-1116\(08\)71811-9](https://doi.org/10.1016/S0166-1116(08)71811-9)
 - [17] Pitt, M.A. (2015) *Inflammopharmacology*, **23**, 17-20. <https://doi.org/10.1007/s10787-014-0224-x>

How the Dirac Sea Idea May Apply to a Spatially-Flat Universe Model (A Brief Review)

Eugene Terry Tatum

Bowling Green, KY, USA

Email: ett@twc.com

How to cite this paper: Tatum, E.T. (2019) How the Dirac Sea Idea May Apply to a Spatially-Flat Universe Model (A Brief Review). *Journal of Modern Physics*, 10, 974-979.

<https://doi.org/10.4236/jmp.2019.108064>

Received: June 17, 2019

Accepted: July 14, 2019

Published: July 17, 2019

Copyright © 2019 by author(s) and Scientific Research Publishing Inc. This work is licensed under the Creative Commons Attribution International License (CC BY 4.0).

<http://creativecommons.org/licenses/by/4.0/>



Open Access

Abstract

The famous Dirac sea idea can be resurrected if one replaces the concept of positive and negative matter mass with positive and negative energy. Utilizing this concept, the perpetually spatially-flat matter-generating FSC model can be shown to be a realistic Milne “empty universe” model. Furthermore, this may be why $R_h = ct$ cosmological models like FSC show an excellent statistical fit with the accumulated data of the Supernova Cosmology Project.

Keywords

Dirac Sea, Dirac Equation, Flat Space Cosmology, Dark Energy, Dark Matter, Inflationary Cosmology, Supernova Cosmology Project, $R_h = ct$ Models

1. Introduction and Background

Mathematical physicist Paul Dirac is perhaps best known for the Dirac equation in its many forms [1]. Not only was he largely responsible for making quantum mechanics relativistic, but his “hole theory” (based upon his equation) suggested to him something about the nature of the cosmic vacuum. Dirac believed that his equation implied that the vacuum could be a many-body quantum state in which all of the negative energy eigenstates (holes) are occupied. In terms of electron eigenstates, for instance, Dirac pictured a “sea” of electrons occupying negative-energy electron eigenstates. Unfortunately, his “Dirac sea” idea was interpreted to imply holes of *negative mass matter*, which is believed to be impossible. The term “antimatter” is used not to imply negative mass matter, but rather gravitationally-attractive positive-energy matter of the same mass as its positive-energy partner, yet *opposite in quantum spin and charge*. The combined mass-energy of an electron and positron, for instance, sums to twice that of the electron alone, rather than summing to zero. Despite the initial apparent failure of the Dirac sea idea, the Dirac equation was correctly credited with pre-

dicting oppositely-charged matter of equal positive mass, for which the term antimatter is restricted.

On a parallel track, there is the currently-favored theory that our universe may have started from a zero-energy state and undergone a brief (10^{-32} s) period of “cosmic inflation” in which all matter and antimatter were created. Nevertheless, this nearly instantaneous matter-generating universe theory would appear to violate conservation of energy. This did not escape notice by its inventor, Alan Guth [2] [3]. Guth has sometimes referred to his theory as a “free lunch” idea. Other somewhat modified inflationary theories [4] [5] of a nearly instantaneous matter-generating universe have followed, although the problem of energy conservation violation appears to be inherent in all such theories [6].

Recently, there have been proposed several *perpetually* matter-generating universe theories [7]-[14], which smoothly expand, are not inflationary in nature, and do not appear to violate conservation of energy. They are also consistent with current observations of a spatially-flat universe. One of the most successful of these theories, in terms of predicting current observations, is the “Flat Space Cosmology” (FSC) model. By following its five basic assumptions, the heuristic FSC model perpetually maintains the Friedmann critical mass density for a spatially-flat universe ($\rho_0 = \frac{3H_0^2}{8\pi G}$) for any theoretical time of observation (o).

Furthermore, the FSC model tightly correlates the current redshifted cosmic microwave background (CMB) temperature of 2.72548 K with a current *predicted* Hubble parameter value of $66.9 \text{ km}\cdot\text{s}^{-1}\cdot\text{Mpc}^{-1}$. This Hubble parameter value fits within the tight constraints of the 2018 Planck Collaboration [15] and 2018 Dark Energy Survey [16] reports.

2. Relevance of the Dirac Sea Idea to the FSC Model

The relevance of the Dirac sea idea to the FSC model pertains to its perpetual matter generation and its perpetual spatial flatness. As detailed in several 2018 publications [11] [12] [13], a *globally* perpetually-flat spacetime implies that the cosmological model must always maintain equal amounts of positive and negative energy. Otherwise, the more dominant energy density component would contribute an observable curvature signifying either cosmic deceleration (positive curvature) or cosmic acceleration (negative curvature). As the excellent statistical fit between $R_h = ct$ cosmological models and observations of the Supernova Cosmology Project indicates, the expansion of our universe appears to be coasting at constant velocity [7] [17] [18] [19] [20]. All $R_h = ct$ models have this “coasting at constant velocity” feature. For specifics concerning the basic features of $R_h = ct$ models, the reader is encouraged to start with these references. FSC is one such $R_h = ct$ model.

The “Dirac sea” idea can be resurrected if one considers a dichotomy of positive and negative *energy* states popping into and out of existence within the vacuum. If one follows the convention that all units of matter mass-energy are

“positive” energy, then one can consider the “holes” in the Dirac sea to be similarly-sized units of “negative” vacuum energy. Furthermore, since the FSC model uses such a sign convention, the negative energy holes in the FSC Dirac sea can now be understood to be units of dark energy exactly offset by the units of matter mass-energy produced in the FSC vacuum. By this perpetually ongoing process, the FSC model accumulates increasingly positive (matter) energy and increasingly negative dark energy of equal magnitude, always *summing to zero total energy*. In this way, a universe which begins in a zero-energy state maintains perpetual conservation of total (*i.e.*, global) cosmic energy.

3. Results: Evidence in Support of FSC and Dirac

The “net zero energy” FSC model can now be contrasted with standard inflationary cosmology, which considers such models to be unrealistic “empty universe” models. The phrase “empty universe” has generally been applied in the past to Milne-type models containing no matter. However, the current $R_h = ct$ models contain matter and, as such, are considered to be more realistic than Milne’s original conception. If one looks carefully at the following open source graph [21] published by the Supernova Cosmology Project (SCP) (Figure 1), one can see the excellent statistical fit of the “empty” universe line demarcating the boundary between accelerating and decelerating universal expansions.

This “empty” universe line falls exactly where the FSC and other $R_h = ct$ models fall. One can also readily see how it is that $R_h = ct$ universe models appear to show an excellent statistical fit with SCP observations to date. For additional proof, another open source graph [22] published by the SCP is provided (Figure 2).

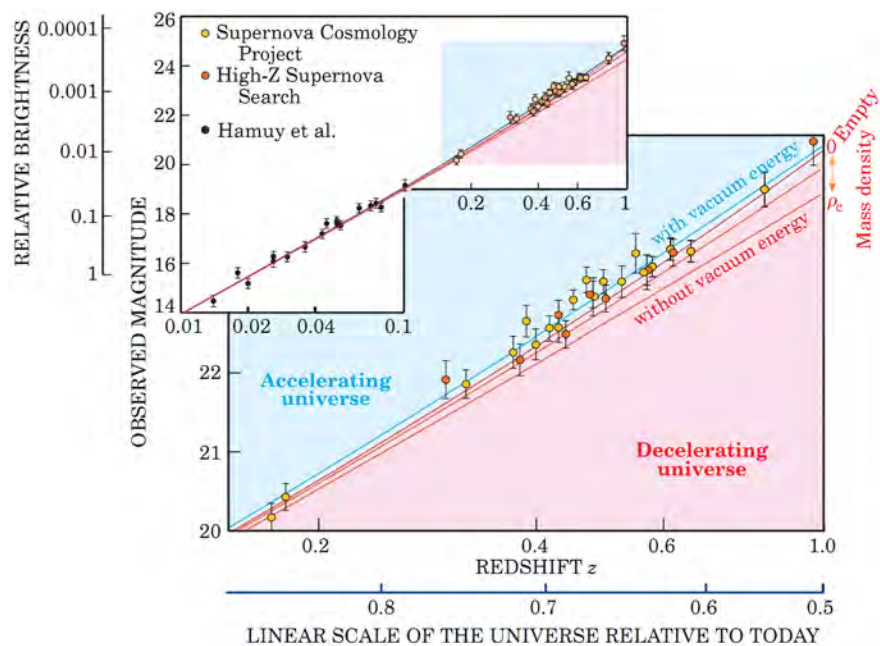


Figure 1. Observed magnitudes of type I a supernovae vs Redshift z.

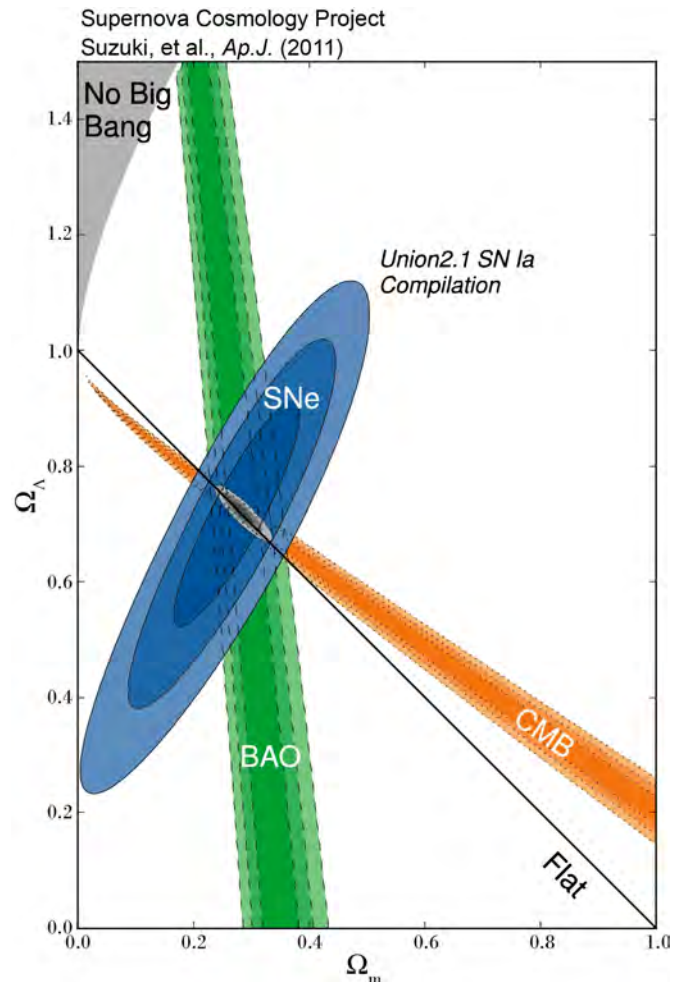


Figure 2. SCP supernovae, BAO and CMB data.

The “flat” line is where the perpetually spatially-flat FSC model falls. Once again, one can readily see that the FSC model shows an excellent statistical fit with the accumulated SCP data.

The significance of the use of the FSC model to resurrect the Dirac sea concept (at least in terms of opposite sign cosmic *energies*) is perhaps best seen in **Figure 3**. This graph is copied, in slightly modified form, from a 2018 FSC publication [23] incorporating the Bekenstein-Hawking entropy into the model in order to represent the cosmic clock as well as the “entropic arrow of time”.

One can readily see that the magnitude of *positive* matter mass-energy (visible plus dark matter) of the FSC model scales in exactly the same way as the magnitude of *negative* dark energy scales. Thus, the “net zero energy” of the universe as a global object is always maintained. In this context, the “net zero energy” FSC model can be thought of as a realistic Milne-type “empty universe” model!

4. Discussion and Summary

This paper provides a brief look at Dirac’s thought process concerning how the cosmic vacuum might behave if it follows his famous equation. The “Dirac sea”

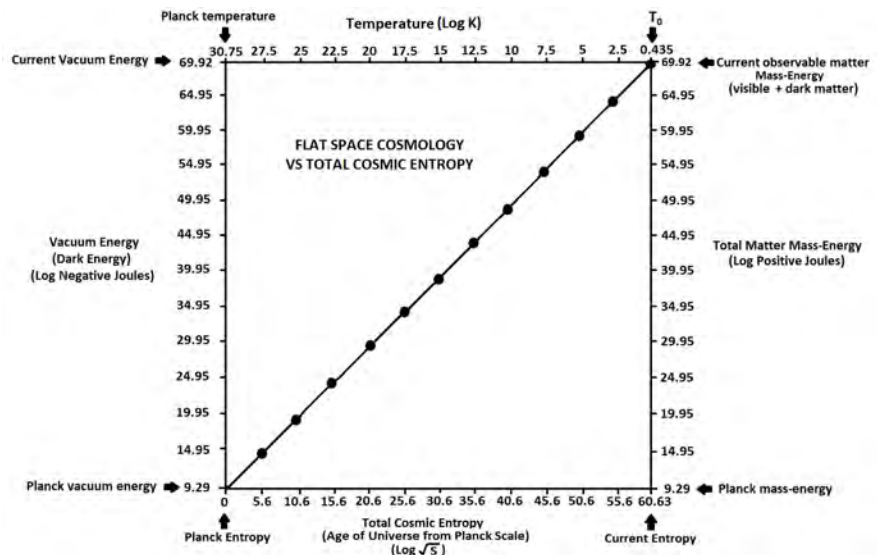


Figure 3. Flat space cosmology positive and negative energies vs cosmic time.

idea is resurrected in terms of a zero-point energy vacuum in which energy has positive (*i.e.*, matter) and negative (*i.e.*, dark energy) values always summing to zero (*i.e.*, “net zero energy”). As it turns out, the FSC model, by its perpetual matter generation and its perpetual spacetime flatness, can be seen as a realistic Milne-type “empty universe” model. The genius of Paul Dirac and his equation can once again be readily seen when his “Dirac sea” idea for positive and negative *matter* (an impossibility) is resurrected in terms of positive and negative *energy*.

Dedications and Acknowledgements

This paper is dedicated to Stephen Hawking and Roger Penrose for their groundbreaking work on black holes and their possible application to cosmology. Dr. Tatum sincerely thanks U.V.S. Seshavatharam for his co-authorship of the seminal FSC papers and some of the more recent FSC publications. He also thanks Dr. Rudolph Schild of the Harvard Center for Astrophysics for his past support and encouragement.

Conflicts of Interest

The author declares no conflicts of interest regarding the publication of this paper.

References

- [1] Wikipedia Contributors (2019) Dirac Equation. Wikipedia, the Free Encyclopedia. https://en.wikipedia.org/wiki/Dirac_equation
- [2] Guth, A.H. (1981) *Physical Review D*, **23**, 347. <https://doi.org/10.1103/PhysRevD.23.347>
- [3] Guth, A.H. (1997) *The Inflationary Universe*. Basic Books, New York.
- [4] Albrecht, A. and Steinhardt, P.J. (1982) *Physical Review Letters*, **48**, 1220-1223.

- <https://doi.org/10.1103/PhysRevLett.48.1220>
- [5] Linde, A.D. (1982) *Physics Letters B*, **108**, 389-392.
[https://doi.org/10.1016/0370-2693\(82\)91219-9](https://doi.org/10.1016/0370-2693(82)91219-9)
- [6] Steinhardt, P.J. (2011) *Scientific American*, **304**, 18-25.
<https://doi.org/10.1038/scientificamerican0411-36>
- [7] Melia, F. (2012) *Astronomical Journal*, **144**, Article ID: 110.
- [8] Tatum, E.T., Seshavatharam, U.V.S. and Lakshminarayana, S. (2015) *International Journal of Astronomy and Astrophysics*, **5**, 116-124.
<https://doi.org/10.4236/ijaa.2015.52015>
- [9] Tatum, E.T., Seshavatharam, U.V.S. and Lakshminarayana, S. (2015) *Journal of Applied Physical Science International*, **4**, 18-26.
- [10] Tatum, E.T., Seshavatharam, U.V.S. and Lakshminarayana, S. (2015) *Frontiers of Astronomy, Astrophysics and Cosmology*, **1**, 98-104.
- [11] Tatum, E.T. (2018) *Journal of Modern Physics*, **9**, 1867-1882.
<https://doi.org/10.4236/jmp.2018.910118>
- [12] Tatum, E.T. and Seshavatharam, U.V.S. (2018) *Journal of Modern Physics*, **9**, 2008-2020. <https://doi.org/10.4236/jmp.2018.910126>
- [13] Tatum, E.T. and Seshavatharam, U.V.S. (2018) *Journal of Modern Physics*, **9**, 1404-1414. <https://doi.org/10.4236/jmp.2018.97085>
- [14] Sapar, A. (2019) *Proceedings of the Estonian Academy of Sciences*, **68**, 1-12.
<https://doi.org/10.3176/proc.2019.1.01>
- [15] Aghanim, N., *et al.* (2018) Planck 2018 Results VI. Cosmological Parameters.
<http://arXiv:1807.06209v1>
- [16] Macaulay, E., *et al.* (2018) First Cosmological Results Using Type Ia Supernovae from the Dark Energy Survey: Measurement of the Hubble Constant.
- [17] Nielsen, J.T., *et al.* (2015) *Scientific Reports*, **6**, Article No. 35596.
<https://doi.org/10.1038/srep35596>
- [18] Wei, J.-J., *et al.* (2015) *Astronomical Journal*, **149**, 102.
<https://doi.org/10.1088/0004-6256/149/3/102>
- [19] Tutusaus, I., *et al.* (2017) *Astronomy & Astrophysics*, **602**, A73.
<https://doi.org/10.1051/0004-6361/201630289>
- [20] Dam, L.H., Heinesen, A. and Wiltshire, D.L. (2017) *Monthly Notices of the Royal Astronomical Society*, **472**, 835-851. <https://doi.org/10.1093/mnras/stx1858>
- [21] Perlmutter, S. (2016) Supernova Cosmology Project. Lawrence Berkeley National Laboratory, Berkeley. <http://www.supernova.lbl.gov>
- [22] Suzuki, N., *et al.* (2011) The Hubble Space Telescope Cluster Supernovae Survey: V. Improving the Dark Energy Constraints above $Z > 1$ and Building an Early-Type-Hosted Supernova Sample.
- [23] Tatum, E.T. and Seshavatharam, U.V.S. (2018) *Journal of Modern Physics*, **9**, 1469-1483. <https://doi.org/10.4236/jmp.2018.98091>

Calculation of the Mass of the Universe, the Radius of the Universe, the Age of the Universe and the Quantum of Speed

Claude Mercier

Independent Researcher, Baie-Comeau, Canada

Email: claudemercier@gctda.com

How to cite this paper: Mercier, C. (2019) Calculation of the Mass of the Universe, the Radius of the Universe, the Age of the Universe and the Quantum of Speed. *Journal of Modern Physics*, 10, 980-1001. <https://doi.org/10.4236/jmp.2019.108065>

Received: June 15, 2019

Accepted: July 16, 2019

Published: July 19, 2019

Copyright © 2019 by author(s) and Scientific Research Publishing Inc. This work is licensed under the Creative Commons Attribution International License (CC BY 4.0). <http://creativecommons.org/licenses/by/4.0/>



Open Access

Abstract

The universe is vast and when we look at the sky, its parameters (dimensions, mass, and age) seems limitless. Lemaitre proposed that the universe began from a primeval-atom [1] which was later ironically nicknamed by Hoyle “Big Bang” in a BBC broadcast in 1949 [2]. From general relativity, Einstein proposed a cosmological model [3] with a spatially finite universe. He assumed a uniform distribution of matter in a huge 4-D sphere. Even if his equations were showing that the universe was either contracting or expanding, Einstein introduced the “cosmological constant” in his equation to force the universe to be static (being consistent with the general way of thinking of his time). In 1929, from observations of galaxies, Hubble found that the universe was expanding. From that moment, Einstein discarded his cosmological constant as an unnecessary fudge factor. Many cosmological models have been built over time. Each of them excels in explaining some aspects of the universe. We consider that the global topology of the universe is not known, but making the assumptions that it is relatively homogenous and isotropic, its extrapolated local topology leads us to some global “apparent” parameters. From our new cosmological model, we calculate the main parameters of the universe which are its apparent mass m_u , its apparent curving radius R_u , its apparent age T_u and the “quantum of speed” ε_v . The quantum of speed is a new notion in physics. It is the smallest speed increment that may exist. For metrology purposes, we calculate these parameters from the most precise physics’ parameters available.

$$m_u \approx 1.73 \times 10^{53} \text{ kg}, \quad R_u \approx 1.28 \times 10^{26} \text{ m}, \\ T_u \approx 13.65 \times 10^9 \text{ years}, \quad \varepsilon_v \approx 2.38 \times 10^{-114} \text{ m} \cdot \text{s}^{-1}$$

Keywords

Mass of the Universe, Hubble Radius, Age of the Universe, Quantum of

1. Introduction

Our universe has astronomic dimensions (mass, radius, and age) that borders limitless for humans. It is also expanding [4]. Astrophysicists always try to describe our universe more accurately according to observations. Our telescopes are more and more powerful which allow us to see further every day. In a previous article [5] we made a new cosmological model from which we can deduce different parameters and dimensions. Because these different dimensions of the universe are directly linked through Dirac's large numbers to infinitely small [6] [7], it is possible to make different calculations to allow finding all the exact values of these dimensions.

This article shows different ways to calculate the apparent mass m_u of the universe, the apparent radius R_u of curvature of the universe and the age of the universe. We want also to make conscious that these values are obtained from an observer at rest, at the center of mass of the universe. Nevertheless, if the observer is traveling on a photon, his point of view will be totally different. For this reason, we will show the notion of quantum of speed. With this notion, we will see that there is an infinitely small difference between the real speed of light and the speed limit that we call the speed of light in vacuum c . For most applications, the real speed of light and the speed limit are approximately the same.

We will then show different links between the infinitely large numbers of the universe and the infinitely small numbers of the universe thanks to Dirac's hypothesis [6] [7].

2. Values of Physics Parameters

We will use the concise form of notation to display tolerances (2.736 (17) K will mean 2.736 ± 0.017 K). The following physics parameters are from CODATA 2014 [8].

- Speed of light in vacuum $c \approx 299792458 \text{ m} \cdot \text{s}^{-1}$
- Electric constant in vacuum $\epsilon_0 \approx 8.854187817 \times 10^{-12} \text{ F} \cdot \text{m}^{-1}$
- Magnetic constant in vacuum $\mu_0 \approx 4\pi \times 10^{-8} \text{ N} \cdot \text{A}^{-2}$
- Planck constant $h \approx 6.626070040(81) \times 10^{-34} \text{ J} \cdot \text{s}$
- Planck length $L_p \approx 1.616229(38) \times 10^{-35} \text{ m}$
- Planck time $t_p \approx 5.39116(13) \times 10^{-44} \text{ s}$
- Planck mass $m_p \approx 2.176470(51) \times 10^{-8} \text{ kg}$
- Universal gravitational constant $G \approx 6.67408(31) \times 10^{-11} \text{ m}^3 \cdot \text{kg}^{-1} \cdot \text{s}^{-2}$
- Electron charge $q_e \approx -1.6021766208(98) \times 10^{-19} \text{ C}$
- Electron mass $m_e \approx 9.10938356(11) \times 10^{-31} \text{ kg}$
- Classical electron radius $r_e \approx 2.8179403227(19) \times 10^{-15} \text{ m}$
- Rydberg constant $R_\infty \approx 10973731.568508(65) \text{ m}^{-1}$

3. Apparent Mass of the Universe

Let us enumerate different ways to calculate the apparent mass of the universe m_u . This mass includes every type of mass (baryonic and dark mass) and the mass associated with all types of energy (photons, dark energy, etc.).

We prefer to talk about the “apparent mass of the universe” instead of talking about the “mass of the universe” because its apparent value is seen from our point of view in the universe. For an observer located somewhere else, the observed value may be different. Please refer to our section talking about the quantum of speed to deepen your notion of “appearance” for the different parameters of the universe.

3.1. Calculation of m_u Using the Principle of Conservation of Momentum

Let us use the principle of conservation of momentum applied to the universe which says that a force F applied during a time Δt will move a mass m_u (the apparent mass of the universe) by increasing its speed by Δv . The luminous universe is expanding at the speed of light in vacuum c . Therefore, we can consider that in Equation (1), $\Delta v = c$.

$$F\Delta t = m_u\Delta v \rightarrow F = \frac{m_u\Delta v}{\Delta t} \rightarrow F = \frac{m_u c}{\Delta t} \quad (1)$$

Let us suppose that the universe is expanding for a time Δt equal to the apparent age of the universe T_u . This value is given by the inverse of the Hubble constant which is about $H_0 \approx 72.1 \text{ km} \cdot \text{s}^{-1} \cdot \text{MParsec}^{-1}$ [5] [9]. Let us note that $1 \text{ MParsec} = 3.085677581 \times 10^{22} \text{ m}$.

$$\Delta t = T_u = \frac{1}{H_0} \approx 13.65 \times 10^9 \text{ years} \quad (2)$$

If we look at the universe as a whole, and if we use Newton’s universal attraction equation to calculate the force F that the universe of apparent radius R_u applies on its own mass m_u , we get Equation (3). The constant G is the universal gravitational constant.

$$F = \frac{Gm_u^2}{R_u^2} \quad (3)$$

In Equation (3), the value of R_u is the apparent radius of curvature of the universe.

$$R_u = cT_u = \frac{c}{H_0} \approx 1.28 \times 10^{26} \text{ m} \quad (4)$$

Let us equate the forces F from Equation (1) and (3). Once we simplify and use Equation (2) and Equation (4), we get Equation (5).

$$m_u = \frac{c^3}{GH_0} \approx 1.73 \times 10^{53} \text{ kg} \quad (5)$$

We get an equation which is the same as Carvalho [10].

3.2. Calculation of m_u Using the Principle of Conservation of Energy

Let us use the principle of conservation of Energy to find the apparent mass m_u of the universe. Initially, at the Big Bang, there was no movement yet. All the energy contained in the universe was contained in the mass m_u of the universe. The total amount of energy E contained in the universe is given by Einstein formula.

$$E = m_u c^2 \quad (6)$$

Since the universe is expanding, the initial energy is converted to potential energy through a gravitational force F applied on a distance R_u (see Equation (4)) from the center of mass of the universe. Let us use Newton's law.

$$F = \frac{Gm^2}{R_u^2} \rightarrow E = FR_u = \frac{Gm^2}{R_u} \quad (7)$$

By equating Equation (6) and Equation (7), and using Equation (4), we get Equation (8).

$$m_u c^2 = \frac{Gm_u^2}{R_u} \quad \text{where } R_u = \frac{c}{H_0} \quad (8)$$

Isolating the apparent mass of the universe m_u from Equation (8), we get Equation (9).

$$m_u = \frac{c^2 R_u}{G} = \frac{c^3}{GH_0} \approx 1.73 \times 10^{53} \text{ kg} \quad (9)$$

One will notice that this is the same equation as Equation (5).

3.3. Calculation of m_u Using the Planck Mass m_p

Let us calculate the apparent mass of the universe m_u by using the Planck mass m_p . By definition, the Planck mass is defined by Equation (10) where h is the Planck constant, c is the speed of light, and G is the universal gravitational constant.

$$m_p = \sqrt{\frac{hc^3}{2\pi G}} \approx 2.18 \times 10^{-8} \text{ kg} \quad (10)$$

Let us define m_{ph} as being the mass associated with the lowest energy photon in the universe [5]. When we look at the energy of a wavelength λ , the energy is at its lowest level when λ is the largest. The largest dimension of the universe is its apparent circumference. Therefore, we can associate a mass m_{ph} to a photon of wavelength $\lambda = 2\pi R_u$ where R_u is the apparent radius of the universe.

$$m_{ph} = \frac{hc}{\lambda c^2} = \frac{hc}{2\pi R_u c^2} = \frac{hH_0}{2\pi c^2} \approx 2.74 \times 10^{-69} \text{ kg} \quad (11)$$

The Planck mass m_p is the geometric average between the smallest mass m_{ph} associated with the lowest energy photon and the biggest mass which is without any doubt the apparent mass of the universe m_u . From this fact, we get the following Equation.

$$m_p = \sqrt{m_{ph}m_u} \approx 2.17 \times 10^{-8} \text{ kg} \quad (12)$$

Equating Equations (12) and (10), and using Equation (11), we get m_u .

$$m_u = \frac{c^3}{GH_0} \approx 1.73 \times 10^{53} \text{ kg} \quad (13)$$

Again, we get, without any surprise, the same equation as Equation (5).

3.4. Calculation of m_u Using the Energy of a Photon

We will calculate the apparent mass m_u of the universe by equating the gravitational energy of a photon with the mass-energy contained in a photon (being a corpuscle) [5]. Let us associate a mass m_{ph} (like in Equation (11)) with a photon of the lowest energy [5] that is at the periphery of the luminous universe (with a wavelength λ equal to the apparent circumference of the universe $\lambda = 2\pi R_u$). Then, if we place this photon at the periphery of the luminous universe, it will have an E_g gravitational energy.

$$E_g = \frac{Gm_um_{ph}}{R_u} \quad (14)$$

According to the special relativity, the mass-energy associated with this photon is E_m .

$$E_m = m_{ph}c^2 \quad (15)$$

By equating Equations (14) and (15), replacing R_u with Equation (4), and isolating m_u , we get the same equation as Equation (5).

$$m_u = \frac{c^3}{GH_0} \approx 1.73 \times 10^{53} \text{ kg} \quad (16)$$

3.5. Calculation of m_u as a Function of the Classical Electron Radius r_e

Recently, with a new cosmological model, the precise values of the universal gravitational constant G and of the Hubble constant H_0 have been found [5] as a function of the classical electron radius r_e , the mass of the electron m_e , the fine-structure constant α , and β (see Equation (19)). Let us use Equations (17) and (18) to evaluate precisely m_u (for metrology purposes).

$$G = \frac{c^2 r_e \alpha^{20}}{m_e \beta} \approx 6.673229809(86) \times 10^{-11} \text{ m}^3 \cdot \text{kg}^{-1} \cdot \text{s}^{-2} \quad (17)$$

$$H_0 = \frac{c \alpha^{19} \sqrt{\beta}}{r_e} \approx 72.09548580(32) \text{ km} \cdot \text{s}^{-1} \cdot \text{MParsec}^{-1} \quad (18)$$

In these two equations, β is defined as the ratio between the expansion speed of the material universe and the expansion speed of the luminous universe. According to our model, the material universe is embedded in a luminous universe, both being spherical and expanding with a speed proportional to their radius [5].

$$\beta = 3 - \sqrt{5} \approx 0.76 \quad (19)$$

with his special relativity theory, Einstein showed that if we accelerate any mass at rest m_0 to a speed v , its energy E would increase because of the Lorentz factor (the square root in Equation (20)) [11]. If v tends towards c , the energy E would tend towards infinity, which is impossible since it cannot get more energy than there is available in the universe. Therefore, v must be slower than c . It also implies that the expansion speed of the material universe is slower (explaining β in Equation (19)) than its luminous counterpart which is expanding at the speed of light (which is c for now). In Equation (20), we show what would happen if we expand Einstein's formula in a series. The first term of the series is the energy at rest and the second one is the kinetic energy which is used in Newton's classical mechanics [12].

$$E = mc^2 = \frac{m_0 c^2}{\sqrt{1 - \frac{v^2}{c^2}}} \approx m_0 c^2 + \frac{1}{2} m_0 v^2 + \frac{3}{8} m_0 \frac{v^4}{c^2} + \dots \quad \text{with } v < c \quad (20)$$

With Equation (17) and Equation (18), we modify Equation (5) to get Equation (21).

$$m_u = \frac{m_e \sqrt{\beta}}{\alpha^{39}} = 1.728098528(26) \times 10^{53} \text{ kg} \quad (21)$$

This equation is one of the most precise of all since it relies on very well-known constants defined in the CODATA 2014 [8]. It also highlights the fact that there are very strong links between the universe's dimensions and its constituents as such as the electron.

3.6. Calculation of m_u as a Function of the Classical Electron Charge q_e

The electron charge q_e may be described as a function of the electron mass m_e , the electron radius r_e and the relative permeability of vacuum ϵ_0 [5].

$$q_e = -\sqrt{\frac{4\pi r_e m_e}{\mu_0}} \approx -1.60 \times 10^{-19} \text{ C} \quad (22)$$

If we isolate the electron mass m_e from Equation (22) and if we put its value in Equation (21), we get an equation that gives the apparent mass of the universe as a function of the electron charge q_e . Its precision is equivalent to Equation (21).

$$m_u = \frac{\mu_0 q_e^2 \sqrt{\beta}}{4\pi r_e \alpha^{39}} = 1.728098528(26) \times 10^{53} \text{ kg} \quad (23)$$

3.7. Calculation of m_u as a Function of the Rydberg Constant R_∞

Let us use the definition of the Rydberg constant R_∞ as a function of the fine-structure constant α and the classical electron radius r_e to find the apparent mass of the universe.

$$R_\infty = \frac{\alpha^3}{4\pi r_e} \approx 1.10 \times 10^7 \text{ m}^{-1} \quad (24)$$

If we replace the classical electron radius r_e from Equation (23) with Equation (24), we get Equation (25) that gives the apparent mass of the universe m_u as a function of the Rydberg R_∞ constant and the electron charge q_e .

$$m_u = \frac{\mu_0 q_e^2 R_\infty \sqrt{\beta}}{\alpha^{42}} = 1.728098528(27) \times 10^{53} \text{ kg} \quad (25)$$

4. Apparent Radius of Curvature of the Universe R_u

Let us enumerate different ways to calculate the apparent radius of curvature of the universe R_u .

We use the term “apparent” because the radius value is seen from our point of view in the universe. For an observer located somewhere else, the observed value may be different. Please refer to our section talking about the “quantum of speed” (further in this article) to deepen our notion of “appearance” for the different parameters of the universe. Also, we prefer to use the term “apparent radius of curvature of the universe” instead of talking about the “radius of curvature” of the universe as mentioned by Einstein [3], the “radius of the universe” [13] or the “radius of the space” [1] [13] like Lemaître because the universe may look spherical from our point of view (and we pretend that it is probably the case). However, what looks like a spherical shape is perhaps only local in the universe. Who knows, maybe the real shape of the universe is a peanut or a toroidal shape? The “apparent radius of curvature” is what we think it could be if we extrapolate the local characteristics and behaviors of the universe to a large scale. Of course, we assume here that the universe is a spherical, homogenous and isotropic. We highlight that the real radius of the universe may well be totally different if we consider other aspects of the universe which may become obvious at large scale.

Let us note that even if we get the same resulting distance as the Hubble radius [14] (which is seen as if the Earth were in the middle of this sphere), we measure here the distance between the center of mass of the universe and the outer limit of the luminous universe. In our model, the Earth is no more the “center of the universe”. The universe is expanding. So, this limit is pushed further every day. The distance that light may travel within a year is only about $7 \times 10^{-9} \%$ of the total radius R_u .

4.1. Calculation of R_u as a Function of the Hubble Constant H_0

The classical way to calculate the apparent radius of curvature of the universe R_u consist in saying that the speed of light in vacuum c was constant and traveled a time-lapse equal to an age of the universe T_u which is a function of H_0 (see Equation (2)).

$$R_u = cT_u = \frac{c}{H_0} \approx 1.28 \times 10^{26} \text{ m} \quad (26)$$

According to different sources, H_0 is between $67.8(9) \text{ km}\cdot\text{s}^{-1}\cdot\text{MParsec}^{-1}$ [15] and $77.6_{-4.3}^{+4.8} \text{ km}\cdot\text{s}^{-1}\cdot\text{MParsec}^{-1}$ [16]. Most measurements of the Hubble constant H_0 rely on inaccurate methods such as the observation of stars. Uncertainties

from different measurement results do not always overlap. For better accuracy, we will use H_0 from our Equation (18). It is compatible with Salvatelli, with $H_0 \approx 72.1_{-2.3}^{+3.2} \text{ km} \cdot \text{s}^{-1} \cdot \text{MParsec}^{-1}$ [9].

4.2. Calculation of R_u as a Function of the Classical Electron Radius r_e

Let us use Equation (18) in Equation (26) to evaluate precisely (for metrology purposes) the apparent radius of curvature of the universe R_u .

$$R_u = \frac{r_e}{\alpha^{19} \sqrt{\beta}} \approx 1.2831078845(57) \times 10^{26} \text{ m} \quad (27)$$

4.3. Calculation of R_u as a Function of the Electron Charge q_e

Let us define the apparent radius of curvature R_u as a function of the Rydberg constant R_∞ . Let us isolate r_e from Equation (22) and use it in Equation (27). We get Equation (28) which gives the apparent radius of curvature of the universe R_u as a function of the electron charge q_e and of the electron mass m_e .

$$R_u = \frac{q_e^2 \mu_0}{4\pi m_e \alpha^{19} \sqrt{\beta}} \approx 1.283107889(13) \times 10^{26} \text{ m} \quad (28)$$

4.4. Calculation of R_u as a Function of the Rydberg Constant R_∞

Like Equation (28) which uses well-known parameters from CODATA and β constant which can be calculated very accurately, we want to define the apparent radius of curvature R_u as a function of the Rydberg constant R_∞ . Let us rewrite Equation (27) with Equation (24) to get the most precise way, up to now, to calculate the apparent radius of the universe R_u .

$$R_u = \frac{1}{4\pi R_\infty \alpha^{16} \sqrt{\beta}} \approx 1.2831078902(48) \times 10^{26} \text{ m} \quad (29)$$

5. Age of the Universe Δt_u

NASA currently estimates the age of the universe by using the inverse of the Hubble constant [17], that is to say, $1/H_0$. The metric based on the work made by the physicists Friedmann [18] [19], Lemaître [1] [13], Robertson [20] and Walker [21] predicts that for a flat universe dominated by the presence of matter, the true age of the universe should be around $2/(3 \cdot H_0)$ [22]. Let us note that sometimes the name of Friedmann or Lemaître is omitted when this metric is cited. This is the case in Carroll's book which refers to this metric under the name "FRW".

Einstein was considering the universe as being static [3], with constant space-time dimensions. When he first noticed that his theory of general relativity leads to a universe in expansion or in contraction, he added a cosmological constant to his equations to force his model of the universe to be static [3]. Let's mention that in his theory of relativity, Einstein was taking for granted that the speed of light in the vacuum was constant [23] [24]. It was entirely consistent

with his view of the universe. A static universe leads to a constant speed of light, except, of course, on the outskirts of large masses as is shown by Einstein with special relativity [24] and Schwarzschild with general relativity [25].

In 1929, Hubble found that the universe was expanding [4]. When Einstein became aware of Hubble's observations, he was forced to admit, according to George Gamow, that adding a cosmological constant to his model of the universe to make it static was the biggest blunder he has made in his life [26]. Let us note that Einstein may have never used these precise words and they may have been falsely reported from Gamow. Nevertheless, Einstein discarded his cosmological constant as an unnecessary fudge factor. It looks like he did not see, at that moment, that the acceleration of light over time was a direct result of an expanding universe. With recent work, we showed that it is possible that the speed of light has never been constant over time [5].

With special relativity, Einstein showed that a gravitational field generated by a mass slows down light [24]. Erroneous by a factor of 2 compared to what happens in reality, his equation, is then corrected by Schwarzschild using general relativity [25]. The universe is expanding [4], and becomes less dense. Therefore, the index of refraction diminishes and light slowly accelerates over time [5].

Initially, we will show how the approximate age of the universe is calculated. In a second step, we will use some results from a work we have done recently [5] to estimate the age of the universe by performing the integral of the inverse of the expansion speed of the material universe according to the curvature radius of the universe. Finally, we will approximate the age of the universe. We will show that $1/H_0$ actually represents a good approximation of the apparent age T_u of the universe and that $2/(3H_0)$ represents the real part of the age of the universe. We can then compare the results and comment.

5.1. Current Methods for the Calculation of the Age of the Universe

In 1929, Edwin Powell Hubble found that galaxies distance themselves from one another at a speed proportional to the distance between them [4]. He deduced a law involving a constant called H_0 . It represents the average recession speed v of galaxies per unit of distance Δr . Let us note that galaxies have their own freedom of movements. Some may move closer to each other and some will move away from each other. But overall, they will move away from each other because of the inflating movement of the universe.

$$\frac{v}{\Delta r} = \frac{1}{\Delta t} = H_0 = 72.1 \text{ km} \cdot \text{MParsec}^{-1} \cdot \text{s}^{-1} \quad (30)$$

As seen in Equation (18), $H_0 \approx 72.1 \text{ km} \cdot \text{MParsec}^{-1} \cdot \text{s}^{-1}$. Let us isolate Δt .

$$\Delta t = \frac{1}{H_0} \approx 13.65 \times 10^9 \text{ years} \quad (31)$$

NASA is currently evaluating the age of the universe with Equation (31) [17]. This way of calculating the age assumes that the expansion rate of the universe is

constant.

According to the model of Friedmann-Robertson-Walker [22], the true age of the universe would be around 2/3 of Equation (31).

$$\Delta t = \frac{2}{3 \cdot H_0} \approx 9.04 \times 10^9 \text{ years} \quad (32)$$

5.2. Calculation of the Age of the Universe Δt_u

The speed of the light in vacuum and the expansion speed of the material universe may have not been constant over time [5]. Our goal here is to calculate the age of the universe (of complex type) by simulating a return to the past by doing the integral of the inverse of the expansion speed $v_m(r)$ of the material universe.

We will use some results of the work cited in [5] to solve the integral of the inverse of the speed $v_m(r)$ of expansion of the material universe as a function of the radius of curvature of the universe. In this way, we will calculate the age of the universe Δt_u .

As mentioned before, the general theory of relativity predicts that the presence of a massive body changes near space-time and increases the index of refraction $n(r)$ (which changes as a function of the distance r from the center of mass of the massive body) of the vacuum around a mass [25]. By moving away from that mass, the gravitational influence is being reduced and the speed of light tends toward c .

We apply the same principle to the universe which is certainly the biggest existing mass. Since the universe is expanding [4], we move away from a certain center of mass and the density of the universe becomes lower over time. Like before, this causes the refractive index to diminish over time and lets the speed of light slowly increase over time tending toward an asymptotic speed that we named k [5]. Of course, the current speed of light in vacuum is c . To keep the total energy of the universe constant meanwhile the speed of light increases, the mass of the universe must slowly decrease over time. The asymptotic speed of light k (when $r \rightarrow \infty$) is given by Equation (33).

$$k = c\sqrt{2 + \sqrt{5}} \approx 2c \approx 6.17 \times 10^8 \text{ m} \cdot \text{s}^{-1} \quad (33)$$

As soon as we try to calculate the speed of light for the time in the past or in the future, we must take into account that the speed of light $v_L(r)$ changes as a function of the apparent radius of curvature r of the universe [5]. The value of Θ is the gravitational potential for the universe and $n(r)$ is the refractive index of the universe as a function of r .

$$v_L(r) = \frac{k}{n(r)} \quad \text{where } n(r) = \sqrt{\frac{1 - 2\Theta/k^2}{1 + 2\Theta/k^2}} \quad \text{and } \Theta = \frac{-Gm_u}{r} \leq 0 \quad (34)$$

In this equation, there is a radius of curvature $r = r_h$ for which the speed of light $v_L(r_h) = 0$. This position r_h is called the horizon of the universe. This is the position for which the denominator of the square root of Equation (34) becomes

zero. In a similar way, in a black hole, the radius of curvature of the horizon r_h is obtained by the Schwarzschild's radius where we replace c by k :

$$r_h = \frac{2Gm_u}{k^2} \approx 6.06 \times 10^{25} \text{ m} \tag{35}$$

It is the same principle as that of a black hole. In fact, the universe is the biggest existing black hole since it has the biggest mass.

Let us note that for a conventional black hole, its entire mass is located in its center of mass. However, for the universe, a big part of the black hole mass lays outside the boundaries of the horizon. The center of mass of the universe coincides with the center of mass of the black hole.

The expansion speed of the universe is currently the speed of light c [5]. Based on the principles of relativity, the matter cannot move at the speed of light without having infinite energy. Consequently, the previous assertion about the expansion of the universe can be true only for light (which we call the luminous universe). The material universe (containing the galaxies, intergalactic dust clouds, etc.) is expanding at a slower speed equal to βc . The factor β , must by necessity be less than 1 since we cannot surpass the speed of light which represents a speed boundary. According to our Equation (19), its value is about 0.76. The apparent radius of curvature r_u of the material universe is, therefore, a portion β of the apparent radius of curvature R_u of the luminous universe [5].

$$r_u = \beta R_u \approx 9.80 \times 10^{25} \text{ m} \tag{36}$$

The expansion speed $v_m(r)$ of the material universe is β times the speed of light $v_L(r)$ because matter must travel slower than light [11].

$$v_m(r) = \beta v_L(r) = \frac{\beta k}{n(r)} \quad \text{where } n(r) = \sqrt{\frac{1-2\Theta/k^2}{1+2\Theta/k^2}} \quad \text{and } \Theta = \frac{-Gm_u}{r} \leq 0 \tag{37}$$

If we take the derivative of the expansion speed $v_m(r)$ of the material universe with respect to the distance r , we get the Hubble constant H_0 [5].

$$\left. \frac{dv_m(r)}{dr} \right|_{r=r_u} = \frac{k\beta y}{r_u} \left(\frac{1}{(1+y)\sqrt{1-y^2}} \right) = H_0 \quad \text{where } y = \frac{2Gm_u}{k^2 r_u} \tag{38}$$

It is important to realize that we do not use the derivative of the expansion speed of the luminous universe to get H_0 since astronomers cannot observe that limit. Through their telescopes, they only see objects like stars and galaxies. Consequently, when Hubble defined its constant H_0 , it was based on the derivative of the expansion speed $v_m(r)$ of the material universe.

At the periphery of the luminous universe (at a distance $r = R_u$ from the center of mass of the universe), light accelerates at an $a_L(R_u) = cH_0$ rhythm.

$$a_L(R_u) = \left. \frac{dv_L(r)}{dt} \right|_{r=R_u} = \left(\frac{dr}{dt} \cdot \frac{dv_L}{dr} \right) \Big|_{r=R_u} = c \left(\frac{dv_L}{dr} \right) \Big|_{r=R_u} = cH_0 \tag{39}$$

However, locally, at a distance $r = r_u$ from the center of mass of the universe, light slowly accelerates at an $a_L(r_u) = cH_0/\beta$ rhythm.

$$a_L(r_u) = \left. \frac{dv_L(r)}{dt} \right|_{r=r_u} = \left. \left(\frac{dr}{dt} \cdot \frac{dv_L}{dr} \right) \right|_{r=r_u} = c \left. \left(\frac{dv_L}{dr} \right) \right|_{r=r_u} = c \frac{H_0}{\beta} \quad (40)$$

Locally, at a distance $r = r_u$ from the center of mass of the universe, matter from the material universe slowly accelerates at an $a_m(r_u) = cH_0$ rhythm.

$$a_m(r_u) = \beta \left. \frac{dv_L(r)}{dt} \right|_{r=r_u} = \beta \left. \left(\frac{dr}{dt} \cdot \frac{dv_L}{dr} \right) \right|_{r=r_u} = \beta c \left. \left(\frac{dv_L}{dr} \right) \right|_{r=r_u} = \beta c \frac{H_0}{\beta} = cH_0 \quad (41)$$

Figure 1 shows the module of the expansion speed $v_m(r)$ of the material universe calculated from Equation (37). It also puts in evidence the Hubble constant H_0 as the slope evaluated precisely at the position $r = r_u$ from the center of mass of the universe (at $r = 0$). Between $r = 0$ (at the Big Bang) and $r = r_h$ (horizon of the universe), the dotted part of the curve shows that the expansion speed of the material universe would normally be negative and of imaginary type. Then, from $r = r_h$ and infinite, the expansion speed of the material universe becomes of real type.

The negative and imaginary value of the speed $v_m(r)$ we get with $r < r_h$ is a mathematical way to show that in a physical world, matter inside the horizon evolves independently than outside the horizon. Here, we cannot see what is happening inside the horizon and vice versa. We could compare it to the cylindrical envelope of an optical fiber. Light can travel inside a fiber from one extremity to the other end, but we cannot see through the envelope (if the fiber is used in its curving limits). It is therefore impossible to know what is happening from outside the fiber and vice versa. Of course, the principles in cause in fiber are not the same. We only bring this example to do an image of the situation happening inside the horizon of a black hole.

Performing the integral of the inverse of $v_m(r)$ with respect to the radius of curvature r , it is possible to calculate precisely the age of the universe more precisely (in its entirety with the real part and its imaginary part) than by using a single tangential projection. In **Figure 1**, the slope of the tangential projection gives the Hubble constant H_0 which can be put in Equation (31) to give the apparent age of the universe.

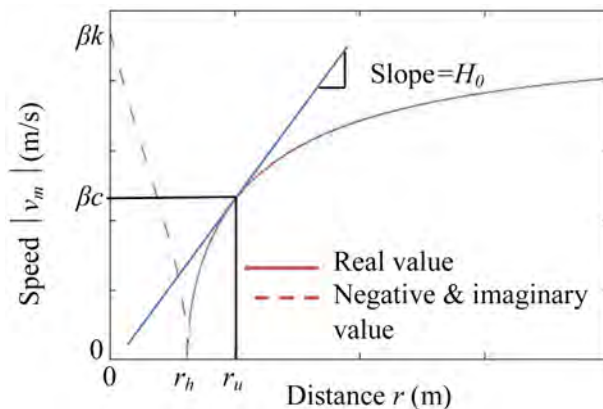


Figure 1. Expansion speed $|v_m|$ of the material universe as a function of distance r .

Let's find the age of the universe $\Delta t_u(r)$ by performing the integral of Equation (42) between the center of mass of the universe (at $r = 0$) and the apparent radius of curvature of the material universe r_u . The resulting value $\Delta t_u(r)$ is of a complex type.

$$\Delta t_u(t) = \int_0^{r_u} \frac{1}{v_m(r)} dr = \Delta t_{hu}(r) + \Delta t_{0h}(r) \quad (42)$$

In Equation (42), the value of $\Delta t_{hu}(r)$ represents the time elapsed between the horizon and the actual age of the universe (see Equation (43)). The resulting value is of real type.

$$\Delta t_{hu}(r) = \int_{r_h}^{r_u} \frac{1}{v_m(r)} dr \quad (43)$$

In Equation (42), the value of $\Delta t_{0h}(r)$ represents the time elapsed between the Big Bang and the horizon (see Equation (44)). The resulting value is of an imaginary type.

$$\Delta t_{0h}(r) = \int_0^{r_h} \frac{1}{v_m(r)} dr \quad (44)$$

Performing the integral calculation of Equation (42), we get Equation (45).

$$\int \frac{1}{v_m(r)} dr = \frac{\left(z(r) + 2G \cdot m_u \ln \left(2 \left[k^2 r + z(r) \right] \right) \right)}{\beta k^3} \quad (45)$$

where $z(r) = \sqrt{k^4 r^2 - 4G^2 m_u^2}$

Consequently, the value of $\Delta t_u(r)$ becomes:

$$\Delta t_u(r) = \Delta t_{hu}(r) + \Delta t_{0h}(r) \approx (9.50 + 10.47i) \times 10^9 \text{ years} \quad \text{where } i = \sqrt{-1} \quad (46)$$

This result is of a complex type. In Equation (46), the first part of the integral (shown in Equation (43)) is of a real type (between r_h and r_u). However, the second part of this latter one (shown in Equation (44)) is of an imaginary type (between 0 and r_h).

If we look carefully to Equation (37), for a radius smaller than the horizon r_h , the speed of light $v_l(r_h)$ becomes of an imaginary type. For this reason, the time T_{0h} become of an imaginary type as well. This mathematical situation just means that time inside the horizon evolves in a completely independent way compared to time outside the horizon, which is why no one can see what happens inside the limits of the horizon of a black hole. The best example we could give is with a fiber optic cable. How light evolves inside the fiber cannot be seen from outside the fiber, and vice versa. Mathematics are a nice language which has to be interpreted to find sense in the real world.

When we wish to consider the time elapsed between position 0 of the Big Bang and the radius of curvature of the horizon r_h , we must calculate the module of the time elapsed $|\Delta t_u|$. We define this value as the apparent age T_u of the universe because it does not necessarily represent the true age of the universe. This

number represents only an apparent age in the likely event that the Big Bang existed. It could also be seen as the time that elapsed if the speed of light had been constant over time since the Big Bang.

$$T_u = |\Delta t_u| = |\Delta_{hu} + \Delta t_{0h}| = \sqrt{\Delta t_{hu}^2 + \Delta t_{0h}^2} \approx 14.14 \times 10^9 \text{ years} \quad (47)$$

We see that the value is only 4.25% over the value of Equation (31).

5.3. Approximation of the Age of the Universe

As for the calculation of power in electrical motors (with the real power, the inductive power and the apparent power), the age of the universe may be seen as follows: the “real” part of the age of the universe, the “imaginary” part of the age of the universe and the “apparent” age of the universe. The module of the two components (real and imaginary) can be calculated using the Pythagorean Theorem by finding the square root of the sum of the squares of the real part and the imaginary part of the age of the universe.

The approximation of the age of the universe will be made in 3 parts: the approximation of the real part of the age of the universe, the approximation of the imaginary part of the age of the universe and the calculation of the module of the apparent age of the universe. In **Figure 2**, we show the parallelogram built from these values.

5.4. Approximation of the Real Part Δt_{hu} of the Age of the Universe

Let's perform the approximation of the real part Δt_{hu} of the age of the universe Δt_u .

For a radius of curvature r_h of the horizon, the square root in Equation (48) equals zero.

$$z(r_h) = \sqrt{k^4 r_h^2 - 4G^2 m_u^2} = 0 \quad (48)$$

So, according to Equation (42) and Equation (45), we get Equation (49).

$$\Delta t_{hu} = \frac{z(r_u) + 2 \cdot G \cdot m_u \cdot \ln\left(2 \cdot \left[k^2 \cdot r_u + z(r_u)\right]\right)}{\beta \cdot k^3} - \frac{2 \cdot G \cdot m_u \cdot \ln\left(2 \cdot k^2 \cdot r_h\right)}{\beta \cdot k^3} \quad (49)$$

where $z(r_u) = \sqrt{k^4 \cdot r_u^2 - 4 \cdot G^2 \cdot m_u^2}$

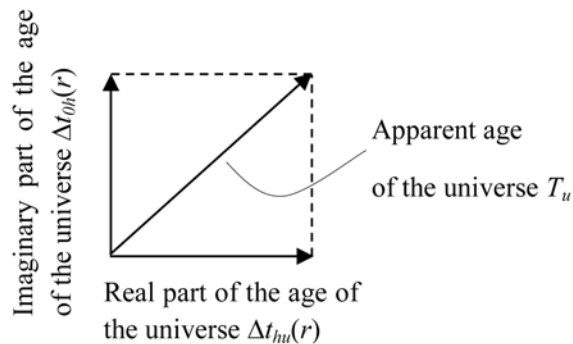


Figure 2. Complex age Δt_u of the universe.

Using Equation (35) with a few simplifications, we get Equation (50).

$$\Delta t_{hu} = \frac{1}{\beta \cdot k} \left(\sqrt{r_u^2 - r_h^2} + r_h \ln \left(\frac{\sqrt{r_u^2 - r_h^2} + r_u}{r_h} \right) \right) \tag{50}$$

Without changing anything, this same equation could be rewritten as follows.

$$\Delta t_{hu} = \frac{r_u}{2 \cdot \beta \cdot c} \cdot \left(1 + \frac{\beta}{2} \right) \cdot y \approx \frac{r_u}{2 \cdot \beta \cdot c} \cdot \left(1 + \frac{\beta}{2} \right)$$

$$\text{where } y = \left[\frac{2 \cdot c}{k \cdot r_u \cdot \left(1 + \frac{\beta}{2} \right)} \cdot \left(\sqrt{r_u^2 - r_h^2} + r_h \ln \left(\frac{\sqrt{r_u^2 - r_h^2} + r_u}{r_h} \right) \right) \right] \approx 1 \tag{51}$$

As shown, the content of the bracket is approximately equal to 1. By doing this approximation and using Equation (36), Equation (51) becomes Equation (52).

$$\Delta t_{hu} \approx \frac{1}{4H_0} (2 + \beta) \tag{52}$$

Further, in this document, we will use Equation (52) to perform the calculation of the apparent age of the universe. For now, let us show that this equation can be approximated to get an equation commonly used by some astronomers to calculate the actual age of the universe.

According to Equation (19), the value of $\beta \approx 0.76$. Let's use this approximation to rewrite Equation (52). After a few simplifications, we get:

$$\Delta t_{hu} \approx \frac{1}{4H_0} \left(2 + \frac{76}{100} \right) \approx \frac{1}{H_0} \left(\frac{69}{100} \right) \approx \frac{2}{3H_0} \approx 9.04 \times 10^9 \text{ years} \tag{53}$$

This last ratio can be deduced from the model of Friedmann-Robertson-Walker [22]. Therefore, Equations (52) and (53) represent good approximations of the real part of the age of the universe.

5.5. Approximation of the Imaginary Part Δt_{0h} of the Age of the Universe

Now, let's find the approximate value of the imaginary part T_{0h} of the age of the universe T_{ir} . From Equation (42), Equation (45) and Equation (48) we get:

$$\Delta t_{0h} = \left[\frac{2 \cdot G \cdot m_u \cdot \ln(2 \cdot k^2 \cdot r_u)}{\beta \cdot k^3} \right] - \left[\frac{\sqrt{-4 \cdot G^2 \cdot m_u^2} + 2 \cdot G \cdot m_u \cdot \ln(2 \cdot \sqrt{-4 \cdot G^2 \cdot m_u^2})}{\beta \cdot k^3} \right] \tag{54}$$

Using Equation (35) and performing a few simplifications, we get Equation (55).

$$\Delta t_{0h} = \frac{r_h}{\beta \cdot k} \cdot [\ln(-i) - i] \text{ where } i = \sqrt{-1} \tag{55}$$

Using the relationship in Equation (56), we rewrite Equation (55), which is the result of a purely imaginary type, to get Equation (57).

$$\ln(-i) = -\frac{\pi}{2} \cdot i \quad (56)$$

$$\Delta t_{0h} = -\frac{r_h}{\beta \cdot k} \cdot \left[1 + \frac{\pi}{2}\right] \cdot i \quad (57)$$

We can rewrite Equation (57) in the following way without changing anything:

$$\Delta t_{0h} = -\frac{r_u}{2 \cdot \beta \cdot c} \cdot \left(1 - \frac{\beta}{2}\right) \cdot \left(1 + \frac{\pi}{2}\right) \cdot x \cdot i \quad \text{where } x = \left[\frac{2 \cdot c}{k} \cdot \frac{r_h}{r_u \cdot \left(1 - \frac{\beta}{2}\right)} \right] \approx 1 \quad (58)$$

As shown, the value of x is approximately 1. Equation (58) then becomes:

$$\Delta t_{0h} \approx -\frac{1}{2 \cdot H_0} \cdot \left(1 - \frac{\beta}{2}\right) \cdot \left(1 + \frac{\pi}{2}\right) \cdot i \quad (59)$$

5.6. Approximation of the Apparent Age T_u of the Universe

Let's calculate the apparent age of the universe by using Equation (47) with Equation (52) and Equation (59). After a few simplifications, we get Equation (60).

$$|\Delta t_u| = |\Delta t_{hu} + \Delta t_{0h}| = \sqrt{\Delta t_{hu}^2 + \Delta t_{0h}^2} \approx \frac{1}{H_0} \chi \approx \frac{1}{H_0} \quad (60)$$

$$\text{where } \chi = \left(\frac{1}{2} \cdot \sqrt{\left(1 + \frac{\beta}{2}\right)^2 + \left(\left(1 - \frac{\beta}{2}\right) \cdot \left(1 + \frac{\pi}{2}\right)\right)^2} \right) \approx 1$$

The value of χ is approximately equal to 1. Consequently, we have shown that the integral of Equation (42) can be approximated by Equation (31). According to us, based on the approximation calculation made at Equation (60), Equation (31) represents only an apparent age T_u of the universe. In fact, it comes from the calculation of the module of a complex sum of the real part and the imaginary part of the age of the universe. We define T_u as the apparent age of the universe.

$$T_u = |\Delta t_u| \approx \frac{1}{H_0} \approx 13.65 \times 10^9 \text{ years} \quad (61)$$

6. Quantum of Speed ε_v

By definition, a quantum (the word "quanta" is plural) represents the smallest indivisible amount of any physical entity. For example, Planck length L_p represents a quantum of distance and Planck time t_p represents a quantum of time. The quantum of speed is the smallest variation of speed that can be obtained. It is so small that it is immeasurable. Nevertheless, it is possible to calculate it thanks to certain physical considerations.

We want to show, among other things, that the different parameters (apparent mass, radius, and age) of the universe are what they are from our point of view. However, they may look different from the point of view of an observer traveling

at the speed of light. Thus, everyone will understand why we consider these parameters as being “apparent”.

In relativity, the speed of light in vacuum c is considered the speed limit. It is used in the Lorentz factor. We will show that even light does not exactly travel at the speed limit c , but a bit less. In fact, the real speed of light is $c - \varepsilon_v$, where ε_v is what we call the quantum of speed. This is the smallest variation of speed that can be measured.

Let us suppose an observer at rest looking at a mass m_0 . According to special relativity [11] [27], if we accelerate the mass at a speed v , for the observer, the mass becomes m' .

$$m' = \frac{m_0}{\sqrt{1 - \frac{v^2}{c^2}}} \quad (62)$$

We would be tempted to say that when $v \rightarrow c$, the mass m' tends towards infinity. However, this is not logical since it is impossible to reach a mass bigger than the mass of the universe m_u . We cannot give to a mass more energy than what is available in the whole universe. This statement imposes a new limit to the speed v .

We make the statement that Planck mass m_p represents the highest level of energy for a particle. It is easy to verify this assertion by equating the energy of an arbitrary mass m with the energy of the smallest wavelength λ possible (which is $2\pi L_p$, where L_p is the Planck length). Planck length L_p is considered, in a quantum world, the smallest unit of length. This is due to the Heisenberg's uncertainty principle which says that we cannot measure precisely the speed of an object and its precise location at the same time [28]. Here, the mass-energy from a particle (given by Einstein's equation [11] [27] $E = mc^2$) is associated to the wave energy (given by Planck's formula $E = hc/\lambda$ [29]).

$$mc^2 = \frac{hc}{\lambda} \quad \text{where } \lambda = 2\pi L_p \quad (63)$$

The standard definition of a Planck length is Equation (64), which implies the universal gravitational constant G , the Planck constant h and the speed of light in vacuum c .

$$L_p = \sqrt{\frac{hG}{2\pi c^3}} \approx 1.62 \times 10^{-35} \text{ m} \quad (64)$$

If we replace L_p in Equation (63) and if we isolate the mass m , we get Equation (65) which is exactly the standard definition of Planck mass m_p .

$$m = \sqrt{\frac{hc}{2\pi G}} = m_p \approx 2.18 \times 10^{-8} \text{ kg} \quad (65)$$

From this statement, we can calculate the maximum speed v_m at which we might move a particle having an initial mass m_{p0} at rest. We give to this mass the same value as the mass associated to a photon of wavelength $\lambda = 2\pi R_u$ (the apparent circumference of the universe). Since this wavelength is the longest that

we can reach in the universe, it corresponds to the lowest amount of energy we can get.

$$\frac{m_{ph}}{\sqrt{1-\frac{v_m^2}{c^2}}} = m_p \rightarrow v_m = c \sqrt{1-\frac{m_{ph}^2}{m_p^2}} \quad (66)$$

Since $m_{ph} \ll m_p$, we can make the following approximation.

$$v_m \approx c \left(1 - \frac{m_{ph}^2}{2m_p^2} \right) \quad (67)$$

In Equation (67), m_{ph} is defined by Equation (11).

Dirac made the hypothesis that all large, dimensionless numbers that could be constructed from the important natural units of cosmology and atomic theory were connected. Let us call N the ratio between the apparent mass of the universe m_u and the mass m_{ph} of associated with the photons of the lowest energy (from Equation (11)).

$$N = \frac{m_u}{m_{ph}} \approx 6.30 \times 10^{121} \quad (68)$$

Let us show that Equation (67) can be defined as a function of N . Let us rewrite Equation (68) with Equation (5) and Equation (11). Then, using the Planck mass m_p (given by Equation (10)), we show that N can be redefined as a function of m_p and m_{ph} (instead of m_u and m_{ph}).

$$N = \frac{c^3}{GH_0} \cdot \frac{2\pi R_u c}{h} = \frac{hc}{2\pi G} \cdot \frac{4\pi^2 R_u^2 c^4}{h^2 c^2} = \frac{m_p^2}{m_{ph}^2} \approx 6.30 \times 10^{121} \quad (69)$$

Let's define the speed v_m in Equation (67) as a function of N with Equation (69).

$$v_m \approx c - \frac{c}{2N} \quad (70)$$

If we replace v_m by $c - \varepsilon_v$, the value of ε_v could be defined as the "quantum of speed".

$$\varepsilon_v \approx \frac{c}{2N} \approx 2.38 \times 10^{-114} \text{ m} \cdot \text{s}^{-1} \quad (71)$$

This speed variation ε_v is the smallest speed unit possible. For an academic purpose, let us rewrite Equation (62) by replacing the speed v per $c - n\varepsilon_v$, where n is an integer > 0 .

$$m' = \frac{m_0}{\sqrt{1-\frac{v^2}{c^2}}} \text{ where } v = c - n\varepsilon_v \text{ and } n = 1, 2, 3, \dots, 2N \quad (72)$$

We see that with Equation (72), we cannot reach an infinite mass anymore and that the real speed of light is at least a quantum of speed slower than the speed limit c . Everyone will admit that ε_v is a so small value compared to any

speed value that it may be neglected most of the time. Nevertheless, it allows putting in evidence some speed boundaries.

The universe is expanding with relativistic speeds. For an observer traveling at the speed of light ($c-\varepsilon_v$), the total mass of the universe would be much smaller. In fact, it would be seen as being only the Planck mass $m_p \approx 2.18 \times 10^{-8}$ kg. If we travel at the same speed as a photon, we have to null out the Lorentz factor that is included at the denominator in the apparent mass of the universe m_u to see what is happening from the observer point of view. We multiply m_u by the Lorentz factor using Equations (70) and (71).

$$m_u \sqrt{1 - \frac{(c - \varepsilon_v)^2}{c^2}} \approx m_u \sqrt{\frac{1}{N}} \approx m_p \approx 2.18 \times 10^{-8} \text{ kg} \quad (73)$$

Planck mass m_p is usually defined by Equation (65).

Similarly, for an observer traveling at the speed of light ($c-\varepsilon_v$), the apparent radius of curvature R_u would look like being only the Planck length $L_p \approx 1.6 \times 10^{-35}$ m.

$$R_u \sqrt{1 - \frac{(c - \varepsilon_v)^2}{c^2}} \approx R_u \sqrt{\frac{1}{N}} \approx L_p \approx 1.62 \times 10^{-35} \text{ m} \quad (74)$$

Planck length L_p is usually defined by Equation (64).

Again, for an observer traveling at the speed of light ($c-\varepsilon_v$), the apparent age of the universe T_u would look like being only the Planck time t_p .

$$T_u \sqrt{1 - \frac{(c - \varepsilon_v)^2}{c^2}} \approx \frac{1}{H_0} \sqrt{1 - \frac{(c - \varepsilon_v)^2}{c^2}} \approx \frac{1}{H_0} \sqrt{\frac{1}{N}} \approx t_p \approx 5.39 \times 10^{-44} \text{ s} \quad (75)$$

Planck time t_p is usually defined by Equation (76).

$$t_p = \sqrt{\frac{hG}{2\pi c^5}} = \frac{L_p}{c} \approx 5.39 \times 10^{-44} \text{ s} \quad (76)$$

On another side, for an observer at rest, if there were no expansion, no movement, and no rotation in the universe, the total mass of the universe would be only the Planck mass m_p . Most of the universe energy (therefore its mass) is coming from different sort of relativistic movement. The demonstration becomes the same as in Equation (73). Obviously, if there were no expansion, the apparent radius of the universe would be the Planck length L_p . If there were no expansion in the universe, the apparent age of the universe would be the Planck time t_p .

7. Different Links between the Universe Dimensions

Dirac made the hypothesis that all large, dimensionless numbers that could be constructed from the important natural units of cosmology and atomic theory were connected [6] [7]. Let us see some about m_u (apparent mass of the universe), m_p (Planck mass), R_u (apparent radius of the universe), L_p (Planck Length), T_u (apparent age of the universe), t_p (Planck time) and H_0 (Hubble con-

stant).

$$N = \frac{m_u}{m_{ph}} = \frac{m_u^2}{m_p^2} = \frac{m_p^2}{m_{ph}^2} = \frac{m_u R_u}{m_p L_p} = \frac{m_p R_u}{m_{ph} L_p} = \frac{m_u T_u}{m_p t_p} = 6.3 \times 10^{121} \quad (77)$$

$$N = \frac{m_p T_u}{m_{ph} t_p} = \frac{m_u}{m_p t_p H_0} = \frac{m_p}{m_{ph} t_p H_0} = \frac{R_u^2}{L_p^2} = \frac{T_u^2}{t_p^2} = \frac{1}{t_p^2 H_0^2} \approx 6.3 \times 10^{121} \quad (78)$$

Let us remind that N represents the maximum number of photons of the lowest energy that may exist in the universe (if we were converting the entire mass of the universe in photons having a wavelength equal to the apparent circumference of the universe $2\pi R_u$).

In Equation (77) and Equation (78), the values of the different parameters of the universe may be obtained from imprecise sources. A precise link between the large number N [5] and the fine-structure constant α can be made.

$$N = \frac{1}{\alpha^{57}} \approx 6.303419702(84) \times 10^{121} \quad (79)$$

By showing Equations (77)-(79), our goal was to highlight the fact that there are tight and precise links between the infinitely large and infinitely small. Once we are aware of these interesting links, we can find more similar precise links with the large number N . More than a hundred other equations may be made about this large number N and various parameters of the universe (temperature, charge, etc.) [30]. From a reverse way, we can get precise values for different parameters of the universe by equating Equation (79) with other equations giving N .

8. Conclusions

In this article, we have shown different ways to calculate the apparent mass of the universe, the apparent radius of curvature of the universe and the age of the universe. We also made the calculation of the quantum of speed. With these parameters, we used Dirac's large numbers hypothesis to show that there are links between all these parameters.

We have defined a new concept that we think must be introduced in physics: the "quantum of speed" ε_v . The "quantum of speed" notion made us conscious that there is a little difference between the real speed of light and the speed limit. For most application, it does not matter to say that both speeds are equal. Although, in some special case, it is necessary to put in evidence the difference. Using common sense, we show that it is evident that we cannot give more energy to any mass than there is energy in the whole universe (which is m_u). Also, since Planck mass m_p is associated to the highest level of energy for an accelerated particle, we cannot give more energy to any particle than what is contained in the Planck mass m_p . Following these two findings, the "quantum of speed" ε_v is naturally introduced.

It was a necessity to introduce the "quantum of speed" to be able to calculate what would be the apparent mass of the universe, the apparent radius of curva-

ture and the age of the universe from the point of view of an observer traveling at the speed of light. Surprisingly, the results are totally different than what common sense would lead to. Only relativity allows us to interpret correctly the results according to the point of view of the observer.

From a metrology point of view, we reach our goal by obtaining precise values for different dimensions of the universe. Using these values will make it easier to see the different links we can make between large numbers of Dirac and the infinitely small. With imprecise values, we can pass beside nice occasions to make rise new theories.

Conflicts of Interest

The author declares no conflicts of interest regarding the publication of this paper.

References

- [1] Kragh, H. (2012) *Astrophysics and Space Science Library*, **395**, 23-38. https://doi.org/10.1007/978-3-642-32254-9_3
- [2] Kragh, H. (2013) *Astronomy & Geophysics*, **54**, 228-230. <https://doi.org/10.1093/astrogeo/att035>
- [3] Einstein, A. (1917) Kosmologische Betrachtungen zur allgemeinen Relativitätstheorie. Springer Link, 130-139. https://doi.org/10.1007/978-3-663-19510-8_9
- [4] Hubble, E. (1929) *Proceedings of the National Academy of Sciences of the United States of America*, **15**, 168-1973. <https://doi.org/10.1073/pnas.15.3.168>
- [5] Mercier, C. (2019) *Journal of Modern Physics*, **10**, 641-662. <https://doi.org/10.4236/jmp.2019.106046>
- [6] Dirac, P.A.M. (1938) *Proceedings of the Royal Society of London A: Mathematical, Physical and Engineering Sciences*, **165**, 199-208. <https://doi.org/10.1098/rspa.1938.0053>
- [7] Dirac, P.A.M. (1974) *Proceedings of the Royal Society of London A: Mathematical, Physical and Engineering Sciences*, **338**, 439-446. <https://doi.org/10.1098/rspa.1974.0095>
- [8] Mohr, P.J., Newell, D.B. and Taylor, B.N. (2016) *Journal of Physical and Chemical Reference Data*, **45**, Article ID: 043102. <https://doi.org/10.1063/1.4954402>
- [9] Salvatelli, V., Andrea, M., Laura, L.-H. and Olga, M. (2013) *Physical Review D*, **88**, Article ID: 023531. <https://doi.org/10.1103/PhysRevD.88.023531>
- [10] Carvalho, J.C. (1995) *International Journal of Theoretical Physics*, **34**, 2507-2509. <https://doi.org/10.1007/BF00670782>
- [11] Einstein, A. (1956) *Physics Today*, **9**, 30. <https://doi.org/10.1063/1.3059795>
- [12] Newton, I. (1686) *Philosophiae Naturalis Principia Mathematica*. Samuel Pepys and the Royal Society Praeses, London, 510. <https://doi.org/10.5479/sil.52126.39088015628399>
- [13] Lemaître, G. (2013) *General Relativity and Gravitation*, **45**, 1635-1646.
- [14] Zichichi, A. (2000) *Proceedings of the International School of Subnuclear Physics*, **36**, 708. <https://doi.org/10.1142/9789812793935>
- [15] Ade, P.A.R., et al. (2016) *Astronomy & Astrophysics*, **594**, A13.

- <https://doi.org/10.1051/0004-6361/201525830>
- [16] Bonamente, M., Joy, M.K., La Roque, S.J. and Carlstrom, J.E. (2005) *The Astrophysical Journal*, **647**, 25-54. <https://doi.org/10.1086/505291>
- [17] Jarosik, N. (2011) *The Astrophysical Journal Supplement Series*, **192**, 17. <https://doi.org/10.1088/0067-0049/192/2/14>
- [18] Friedmann, A. (1922) *Zeitschrift für Physik*, **10**, 377-386. <https://doi.org/10.1007/BF01332580>
- [19] Friedmann, A. (1924) *Zeitschrift für Physik*, **21**, 326-332. <https://doi.org/10.1007/BF01328280>
- [20] Robertson, H.P. (1933) *Reviews of Modern Physics*, **5**, 62-90. <https://doi.org/10.1103/RevModPhys.5.62>
- [21] Walker, A.G. (1937) *Proceedings of the London Mathematical Society*, **42**, 90-127. <https://doi.org/10.1112/plms/s2-42.1.90>
- [22] Carroll, S.M. (2004) *Spacetime and Geometry: An Introduction to General Relativity*. Addison Wesley, Boston, 513.
- [23] Einstein, A. (1916) *Annalen der Physik*, **49**, 769-822. <https://doi.org/10.4324/9780203198711>
- [24] Einstein, A. (1911) *Annalen der Physik*, **35**, 898-908. <https://doi.org/10.1002/andp.19113401005>
- [25] Grøn, Ø. (2016) *American Journal of Physics*, **84**, 537. <https://doi.org/10.1119/1.4944031>
- [26] Weinberg, S. (2005) *Physics Today*, **58**, 31-35. <https://doi.org/10.1063/1.2155755>
- [27] Einstein, A. (1905) *Annalen der Physik*, **322**, 891-921. <https://doi.org/10.1002/andp.19053221004>
- [28] Heisenberg, W. (1927) *Zeitschrift für Physik*, **43**, 172-198. <https://doi.org/10.1007/BF01397280>
- [29] Planck, M. (1899) *Natuerliche Masseinheiten*. Der Königlich Preussischen Akademie Der Wissenschaften, 479.
- [30] Mercier, C. (2016) *More than a Hundred Ways to Get the Large Number N. Hypothesis and Thoughts on the Universe*, 14. http://www.pragtec.com/physique/index_en.html

Topologically Stable States of the Anti-Centrifugal Potential

Rossen Dandoloﬀ

Laboratoire de Physique Theorique et Modelisation, Universite de Cergy-Pontoise, Cergy-Pontoise, France

Email: rdandoloﬀ@yahoo.com

How to cite this paper: Dandoloﬀ, R. (2019) Topologically Stable States of the Anti-Centrifugal Potential. *Journal of Modern Physics*, 10, 1002-1005.
<https://doi.org/10.4236/jmp.2019.108066>

Received: June 9, 2019

Accepted: July 16, 2019

Published: July 19, 2019

Copyright © 2019 by author(s) and Scientific Research Publishing Inc. This work is licensed under the Creative Commons Attribution International License (CC BY 4.0).

<http://creativecommons.org/licenses/by/4.0/>



Open Access

Abstract

We present a study of the anti-centrifugal potential based on the incorporation of the quantum geometric potential of a surface [1] into the generalised anti-centrifugal potential [2]. As a basic variable we will use the unit normal to the surface. Then the total quantum effective potential appears to be the nonlinear sigma model plus positive terms. A 2d bilayer geometry smoothly connected by a neck is used to show that the anti-centrifugal potential creates topologically stable states.

Keywords

Anti Centrifugal Potential, Topology, Quantum States

1. Introduction

Recently a peculiar quantum behaviour of a free particle on a plane (R^2) was discussed [3], where free particles with 0 angular momentum ($m = 0$) appear to be attracted to the origin of the plane (the origin of the coordinate system on the plane). The authors [3] have considered a Dirac δ -function potential at the origin, which breaks the translational invariance of the plane and introduces a length scale in the problem. It turns out that a Hamiltonian with a Dirac δ -function potential on the plane is equivalent to a free Hamiltonian on a plane with one point (at the origin) taken out [4]. Then the plane becomes non simply connected and the consequences for quantum mechanics are studied in [4]: namely the self adjointness of operators. In the present paper we will discuss a non simply connected surface and will study the consequences of this topological property of the surface for the stability of the anti centrifugal states. We will follow our previous work [2] on the generalised anti centrifugal potential. In this paper [2] we have analysed the Laplace-Beltrami (LBO) operator on a surface where we have introduced *half-geodesic coordinates* [5]. The radial coordinate

ξ represents the geodesic and the other η closes around the hole at the origin. The line element in these coordinates is given by: $ds^2 = d\xi^2 + h(\xi)d\eta^2$. The LBO separates in two parts: kinetic and potential part V for the radial coordinate ξ given by

$$V = -\frac{\hbar^2}{2m_0} \left[\frac{1}{4}k_g^2 - \frac{1}{2}K - \frac{m^2}{r_0^2} \right] \quad (1)$$

Here $K = -h^{-1}\partial_\xi^2 h$ represents the Gaussian curvature of the surface and $k_g = -h^{-1}\partial_\xi h$ is the geodesic curvature. For angular momentum $m=0$ (note that the anti centrifugal potential appears only for $m=0$) the above potential takes the form:

$$V = -\frac{\hbar^2}{2m_0} \left[\frac{1}{4}k_g^2 - \frac{1}{2}K \right] \quad (2)$$

In addition for a general surface there is a quantum geometric potential (QGP). Usually it is shown that this potential is induced on a surface, using the method of a very high sandwich potential around the surface. This potential has the form [1]

$$V = -\frac{\hbar^2}{8m_0} (\kappa_1 - \kappa_2)^2 = -\frac{\hbar^2}{2m_0} (M^2 - K). \quad (3)$$

Here κ_i 's are the principal curvatures of the surface, \hbar is the Planck's constant and m_0 is the effective mass. M is the Mean curvature and K is the Gauss curvature of a two-dimensional surface embedded in three-dimensional space.

The combined potential V_{tot} reads:

$$V_{tot} = -\frac{\hbar^2}{2m_0} \left[\frac{1}{4}k_g^2 - \frac{3}{2}K + M^2 \right] \quad (4)$$

2. The Normal \mathbf{n} of a Surface as a Main Variable

The investigations until now were concentrated on different geometries and the corresponding QGP. So far the link between the QGP and the topology of the underlying geometry has not been discussed.

In this paper we will use the normal to the surface \mathbf{n} as the basic variable describing the surface. Indeed the link between the normal \mathbf{n} of a surface and its Gaussian and Mean curvatures is given by the following expressions [6]:

$$M = -\nabla \cdot \mathbf{n}, \quad (5)$$

$$2K = \mathbf{n} \cdot \nabla^2 \mathbf{n} + (\nabla \cdot \mathbf{n})^2. \quad (6)$$

Now we are ready to express V_{tot} in terms of the normal \mathbf{n} only.

$$V_{tot} = -\frac{\hbar^2}{2m_0} \left[\frac{1}{4}k_g^2 + \frac{1}{4}(\nabla \cdot \mathbf{n})^2 + \frac{3}{4}(\nabla \mathbf{n})^2 \right] \quad (7)$$

Here we have used the following identity:

$$\mathbf{n}^2 = 1 \Rightarrow \mathbf{n} \cdot \nabla^2 \mathbf{n} = -(\nabla \mathbf{n})^2 \quad (8)$$

Now we will consider here a surface that represents a double layer connected by a smooth neck. The normals \mathbf{n} to this surface at the infinity on the upper layer are directed upwards and on the lower layer are directed downwards. Let us note that the catenoid possesses the same topology as the above described double layer. Usually the anti centrifugal potential is considered in cylindrical coordinates because there its presence becomes immediately evident. In this case: $V_{eff} = V(r) + \frac{m^2}{2m_0 r^2}$ where r is the radial coordinate—in our case this is ξ .

3. The Number of States

Now we would like to estimate the number of radial states (for the effective one dimensional Schrödinger equation in the ξ direction). The momenta p_ξ in the potential $V_\xi = V_{tot}$ vary between 0 and p_ξ where

$$p_\xi = \sqrt{-2m_0 V_\xi} = \frac{\hbar}{2} \sqrt{(\nabla \cdot \bar{\mathbf{n}})^2 + 3(\nabla \bar{\mathbf{n}})^2 + k_g^2} \geq \frac{\hbar}{2} \sqrt{3(\nabla \bar{\mathbf{n}})^2}. \tag{9}$$

In the inequality we have used the fact that k_g^2 and $(\nabla \cdot \bar{\mathbf{n}})^2$ are always positive. When $\xi \rightarrow \infty$ $\bar{\mathbf{n}} \rightarrow \bar{\mathbf{n}}_0 = \text{constant vector field}$, therefore $V_\xi \rightarrow 0$ (note that $k_g \rightarrow 0$ for $\xi \rightarrow \infty$ and that the potential $V(\xi)$ represents a smooth function of ξ because we assume that the surface is smooth surface and as a consequence $\bar{\mathbf{n}}$ is a smooth function of ξ) and $p_\xi = 0$ for $\xi = \infty$, so $\xi = \infty$ represents a turning point for the quasi-classical approximation in the framework of which we are estimating the number of localised states. Now we are ready to evaluate the density of states along the ξ axis. The density of states is given by the following expression [7]:

$$d\mathcal{N} = \frac{p_\xi d\xi}{2\pi\hbar} = \frac{p_\xi d\xi}{h} \geq \frac{\sqrt{3}}{4\pi} |\nabla \bar{\mathbf{n}}| d\xi = \frac{\sqrt{3}}{4\pi} d\theta. \tag{10}$$

where $\theta(\xi)$ is the azimuthal angle in the ξ direction. The unit vector that represents the normal to the surface is given by $\bar{\mathbf{n}} = (\cos\theta(\xi), \sin\theta(\xi))$. Note that usually in the context of different spin models $(|\nabla \bar{\mathbf{n}}|^2 d\xi)$ represents the energy density and is the one dimensional non linear sigma model. Then the total number of states is:

$$N = \oint d\mathcal{N} = \oint \frac{\sqrt{3}}{4\pi} d\theta = \frac{\sqrt{3}}{2} > 0. \tag{11}$$

The integration path represents the equivalence of two disconnected half circles to the left of the origin and to the right of the origin of the coordinate system. The total gives 2π ($\oint d\theta = 2\pi$).

4. Conclusion

It is clear that using topological arguments we cannot determine the exact number of states. But on the other hand the localised states cannot be destroyed by any smooth deformation of the considered surface *i.e.* they are topologically stable. These topological considerations give the localised anti-centrifugal states addi-

tional legitimacy.

Conflicts of Interest

The author declares no conflicts of interest regarding the publication of this paper.

References

- [1] da Costa, R.C.T. (1981) *Physical Review A*, **23**, 1982.
<https://doi.org/10.1103/PhysRevA.23.1982>
- [2] Dandoloﬀ, R., Jensen, B. and Saxena, A. (2014) *Physics Letters A*, **378**, 510.
<https://doi.org/10.1016/j.physleta.2013.12.016>
- [3] Cirone, M.A., Rzazewski, K., Schleich, W.P., Straub, F. and Wheeler, J.A. (2001) *Physical Review A*, **65**, Article ID: 022101.
<https://doi.org/10.1103/PhysRevA.65.022101>
- [4] Kowalski, K., Podlaski, K. and Rembielinski, J. (2002) *Physical Review A*, **66**, Article ID: 032118. <https://doi.org/10.1103/PhysRevA.66.032118>
- [5] Forsyth, A.R. (2012) *Lectures on the Differential Geometry of Curves and Surfaces*. Forgotten Books, London.
- [6] Weatherburn, C.E. (1961) *Differential Geometry of Three Dimensions*. Vol. 1, Cambridge University Press, Cambridge.
- [7] Landau, L.D. and Lifshitz, E.M. (2004) *Quantum Mechanics*. Butterworth-Heinemann, Oxford.

Explanation of Dark Matter, Dark Energy and Dark Space: Discovery of Invisible Universes

Alexander Alexandrovich Antonov

Independent Researcher, Kiev, Ukraine

Email: telan@bk.ru

How to cite this paper: Antonov, A.A. (2019) Explanation of Dark Matter, Dark Energy and Dark Space: Discovery of Invisible Universes. *Journal of Modern Physics*, 10, 1006-1028.

<https://doi.org/10.4236/jmp.2019.108067>

Received: June 4, 2019

Accepted: July 22, 2019

Published: July 25, 2019

Copyright © 2019 by author(s) and Scientific Research Publishing Inc.

This work is licensed under the Creative Commons Attribution International License (CC BY 4.0).

<http://creativecommons.org/licenses/by/4.0/>



Open Access

Abstract

Theoretical and experimental studies of special processes in linear electric circuits have proved the principle of physical reality of imaginary numbers discovered 500 years ago. This principle of physical reality of imaginary numbers has allowed astrophysics to prove the existence of invisible parallel universes and explain the phenomena of dark matter, dark energy and dark space associated therewith. Physical entities corresponding to imaginary, complex and hypercomplex numbers in the other exact sciences together form an invisible and still unknown world that is to be learned by science of the future.

Keywords

Imaginary Numbers, Dark Matter, Dark Energy, Dark Space, Multiverse, Hyperverses

1. Introduction

At the turn of the twentieth century William Thomson, 1st Baron Kelvin the President of the Royal Society in 1890-1895, asserted: “*There is nothing new to be discovered in physics now. All that remains is more and more precise measurement.*” However, the twentieth century denied this assertion, as theory of relativity and quantum mechanics were developed, radioactivity and X-ray radiation, a planetary model of atom and black holes, dark matter and dark energy were discovered, atomic and hydrogen bombs were exploded, transistors, integrated microcircuit, lasers and many other things were created.

History repeats itself. And now, at the turn of the twenty-first century, it is often asserted that we just need to create a “theory of everything”, thereby allowing one to assume that everything else in physics has already been learned¹.

But, firstly, it is more correct to assume that the learning process is infinite

¹Therefore, unified field theory is more correct name of this theory.

and there are always more unlearned things in physics than learned ones. Therefore, for example, the achievements of twentieth-century physics from the standpoint of physics of the third millennium would be much more modest than we imagine today. Secondly, many theories developed in physics up to date, including the theory of relativity and quantum mechanics, are not actually completely accurate and require correction in accordance with the principle of physical reality of imaginary numbers.

Finally, authors of a number of fundamental discoveries have been honoured with the Nobel Prize already in the twenty-first century:

- 2006: John C. Mather and George F. Smoot, who confirmed the Big Bang theory by their studies of cosmic microwave background and black holes;
- 2011: Saul Perlmutter, Brian P. Schmidt and Adam G. Riess, who discovered dark energy;
- 2013: François Englert and Peter Higgs, who discovered the Higgs boson.

There can be no doubt that there will be other outstanding discoveries and new theories in the present century.

In this regard, the hypothesis of the hidden Multiverse developed in the twenty-first century is also of interest, as it has solved many problems that arose in astrophysics of the twentieth century. This hypothesis is based on the principle of physical reality of imaginary numbers proved theoretically and experimentally. Moreover, there are even several proofs [1]-[17] that have been offered. And since previously unknown experiments² corresponding to them can be repeated in any radio engineering and electrotechnical laboratory, they, unlike the unsuccessful OPERA experiment, which attempted to solve the same problem essentially, are absolutely reliable and undoubtedly demonstrative.

The simplest and most understandable of these proofs is the proof using the Ohm's law in the interpretation of Steinmetz [10] [11] [12] [13] [14]. This interpretation of the Ohm's law, in addition to its direct purpose of enabling calculation of linear electric AC circuits, also has allowed the author to:

- prove physical reality of imaginary and complex numbers³ [1]-[17];
- create correct theory of resonance [1] [2] [3] [4] [7] [9] [15] [16];
- correct the special theory of relativity (STR) [7] [10] [13] [18];
- create verifiable hypothesis of the hidden Multiverse [19]-[34];
- explain the phenomenon of dark matter and dark energy [8] [11] [14] [17] [23]-[30] [35] [36] [37] [38];
- explain where antimatter is and why it does not annihilate with matter [38];
- explain where tachyons are and why they do not violate the causality principle [38];
- discover the phenomenon of dark space and a Hyperverse [17] [39].

²Including those described in articles [1] [2] [3] [5], published before the end of the OPERA experiment and therefore made this experiment unnecessary.

³Physical reality of imaginary, complex, hyper-complex and real numbers is actually reasonable to speak of only in respect of concrete numbers provided with references to units of measurement used for the corresponding parameters of physical objects.

2. Proof of Physical Reality of Concrete Imaginary Numbers

In 1826 Georg Simon Ohm discovered the law, which now bears his name, as a result of nine years of experimental research. In order to realize how difficult it was to discover the law, it's enough to remember that there were no electric measuring instruments at that time. Moreover, experimental research and mathematical processing of its results were not encouraged in physics of that time. Famous physicist Alexander Grigorievich Stoletov wrote in this regard: "...*physics especially tempted natural philosophers. What a favourable theme were electric phenomena for the most riotous imaginations... Attractive and vague deductions were in the foreground: hard work of experimenter and exact mathematical analysis were not honoured; they seemed superfluous and harmful in the study of nature...*" Therefore, in 1828 Ohm was even fired by the Minister of Education for his discovery. The Minister considered that the use of mathematics in physics was inappropriate. However, later, Ohm's research received deserved recognition. In 1881 International Congress of Electricians in Paris gave his name to the unit of electric resistance.

Nevertheless, exceptional ideological significance of Ohm's law for all exact sciences has not been still realized. Therefore, except solution of the above-specified problems, this article aims to fill this gap in science and pay tribute to the great scientist.

In 1826 Georg Simon Ohm proposed his law in the formulation applicable to electric DC circuits [40]. And its interpretation applicable to electric AC circuits was proposed by Charles Proteus Steinmetz [41] in 1893. This interpretation is now commonly referred to as the symbolic method of calculating electric circuits. We will use it below.

According to Steinmetz theory resistance of a resistor is equal to a real number R , the value of which does not depend on frequency ω of sinusoidal voltage applied to thereto. Inductive reactance L is equal to a positive imaginary number⁴ $j\omega L$, the value of which depends on frequency ω . Capacitive reactance C is equal to a negative imaginary number $-j/\omega C$, the value of which also depends on frequency ω , although in a different way.

Consequently, resistance of any electric LCR circuit would depend on frequency ω , if imaginary inductive and capacitive reactances are actually physically existent and would not depend, if otherwise. Therefore, an experiment determining whether inductive and capacitive imaginary reactances are physically existent would be extremely simple. In this experiment, it is only needed to change the frequency of sinusoidal voltage applied to LCR circuit and check whether value of electric current flowing through the circuit changes. The result of the experiment conducted by millions of engineers in the course of their everyday practical activities (for example, when creating electric filters that are indispensable for radio engineering, telecommunication, television, radiolocation

⁴In the theory of electric circuits, unlike mathematics, the imaginary unit $\sqrt{-1}$ is usually denoted by the letter j , since the letter i denotes electric current.

and other exact sciences) has long been known. In this experiment intensity of current always changes.

Besides, physical reality of imaginary inductive and capacitive reactances is also confirmed by the power factor, also called the $\cos \varphi$, a concept available in power engineering, characterizing the presence in the load of a physically existent imaginary component of the power consumed.

Consequently, imaginary inductive and capacitive reactances are actually physically existent. Hence, ***any other concrete imaginary numbers are also physically existent.***

The utmost importance of imaginary numbers in the science was emphasized by Sir Roger Penrose: "...the very system of complex numbers has a profound and timeless reality which goes beyond the mental constructions of any particular mathematician... They were put there neither by Cardano, nor by Bombelly, nor Wallis, nor Coates, nor Euler, nor Wessel, nor Gauss, despite the undoubted farsightedness of these, and other, great mathematicians; such magic was inherent in the very structure that they gradually uncovered..."

Discovery of the experimentally proven principle of physical reality of imaginary numbers is extremely important from ideological point of view. The principle suggests that in addition to the visible world known to us there is another world which is invisible and still unknown. And, as shown below, under certain circumstances people can visit this unknown physical world even passing into it on foot.

Thus, Ohm's law is important in science because it allows calculation of electric circuits, and even more important because it allows proof of existence of the invisible and unknown world, which the science of future has yet to discover. As well as because, in accordance with the principle of physical reality of imaginary numbers, all existing theories and hypotheses in exact sciences should now be corrected. Their existing interpretations, as shown below with the example of the currently accepted version of the special theory of relativity, are imperfect.

3. Correction of the Special Theory of Relativity

The special theory of relativity [42] [43] [44] created by Joseph Larmor [45], Nobel laureate Hendrik Antoon Lorentz [46], Jules Henri Poincaré [47], Nobel laureate Albert Einstein [48] and other outstanding scientists has always been criticized throughout its century-old history. The criticism⁵ has not always been constructive, although sometimes it has been fair and incontestable. For example, ***the principle of non-exceedance of the speed of light postulated in the STR,***

⁵The STR has been criticized from the very beginning by Oliver Heaviside, Nikola Tesla, Nobel Prize winner Albert Abraham Michelson, Nobel Prize winner Friedrich Wilhelm Ostwald, Nobel Prize winner Joseph Noble Prize winner Nobel Prize winner Svante August Arrhenius, Nobel Prize winner Prize winner Alvar Gullstrand, Nobel Prize winner Wilhelm Carl Werner Otto Fritz Franz Wien, Nobel Prize winner Walter Hermann Nernst, Nobel Prize winner Ernest Rutherford, 1st Baron Rutherford of Nelson, Nobel Prize winner Johannes Stark, Nobel Prize winner Frederick Soddy, Nobel Prize winner Percy Williams Bridgman, Nobel Prize winner Edwin Mattison McMillan, Nobel Prize winner Hideki Yukawa, Nobel Prize winner Hannes Olof Gösta Alfvén and many other outstanding scientists.

⁶As it has not been yet proved by anybody.

which has the effect of denying the physical reality of imaginary numbers, is experimentally refuted by the principle of physical reality of imaginary numbers proved above.

The Nobel Prize winner Steven Weinberg spoke about the unproven experimental theories very clearly: “Scientific theories cannot be deduced by purely mathematical reasoning”.

The principle of physical reality of imaginary numbers also proves incorrectness of all relativistic formulas of the STR, in particular,

$$m = \frac{m_0}{\sqrt{1-(v/c)^2}} \quad (1)$$

$$\Delta t = \Delta t_0 \sqrt{1-(v/c)^2} \quad (2)$$

$$l = l_0 \sqrt{1-(v/c)^2} \quad (3)$$

where m_0 is the rest mass of a physical body;

m is the relativistic mass of a moving physical body;

Δt_0 is the rest time of a physical body;

Δt is the relativistic time of a moving physical body;

l_0 is the rest longitudinal length of a physical body;

l is the relativistic longitudinal length of a moving physical body;

v is the velocity of a moving physical body;

c is the speed of light.

Explaining the formulas, the STR asserts that as relativistic mass m , time Δt , longitudinal length l and other physical quantities assumes imaginary values at $v \geq c$, they are physically nonexistent. However, as follows from the principle of physical reality of imaginary numbers, this assertion is erroneous and made due to misunderstanding of some aspects of the STR by its authors, particularly, inability to prove physical reality and explain physical nature of concrete imaginary numbers.

In fact, according to the principle of physical reality of imaginary numbers, physical world corresponding to them exists in the STR, and therefore needs an explanation. This is as follows. When $v \geq c$ physical world must exist if formulas (1), (2) and (3) are valid. But formulas (1), (2) and (3) are valid only in the range $0 \leq v < c$. And in the range $v \geq c$ they do not meet this condition (see **Figures 1(a)-(c)**). Therefore, they should be corrected for the range $v > c$ as follows

$$m = \frac{m_0 i^q}{\sqrt{1-(v/c-q)^2}} = \frac{m_0 i^q}{\sqrt{1-(w/c)^2}} \quad (4)$$

$$\Delta t = \Delta t_0 i^q \sqrt{1-(v/c-q)^2} = \Delta t_0 i^q \sqrt{1-(w/c)^2} \quad (5)$$

$$l = l_0 i^q \sqrt{1-(v/c-q)^2} = l_0 i^q \sqrt{1-(w/c)^2} \quad (6)$$

where $q = \lfloor v/c \rfloor$ is the “floor” function of argument v/c ;

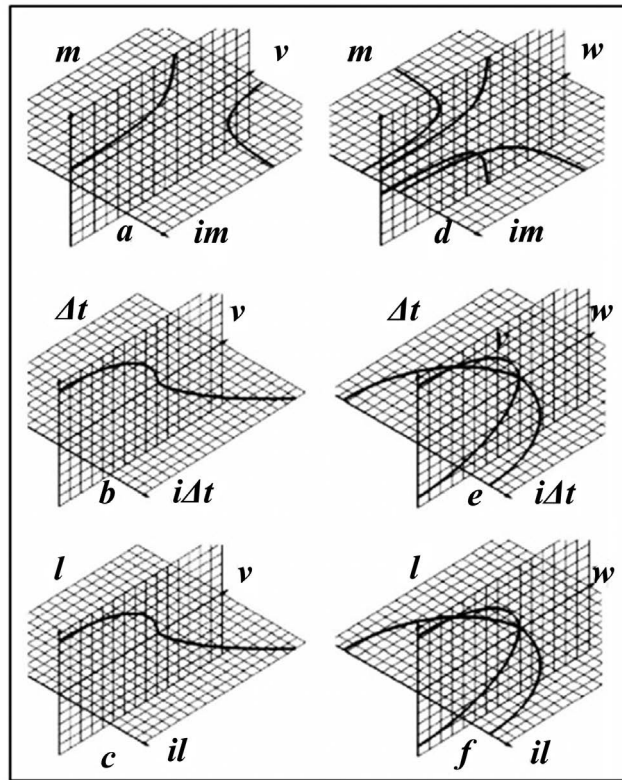


Figure 1. (a) is graph of the function (1); (b) is graph of the function (2); (c) is graph of the function (3); (d) is graph of the function (4); (e) is graph of the function (5); (f) is graph of the function (6).

$w = v - qc$ is the local velocity for each universe, which can take values only in the range $0 \leq w < c$;

v is the velocity measured from our universe;

c is the speed of light.

Albert Einstein did not exclude the adjustment of the STR in future. He wrote: “No single idea, which I would be sure that it will stand the test of time”.

4. Hypothesis of the Hidden Multiverse

In formulas (4), (5), (6) the value $q = 0$ corresponds then to our universe and the value $q = 1$ corresponds to the adjacent universe, in which $c \leq v < 2c$ and which is invisible from our universe, as it is beyond the horizon of events. This universe contains tachyons [49]-[54], so it shall be for definiteness referred to as tachyon universe. Recognizing physical reality of imaginary time corresponding to the formula (5), Stephen William Hawking wrote in this regard: “Imaginary time is a new dimension, at right angles to ordinary, real time”.

For similar reasons, our universe is called tardyon. Consequently, we actually live in a Multiverse, which shall be called hidden due to mutual invisibility of parallel⁷ universes contained therein, rather than in a Monoverse.

However, in formulas (4), (5), (6) the quantity q can also assume greater val-

⁷Since despite their infinity they never intersect.

ues⁸. Thus, the quantity $q=2$ corresponds to the tardyon antiverse (as $i^2 = -1$), the quantity $q=3$ corresponds to the tachyon antiverse (as $i^3 = -i$), the quantity $q=4$ corresponds to another⁹ tardyon universe (as $i^4 = 1$), the quantity $q=5$ corresponds to another tachyon universe (as $i^5 = -1$), etc. It can be assumed that these universes can form both closed¹⁰ (**Figure 2**) and open (**Figure 3**, **Figure 4**) screw structure. Herewith, if the hidden Multiverse has the structure of a closed screw ring¹¹, then it should be assumed unique. If the hidden Multiverse has the structure of an open screw ring, then its edges would be connected to other Multiverses: twice with the same Multiverse as in **Figure 3**, or with two different Multiverses¹², as in **Figure 4**. And together they form a Hyperverse.

It's time answer one more obvious question: Why parallel universes do not intersect? There can be only one answer: Because they exist in space that has more than three dimensions. In formulas (4), (5) and (6) this circumstance is taken into account by the parameter q , which is the fourth spatial dimension. Consequently, distribution of material contents in such a hidden Multiverse is described by function $f_q(x, y, z) + iq$ in which x, y, z are the coordinates of the material contents in the corresponding parallel universe, and q is the coordinate of this universe in the fourth spatial dimension.

Besides, parallel universes naturally do not stand still in this four-dimensional space. They continuously drift and often touch each other in numerous spots or even slightly penetrate into each other. In the places of interpenetration certain transition zones¹³ occur, which are usually referred to as portals¹⁴ or star gates [19] [20] [21] [29] [30] [31] [55] [56] [57]. In **Figures 2-4**, these multiple bidirectional portals¹⁵ are denoted by single two-sided arrows.

5. Where Are Antimatter and Tachyons?

The great advantage of the hidden Multiverse hypothesis is that it gives answers to many questions that have not yet been explained in astrophysics.

Thus, it is quite obvious that tachyons are in tachyon universes and antiverses. Herewith, it immediately becomes clear that they do not violate the principle of causality, as they are not in our tardyon universe.

It is no less obvious that antimatter [58] [59] [60] [61] [62] is in antiverses. Besides, tardyon antiverse turns out to exist not only relative to our tardyon universe, but there are other tardyon antiverses relative to other tardyon universes.

⁸This is proved below.

⁹Since there are totally not less than twenty universes in the hidden Multiverse.

¹⁰Same-type universes and antiverses in all figures are indicated by the same colour combination of frame and fill. Besides, colour combinations of frame and fill of the similar universes and antiverses are mutually opposite.

¹¹In fact, as is shown below this structure cannot exist in nature.

¹²In which, therefore, frames are of the same color and fills are of different colors for all Multiverses.

¹³In which the quantity q varies by one from one integer value to another, corresponding to the adjacent parallel universes.

¹⁴Which have nothing to do with "wormholes" in the general theory of relativity.

¹⁵Through which the material contents of adjacent universes have been exchanged.

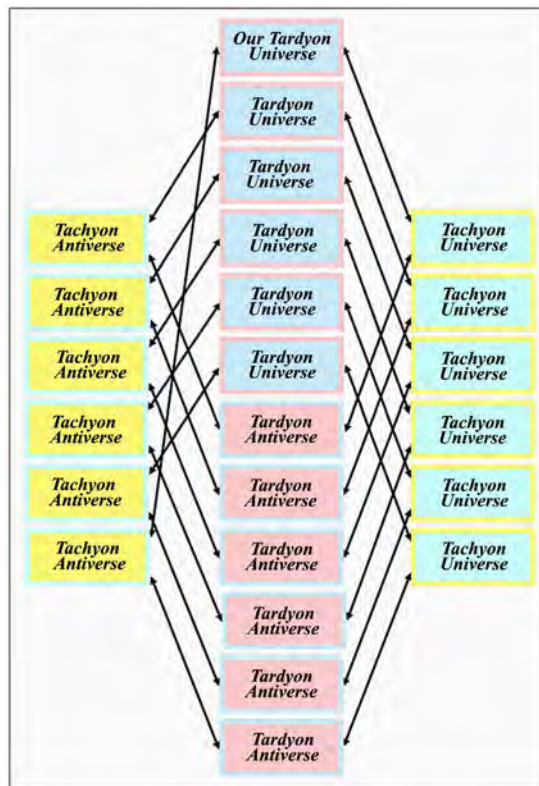


Figure 2. Structure of the hidden Multiverse corresponding to the principle of physical reality of complex numbers.

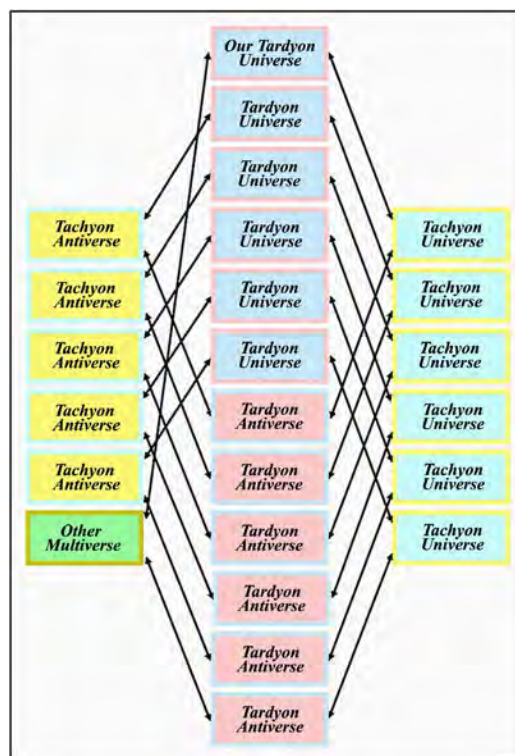


Figure 3. Another structure of the hidden Multiverse corresponding to the principle of physical reality of complex numbers.

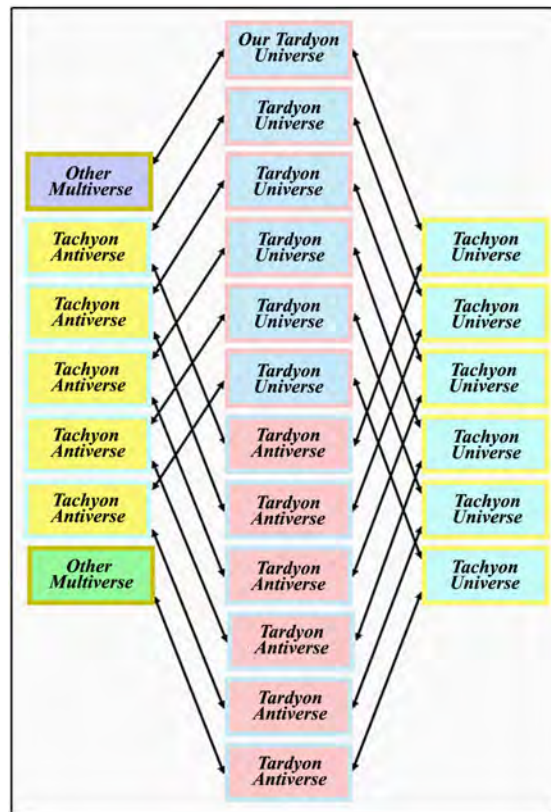


Figure 4. One more structure of the hidden Multiverse corresponding to the principle of physical reality of complex numbers.

Moreover, there are tachyon antiverses relative to their tachyon universes. Therefore, matter and antimatter do not annihilate in the hidden Multiverse, as tardyon universes and antiverses alternate with tachyon universes and antiverses.

6. Explanation of Dark Matter and Dark Energy

In the twentieth century two extremely important scientific discoveries were made in astrophysics [63]-[69]. One of them was made in 1932-33 by Jan Hendrik Oort [70] and Fritz Zwicky [71] and called dark matter. Another one, called dark energy, was made in 1998-1999 by Saul Perlmutter [72], Brian P. Schmidt [73] and Adam G. Riess [74] who were awarded the Nobel Prize for this discovery. Adam G. Riess argued on this point: “Humanity is on the verge of a new physics of the Universe¹⁶. Whether we want it or not, we will have to accept it”.

But what dark matter and dark energy themselves are, until very recently, could not be explained. It was for these incomprehensibility that these physical entities were called dark.

Therefore Michio Kaku came to the following conclusion [75]: “Of course, a whole bunch of Nobel Prizes is waiting for the scientists who can reveal the secrets of the ‘dark energy’ and ‘dark matter’”.

¹⁶The foundations of which are set forth in this paper.

There are many hypotheses of the Multiverse [75]-[83]. However, they have a very significant drawback: none of them explains the phenomenon of dark matter and dark energy. The phenomenon of dark matter and dark energy also is not explained by the Monoverse hypothesis corresponding to the current version of the STR, within the framework of which all unsuccessful attempts to explain this phenomenon have been carried out so far. In this regard, it seems appropriate to take into account Albert Einstein's point of view: "*Insanity: doing the same thing over and over again and expecting different results*".

The phenomenon of dark matter and dark energy can be quite explicable in terms of the hypothesis of the hidden Multiverse [35] [36] [37] [38]:

- invisibility of dark matter and dark energy is explained by mutual invisibility of parallel universes of the hidden Multiverse;
- failure to detect any of well-known chemical elements in composition of dark matter and dark energy is explained by inability to analyze contents of other universes located in other dimensions by tools we use on Earth;
- dark matter is other parallel universes of the hidden Multiverse adjacent to our universe;
- dark energy is other parallel universes of the hidden Multiverse, besides our universe and universes adjacent to it.

7. Analysis of Data of WMAP and Planck Spacecrafts

This structure of the hidden Multiverse can be defined more exactly due to data obtained by WMAP [84] and Planck [85] spacecrafts. Thus, according to WMAP data, our universe (in fact, our hidden Multiverse) is composed of 4.6% baryonic matter, 22.4% dark matter and 73.0% dark energy. And according to later measurements of the Planck spacecraft, our universe (again, in fact, our hidden Multiverse) is composed of 4.9% baryonic matter, 26.8% dark matter and 68.3% dark energy.

Therefore, believing that mass-energy of parallel universes has been substantially averaged over billions of years due to the existence of portals, *i.e.* their mass-energy can be accurately assumed to be equal, we find:

- the total number of parallel universes in the hidden Multiverse, which is $100\%/4.6\% = 21.7$ universes according to WMAP data and $100\%/4.9\% = 20.4$ universes according to Planck data, *i.e.* 20 ... 22 universes;
- the number of parallel universes in dark matter, which is $22.4\%/4.6\% = 4.9$ universes according to WMAP data and $26.8\%/4.9\% = 5.5$ universes according to Planck data, *i.e.* 5 ... 6 universes;
- the number of parallel universes in dark energy, which is $73.0\%/4.6\% = 15.9$ universes according to WMAP data and $68.3\%/4.9\% = 13.9$ universes according to Planck data, *i.e.* 14 ... 16 universes.

Thus, dark matter and dark energy turned out to be invisible parallel universes of the hidden Multiverse, beside ours, rather than some new microstruc-

tures of our visible universe, which are currently looked for at the Large Hadron Collider. In other words, these are just other names of these universes.

Apparently, the foregoing does not fully correspond to assertions generally accepted in relativistic physics and astrophysics. Sir Isaac Newton wrote: “No great discovery was ever made without a bold guess”. The same opinion was held by Niels Henrik David Bohr who said his catchphrase: “There is no doubt we have faced a mad theory. But the question is this. Is it really crazy enough to be right?”

However, the results of WMAP and Planck data analysis that give such evident explanation do not correspond to the probable structures of the hidden Multiverse shown in **Figures 2-4**. In these structures, tardyon universes cannot be adjacent to five-six tachyon universes and antiverses, since there is no space for two-three infinitely large parallel universes in the same dimension with the coordinate q .

Consequently, the structures of the hidden Multiverse shown in **Figures 2-4** do not correspond to the WMAP and Planck data. And their fallacy is explained by the fact that they correspond only to the simplest case of implementation of the hidden Multiverse, which has only one extra dimension, *i.e.* they correspond to the principle of physical reality of complex numbers containing only one imaginary unit, for which formulas (4), (5) and (6) are right.

However, as follows from the WMAP and Planck data, implementation of the structures of the hidden Multiverse corresponding to calculation result obtained requires three extra dimensions. That is, formulas (4), (5), and (6) shall be corrected in accordance with the principle of physical reality of quaternions $\sigma + i_1\omega_1 + i_2\omega_2 + i_3\omega_3$ [86], containing three imaginary units i_1, i_2, i_3 connected by relations

$$i_1^2 = i_2^2 = i_3^2 = 1 \quad (7)$$

$$i_1 i_2 i_3 = i_2 i_3 i_1 = i_3 i_1 i_2 = -1 \quad (8)$$

$$i_1 i_3 i_2 = i_2 i_1 i_3 = i_3 i_2 i_1 = 1 \quad (9)$$

In this case the corrected relativistic formulas will be as follows

$$m = \frac{m_0 (i_1)^q (i_2)^r (i_3)^s}{\sqrt{1 - [v/c - (q + r + s)]^2}} = \frac{m_0 (i_1)^q (i_2)^r (i_3)^s}{\sqrt{1 - (w/c)^2}} \quad (10)$$

$$\begin{aligned} \Delta t &= \Delta t_0 (i_1)^q (i_2)^r (i_3)^s \sqrt{1 - [v/c - (q + r + s)]^2} \\ &= \Delta t_0 (i_1)^q (i_2)^r (i_3)^s \sqrt{1 - (w/c)^2} \end{aligned} \quad (11)$$

$$\begin{aligned} l &= l_0 (i_1)^q (i_2)^r (i_3)^s \sqrt{1 - [v/c - (q + r + s)]^2} \\ &= l_0 (i_1)^q (i_2)^r (i_3)^s \sqrt{1 - (w/c)^2} \end{aligned} \quad (12)$$

where q is the total number of parallel universes, penetration into which is made through portals, corresponding to the imaginary unit i_1 , with increasing distance from our tardyon universe;

r is the total number of parallel universes, penetration into which is made through portals, corresponding to the imaginary unit i_2 , with increasing distance from our tardyon universe;

s is the total number of parallel universes, penetration into which is made through portals, corresponding to the imaginary unit i_3 , with increasing distance from our tardyon universe;

v is the velocity measured from our tardyon universe, which, therefore, can be called tardyon velocity;

c is the speed of light;

$w = v - (q + r + s)c$ is the local velocity for corresponding universe, which can take values only in the range $0 \leq w < c$.

The structure of the hidden Multiverse corresponding to the formulas (10), (11) and (12) can be as in **Figure 5**. As can be seen, this structure is distinguished from the structure shown in **Figure 4** by the fact that it contains three tachyon universes i_1, i_2, i_3 and three tachyon antiverses i_1, i_2, i_3 , which provides required three extra dimensions. Thus, six-dimensional space of the hidden Multiverse has actually three extra dimensions q, r, s including parallel universes, and three dimensions x, y, z including material contents of each of these universes. So, space of the hidden Multiverse [87] is described by the formula $f_{q,r,s}(x, y, z) + i_1q + i_2r + i_3s$ where the function $f_{q,r,s}(x, y, z)$ describes

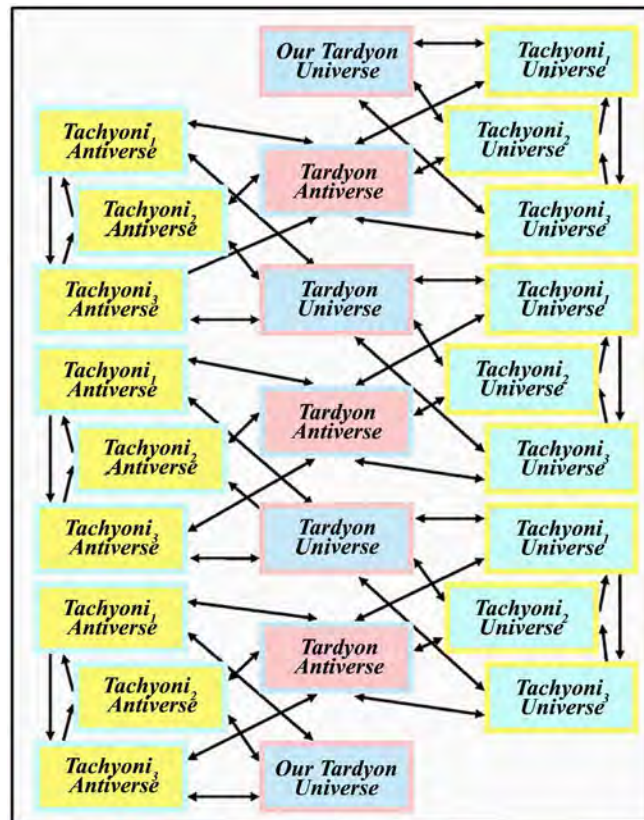


Figure 5. Structure of the hidden Multiverse corresponding to the principle of physical reality of quaternions.

distribution in the coordinates x, y, z of material contents in the corresponding parallel universe with coordinates q, r, s .

Lisa Randall wrote in this regard: “*maybe we live in a three-dimensional spatial slit of a multidimensional universe*”.

Besides, the quaternion structure is distinguished by presence in it of both bidirectional portals corresponding to the formula (7) and unidirectional portals corresponding to formulas (8) and (9). It means that there is a danger to get into a unidirectional portal while travelling in the hidden Multiverse and never return back therefrom.

However, this structure of the hidden Multiverse also does not correspond to the results of WMAP and Planck data analysis, since it contains twenty-four parallel universes, rather than twenty to twenty two parallel universes. As explained above, this proves that our hidden Multiverse is connected to other Multiverses through corresponding portals and together with them forms a Hyperverse. Therefore, it can be argued that other invisible Multiverses of the Hyperverse, beside ours, form a dark space. In other words, the ***Hyperverse is a multidimensional (and possibly infinite-dimensional) Universum¹⁷ containing a very large number of Multiverses.***

Besides, our hidden Multiverse can be connected to other Multiverses in various ways. Firstly, it can be connected to a different number of other Multiverses. Secondly, it can be connected to other Multiverses in various ways. Some probable variants of connection are shown in **Figures 6-8**. And finally, it can be connected to other Multiverses which have different structures and number of parallel universes. Herewith, there is a possibility that it is connected to other Multiverses corresponding to the principle of physical reality of various complex and hypercomplex numbers.

Figure 6 shows a structure diagram of our hidden Multiverse containing twenty-two parallel universes and connected twice to the same Multiverse of dark space, instead of its two missing parallel universes. In this structure diagram our tardyon universe is connected through corresponding portals to five adjacent parallel universes: two tachyon universes i_1, i_2 and three tachyon antiverses i_1, i_2, i_3 .

Figure 7 shows another structure diagram of our hidden Multiverse containing twenty-one parallel universes and connected to three different Multiverses of dark space, instead of its three missing parallel universes. In this structure diagram our tardyon universe is connected through corresponding portals to five adjacent parallel universes: two tachyon universes i_1, i_2 and three tachyon antiverses i_1, i_2, i_3 .

Figure 8 shows one more structure diagram of our hidden Multiverse containing twenty parallel universes and connected to three different Multiverses of dark space, instead of its four missing parallel universes. In this structure diagram our tardyon universe is connected through corresponding portals to six

¹⁷It is similar to a large city, in which our three-dimensional visible universe is just one of apartments.

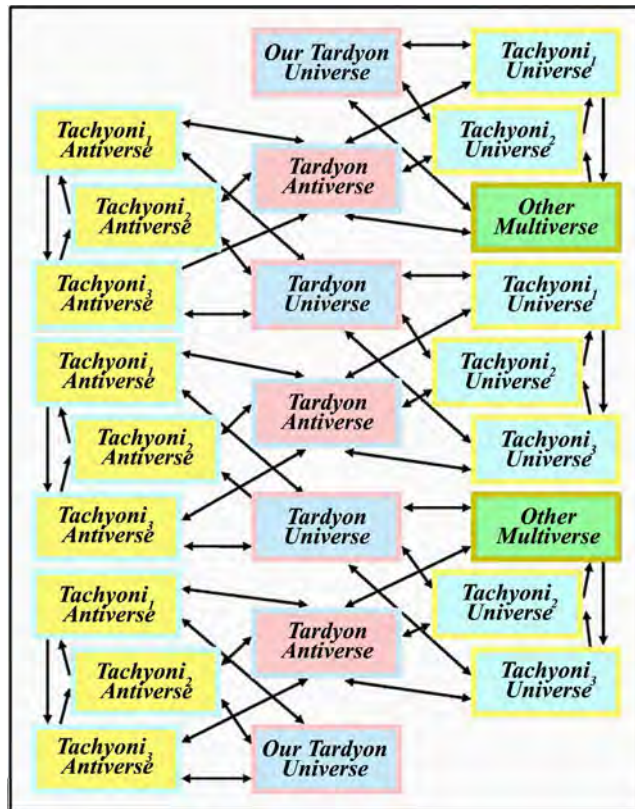


Figure 6. Quaternion structure of the hidden Multiverse.

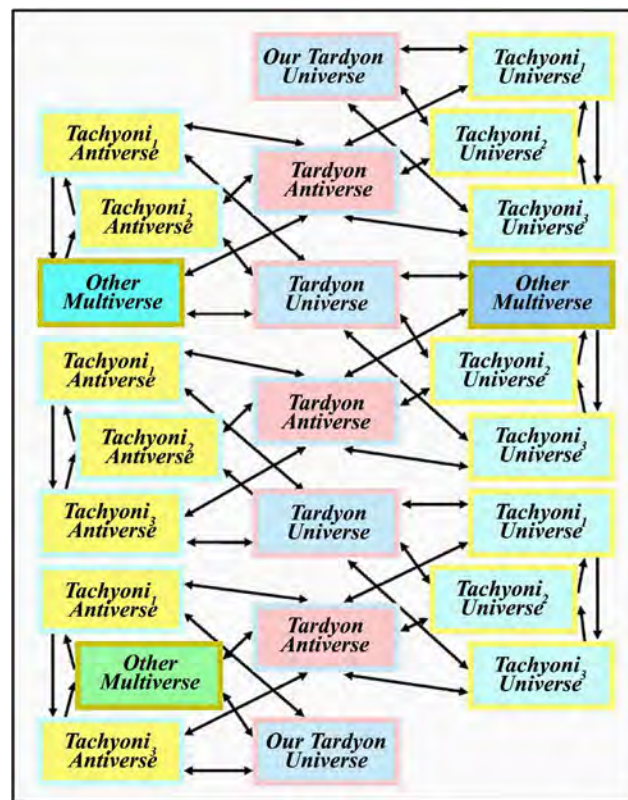


Figure 7. Another quaternion structure of the hidden Multiverse.

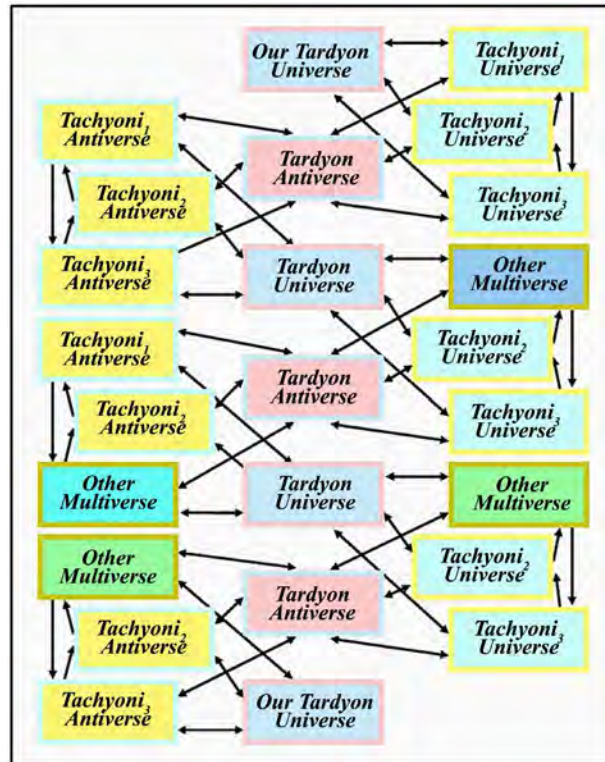


Figure 8. One more quaternion structure of the hidden Multiverse.

adjacent parallel universes: three tachyon universes i_1, i_2, i_3 and three tachyon antiverses i_1, i_2, i_3 .

8. Discovery of Dark Space

There can be a lot of similar examples of structures of the hidden Multiverse provided. However, we are not currently able to say which of them actually exists, as we have not got enough experimental data. So, to answer this question we need additional astrophysical studies, including those aimed at experimental confirmation of dark space existence.

And this is presumably possible, although the above-mentioned phenomenon of dark space is just as invisible and unlearned, as the phenomenon of dark matter and dark space. Moreover, in contrast to the phenomenon of dark matter and dark space, it turned out to be undetectable by its physical manifestations. Therefore, it hasn't been discovered until very recently. It has been detected only due to mathematical processing of data obtained by the WMAP and Planck spacecrafts [17] [39], aimed at checking them for compliance with hypotheses of the hidden Multiverse and Hyperverses. However, since the structure of the Hyperverses includes the hidden Multiverse, in which our tardyon universe can have not only six (as in **Figure 9(a)**), but also five (as in **Figure 9(b)**) adjacent parallel universes, there can be portals on Earth to the universes of dark space. Therefore, existence of dark space can be confirmed by geophysical studies of portals and afterportal spaces and with the help of astrophysical studies.

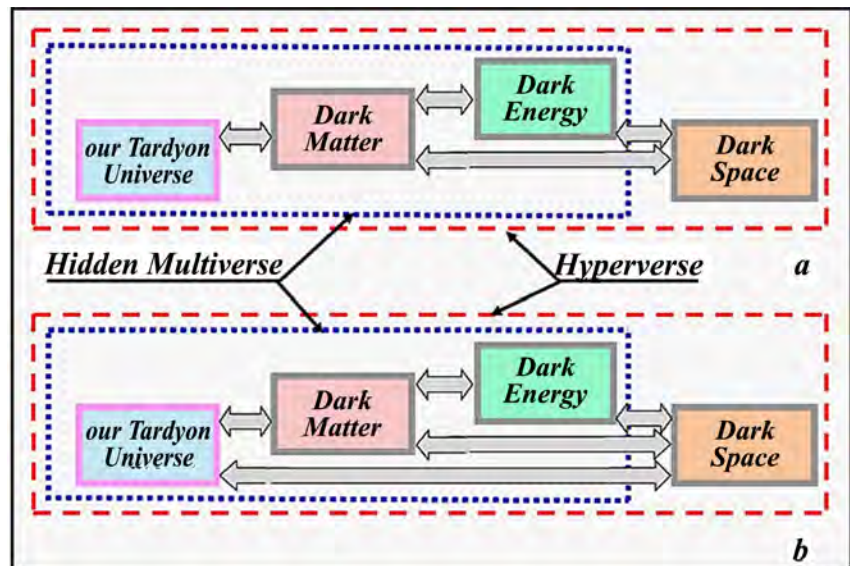


Figure 9. Structure of the Hyperverses.

9. Verifiability of the Hypothesis of the Hidden Multiverse

A large number of interesting hypotheses of Multiverse have been to date proposed, all of which are, however, unverifiable. Nevertheless, the proposed hypothesis of the hidden Multiverse is verifiable, since:

- the phenomenon of dark matter and dark energy, as is shown above, is its experimental confirmation. It is also experimentally confirmed by mass defect that is often detected in experiments at the Large Hadron Collider, *i.e.* a situation in which the total mass of subatomic particles turned out to be greater before acceleration than their total mass near the point of astrophysical singularity $v \rightarrow c$. This situation can be explained by formation of tachyons and their transition to adjacent tachyon universes and antiverses through micro portals.

Although these two statements logically follow from the foregoing and correspond to common sense, they raise some doubts, since they do not presumably exclude other explanations of the mentioned experimental data. However, the third proof of existence of invisible universes given below leaves no doubt whatsoever. The point of this proof is as follows. Since stars are placed differently in invisible parallel universes adjacent to our visible universe, star maps in areas beyond the portals might be other than those observed from Earth. Therefore, as we move from our universe to one of the adjacent universes through portals, which are the so-called anomalous zones [88], star maps of our visible universe are gradually replaced with star maps corresponding to adjacent universes that are not visible from Earth. And even given shallow penetration into portals such differences would likely be more noticeable than in astronomical observations of Sir Arthur Stanley Eddington in 1919 that confirmed the deviation of light rays near the Sun, predicted by the general theory of relativity. Thus, in order to make sure that universes unobservable from Earth exist, one should take a pic-

ture of starry sky in portals, which are numerous on Earth, and define differences comparing these pictures with those taken in observatories. Therefore, the discovery of the invisible universes in the proposed way seems quite convincing and expected in the near future.

Consequently, the hypothesis of the hidden Multiverse considered has every reason to be called a theory.

10. Dark Dimensions

However, one should not think that other physical worlds are just other parallel universes. As proved above, all concrete imaginary numbers are physically real. And physical entities corresponding to them also form their parallel worlds.

For example, in the Euler formula $\exp(ix) = \cos x + i \sin x$, describing oscillatory processes of any physical nature, such as mechanical, hydraulic, acoustic, electromagnetic, etc., both summands of its right part are physically real. However, no one can currently say what the component $i \sin x$ is, if the component $\cos x$ corresponds to mechanical oscillations of a pendulum. It's the same as in the case when the component $\cos x$ describes other oscillatory processes, or when concrete imaginary numbers describe any physical objects and processes described by other formulas. Special research is needed for each specific case, like that conducted earlier when clarifying physical nature of imaginary reactances in the theory of electric circuits or physical nature of relativistic formulas at superluminal speeds in the STR. Such research will allow us to learn a structure of contents of parallel universes and relationship between contents of our and other universes. However, this is a task of future.

In the meantime, we just note that any concrete numbers, both real and imaginary, always correspond to the results of measurements. Therefore, concrete imaginary numbers shall be called dark dimensions by analogy with dark matter and dark energy, since they are still absolutely inexplicable and objects of measurements corresponding to them are absolutely invisible.

11. Conclusions

The monograph has proved that dark matter and dark energy discovered in the previous century still seem completely inexplicable only because their explanation is not sought where it is. Everybody looks for the explanation exclusively in our visible Monoverse, the hypothesis of which follows from the principle of light speed non-exceedance postulated in the STR. The hypothesis of the Monoverse supposes that there seems to be nowhere to look for the explanation of the phenomenon of dark matter and dark energy.

The principle of light speed non-exceedance in the STR turned out to be in demand, because all its relativistic formulas in this theory were inexplicable. They couldn't be explained, as they implied that mass, time, distance and other physical quantities at superluminal speeds took values measured by imaginary numbers. Creators of the STR did not know what this meant, and therefore

could not explain their theory. Therefore, they needed this principle in order to avoid the necessity to recognize it.

However, this postulate didn't convince other scientists, who were more interested in scientific truth than prestigious considerations. In addition, some physical discoveries, for example, Cherenkov radiation produced by charged particles moving faster than light, could cause such doubts. Therefore, it was quite natural to search for other physical phenomena that could disprove the principle of light speed non-exceedance.

As a result, the OPERA collaboration attempted to refute the postulate on light speed non-exceedance by proving the existence of superluminal neutrinos. On September 22, 2011 a sensational report on successful completion of this very complex experiment was published. However, in half a year the OPERA experiment was refuted by the ICARUS experiment. Therefore, the question of existence of superluminal neutrinos and physical reality of imaginary numbers remained open.

However, *in 2008-2010, i.e. before completion of the OPERA experiment, results of other experiments were published. They successfully proved physical reality of concrete imaginary numbers, and therefore made the OPERA experiment unnecessary.* These and subsequent publications on experimental studies of oscillatory processes in linear electric circuits have also refuted the principle of light speed non-exceedance, which is just an unproved assumption.

Therefore, the conclusion about existence of the Monoverse derived from the principle of light speed non-exceedance in the STR also turned out to be wrong. Until recently an explanation for dark matter and dark energy was unsuccessfully sought in the Monoverse. However, they weren't found there. *The corrected relativistic formulas of the STR have allowed creating a verified hypothesis of the hidden Multiverse. Existence of invisible parallel universes therein has explained the phenomenon of dark matter and dark energy.* Moreover, existence of other Multiverses outside the hidden Multiverse has also discovered and explained a previously unknown phenomenon of dark space. It has been shown that our visible universe together with invisible parallel universes of dark matter, dark energy and dark space form the Hyperverse.

The structure of the hidden Multiverse has been clarified in the course of mathematical analysis of experimental data obtained by the WMAP and Planck spacecrafts. Their mathematical processing has made it possible to determine that the hidden Multiverse has a quaternion structure in six-dimensional space and contains twenty-two parallel universes. Of them, five-six invisible parallel universes of dark matter are adjacent to our visible universe, and the remaining invisible parallel universes of dark energy in the hidden Multiverse are further away from our visible universe. These universes are interconnected by unidirectional and bidirectional portals. And some portals connect them with invisible parallel universes of the Hyperverse, which are outside the hidden Multiverse.

In this book, there are naturally no answers to many other issues of astrophysics. But they cannot but be, since each new theory giving answers to questions posed by previous theories in turn inevitably gives rise to new questions. And the authors of other even more new theories and hypotheses are to answer them. This is the inevitable logic of science development.

Nevertheless, *the main features of dark matter and dark energy—why they are invisible and why no molecules, atoms and subatomic particles are found in them—are clearly and convincingly explained in section 6. And in section 9 it is explained how the existence of invisible universes, by which the phenomenon of dark matter and dark energy is generated, can be proved in the most indisputable way with the help of photographs of the starry sky in the portals.*

However, imaginary numbers are used not only in the theory of electric circuits, the special theory of relativity and astrophysics. They are also used in all other exact sciences. Imaginary physical quantities corresponding to them are called dark dimensions. Learning of their physical nature would require additional studies, which would largely determine the content of future science.

Conflicts of Interest

The author declares no conflict interest regarding the publication of this paper.

References

- [1] Antonov, A.A. (2008) *European Journal of Scientific Research*, **21**, 627-641.
- [2] Antonov, A.A. (2009) *European Journal of Scientific Research*, **28**, 193-204.
- [3] Antonov, A.A. (2010) *American Journal of Scientific and Industrial Research*, **1**, 342-349. <https://doi.org/10.5251/ajsir.2010.1.2.342.349>
- [4] Antonov, A.A. (2010) *International Journal of Pure and Applied Sciences and Technology*, **1**, 1-12.
- [5] Antonov, A.A. (2010) *General Mathematics Notes*, **1**, 11-16. https://doi.org/10.17686/sced_rusnauka_2010-887
- [6] Antonov, A.A. (2013) *International Journal of Management, IT and Engineering*, **3**, 219-230.
- [7] Antonov, A.A. (2014) *American Journal of Scientific and Industrial Research*, **5**, 40-52.
- [8] Antonov, A.A. (2015) *Journal of Russian Physical and Chemical Society*, **87**, 328-355. (In Russian)
- [9] Antonov, A.A. (2015) *General Mathematics Notes*, **31**, 34-53. http://www.emis.de/journals/GMN/yahoo_site_admin/assets/docs/4_GMN-9212-V31N2.1293701.pdf
- [10] Antonov, A.A. (2015) *American Journal of Electrical and Electronics Engineering*, **3**, 124-129.
- [11] Antonov, A.A. (2015) *Global Journal of Physics*, **2**, 145-149. http://gpcpublishing.com/index.php?journal=gjp&page=article&op=view&path%5B%5D=294&path%5B%5D=pdf_14
- [12] Antonov, A.A. (2016) *PONTE*, **72**, 131-142.

- <https://doi.org/10.21506/j.ponte.2016.7.9>
- [13] Antonov, A.A. (2016) *Journal of Modern Physics*, **7**, 2299-2313.
<https://doi.org/10.4236/jmp.2016.716198>
- [14] Antonov, A.A. (2016) *International Review of Physics*, **10**, 31-35.
<https://www.Praiseworthyprize.org/jsm/index.php?journal=irephy&page=article&p=view&path%5B%5D=18615>
- [15] Antonov, A.A. (2016) *General Mathematics Notes*, **35**, 40-63.
http://www.geman.in/yahoo_site_admin/assets/docs/4_GMN-10932-V35N2.31895146.pdf
- [16] Antonov, A.A. (2017) *Norwegian Journal of Development of the International Science*, **6**, 50-63. <http://www.njd-iscience.com>
- [17] Antonov, A.A. (2018) *Natural Science*, **10**, 11-30.
<https://doi.org/10.4236/ns.2018.101002>
- [18] Antonov, A.A. (2014) *Global Journal of Science Frontier Research: A Physics & Space Science*, **14**, 51-59.
https://globaljournals.org/GJSFR_Volume14/7-Verification-of-the-Second-Postulate.pdf
- [19] Antonov, A.A. (2011) *British Journal of Science*, **2**, 51-60.
https://doi.org/10.17686/sced_rusnauka_2011-892
- [20] Antonov, A.A. (2012) *Encyclopedia of Russian Thought: Reports to Russian Physical Society*, **16**, 3-20.
- [21] Antonov, A.A. (2012) *International Journal of Pure and Applied Sciences and Technology*, **12**, 43-56.
- [22] Antonov, A.A. (2015) *International Journal of Advanced Research in Physical Science*, **2**, 25-32.
- [23] Antonov, A.A. (2015) *American Journal of Modern Physics*, **4**, 1-9.
<https://doi.org/10.11648/j.ajmp.20150401.11>
- [24] Antonov, A.A. (2015) *International Journal of Physics*, **3**, 84-87.
- [25] Antonov, A.A. (2015) *Cosmology*, **19**, 40-61.
- [26] Antonov, A.A. (2015) *Optics*, **4**, 43-47.
- [27] Antonov, A.A. (2015) *American Journal of Modern Physics*, **4**, 180-188.
<https://doi.org/10.11648/j.ajmp.20150404.14>
- [28] Antonov, A.A. (2016) *Frontiers of Astronomy, Astrophysics and Cosmology*, **2**, 1-9.
- [29] Antonov, A.A. (2016) *Journal of Modern Physics*, **7**, 1228-1246.
<https://doi.org/10.4236/jmp.2016.710111>
- [30] Antonov, A.A. (2016) *American Journal of Modern Physics*.
<http://www.sciencepublishinggroup.com/news/sciencepgfrontiersinfo?articleid=93>
- [31] Antonov, A.A. (2016) *Journal of Modern Physics*, **7**, 1933-1943.
<https://doi.org/10.4236/jmp.2016.714170>
- [32] Antonov, A.A. (2016) *Global Journal of Science Frontier Research: A Physics and Space Science*, **16**, 4-12.
- [33] Antonov, A.A. (2017) *Global Journal of Science Frontier Research*.
<http://blog.gjsfr.org/2017/02/verifiable-hidden-multiverse.html>
- [34] Antonov, A.A. (2017) *Natural Science*, **9**, 43-62.
<https://doi.org/10.4236/ns.2017.93005>
- [35] Antonov, A.A. (2015) *Journal of the Russian Physical and Chemical Society*, **87**,

- 63-76. (In Russian) <http://www.rusphysics.ru/files/Antonov.Obsor.pdf>
- [36] Antonov, A.A. (2016) *Global Journal of Science Frontier Research*, **15**.
<http://blog.gjsfr.org/2016/09/explanation-of-dark-matter-and-dark.html>
- [37] Antonov, A.A. (2017) *Journal of Modern Physics*, **8**, 567-582.
<https://doi.org/10.4236/jmp.2017.84038>
- [38] Antonov, A.A. (2016) *PONTE*, **72**, 288-300.
<https://doi.org/10.21506/j.ponte.2016.9.22>
- [39] Antonov, A.A. (2018) *Journal of Modern Physics*, **9**, 14-34.
<https://doi.org/10.4236/jmp.2018.91002>
- [40] Ohm, G.S. (1826) *Journal fur Chemie und Physik*, **46**, 137-166.
- [41] Steinmetz, C.P. (2010) *Theory and Calculation of Electric Circuit*. Nabu Press, Charleston.
- [42] Larmor, J.J. (1897) *Philosophical Transactions of the Royal Society A: Mathematical, Physical and Engineering Sciences*, **190**, 205-300.
<https://doi.org/10.1098/rsta.1897.0020>
- [43] Lorentz, H.A. (1899) *Proceeding of the Royal Netherlands Academy of Arts and Science*, **1**, 427-442.
- [44] Poincaré, H. (1905) *Comptes Rendus*, **140**, 1504-1508.
- [45] Einstein, A. (1905) *Annalen der Physik*, **17**, 891-921.
<https://doi.org/10.1002/andp.19053221004>
- [46] Einstein, A. (1920) *Relativity: The Special and General Theory*. H. Holt and Company, New York.
- [47] Bohm, D. (2006) *The Special Theory of Relativity*. Routledge, Abingdon-on-Thames.
- [48] Hawking, S.W. and Penrose, R. (2010) *The Nature of Space and Time*. Princeton University Press, Princeton. <https://doi.org/10.1515/9781400834747>
- [49] Tanaka, S. (1960) *Progress of Theoretical Physics (Kyoto)*, **24**, 171-200.
<https://doi.org/10.1143/PTP.24.171>
- [50] Terletsky, Y.P. (1966) *Paradoxes of the Relativity Theory*. Nauka Publishing, Moscow. (In Russian)
- [51] Feinberg, G. (1967) *Physical Review*, **159**, 1089-1105.
<https://doi.org/10.1103/PhysRev.159.1089>
- [52] Bilaniuk, O.-M.P. and Sudarshan, E.C.G. (1969) *Physics Today*, **22**, 43-51.
<https://doi.org/10.1063/1.3035574>
- [53] Recami, E., Fontana, F. and Garavaglia, R. (2000) *International Journal of Modern Physics A*, **15**, 2793-2812. <https://doi.org/10.1142/S0217751X00001403>
- [54] Hill, J.M. and Cox, B.J. (2012) *Proceeding of Royal Society A: Mathematical, Physical and Engineering Sciences*, **468**, 4174-4192.
<https://doi.org/10.1098/rspa.2012.0340>
- [55] Antonov, A.A. (2015) Where to Look for Alien Civilisations, *Cosmology*. Commentaries: Stephen Hawking's Aliens. The Search for Intelligent Extraterrestrial Life. Project Breakthrough Listen. <http://cosmology.com/Aliens1.html>
- [56] Antonov, A.A. (2016) How Portals of the Invisible Multiverse Operate. *Science PG Frontiers*.
<http://www.sciencepublishinggroup.com/news/sciencepgfrontiersinfo?articleid=147>
- [57] Antonov, A.A. (2016) *Philosophy and Cosmology*, **6**, 11-27.

<http://ispcjournal.org/journals/2016-16/Antonov16.pdf>

- [58] Alfvén, H. (1966) *Worlds-Antiworlds: Antimatter in Cosmology*. W. H. Freeman & Co., San Francisco.
- [59] Foot, R. (2002) *Shadowlands: Quest for Mirror Matter in the Universe*. Universal Publishers, Parkland.
- [60] Frazer, G. (2004) *Antimatter: The Ultimate Mirror*. Cambridge University Press, Cambridge.
- [61] Santilli, R.M. (2006) *Isodual Theory of Antimatter: With Applications to Antigravity, Grand Unification and Cosmology*. Springer Netherlands, Dordrecht.
- [62] Mazure, A. and Le Brun, V. (2012) *Matter, Dark Matter, and Anti-Matter: In Search of the Hidden Universe*. Springer-Verlag, Berlin.
<https://doi.org/10.1007/978-1-4419-8822-5>
- [63] Freeman, K. and McNamara, G. (2006) *In Search of Dark Matter*. Springer, Berlin.
- [64] Nicolson, I. (2007) *Dark Side of the Universe: Dark Matter, Dark Energy, and the Fate of the Cosmos*. Johns Hopkins University Press, Baltimore.
- [65] Ruiz-Lapuente, P. (2010) *Dark Energy: Observational and Theoretical Approaches*. Cambridge University Press, Cambridge.
<https://doi.org/10.1017/CBO9781139193627>
- [66] Amendola, L. and Tsujikawa, S. (2010) *Dark Energy: Theory and Observations*. Cambridge University Press, Cambridge.
<https://doi.org/10.1017/CBO9780511750823>
- [67] Bertone, G. (2013) *Particle Dark Matter: Observations, Models and Searches*. Cambridge University Press, Cambridge.
- [68] Sanders, R.H. (2014) *The Dark Matter Problem: A Historical Perspective*. Cambridge University Press, Cambridge.
- [69] deGrasse, T.N. (2017) *Astrophysics for People in a Hurry*. W. W. Norton & Company, London.
- [70] Oort, J.H. (1932) *Bulletin of the Astronomical Institutes of the Netherlands*, **6**, 249-287. <http://adsabs.harvard.edu/abs/1932BAN.....6..249O>
- [71] Zwicky, F. (1933) *Helvetica Physica Acta*, **6**, 110-127.
<http://adsabs.harvard.edu/abs/1933AcHPh...6..110Z>
- [72] Perlmutter, S. (2012) *Reviews of Modern Physics*, **84**, 1127-1149.
<https://doi.org/10.1103/RevModPhys.84.1127>
- [73] Schmidt, B.P. (2012) *Reviews of Modern Physics*, **84**, 1151-1163.
<https://doi.org/10.1103/RevModPhys.84.1151>
- [74] Riess, A.G. (2012) *Reviews of Modern Physics*, **84**, 1165-1175.
<https://doi.org/10.1103/RevModPhys.84.1165>
- [75] Kaku, M. (2005) *Parallel Worlds: A Journey through Creation, Higher Dimensions, and the Future of the Cosmos*. Doubleday, New York.
- [76] Deutch, D. (1998) *The Fabric of Reality: The Science of Parallel Universes and Its Implications*. Penguin Books, New York.
- [77] Greene, B. (2005) *The Fabric of the Cosmos: Space, Time, and the Texture of Reality*. Penguin Books, London.
- [78] Vilenkin, A. (2007) *Many Worlds in One: The Search for Other Universes*. Hill and Wong, New York.
- [79] Carr, B. (2009) *Universe or Multiverse?* Cambridge University Press, Cambridge.

- [80] Gribbin, J. (2010) *In Search of the Multiverse: Parallel Worlds, Hidden Dimensions, and the Ultimate Quest for the Frontiers of Reality*. Wiley & Sons Inc., Hoboken.
- [81] Greene, B. (2011) *The Hidden Reality: Parallel Universes and the Deep Laws of the Cosmos*. Vintage, New York.
- [82] Hawking, S. and Mlodinow, L. (2012) *The Grand Design*. Bantam, New York.
- [83] Tegmark, M. (2014) *Our Mathematical Universe: My Quest for the Ultimate Nature of Reality*. Vintage, New York.
- [84] Hinshaw, G., Larson, D., Komatsu, E., Spergel, D.N., Bennett, C.L., Dunley, J., *et al.* (2013) Nine Year Wilkinson Anisotropy Probe (WMAP) Observations: Cosmological Parameter Results.
- [85] Adam, R., Ade, P.A.R., Aghanim, N., Akrami, Y., Alves, M.I.R., Argüeso, F., *et al.* (2015) Planck 2015 Results. 1. Overview of Products and Scientific Results.
- [86] Kantor, I.L. and Solodovnikov, A.S. (1989) *Hypercomplex Numbers*. Springer Verlag, Berlin. <https://doi.org/10.1007/978-1-4612-3650-4>
- [87] Antonov, A.A. (2015) *Global Journal of Science Frontier Research A: Physics and Space Science*, **15**, 8-15.
https://globaljournals.org/GJSFR_Volume15/2-Quaternion-Structure-of-the-Hidden.pdf
- [88] Chernobrov, V.A. (2000) *Encyclopaedia of Mysterious Places of the Earth*. Veche Publishing, Bucharest. (In Russian)

Space-Time Universe versus Energy Driven Time Arrow Universe: Time-Neutrality Confronted with Fundamental Irreversibility

Helmut Tributsch^{1,2*}

¹Institute for Physical and Theoretical Chemistry, Free University Berlin, Berlin, Germany

²Helmholtz Centre Berlin for Materials and Energy, Berlin, Germany

Email: helmut.tributsch@alice.it

How to cite this paper: Tributsch, H. (2019) Space-Time Universe versus Energy Driven Time Arrow Universe: Time-Neutrality Confronted with Fundamental Irreversibility. *Journal of Modern Physics*, 10, 1029-1064. <https://doi.org/10.4236/jmp.2019.108068>

Received: June 15, 2019

Accepted: July 26, 2019

Published: July 29, 2019

Copyright © 2019 by author(s) and Scientific Research Publishing Inc. This work is licensed under the Creative Commons Attribution International License (CC BY 4.0).

<http://creativecommons.org/licenses/by/4.0/>



Open Access

Abstract

A dynamic interpretation of quantum phenomena based on an energy driven time arrow requires a combined description of matter and information on matter. This information around matter turned out to be gravitation and the fact that a photon is continuously recycled via this information generates an always constant light velocity. These two phenomena, simple consequences of fundamental irreversibility, have mathematically been imposed on empty space for time-neutral spacetime in General Relativity theory. In an irreversible universe such a four-dimensional spacetime would not anymore be required. Another striking difference is the role of time. Clock-time, used in Relativity Theory and found to be relative, is not associated with a generation of changes, being only a scale for measuring changes, based on selected periodic phenomena. The real time in an irreversible world, action time, is the flow of action, as generated by the principle of least action, or, alternatively, the loss of information on the past. In contrast to clock-time, action time is invariant with respect to relativistic transformation and also facilitates self-organization of matter and information. Gravitation as information on matter with the aim of imposing the principle of least action also provides the link between quantum world and cosmology, which Relativity Theory cannot provide. Relevant aspects of both theoretical approaches, with special emphasis on already experimentally verified spacetime phenomena, are critically analysed. While Relativity Theory, which is relying on time-neutral laws, is applied to support a chaotically exploding Big Bang scenario, the fundamentally irreversible universe subject to an energy driven time arrow is characterized by self-organization of energy, matter and information yielding an intelligent and creative “Self-Image” universe, which is able to periodically regenerate itself. Arguments for a fundamentally irreversible energy driven nature

*Retired.

include, apart from explaining experimental support for Relativity Theory differently, the simple, straightforward derivation from a dynamically interpreted principle of least action, the elimination of quantum and cosmological paradoxes and the more sensitive and flexible information-technology based (digital) nature of gravitation as compared with the analogue “bent space” gravitation.

Keywords

Time-Neutrality, Irreversibility, General Relativity Theory, Big Bang Universe, Self-Image Universe, Information

1. Introduction

1.1. Why Is It Necessary to Question Space-Time

When ad-hoc postulates of an established time-neutral theory can readily be derived from a new, simpler irreversible one, a review of the scientific situation concerned is required. This is done with this publication. During a recent effort, aimed at investigating and eliminating paradoxes in physical theories the principle of least action was interpreted in a dynamic way leading to the conclusion that energy should not be considered to be a scalar quantity, only with the ability, not the interest to do work. It should be considered to be a dynamic variable, a vector, with an interest to do work and the ability to drive time [1]. The drive of free energy to do work should be expressed in the property to decrease its presence per state towards a redistribution of energy on many states in form of entropy increase and not anymore available energy. Since energy is conserved, the real changes proceeding during this reaction concern the abandonment and a reduction of information on the way from available to not anymore available energy (equivalent to a low information content). As a result, a dynamic time is obtained, expressed as a flow of action (energy times time) as a consequence of approaching least action. Alternatively, the turnover, the drain of information during energy conversion (the loss of information on the past) can also be defined as time arrow. They are, in both expressions, invariant against transformation to moving systems and represent the “dynamic” time arrow as trace of energy. It makes, in contrast to the presently established paradigm of time-neutrality, nature fundamentally irreversible and time oriented. This had also to be considered in quantum theory with the consequence that particle and wave are not energetically equivalent but that the spread-out wave, with its higher entropy content, has to be restored into a particle with the help of information, set aside for this purpose. As a consequence, a quantum state has to be described in terms of particle or wave including the information on the state of both of them. This information image on matter not only eliminated quantum paradoxes, but also helped to get insight into relevant physical contexts, which remained blurred by irrationality and paradoxes [1] [2]. The argument that a particle-wave duality cannot be considered as given (as assumed in conventional

quantum theory), but has to be mediated by information can be supported with the example of technical analogue-digital-analogue converters, e.g. applied in cellular phones, which also have to use information for analysing, digitalizing, processing and reconstruction, but also for minimising energy needs required for handling information. Without information two different manifestations of energy, the analogue and the digital signal, could technically not be interconverted. Why has this principle not been considered in the particle-wave duality?

The information on matter, needed to mediate particle-wave duality in an irreversible world, which has an energy content, turned out to be what is called gravitation, and a photon, travelling and using this information for particle-wave interconversion (compare **Figure 1**, top right), maintains the same properties,

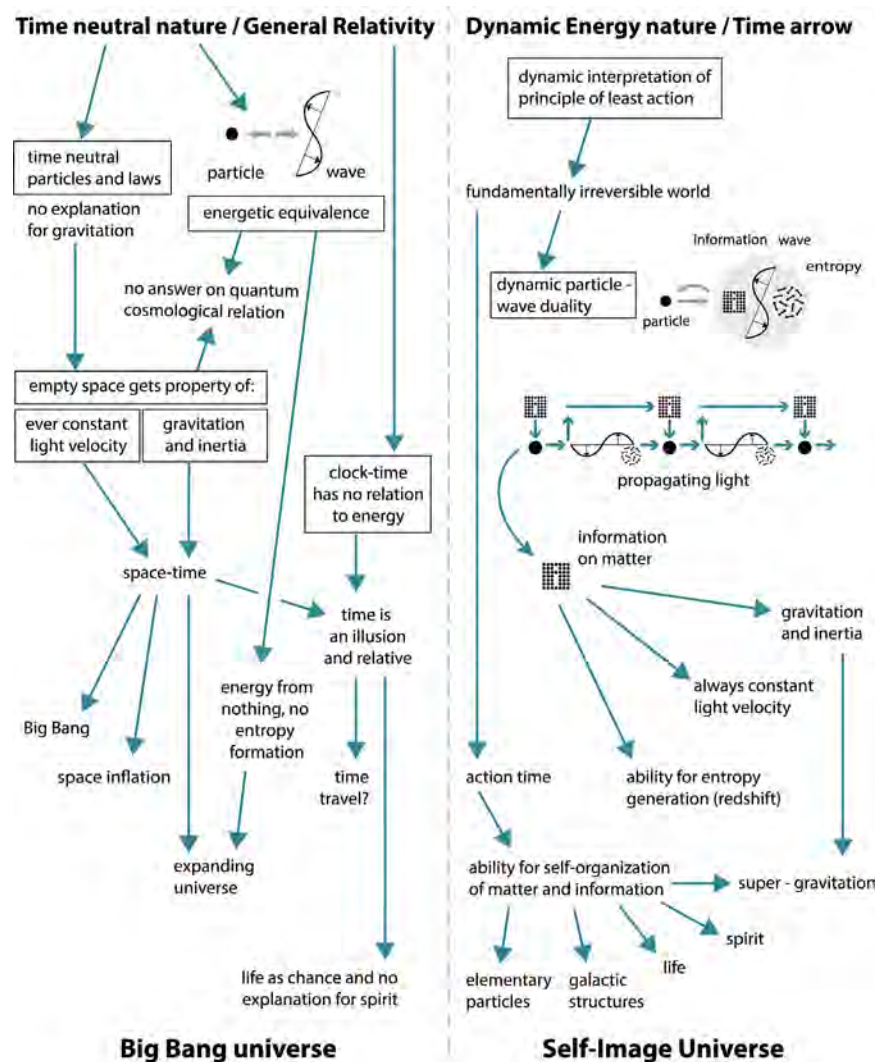


Figure 1. Schemes explaining assumptions (in rectangles) involved in the Time Neutrality paradigm and General Relativity theory (left) as compared with the starting assumptions, derived from the principle of least action, related to the Dynamic Energy (Time Arrow) theory (right). Also simplified explained are the dynamic quantum state with the mediating information and propagating light with the intermediate form as information (visualized as dotted square expressing “i”). Consequences and explanations are also included.

including its always constant velocity, in relative reference systems. It is like transmitting digital information to a flying airplane. The information received is independent of flight direction and flight velocity. Summarizing, the irreversible world, subject to the energy driven time arrow, yields the always constant, absolute light velocity and gravitation (including inertia within a situation of equivalence, when the drive to reduce the presence of energy per state is violated) as fundamental properties deducible from dynamic quantum states.

This is a very stimulating result, however also highly intriguing, since the established and experimentally well tested Relativity Theories were, one century ago, developed for the purpose of explaining exactly these two phenomena. It is well known that after efforts with an ether theory failed, Einstein simply stated that these experimentally verified phenomena of the always constant light velocity and of gravitation (including inertia) are imposed by empty space, claiming space-time properties. The necessary field equations for space were developed and adapted accordingly. Now, after one century of discussions and experimentation the Relativity Theory is so well accepted that criticism is considered not anymore relevant. The four-dimensional spacetime, as well as various relativity phenomena and ideas, including time dilation and time travel, the Big Bang scenario, space inflation, universe expansion, black holes and gravity waves are already discussed even in schools as part of the now established space-time concept of our universe [3].

The situation encountered is quite remarkable: On one hand there is the fully developed science structure based on time-neutral concepts with clock-time only used as a scale for measuring changes, and with experimentally well confirmed theories with significant paradoxes and irrational explanations (energy from nothing, effect without cause, inflation of empty space, non-locality, zero point energy, additional dimensions, multi-worlds). On the other hand there is a starting effort [1] [2] [4] [5] in considering nature as fundamentally irreversible, attributing to energy time driving properties and learning how to describe the universe as a fully rationally functioning system.

The time-neutral world concept sees absolute light velocity, gravitation and inertia as properties of empty space. The long searched for link between quantum world and cosmos could still not be identified. Clock-time, with its function as scale for measuring changes and with its origin from periodic phenomena such as pendulum movements, quartz oscillations and electronic transition frequencies in atoms, turned out to be an illusion (opinion also expressed by Einstein).

The Dynamic Energy concept (in the following also named Time Arrow concept), in contrast, sees absolute light velocity and gravitation as local particle properties reflecting mechanisms of information on matter, the information engaged in dynamic particle-wave duality [1]. The connection between quantum world and cosmos is thus immediately given. Time is the flow of action or information lost about the past, invariant upon transformation.

A fundamental difference between the two models is also that in the Dynamic Energy approach the two properties, absolute light velocity and gravitation, are just side results of quantum reasoning, while, in the Time-Neutrality world model they are, via Relativity Theory, additionally postulated to be properties of empty space. They are postulated as additional phenomena.

As a basis for discussion **Figure 1** compares the basic assumptions of the Time-Neutrality paradigm including General Relativity theory (left) with those of the Dynamic Energy concept (right). On the left side it is shown, marked with rectangles, how the (postulated) time-neutral world implemented a (postulated) space-time concept and an (adopted) futile, relative clock time to describe a chaotically exploding universe (here considered necessary, since entropy formation by expanding, propagating photons cannot be adequately considered).

On the right side it is explained, how the Dynamic Energy approach derives irreversibility from the principle of least action and imposes a dynamic particle wave duality mediated by information on matter (marked with dotted squares, visualizing an “i” indicating information). This, together with the notion, equally deducible from the principle of least action, that energy driven time is the flow of action, or the loss of information on the past, is all what is needed to deduce the always constant light velocity, gravitation, entropy formation by spreading, propagating photons, and an entirely different, information dominated universe. The Dynamic Energy approach claims to be able to eliminate quantum paradoxes (effect without cause, non-locality, fundamental uncertainty, zero-point energy) and paradoxes in cosmology (energy from nothing, space inflation, dark matter and energy) [1] [2] [6].

From this comparison it can be deduced, that the two approaches are not compatible in their dealing with always constant light velocity and gravitation (including inertia) and time. The Dynamic Energy model derives its basic claim that energy is fundamentally dynamic and oriented from the principle of least action [1]. The flow of action turns out to be the real time, action time (see below) responsible also for the self-organizing creativity of life and the universe, since feedback processes are facilitated. When applied to quantum processes, dynamic energy requires consideration also of the role of space for energy. It reduces its presence per state, its information content, with respect to both, time and space, while conserving the energy. This is the reason why a particle adopts the form of a wave. In this spread-out form its ability to do work is decreased due to entropy formation (compare particle-wave duality expressed in symbols in **Figure 1**, top right). The consequence is the need to introduce an information on matter, which is mediating the reversibility of the particle-wave duality. Besides of these reasonable considerations no further assumptions were needed. The meaning of gravitation, the explanation of the ever-constant light velocity, the link between quantum physics and cosmology and the reason for the structural creativity and function of self-organized systems turned out to be logical consequences. In addition, the interpretation of gravitation as information, to-

gether with the possibility of self-organisation of information, of information on matter, opened the way towards an explanation of super-gravitation in space. Self-organization of information also opens the way towards a more intelligent handling of genetic information and of information of neuronal origin in the brain. It opens the way towards the explanation of mind and spirit.

In contrast, on the basis of the Time-Neutrality paradigm and the General Relativity theory significant claims had to be made in relation to space (**Figure 1**, left). Space is imagined such that it imposes the always constant light velocity and accelerates matter in such a way that it generates gravitation and inertia. It cannot provide a link to quantum physics, involves irrational mechanisms, daring theoretical interpretations, and cannot explain dark matter (super-gravitation).

However, due to its one century long history and many experimental efforts, there is at present overwhelming support for Relativity Theory. This is, last not least also due to very costly experiments, which have produced quite tiny measured values, interpreted in favour of Relativity Theory (the LIGO and the Gravity B probe experiments alone have together cost two billion dollars).

What are the prospects of challenging General Relativity under such conditions? Comparing General Relativity theory with the new Dynamic Energy approach may sharpen our understanding of the universe, especially since it is essentially a confrontation of a time-reversible nature with a fundamentally irreversible one. Is nature fundamentally time-neutral even though everything is moving into one direction only and far from equilibrium processes are so dominating in shaping galactic structures and living organisms? The challenge of confronting both theories is also justified because the Dynamic Energy approach is claiming to eliminate the increasing number of paradoxes and irrationalities, which the paradigm of Time-Neutrality and Space-Time has generated. In addition, only one of the two approaches to describe nature can be correct.

In the following it will be attempted to compare and evaluate essential features of the two theories to understand the crucial differences and to identify experimental and theoretical steps for answering the questions posed. While the Dynamic Energy (Time Arrow) approach pictures a highly intelligent, spiritual universe, the Big Bang universe, explained by General Relativity theory, describes a quite primitive, exploding universe, in which life developed by chance without aim, and mind and spirit get no explanation.

The energy driven time arrow approach is still in its infancy and lacks an elaborate mathematical framework. However, it offers explanations for gravitation and the absolute light velocity, which were not artificially attributed to space (as in General Relativity theory), but simply followed from the quest for a description of nature on the basis of an irreversible, energy driven Time Arrow. It also claims, that clock time is just a time scale for measurement, but not representing the real time flow, which is generated by a dynamic energy. The quite dramatic turning-point generated by postulating a fundamentally irreversible world (**Figure 1**, right) is shown with the following example: Time-neutral energy and

clock-time enter Heisenberg's uncertainty relation with its controversial consequence for zero-point energy, which turned out to be a relevant point for speculations on evolution of the universe. For a fundamentally irreversible world with a dynamic energy and an energy driven time an entirely different interpretation is unavoidable even for such a very established relation. The energy driven time arrow supports a much more intelligent and creative universe, which can logically be understood and has the potential for renewal and perpetuation via information on matter (see later).

1.2. History of Criticism and Theoretical Background of Space-Time

Einstein's two Theories of Relativity find so much support that critical analyses are usually no longer accepted for publication. Is this persuasiveness of the theories based on irrevocable theoretical and experimental facts? Einstein himself once commented to a journalist that it is the "mystery of not understanding that attracts many people who indeed do not understand" [7]. Some understood physics and mathematics, but still could not accept the Relativity Theory. One example is the famous French mathematician Henri Poincaré. Until his death around 1912 he opposed the theory, as Einstein himself reported [7]. Another famous scientist, Paul Ehrenfest, an Austrian professor who taught in Amsterdam, committed suicide in 1933. In a letter to his colleagues, including Einstein, he commented that he could not continue to teach a science that he could no longer follow. Even Albert A. Michelson, who for the first time, long before Einstein took it into account in his theory, demonstrated the amazing constancy of the speed of light, was by no means pleased with the Relativity Theory. He said he would prefer to believe that his measurements were wrong before he believed this theory (quoted in [8]). Other famous scientists who witnessed the rise of relativity and did not accept it were, for example, Ernest Rutherford, Robert A. Millikan, Ernst Mach, Wilhelm C. Röntgen and Nicola Tesla. During the further 20th century and until today many scientists have wondered about and criticized the Theory of Relativity. The "Worldwide List of Dissident Scientists" compiled by Jean de Climont gives many examples [9]. The theoretical physicist and then vice-director at the Space Research Institute of the Russian Academy of Sciences, S. N. Arzhanov proceeded very thoroughly with his analysis of problems. He produced a book with the title "Criticism of the Foundations of the Relativity Theory" [10]. In it he physically and mathematically investigates every conceivable aspect of both theories of relativity, including their experimental verification, and finds serious contradictions and inconsistencies. He advises a return to the classical idea of space and time.

It is not the subject of the present paper to deal with questions related to the mathematical formalism of Relativity Theory. It should only be mentioned that it is conspicuous, that conservation of energy, momentum and angular momentum are not considered in it, even though far reaching conclusions are drawn on highly dynamic energetic phenomena in the universe (Big Bang, inflation of

space, Black Holes, expansion of the universe). There is also no explanation on how empty space, without matter and structure in it, can physically develop such sophisticated properties as space-time theory claims (e.g. acceleration of objects, manipulation of time, adjustment of light velocity). Space-time, which will never reveal the physical origin of its properties is, in this respect, a dead end for scientific understanding.

Why is it, after one century of continuous rise and confirmation of Relativity Theory and much unsuccessful criticism now justified to challenge this theory again? There is a significant reason: One is not any more just dealing with a mere criticism, like in numerous earlier efforts. It is for the first time that a counter theory on the basis of much simpler and more reasonable assumptions, which explain the always constant light velocity, gravitation, inertia and time differently, takes shape. It also naturally explains the relation between the quantum world and the cosmos, which Relativity Theory and Standard Model of elementary particles could not provide. This new, alternative universe turns also out to behave much more intelligent than deducible on the basis of the Big Bang scenario. It can explain the thrust of biological evolution as well as evolution of spirit through self-organization of information and replaces the Big Bag explosion of energy from nothing, inflation of empty space as well as accelerating expansion of the universe with a more logic interpretation. In addition, the challenge of questioning Relativity Theory means to simultaneously discuss, whether nature is fundamentally time-neutral, as presently assumed in physics, or fundamentally irreversible, as the Dynamic Energy theory claims. Is our universe governed by fundamentally time-neutral laws and mechanisms, and is time an illusion, even though everything is visibly moving in one direction only? This alone already gives justification for this attempt to question the time neutral world of space-time.

2. Results

2.1. Time Neutrality against Fundamental Irreversibility

It is well known that present concepts of nature including elementary particle (Standard Model) theory, quantum theory and relativity theory are based on time-neutral concepts. All mechanisms can proceed in positive as well as negative time direction and fundamental laws of physics allow that. The only time orientation presently accepted in physics is that in direction of increasing probability and increasing entropy. A system assumes a more disordered condition characterized by a minimum information on it.

The author, in his effort to demonstrate fundamental irreversibility, has criticised such a concept and its mathematical basis [6] [11]. During mathematical derivation, within the H-theorem, of the entropic time, information on time-neutral particles is reorganized, simplified and partially abandoned. This is done by replacing the initially very exact description by an estimation (Markovian mixture), a statistical procedure, aimed at predicting the future on the basis of re-

duced information. Since information has an energy content ($1 \text{ bit} = kT \ln 2$) energy is thereby thrown away. This explains, why the system assumes directionality and cannot be reversed. There is an additional argument against the entropic time arrow. The system concerned approaches a situation of maximum disorder or minimum information content moving with the entropy content from S_1 to S_2 by ΔS . It loses thereby information. Since information has an energy content, where does this energy go? Energy has to be conserved. The concept of a purely entropic time arrow does not work. The author argues that the entropy increase by ΔS can be multiplied by the absolute temperature T to yield the energy quantity $T\Delta S$, “entropic” energy. Now, considering the first law of thermodynamics on energy conservation one can ask, where this entropic, not anymore available energy came from. It could only have been derived from Gibbs free energy ΔG . This however means that not the statistical drive towards disorder, but that a “dynamic” (free) energy as a dynamic variable is the real source of changes towards increasing entropy. Energy has an interest in doing work! This is, of course, not consistent with the presently established concept of a “scalar” energy as a quantity of state, with the ability, but no interest to do work.

When the author studied the important principle of least action he found that also energy within this principle has to be considered “dynamic”, because only that way extremal, least action values can be reached at all, and that the principle is expressing a fundamentally irreversible world [1]. The proposed definition of this “dynamic” energy was that it “decreases and minimises its presence per state” thus generating, chaotic, not any more useful energy. This is equivalent to a decrease and minimization of information. Such properties define a fundamentally dynamic time arrow with all its different consequences for explaining the universe.

2.2. What Is Time in Reality?

Since antiquity many thoughts have been reported on the meaning of time, and during the last century numerous books have been written on the subject (e.g. [12] [13] [14] [15]). The impression is that no final conclusion has yet been reached. The author has also contributed to the search for the meaning of time [11] leading to the view explained here.

For present science, with its time-neutral particles and laws, and emphasized by personalities like Einstein, time is an illusion. It is just used as an ordering parameter to monitor changes. The Theory of Relativity shows, that time depends on relative movement and each system has its own time. The time used is clock-time, which is just a sequence of numbers, a scale or ruler for measuring changes, without any relation to matter or energy. It can therefore not be directly measured, but has to be derived from energy converting clocks. These clocks, however, do nothing more than to activate a periodical process, such as a pendulum movement, the oscillation of a quartz platelet, or the electron relaxation in an atom. Such time lapses during oscillations, which are just determined by

natural or material constants and have no relation to energy turnover themselves, are summed up and calibrated against periodic astronomical phenomena to yield seconds, hours and days (compare **Figure 2(a)**).

It is this clock time, which is just a scale and has nothing to do with energetic processes, which is multiplied with light velocity and became the axis of the fourth dimension in the four-dimensional space-time of Relativity Theory. It is this clock time, which, in the Theory of Relativity is relativistic dilated when calculated for a fast moving reference system. For an atomic clock this means that atomic parameters are thereby changed. This actually happens. Atomic clocks travelling around the globe show time dilations in the order of fractions of a microsecond (e.g. Hafele-Keating experiment). Within the Theory of Relativity part of this effect is attributed to gravitational effects, part to relative movements. But, in fact, only the properties of a scale have been changed due to changed physical parameters. Within the Dynamic Energy concept, it is not the real time which changed but only the scale for measuring it.

Within the concept of a “dynamically” understood energy, and with such a dynamic energy acting via the principle of least action, a real, irreversible energy driven time can readily be defined. It is the flow of action (energy times time), which is activated as the consequence of the principle of least action and can be called action time (**Figure 2(b)**). It is, for example, the tickling of sand in an hourglass or a stone rolling down a hill and describable as a flow of action. This is, more or less, what the Greek naturalist and philosopher Aristotle, who lived

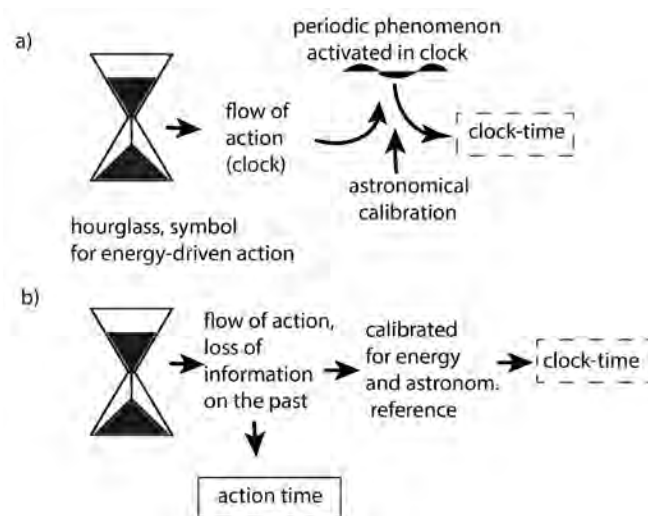


Figure 2. Scheme explaining the difference between clock time (a), which is just a scale for measuring change, and action time, which is here considered to be the real, energy-driven time (b). The symbols on the left side of depictions show a simplified hourglass representing energy turnover and a flow of action, the flowing sand, on the way of fulfilling the least action condition. In an ordinary clock action is just used to activate a calibrated oscillating mechanism, which provides a scale for measuring change. The real time flow is action time, the flow of action as a consequence of energy conversion, or the loss of information (supplied by free energy) on the past. If normalized for energy, clock-time can also be deduced (b).

in the 4th century BC, observed. He said: “Time is the measure of a movement that takes place from a before to an after”. Movement requires energy. Then time is a measure for energy turnover. This is exactly what the Dynamic Energy approach states and it can give additional information: Since dynamic processes are proceeding via a reduction of energy per state this action time equally means “loss of information on the past”. Such a statement is comprehensible and fully logical: the information, which we have recognized just instances before in our environment, is gone. Just some fragments of memory remain in our brain.

Why is sand moving in an hourglass? It is moving, because energy (gravitational energy) is dynamically active. What is this activity like, when energy, during energy conversion, remains fully conserved? The above given definition, that “it decreases and minimizes its presence per state” implies that order, available within the energy system is being reduced. This way energy is redistributed. In the case of chemical energy (e.g. a carbon-hydrogen bond), or of a photon as primary energy source, elaborate arrangements of energy and materials are abandoned during the energy conversion process to finally only show low temperature kinetic energy. This shows, that it is order, information about the energy system, which is given up during the energy conversion process to yield disorder while energy in total is conserved. The flow of action (energy times time) in such an energy conversion process $(d(\Delta Et)/dt)$ is thus generated by a reduction of order (information) within the energy system. It is consequently equivalent to say that it is the flow of abandoned information on the past (dI_{ab}/dt) that characterizes fundamental energy driven time. In this case, since the lost information concerned is linked to energy, there is no problem with energy conservation. It is considered in the energy balance of the entire process. It is this abandonment of information (on energy) that implements the redistribution and conversion of energy thus causing the flow of action.

Energy driven time, or action time, can therefore be formally written in the following way (here t is the clock time and ΔE the energy turned over:

$$\text{energy driven time} = \text{action time} = \frac{d(\Delta Et)}{dt} = \frac{dI_{ab}}{dt} \quad (1)$$

and from this equation clock-time can be deduced

$$\text{clock time } t = \frac{I_{ab}}{\Delta E} \quad (2)$$

This clock-time does not any more correspond to the flow of abandoned information due to energy turnover. It is an energy neutral statement of abandoned information per energy turned over. Clock-time is a standard, a calibrated scale for measuring changes. It is for this reason, that clock time is subject to dilation, when transformed within Relativity Theory, since it refers to the energy of moving systems, where energy can be determined to be correspondingly larger.

Both equivalent definitions of the proposed real time arrow (1), the flow of action, and the flow of abandoned information on the past are invariant with re-

spect to relativistic transformation and can directly be measured, because they are characterized by an energy content. But clock time (2) is not, since the invariant information flux is considered per energy turned over. It is just a scale for measuring time. A certain amount of information turnover per energy is considered and counted as a scale. Relativity theory uses clock time for constructing the fourth dimension and draws important conclusions from relativistic time properties. On the basis of the here given definition of energy driven time, action time (1), it should be this time, action time, and not clock-time (2), which should be used in formulas, which aim at the description of the universe, when highly dynamic mechanisms are to be derived as conclusions.

Figure 2 explains in a simple scheme the difference between clock time (above) and action time (below). In the first case (a) a flow of action is only used to activate periodic phenomena for measuring changes via the clock time. In the second case (b) the flow of action itself is considered to be the energy driven time flow. By dividing it through the turned over energy, clock-time can be obtained also in this case as calibrated scale for measuring change.

2.3. What Means Gravitation and Always Constant Light Velocity for Space-Time

Relativity theory implements, via the field equations, relevant experimentally verified properties into empty space: they concern the ability of always sustaining the absolute light velocity and the capacity to simulate gravitation and inertia, while respecting the equivalence principle, by adequately accelerating masses. Since these introduced properties actually prevail, this may explain the astonishing apparent experimental meaningfulness of General Relativity theory. The properties of space yield what has been introduced as a theory. But it is well known that these introduced properties cause the now four-dimensional space-time to bend, since gravity has become a geometric property of space-time. A satellite around a celestial body thereby feels a force at close distance, since it is moving along a curved space tracing its trajectory. For understanding, what it means in practice, when a body is deviated by a bent space around a mass let us look at an example. The difference in gravitation forces, and the degree of bent space, between two neutrons and two weights of one kilo is of the order of 10^{54} . Gravitation means bending of space and bending is induced by the energy momentum tensor in relativity theory. Can one imagine a detectable bending of space, equivalent to gravitational acceleration, around spherical objects differing by a factor of the order of 10^{54} ? A passing and interacting particle should nevertheless be able to register the differences and to respond properly to a highly varying gravitation. A bent space around a mass must communicate itself as an analogue signal. Technical experience shows that an analogue signal (which continuously varies as quantity to be registered) can only be measured within 0.01% of its maximum signal (three digits behind the comma), and has to be regularly calibrated. Gravitational changes of up to and trespassing a range of 10^{54} can never be registered via an analogue signal of bent space around a sphere. How accurate

are gravitation signals measured in practice? This question will be discussed later.

Within the Dynamic Energy theory gravitation is information with the requirement to reduce energy per state while imposing the principle of least action. Phenomena controlled by information are not limited by analogue restrictions and also readily explain, what happens, when the mentioned requirement is violated and the energy per state tends to increase. If this minimisation condition is violated and energy per state increases, then a counter force results, equivalent to energy per distance travelled. This is inertia fulfilling the equivalence principle. It responds to the gravitation of matter from the entire universe, as Ernst Mach proposed. The Dynamic Energy theory has no problem explaining inertia.

Another question is to understand the implementation of absolute light velocity within the four-dimensional space time. Let us imagine a photon approaching an object coming closer at very high speed. When hitting it light velocity measured on the object must be the known absolute value. When, before the encounter, and how is such an adjustment made in a time-neutral world? It formally works, of course, because mathematics imposes it, but it is not easily understandable. This also concerns the time around masses in space-time. Within the Theory of Relativity time is actually variable and manipulated depending on the distance of a mass. How can, on a physical basis time be manipulated? In terms of an atomic clock this means, as explained before, that atomic parameters must change. They can change due to a changed gravitation, but this does not mean that time itself, the energy driven time, is dilated that way.

When the concept of an energy driven time arrow was applied to quantum phenomena, it turned out that matter (energy), concentrated in a particle, and energy spread out as wave had to be linked via an information image of matter (energy). It has to be set aside to support the back conversion of the wave into the particle [1] [6]. This information around matter has an energy content and was identified as gravitation. Propagating photons, changing from the wave form into the particle form via information imply information-controlled photon properties (compare propagating photon expressed in symbols in **Figure 1**, top right). Photons are continuously reassembled via information (represented in form of dotted squares), independent of relative movements of the receiver. This works similar as programs for television or information for a 3D printer are registered on an airplane [2]. They function independent of flight velocity and flight direction. The program for a 3D printer can be used to produce a toy car which travels at an always constant speed. In fact, as a side product of applying the energy driven time arrow to quantum states new explanations both for gravitation and the always constant absolute light velocity in free space were found. Surprisingly, gravitation turned out to be information on matter and the absolute light velocity simply the consequence of involvement of information in the quantum process. The just mentioned problems in understanding gravitation or the always constant light velocity in terms of the space-time concept simply dis-

appear with the information nature of gravitation. Information can work like that and no postulation needs to be made on highly elaborate properties of empty space as General Relativity theory does it.

This, of course, motivated and urged to explore, whether this supports a fundamentally irreversible universe subject to an energy driven time arrow. It became necessary to confront it with the time-neutral, already well-established universe shaped by General Relativity (**Figure 1**).

Such a confrontation is, in fact, unavoidable, because only one of these two world models for explaining nature can survive. Absolute light velocity and gravitation are either information-controlled properties of an energy driven time arrow, or they are properties of free space, as General Relativity implemented them. The first approach is entirely rational and quite simple, the second a mathematical construction which generates numerous paradoxes and irrationalities (four dimensions, relativistic time and length changes, time travel, space inflation) which, however, already, according to specialists, has produced surprising experimental support.

2.4. Relation between Quantum World and Universe

Since the rise of quantum and Relativity Theory scientists have searched for a unifying link between them. The discipline of quantum gravitation, for example, studies that, aiming for a “Theory of Everything”. String-theory is another research orientation, which searches for such a connection. Up to now it was not found.

The energy driven Time Arrow approach, in dealing with quantum phenomena, found this link quite naturally. The self-image of matter in form of information, mediating the particle wave exchange was identified with gravitation and the same information (or gravitation) also controls the dynamics of the universe. A remarkable consequence of this finding is, that what we call gravitation is in fact information on matter. This implies that our universe is essentially controlled by information, which has significant further consequences (see later). But it also readily explains, why the measured difference in gravitation between two neutrons and two weights of one kilo of 10^{54} does not pose problems for function and detection. It is a difference in numbers, registered as information without the need of an intermediate registration as analogue signal of space bending. Of course, a big task for the future will be to decipher the information code of nature and to understand, how information can be turned over during generation of action.

2.5. To What Extent Can Relativistic Phenomena Be Understood Differently?

Special and General Theory of Relativity have puzzled with their very characteristic phenomena. Below, with relation (3), it is shown how the length of an object is reduced, when its velocity v is approaching the speed of light c . It is seen, that it is shrinking and finally disappearing. The next formula (4), also well known,

is showing, how the time interval Δt_0 between two subsequent instances (e.g. seconds) is increasing with increasing velocity v of an object. Approaching the light velocity the clock cycle is getting larger and larger until finally clock-time stops. The first example of a rocket, shrinking at high speed, rises the question, how this could occur with a stiff object, which subsequently may land in full size. The second example of time dilation, in turn, is the basis of numerous paradoxes which deal with time travel.

When trying to judge these well known predicted phenomena it is of interest to point out, that these relativistic phenomena are only seen, when the object is analysed in direction of movement. Observers analysing it perpendicular to the movement will not see this effect (Figure 3).

Since objects with simultaneously different spatial measures and different time cannot exist, one is apparently dealing with a problem of measurement. The measurement occurs with light, which serves for transmitting the signals. Two measurements have to be made for measuring length and a time interval respectively. During that interval the object is moving with the velocity v . It is learned how the ratio of object velocity v and light velocity c is affecting measured data. This is definitively a measurement artefact due to the limited light velocity and not information on the studied object. Indeed, when the light velocity in these formula (3) and (4) is set to become infinite, the relativistic effects just disappear.

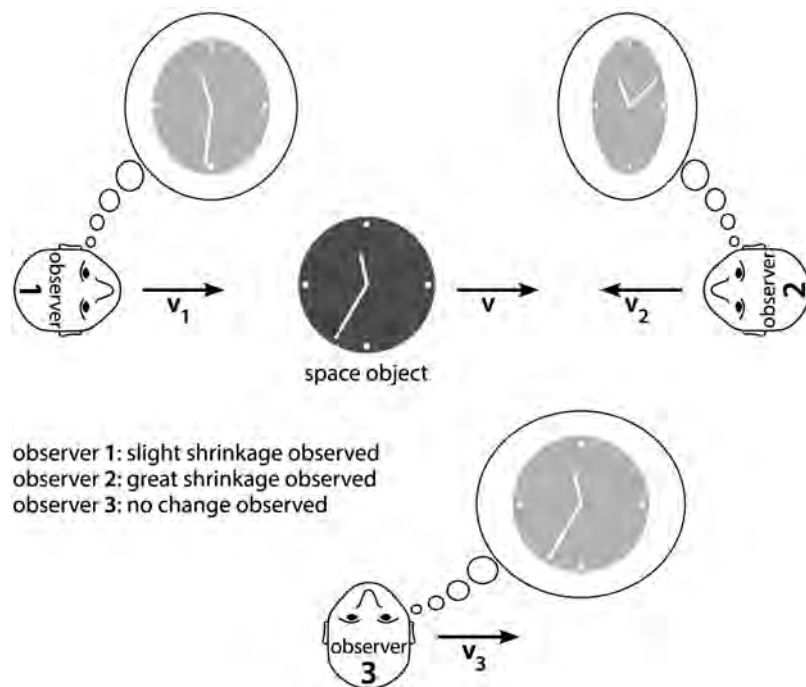


Figure 3. Scheme visualizing a paradox of relativity theory. Three observers with three relative velocities will, according to relations (3) and (4), see the spacecraft shrinking differently and recognize different “time flows” on it. In the direction of the spacecraft’s motion, the spacecraft will shrink and there will be a time dilation, different for observers at different speeds. No length or time dilation will be observed perpendicular to the movement. What is the actual length of the spacecraft, what time does it run?

This means that, in this case of simultaneity, the scale for measuring changes is not compressed or stretched due to a finite transmitting light velocity.

$$l = l_0 \sqrt{1 - \frac{v^2}{c^2}} \quad (3)$$

$$\Delta t = \frac{\Delta t_0}{\sqrt{1 - \frac{v^2}{c^2}}} \quad (4)$$

The energy driven Time Arrow approach states, that energy converting systems do not follow clock-time (2), but are subject to action time (1). Within the energy driven Time Arrow universe one would not transform the clock-time which is just a ruler or scale for passive measurements of changes. One would transform the real time (1), the flow of action or the flow of abandoned information on the past. Both are relativistic invariant so that moving energy converting objects would see the same time flow. All paradoxes with time travelling then simply disappear.

If one would like to find out clock-time on a moving object, the travellers would have to determine action time, measured for their object, and divide it by the locally turned over energy (2). When the conditions and calibration procedures are the same, also clock-time would be the same. This does not support the statement that every relatively moving object has its own time and that time is an illusion (comment also by Einstein). There is a simple intellectual consideration, that could support such a conclusion. The presently as one of the most distant recognized galaxies, Abell 1835 IR 1916, has a redshift, which indicates it is drifting away with 97% of light velocity. Clocks there on a similar planet, calculated via relativistic theory, should proceed 4 times slower. Observers there would, however, conclude the same from our galaxy. Does this make sense? Do we have a slowed down evolution, because we see galaxies escaping at a high speed?

The energy driven Time Arrow approach would not expect any difference in time flow when similar environmental conditions prevail. And it would also challenge the claimed high relative velocity seen in the (cosmological) redshift. It is not caused by the expansion of space, but is a consequence of entropy loss by propagating photons (see later).

2.6. Spacetime Critically Seen in Terms of the Energy Driven Time Arrow

A significant problem with General Relativity theory, according to the author, is, that the clock-time used is not relevant for transmitting useful information on changes and for calculating action. It is a scale for change only, a sequence of numbers. Another one is that matter and laws which control it were defined to be time neutral. Nevertheless, General Relativity theory is used to justify and describe highly dynamic phenomena, the Big Bang scenario, the inflation of space, to understand Black Holes and to investigate the accelerating expansion of the

universe.

Today the dynamics of the universe is deduced by back and forward calculating the field equations of General Relativity, which describe the relation between the geometry of space time and the energy-momentum distributed in it. Considering the apparent dynamics of the redshift of galaxies and stars they attribute to the universe an age of 13.8 billion years while it was stretched to a dimension of approximately 78 billion light years. That this rate of expansion exceeded light velocity is not considered a problem, since it is the empty space, which is assumed to have supported this stretching activity. But how can empty space, with no material properties defining it, do this?

The energy driven Time Arrow approach identified time flow as flow of action with changes in the environment (1). It is not just a scale for monitoring changes (2) (compare **Figure 2**). In addition, gravitation was identified to be information on matter with its root in quantum phenomena. Inertia is just the counter reaction to the fundamental law of Dynamic Energy aiming at reducing the presence of energy per state against a violation of this law. Gravitation and inertia are here not a property of empty space, but information mechanisms implemented on quantum level and, via this information, gravitation, widely present in the universe. The same is true for the interpretation of absolute light velocity. It is simply a property of information handling within the photon and not a property of space either. When these three properties, which, via Relativity Theory have been mathematically and ad hoc implemented into space, are explained in this different way, there is theoretically no basis left for a spacetime universe. However, how can one deal with the significant experimental evidence claimed in support of General Relativity theory and space-time?

With imposed conditions of absolute light velocity and a gravitation subject to the equivalence principle both theories, the General Relativity theory and the Dynamic Energy approach, should have the ability to explain at least part of existing phenomena. One significant difference is, however, the fourth dimension in the General Relativity theory, which gives rise to a very different space structures and phenomena. What can one learn from the different types of experimental tests of General Relativity theory?

2.7. Relativity Theory Is Sensitive for Specific Mechanisms, But less for Space Phenomena

Among the successful predictions of General Relativity one could mention the deflection of light by the sun, the gravitational redshift of light, gravitational lensing, equivalence principle testing. These phenomena are just consequences of gravitation, including the equivalence principle and the absolute light velocity, introduced in the General Relativity theory as property of space. These mechanisms really exist, and therefore act. But for the success of experiments it is not clear whether they originate from empty space or from quantum processes.

General relativity is less sensitive with respect to predictions concerning space

properties. It cannot tell whether the universe is static or dynamic. It cannot account for the inhomogeneous, granular appearance of the universe, since it treats it as homogeneous. It cannot say anything about the value of the Hubble constant nor about dark energy and dark matter, which are expected to occupy large areas in the universe. Singularities can be identified, but whether they are really Black Holes or just indicate where the theory fails remains an open question.

The author believes that this poor ability in dealing with space properties may in part be caused by the introduction of clock time into the fourth dimension of spacetime. It acts as a scale for measuring changes only, and, since it has no direct relation to matter or energy, cannot implement and communicate action.

However, in General Relativity tests, certain phenomena, attributed to gravitational distortion of space-time could be predicted and were tested: The perihelion precession of Mercury, in part attributed to spacetime distortions, can be calculated. For Mercury's perihelion movements by 575 arcsec/century, of which only 532 arcsec/century could be accounted for by classical Newtonian gravity calculations, General Relativity theory could explain the difference. Also deviations from geodetic precession (6 arcsec/year) and a Frame-Dragging Precession (0.039 arcsec/year) from Gravity Probe B Satellite experiments appear to support General Relativity and its four-dimensional space. But the effects observed are very small. The LIGO experimental setup, a Michelson-Interferometer for observation of gravitation waves, in 2015 detected a transient change of length of the order of one atomic diameter in form of half a dozen irregular maxima lasting together 2 tenth of a second. Are such tests a proof of space-time and gravitation waves or are other explanations imaginable?

The Dynamic Energy approach explains gravitation as information image of matter, aiming at decreasing and minimizing energy per state. It does that when interacting with matter and guides it like a remote-control system in an orbit subject to least action. This is different from the far-reaching action of Newton's gravitation and the near field action of gravitation in Relativity Theory. Already this is an interesting result, because remote control works technically and is commonly applied in steering drones.

When a travelling photon, particle and wave mediated via information on matter, is interacting with gravitation (information), there will be an effect of information acting on and changing due to additional information. There will be definitively an effect. This way deflection of light by heavy masses, the gravitational redshift, and gravitational lensing should in principle be explainable. It is also remarkable, that in form of remote control, using information (gravitation) on the spot to guide objects, irreversible nature applies a technology which our civilization has witnessed to be working. The open question remains, how natural objects can implement the provided information, when responding to gravitation. It should be recalled, that the Dynamic Energy theory is considering elementary particles as self-organized systems, comparable to virions, viruses de-

coupled from energy supply and not characterizable as “living” organisms [4]. They are expected to “know” how to respond to natural laws.

The situation in challenging General Relativity is more complicated with phenomena interpreted as space-time properties. However, they are very small and there is also the possibility to find explanations on the basis of the energy driven Time Arrow approach. Here again gravitation fields are fields expressing and mediating information. Information has an energy content and energy can generate gravitation. Information fields can therefore interact with masses and can be distorted through their presence. This could account for some of the space related effects identified with General Relativity theory. A Frame-Dragging effect (Lense-Thirring effect), for example, should also be expected with an information (gravitation) cloud around a rotating mass. Significant efforts have been developed (especially via String-Theory and Supergravitation-Theory) to introduce quantization of gravity into General Relativity. They failed and Dynamic Energy theory can comment on that from its point of view: The function of information on matter during the dynamic particle-wave duality can be compared to that of a technical analogue-to-digital converter. Such a converter involves an algorithmic function which performs quantization of the analogue signal and is called a “quantizer”. Information on matter, mediating the dynamic particle-wave duality (Figure 1 top right) may also act as such a quantizer, and by minimizing energy per state for an electron in an orbit of an atom or molecule it definitively can induce quantization of electronic states of atoms and molecules [1]. Within the Dynamic Energy approach the search for quantum gravity within General Relativity should be replaced by a profound study of information on matter. It plays a crucial role in quantum states and, as gravitation, is also decisive for understanding the universe.

2.8. How to Deal with the Specific Experimental Evidence for Relativity Theory

Because of the overwhelming experimental evidence claimed for Relativity Theory, criticism is not any more accepted by established journals. However, up to now critics could not present a reasonable alternative theory for explaining the always constant light velocity, gravitation, inertia, time behaviour and space properties. The Dynamic Energy model does this and claims in addition the potential of eliminating paradoxes and irrationalities of General Relativity. It also entirely naturally provides the link between quantum behaviour and cosmological function, and introduces, for the first time, the concept and mechanistic creativity of information technology into fundamental physical mechanisms. Our industrial civilization experiences the amazing potential of information technology, which is based on natural laws. Why should nature not apply them?

Here alternative explanations for experimental observations claimed to support Relativity Theory are sketched.

Time shifts of atomic clocks: Atomic clocks sent around the Earth or clocks in space show time dilation. It is interpreted to fully confirm Relativity Theory.

These phenomena seen with atomic clocks in the sub-microsecond range occur with time intervals determined by atomic parameters only. According to the Time Arrow approach not the time changed, but a changed gravitation acting on the atomic clock modified the time lapses, determined by electronic transition in the atoms. Something similar would happen, if an ordinary pendulum clock would be taken up a mountain, where gravity, the acceleration imparted to objects, is lower. Its oscillation period inversely depends on the root of gravity and would become longer and correspondingly its oscillation frequency lower. This, however, does not mean that the time measured with the pendulum clock has changed. Just the scale used for measuring changes, the oscillations of the pendulum clock, experienced an alteration in the parameters controlling them. One would have to recalibrate the clock.

The Time Arrow approach explained quantization in atoms as consequence of minimization of information on matter [1] [6]. When additional gravitation (which itself also constitutes information on matter) is applied, the obtained minimum approached for quantization of electronic levels will be shifted and thus the distribution of the concerned electron orbits within the atom. This will change the time lapse during an electronic transition. Atomic clocks, today, can even register gravitation changes generated by the tides produced by the moon and react to a change of one meter in altitude. This has nothing to do with relativity theory. It cannot be claimed via experiments of travelling atomic clocks that time is relative, since the time lapses concerned are not the real dynamic time. What is observed is that a scale for measuring changes, the sequence of time lapses, which, when calibrated, we use as a clock, is altered by gravitation and additional parameters. Since such clocks are technologically important, this behaviour has, of course, to be technologically considered, but it does not support the claim of Relativity Theory that time is relative. It is also not a real space-time, but a “space-time scale”, when just a scale for measuring changes is used to construct “space-time” and varies its intervals in dependence of gravity and other parameters. Relativity theory does not understand the real nature of time properly. It tries to understand the universe by linking it with a scale, lacking any relation to energetic processes and change, the properties of which are influenced by physical parameters.

Diversion of light by gravitation

Gravitation, being interpreted as information on matter, will have an effect on the trajectory of light, which is equally controlled and mediated by information on matter. A quantitative theory will be able to deal with this phenomenon, during which information enforces a minimisation of energy per state towards an implementation of the principle of least action in presence of additional information from outside. When gravitation (information) becomes strong enough, light will be visibly deviated and, in the case of a Black Hole environment, prevented from escaping. One is dealing with the effect of a “remote control” on elementary particles via information.

Increase of weight with increasing velocity

The Dynamic Energy approach explains elementary particles and matter as self-organized energy [4]. Self-organized systems can grow in mass with energy from outside. Examples are a hurricane, a green plant growing in sunlight, a living species consuming food. The increase of mass during acceleration of elementary particles to very high velocities can be interpreted that way. Kinetic energy, when provided to a sufficient extent, is converted into mass. This is possible when mass is behaving as self-organized energy. The author believes, that Relativity Theory formally comes to the same conclusion, because of the physics introduced on the basis of its mathematical construction.

The formula $E = mc^2$

The famous relationship $E = mc^2$ derived from Einstein's theory of relativity describes the energy of a mass m at zero velocity. It is considered synonym with Relativity Theory and any counter theory will have to deal with this situation. It is therefore important to learn that the derivation of this formula was not really based on logical considerations, but was already anticipated in the derivation of the result (see [16]). Classical deductions of analogue formulas were also described in the literature [17]. Einstein speculated that the energy formula he deduced for light, which included arbitrary assumptions, should also apply generally to any other energy form. Two years before Einstein, an Italian geologist, Olinto de Pretto, published the same relationship between energy and mass. He derived it from a non-relativistic consideration [18]. He observed how the mass of uranium and thorium transformed into energy during radioactive decay. Before him, around 1900, Henri Poincaré apparently brooded over the same formula. The point here is not to diminish the accomplishments of Albert Einstein. The point is that we want to understand what this formula actually means in the context of Relativity Theory. Do we need the Theory of Relativity to derive this proven formula? In reality, the formula $E = mc^2$ has nothing to do with relativity. It would still be valid if the four-dimensional space did not exist. Einstein had anyhow neglected relativistic considerations before deriving the famous energy-mass formula. This formula can be derived purely from classical arguments. The important energy-mass relationship can therefore not be used as a support and justification for a four-dimensional space-time. This is an important argument for the considerations here and justifies the discussion. One does not need the Theory of Relativity to obtain this important formula. And there is an additional relevant fact: The Dynamic Energy theory also conveniently establishes the connection between energy and mass. Mass is simply self-organized energy, it is consequently proportional to energy [4]. Self-organization is doing with energy what it does with water on a hotplate, when generating droplets erratically moving around (Leidenfrost-phenomenon). These water droplets made from water correspond to elementary particles generated from energy via self-organization. However, because of the complex mechanism of self-organization, the proportionality factor between energy and mass is ex-

pected to be more complicated than c^2 , which, in this simple form, accounts for the appropriate dimensions.

Gravitation singularities are information singularities

Gravitational singularities are locations within space-time, characterized by infinitely growing gravitation and undefined space-time properties. Dynamic Energy theory explains gravitation as information on matter with the task to decrease energy per state and thereby to reduce information contained in free energy. Such a developing singularity, called a Black Hole, is thus an extremely dynamic information phenomenon aiming at disrupting matter and generating entropy. During the proceeding mechanism information (gravitation) is increasingly concentrated. As explained in a preceding publication [2], this is a highly dynamic process, including self-organization and even structuring of information (gravitation). As a far from equilibrium self-organizing open energy consuming system it approaches maximum entropy generation, within given constraints, like derived for living systems [5]. The information driven matter consuming self-organizing Black Hole moves further and further away from equilibrium and finally develops quasar properties to get rid of accumulating entropy. One is dealing with an information controlled inorganic phenomenon comparable to primitive living organisms with a directional evolution and different development stages towards maximum entropy turnover.

Gravitational waves as information pulses

Within Dynamic Energy gravitation is explained as information on matter and information itself does not produce waves. But when self-organized, which is possible within the Dynamic Energy theory [6], time dependent, propagating information (gravitation) phenomena are to be expected. They have nothing to do with perturbations of a space-time structure of the universe and do not show a time—component of the assumed space-time perturbation (clock-time perturbations were not registered during the LIGO experiments). If space-time would exist, “gravitation waves” should be frequent, since the presently known universe contains 500 billion galaxies with over 100 billion stars in each. Space would be vibrating.

Dark matter means self-organized information on matter

Dark matter cannot be explained by the Theory of Relativity and when not found constitutes a problem for it. Dynamic Energy explains the dark matter phenomenon as self-organized information on matter (gravitation) [2] [6]. The time arrow allows feedback and thus a self-organization of information into a higher hierarchy of information handling with the task of reducing energy presence per state. The additional energy needed comes from the energy flow sustaining self-organization of information on matter. The result is much higher gravitation, powered by the energy consumed for the self-organization of information. Gravitation (information) could even get structured in space like observed in living organisms. No dark matter is needed and expected for explaining super-gravitation and gravitational lensing in the universe. The mirage effect

is generated by self-organized gravitation (information) in a similar way as terrestrial mirage effects are generated by special, self-organized weather conditions.

Space-time distortions versus dynamics of information clouds

In the Dynamic Energy approach phenomena like the perihelion motion and curvature of space time could be reinterpreted as distortions and behaviour of information (gravitation) halos or information clouds around space objects. They have an energy content and may interact, for example, by responding to a rotating or otherwise moving mass. The behaviour of gravitation fields as fields of information and their mutual interaction need to be studied. How are information clouds behaving, which make up gravitation around masses?

Cosmological redshifts versus information handled “tired light”

Expanding radiation is, like an expanding gas subject to entropy production. The equivalence of the entropy formula applicable has already been used by Einstein in 1905 to justify the existence of light in form of particles (photons) [19]. His argument was that, subject to the same entropy formula upon expansion light should behave like particles of a gas. However, in time-neutral quantum physics photons, once released, are only allowed to lose energy by interacting with matter or gravitation. Entropy generation is not any more taken into consideration. Dynamic quantum physics requires and allows entropy generation of propagating photons via the mediating presence of information on matter. Since the logarithmic formula for entropy generation by expanding radiation into a larger and larger volume goes towards infinity, the energy of expanding, propagating photons should finally be consumed at the expense of released microwave radiation [2]. In contrast to abandoned classical theories on “tired light”, which have already been discussed one century ago (Ritz, 1908 [20]; Zwicky 1929 [21]), light particles are not deviated by dust to produce a blurred sky, but get rid of microwave radiation without deviation from the photon path via the information on matter involved in energy redistribution. The redshift observed from distant stars and galaxies could therefore to a large extent be due to entropy generation by expanding, propagating photons and not to an explosive expansion of empty space (cosmological redshift) and accelerating escape movements of galaxies. On the basis of Dynamic Energy a new evaluation of structure and dynamics of the universe is required. It could be much more static than presently assumed.

How accurate can bent space gravitation be measured?

As scientific experience shows, a phenomenon such as gravitation is perfectly considered and implemented in natural processes. For this to work bent space gravity has to be registered with sufficient accuracy. Is this possible with a gravitation coined by a bent space, which has to be registered as an analogue signal? An indication of the accuracy in measuring gravity is provided by measurements (e. g. via torsion balances) of the gravity constant, which is deduced via the well-known formula relating gravitation forces to masses and their distance. Its presently recommended value is $6.67430 \times 10^{-11} \text{ m}^3\text{kg}^{-1}\text{s}^{-2}$ with an uncertainty of 2.2×10^{-5} , which is mostly due to the fact, that the mass of the earth is not well

known. This requires measurements in the laboratory with correspondingly quite small test masses and associated inaccuracies. The expectation prevails that an accuracy of 6 digits can be reached for the gravity constant. On the Earth surface the variations in gravity itself, which in average is $g = 9.81 \text{ ms}^{-2}$, due to latitude amount to ± 0.03 , due to local geological variations to ± 0.0006 , and due to tides to ± 0.000003 [22]. The best accelerometers can measure gravity to two parts per billion, that is to ± 0.00000002 [23]. Such an accurate measurement can be performed on just the selected location. How can a bent space be measured so exactly without access to information on the degree and orientation of space bending?

The role of self-organization

Every self-organization requires a directed time which provides a “before” and an “after”. A clock time does not provide that, because it only represents a scale, provided by oscillation phenomena, for measuring change. The Dynamic Energy approach, however, provides an energy driven time arrow which readily supports self-organization of matter and information (which has an energy content). The time orientation may be enforced by information loss accompanying energy processes from usable to unusable energy. Time is the loss of information on the past. This way, and because of the existence of a directed time, the complex space structures seen in the universe or in the structural complexity of life can readily be understood and explained. Such a creativity of the universe would not be possible within the time-neutral approach. Here daring mathematical procedures had to be applied to justify time orientation for self-organization (e. g. symmetry breaking). In practice, relevant disciplines, dealing with feedback and self-organization, e.g. control theory, presuppose a functioning of feedback processes, even though time neutrality and time as an illusion should not permit it.

The “Big Bang universe” of time-neutrality versus the “Self-Image universe” of irreversibility

The Big Bang universe (Figure 4, top) with the origin of energy from nothing, the inflation of empty space, with its quantum fluctuations, dark matter and the accelerating expansion of galaxies via dark energy is well known to be characterized by irrational assumptions (marked as I_1 to I_5 in Figure 4, top). However, practically full experimental verification is claimed [24] [25].

The Dynamic Energy approach for understanding the universe emphasizes the importance of information mediating between concentrated and distributed, chaotic energy. Such a mechanism applies for the particle-wave duality and is, since gravitation (information) dominates space, also expected to apply for the entire universe. A terminal, worn-out universe with a high entropy content will consequently be reconverted, by set aside information, into the free energy rich initial, original universe (Figure 4, bottom). We are dealing with a fractal universe, which shows parallel behaviour on quantum and cosmological level [2]. Such a behaviour is only to be expected from a fundamentally irreversible world, which is able to self-organize. Since the redshift of galactic light can, to a large

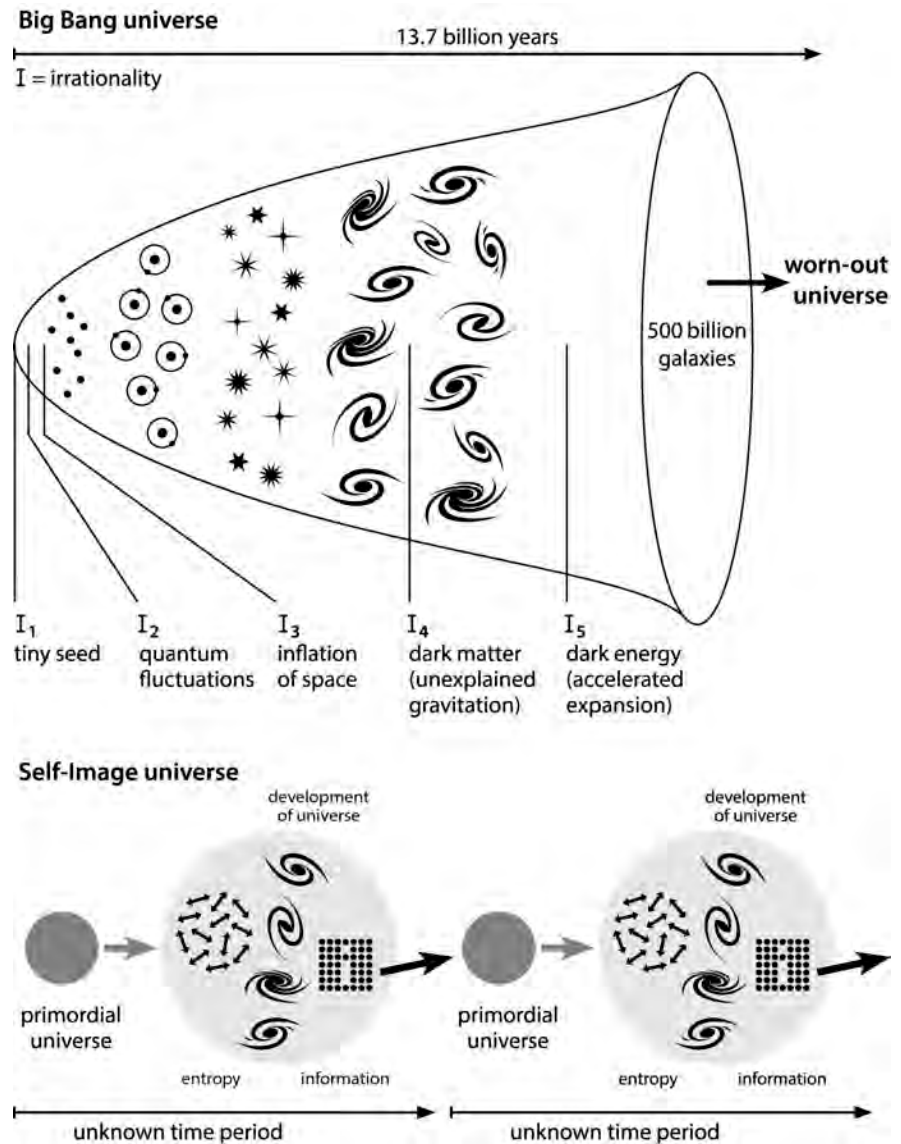


Figure 4. The Big bang scenario, which is sustained by the time-neutrality paradigm, shaped by General Relativity, and characterized by irrationalities (top) is compared with the Self-Image universe, resulting from Dynamic Energy considerations (bottom). The first describes an explosion of energy, matter and empty space without understandable sense, with life as chance phenomenon and an end in cold and darkness. The second starts via information, evolves galactic structures, live and spirit as an aim of self-organization, within an information-controlled universe, and regenerates itself finally again via set aside information.

extent, be understood as entropic energy losses (discussed above), most evidence for a Big Bang scenario can be interpreted differently and in support of the Self-Image universe [6].

But the Self-Image universe has additional striking properties. Because of its directionality (due to feedback-coupled mechanisms as shown for cybernetic systems [26]) and the role and importance of information it can explain evolution of consciousness and spirit. As matter can self-organize to living species,

also information (related to energy and matter) can do this and reach a higher ranking or hierarchy and function. This occurs on the level of chemical information in relation to the genetic code and it also occurs in the brain, where upgraded, self-organized information leads to consciousness and spirit. Information on matter, gravitation, as well can self-organize under appropriate conditions and sufficient energy supply to yield super-gravitation, which can serve as a substitution for “Dark Matter”, without the need for undiscovered dark matter particles (compare above). Feedback-coupled processes have teleologic character and follow an intrinsic aim [26], including in biological evolution, where genetic control is superposed to a strive of biological systems for maximum entropy production within their restraints [5]. The Self-Image universe is dominated by information (gravitation), and favours evolution of mind and spirit [6]. In contrast to the Big Bang universe without aim and with life just being a chance development, it is intelligent and creative, is logic and sophisticated [6], expecting further exploration.

3. Discussion

3.1. A Credible Explanation of the Universe Is Simple and Rational

For the first time, and based on reasonable starting assumptions (fundamental irreversibility in nature) a rational counter theory is proposed, which challenges the space-time understanding of the universe. **Figure 1** explains, why the well-established time neutral world of space-time (**Figure 1**, left) has to be challenged by the energy driven Time Arrow world. The essential postulates by General Relativity theory, the always constant light velocity, gravitation and inertia as properties of empty space, can be explained differently, on quantum level and in a more straightforward way as consequences of a dynamically understood principle of least action. Information on matter, needed as a link between wave and particle aspect of matter, turned out to be a crucial aspect of fundamental irreversibility. Only one of the two theories, based on different paradigm, can be correct. If nature is fundamentally energy driven and irreversible, then a Big Bang scenario based on space-time concepts is wrong.

The “energy-driven Time Arrow” approach towards understanding a fundamentally irreversible universe, as an alternative to the established time-neutral one, which is shaped by General Relativity theory, is faced with a complex challenge. On one hand there is the claim that Relativity theory has passed every test. On the other hand the quest for fundamental irreversibility and an energy driven time has opened a very promising path: it eliminates paradoxes in quantum physics and has given straightforward explanations for gravitation (and inertia) and the absolute light velocity, without the need to introduce them as property of empty space. They are implemented on quantum level so that also the link with processes in the universe is automatically given. Gravitation turned out to be information on matter with the aim of decreasing the presence of energy per state. This yielded an explanation of gravitational forces in terms of a remote

control of masses, distinct from Newton's long-distance action of gravitation forces and the close distance action of gravitation in General Relativity. Due to the orientation of the energy driven Time Arrow, a "before" and an "after" are readily given and consequently the route to self-organization is entirely open. It is open for energy, which self-organizes to elementary particles, for matter, which self-organizes to galaxies and life, and for information (which contains energy which is related to mass) which self-organizes to a higher hierarchy of information processing [27]. It yields a higher ranking of genetic information, when genetic information self-organizes. It is consciousness and spirit, when information in the brain self-organizes. It is super-gravitation when gravitation (information on matter) self-organizes. All together looks like a promising starting situation for the exploration of an intelligent universe.

When information on matter (gravitation) self-organizes in the inorganic environment of space, it moves up into a higher hierarchy. Then it also increases its order, or the information it contains. It may structure itself, with areas of high gravitation near others of low or no gravitation. The gravitational effect exerted becomes much stronger. The additional energy required for this super-gravity comes from the self-organization of gravity, which demands a sustaining flow of energy. In any case, the supergravity proposed here, as self-organized information, does not require any dark matter. This dark matter has been searched for during four decades now. The complex experiments with the liquid Xenon probe in the Gran Sasso mountain in Italy were negative. The Chinese Panda-X-II experiments and the Swiss experiments with ultracold neutrons were also unsuccessful. The time arrow as a trace of energy does not need dark matter. Its effect is due to a dynamic self-organization property of gravitation, information about matter, which may regulate and dominate our universe in other respects as well.

Another thrust of the Dynamic Energy approach is access to irreversible thermodynamics of matter which the time arrow facilitates. The recognized limiting entropy law is "maximum entropy turnover within the constraints of the system" [5]. This applies for life (with the genetic mechanism superposed), as well as for galactic objects such as Black Holes [2]. In these it is information (explained to be gravitation), with the tendency to decrease energy per state, which increasingly concentrates and degrades matter. Because the products of entropy generation can, in an initial period, not leave the Black Hole due to gravitational attraction, its system is pushed further away from equilibrium. A new organization of the Black Hole and a structuring of gravitation is assumed which represents a Black Hole-Quasar association, which is able to exhibit maximum entropy (energy) turnover. The time arrow as a trace of energy implements this and is thus a key to the irreversibility and thus creativity of the universe. The Dynamic Energy universe explains observed phenomena rationally and in a straightforward way. Irreversibility and feedback mechanisms of self-organization are creative tools towards a structured and intelligent universe.

However, time-neutral physics and the space-time world of General Relativity are well established [24] [25]. It is often stated that Special and General Relativity have passed every test. Some of these experiments were discussed, questioned and reinterpreted above. Since absolute light velocity and gravitation subject to equivalence with inertia are actually implemented in nature and were imposed on empty space via Einstein's field equations, some of the "verification" experiments may just reflect that. One verifies what the theory considered. But, as the "Dynamic Energy" approach shows, the ever-constant light velocity and gravitation could also have different origin. What is different, when light velocity and gravitation is controlled by information and originating from quantum processes? First, gravitation indeed occurs on elementary particle level. Towards a weight of one kilogram it increases by a factor of 10^{54} . Second, important "demonstrations" of General Relativity have to be explained differently. As discussed above, the time dilation registered with travelling atomic clocks is not considered a change of time flow but simply to be the influence, which a change in gravitation is exerting on electronic states in the atoms, controlling the time lapses induced by electronic transitions in atomic clocks. It is well known that the Standard Model of elementary particles, which is based on time-neutrality, cannot explain gravitation at all. The "Dynamic Energy" approach, which considers matter as self-organized energy, can do it: particles exist and react as self-organized mechanisms. They grow and change during energy turnover like a hurricane. This permits also that accelerated particles increase their mass [4]. It explains also the diversity of elementary particles, of which only a few serve as useful building stones for matter. As discussed above, the equivalence of energy and mass is equally not a privilege of Relativity Theory. The Dynamic Energy theory has also the potential to provide alternative explanations for experimental results related to gravitation phenomena, interpreted as proofs for space-time. For this purpose more has to be learned about the dynamics of information (gravitation) clouds.

3.2. The Time Arrow Universe Is Rational, Intelligent and More Fascinating

The Self-Image universe drawn by the Dynamic Energy theory is recreated from a worn-out universe by set aside information on matter and can develop successive activity periods (Figure 4, bottom). The energy driven Time Arrow leads to a self-organization of energy to elementary particles [4]. Among these, which were compared with virions, viruses without access to energy, some are useful as building stones of matter. Also matter can self-organize and thereby already uses self-organized genetic information to upgrade its creative and sustaining abilities. Structured, self-organized matter aims at maximum entropy turnover and thereby prepared the conditions to support self-organization of information in the brain. The brain requires a high rate of energy turnover for self-organization. Consciousness and spirit evolved [5]. Evolution of spirit within an information-based universe turned out to be the aim of evolution. Its origin is purely

materialistic and rooted in the feedback-controlled nature of self-organization processes [26]. All together the contours of a spiritual universe appear, which sees evolution and life not as a coincidence, but as part of a gigantic experiment triggered by energy acting via the time arrow. Far reaching philosophical considerations result. Also the question can be answered, what nature actually is. It is a question which could not be answered on a purely materialistic basis before. The Time Arrow can now do it:

“Nature is the self-realization of energy over the time arrow”.

Due to its fundamental irreversibility, energy can self-organize to elementary particles and to matter [4]. Matter can self-organize to structured objects and life [5]. Information in structured matter can self-organize to generate mind and spirit [6]. The time arrow, of course, is action time, the flow of energy driven action, equivalent to the loss of information on the past. Relevant questions around such conclusions and arguments leading to them are discussed in a recent monograph [27].

The paradigm of time neutrality and Relativity Theory has, in contrast, sketched a universe which starts with energy from nothing in a Big Bang explosion. It involves a (bizarre) expansion of empty space and recognizes an evolution, which functions by pure chance and natural selection. This concept of evolution is characterized by no aim, cannot explain its obvious thrust and is unable to explain consciousness and spirit. The chaotically starting and dramatically expanding universe consumes its energy resources and is finally heading towards a cold death in infinite expansion. Mostly puzzling is the fact, that such a highly dynamic universe was constructed starting from assumed time-neutral particles and natural laws. Critically seen it does not explain the dynamics it created. Such a concept does not allow relevant philosophical questions either.

The new vision of the universe, the Self-Image universe (**Figure 4**, bottom), which is started, largely controlled, and regenerated by information, is fundamentally irreversible, explains dynamic change, aim and creativity, and interestingly shows rationally understandable contours of development and destination. It is profoundly logic and philosophically highly attractive, because questions can be asked with respect to the role, development and aim of spirit, which is part of its character [27].

3.3. Time Neutrality versus Fundamental Irreversibility

The Dynamic Energy approach claims that the Time-Neutrality paradigm, applied to highly dynamic processes, is largely responsible for relevant paradoxes and finally also was responsible for the rise of Relativity Theory based on clock time, which has no relation to energetic processes. How the basic assumptions of the time-neutrality paradigm led to well-known, presently still tolerated, paradoxes is analysed in **Figure 5**.

Time-neutrality and an energy which is just a scalar without any relation to change is seen as the reason why the dynamic nature of the principle of least

has been assumed in support of the Big Bang scenario.

The energy driven Time Arrow approach thus also provides, in **Figure 5**, explanation for the cause and development of paradoxes and irrationality within the time-neutral space-time concept. This is an additional argument for the reality of a fundamentally irreversible world and the need for a paradigm change.

The Dynamic Energy theory which can be derived from a dynamic interpretation of the principle of least action [1] applies just the additional condition for quantum physics that energy, diluted in time and space, has less ability for work compared to concentrated energy. Starting from the paradigm change of dynamic energy and respecting the role of space and time for energy appears to be sufficient for explaining essential quantum and cosmological phenomena and arriving also at a reasonable philosophical interpretation of evolution and the universe (**Figure 1**, right side).

The above given alternative interpretations of experiments, that successfully seem to support Relativity Theory, show that they do not contradict a fundamentally irreversible nature. Alternative, and in addition logic and simpler interpretations in line with Dynamic Energy theory are possible. No experiment has up to now been communicated that unambiguously shows that a natural phenomenon can be inverted in time without additional changes in the environment. Such efforts should be continued as an attempt to support or challenge Relativity Theory based on the time-neutrality paradigm. Also, answers should be found to questions on relativity as sketched in **Figure 3**. The author insists that there should be no tolerance for irrational concepts in science and the step from clock-time to an energy driven action time (**Figure 2**) would quite radically change understanding in cosmology.

In support of such a step it should be explained how measurement values for gravitation covering 54 orders of magnitude (between two neutrons and two one kilogram weights) can be expressed and registered in form of a bent space around spherical material objects. For the expected analogue signals expressing gravitation based on a bent space this appears to be impossible. Only 4 orders of magnitude (0.01% of full value) can reliably be measured with such systems. On the other hand, gravity measurements with an accuracy of 2 parts per billion have been achieved, as explained above (compare [23]). Besides of the LIGO experiment the gravity probe B experimental results provide another example of surprising accuracies while dealing with quite small signals. The already mentioned measured frame dragging drift around rotating Earth, which was claimed to be in good agreement with General Relativity, amounted to approximately 10^{-5} parts of one degree per year [28].

Can the bent space of General Relativity around Earth be registered within an accuracy of 5 to 9 digits (decimal positions)? In order to do that the instrument (or the physical object concerned) must be able to retrieve or register the corresponding information from the curved structure of space, which is expected to

be present and active during measurement (or interaction). The discussed measurable gravity values already indicate a two to six orders of magnitude higher accuracy than expected for a measurement of an analogue signal which a bent space is able to provide on the basis of practical experience: the error of an analogue instrument due to gain is generally estimated to be 0.01% or three digits behind the comma, to which an offset error has to be added (e.g. [29]). And there is an additional problem: bent interfaces or space regions as measure for gravitation cannot be properly evaluated by just measuring one point. A particle arriving and selecting a curved trajectory around a spherical object has to monitor curved space gravitation. Several or many points apart are needed to approach such a bent trajectory or space or one needs to scan it for digitalization and evaluation. This is evident, since the degree of bending is a measure for the intensity of gravity. Can a bent space reflecting gravity, which undoubtedly provides an analogue signal, really be measured with such an accuracy, and at one location only, as explained above? How can a gravity measurement of bent space on just one location yield an accuracy of 9 digits [23]? The author's conclusion is that this is not possible with the space-time gravitation mechanism of General Relativity. This is a strong, experimentally verifiable argument against bent space gravity. In spite of many contrary claims, and an elaborate created knowledge basis on Relativity Theory [30] [31] [32] [33] [34] such a concept of space-time and gravity does not match reality.

With a gravitation in form of information in numbers, on the other hand, registering and handling such a signal over many orders of magnitude, and providing such a sensitivity on any single location where gravitation exists would work. Measurement of gravitation on one location only is sufficient for obtaining the necessary information, as actually possible in reality. The measurement is then dealing with an information cloud around matter, in which information on matter, gravity, is present, properly distributed and available and active in form of numerical data. Can information better explain gravity? In a given gravitational field, all bodies, whether light as a feather or heavy as a hammer, are subjected to the same acceleration. They approach the ground at the same speed, provided that no air is present to exert varying amounts of friction. Such an experiment was actually carried out successfully in 1971 by Apollo 15 astronaut David Scott on the moon. One can rationally understand that the information image imposes such a behaviour, an equally strong acceleration, on masses. The information given in an identical gravitational field for a reduction of energy per state is simply the same for differently shaped objects. So also the observed acceleration is identical for a feather and a hammer. The principle, according to which acceleration does not depend on mass, shape or density of an object, is thus comprehensible, logically understandable. It is triggered by the same implemented information. However, the force experienced by unequal objects is different, since the triggered acceleration must be multiplied by the corresponding mass.

How nature is actually handling information on matter in the form of gravitation needs, of course, to be explored. It may be a demanding task, but a realistic one, compared to the claim of Relativity Theory that curving of empty space is doing that. Elementary particles are already showing gravity properties so that the phenomenon must originate in them as derived by Dynamic Energy considerations. One knows what to search for, and what questions to ask. Experience within our evolving information age may provide more and more technical clues.

Such a measurement challenge, the distinction between analogue space-time signals on gravity and digital Dynamic Energy signals of gravity is proposed here as a falsification criterion (according to Popper [35]) for Relativity theory and Dynamic Energy theory respectively. Dynamic Energy involves information on matter in form of clouds around masses as explanation for gravity, in conflict with General Relativity with its bent space around masses. Since information on matter, as gravitation, turned out to be so essential as the link between quantum physics and cosmology, and as a key to a more intelligent Self-Image universe (Figure 4), another falsification effort should concern this information: It should be attempted to demonstrate that for a mutual transformation between two different material phenomena such as particle and wave no mediating information would be needed. The author has pointed to the example of analogue-digital-analogue converters in cell phones as functioning technical devices for digitalizing, evaluation and reconstruction [27], which show that natural laws require a mediating information program for a working exchange between wave and particle (compare Figure 1, top right). Omitting this information (as occurring in classical quantum theory on the basis of time-neutrality) prevents dynamic function and must lead to problems and contradictions in understanding. The Dynamic Energy approach requires this mediating information, which also turned out to be crucial for eliminating quantum paradoxes and for building a rational link to cosmology. Falsification is successful, if it can be demonstrated that the mediating information between particle and wave (dotted squares in Figure 1, right side) is not needed.

The Franciscan monk William of Ockham proposed in the 14th century that “no more causes for natural events should be allowed than absolutely necessary for their explanation”. This rule of thumb for scientists, also known as Ockham’s razor, would clearly favour the Dynamic Energy approach claiming a fundamentally irreversible nature, presented here, over the irrational theories, including General Relativity theory, for various natural phenomena, based on time neutrality and criticised in this paper. Figure 1 shows that much less and more reasonable starting assumptions (marked with rectangles) are required (right) compared to the time-neutral space-time approach (left). In addition, irreversibility is not a claim but results from a dynamic interpretation of the principle of least action [1]. Within the paradigm of an energy-driven Time Arrow historically evolved time-neutral theories that lead to irrational conclusions could be

challenged, adapted and replaced, and this with significantly more reasonable basic assumptions [6] [27]. Moreover, it is not the same to describe nature through paradoxes and to declare them fundamental as to explain nature rationally as the Dynamic Energy approach can. Common sense would always prefer rational explanations and consider them simpler and making more sense. Last not least the fundamentally irreversible nature, as derivable from a dynamic interpretation of the principle of least action, explains evolution of spirit in context with a more conciliatory and supporting universe, which is rational and in principle much simpler than the Big Bang scenario. Relativity Theory would not allow that, because it relies on time-neutral particles and laws, claims a complex space-time, uses a clock which does not reflect, but only monitors change, claims empty space as origin for the always constant light velocity as well as for gravitation and inertia, speculates with an exploding vacuum and more recently even with multi-worlds.

Dynamic Energy pictures a much simpler, rational and more attractive universe. It is a promising alternative, because truth regularity proved to be simpler and philosophically more rewarding. It especially promises to allow penetrating deeper into natural contexts. There will never be a reasonable scientific understanding of bent empty space gravity of Relativity Theory, but the information technology expected behind the information-based gravity of the Time arrow approach promises a deep penetration into the secrets of the universe. The proposed new truth is that nature is fundamentally irreversible, that real time flow is the loss of information on the past, that the two Relativity Theories design a fictional universe by assuming that gravity and always constant light velocity are properties of empty space. Existing nature is, in principle, much simpler than presently seen and it is rational, while able to creatively evolve sophisticated structured systems including galactic objects, life and spirit within a universe dominated by information.

Conflicts of Interest

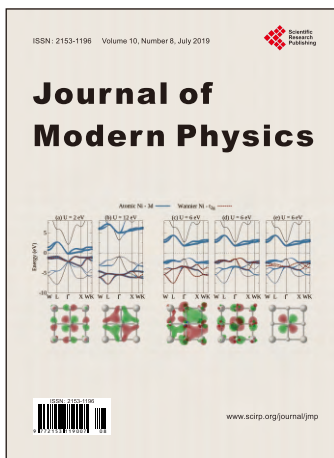
The author declares no conflicts of interest regarding the publication of this paper.

References

- [1] Tributsch, H. (2016) *Journal of Modern Physics*, **7**, 365-374.
<https://doi.org/10.4236/jmp.2016.74037>
- [2] Tributsch, H. (2016) *Journal of Modern Physics*, **7**, 1455-1482.
<https://doi.org/10.4236/jmp.2016.712133>
- [3] Susskind, L. (2012) *Modern Physics, General Theory of Relativity*, Fall 2012, Stanford.
<https://podcasts.apple.com/us/podcast/modern-physics-general-theory-of-relativity-fall-2012/id571368922>
- [4] Tributsch, H. (2018) *Journal of Modern Physics*, **9**, 1361-1380.
<https://doi.org/10.4236/jmp.2018.97082>

- [5] Tributsch, H. (2018) *Advances in Anthropology*, **8**, 140-174.
<https://doi.org/10.4236/aa.2018.83008>
- [6] Tributsch, H. (2015) *Irrationality in Nature or in Science? Probing a Rational Energy and Mind World*. CreateSpace.
- [7] Pais, A. (1979) *Reviews of Modern Physics*, **51**, 863-914.
<https://doi.org/10.1103/RevModPhys.51.863>
- [8] <http://www.kritik-relativitaetstheorie.de>
<http://www.anti-relativity.com>
- [9] Climont, J. (2012) *The Worldwide List of Dissident Scientist*.
<https://de.scribd.com/doc/229428780/The-Worldwide-List-of-Dissident-Scientists-Jean-de-Climont>
- [10] Arteha, S.N. (2003) *Criticism of the Foundations of the Relativity Theory*.
<http://vixra.org/pdf/1201.0082v1.pdf>
- [11] Tributsch, H. (2008) *Energie, Zeit und Bewusstsein*. Shaker Media, Aachen.
- [12] Withrow, G.J. (1980) *The Natural Philosophy of Time*. Clarendon Press, Oxford.
- [13] Zeh, H.D. (1992) *The Physical Basis of the Direction of Time*. Springer, Berlin.
<https://doi.org/10.1007/978-3-662-02759-2>
- [14] Reichenbach, H. (1956) *The Direction of Time*. University of California Press, Berkeley. <https://doi.org/10.1063/1.3059791>
- [15] Davies, P.C.W. (1974) *The Physics of Time Asymmetry*. Surrey University Press, Guildford.
- [16] Ives, H.E. (1952) *Journal of the Optical Society of America*, **42**, 540-543.
<https://doi.org/10.1364/JOSA.42.000540>
- [17] Gut, B.J. (1981) *Immanent-logische Kritik der Relativitätstheorie*. Oberwil b. Zug: Kugler, 151S.
- [18] Olinto De Pretto (1903). http://en.wikipedia.org/wiki/Olinto_De_Pretto
- [19] Einstein, A. (1905) *Annalen der Physik*, **17**, 132.
<https://doi.org/10.1002/andp.19053220607>
- [20] Ritz, W. (1908) *Annales de Chimie et de Physique*, **8**, 145.
- [21] Zwicky, F. (1929) *Proceedings of the National Academy of Sciences*, **15**, 773-779.
<https://doi.org/10.1073/pnas.15.10.773>
- [22] <https://web.calpoly.edu/~gthorncr/ME302/documents/AccuracyofGravity.pdf>
- [23] <https://en.wikipedia.org/wiki/Gravimetry>
- [24] Will, C.M. (2006) *Living Reviews in Relativity*, **9**, 3.
<https://doi.org/10.12942/lrr-2006-3>
- [25] Fließbach, T. (2003) *Allgemeine Relativitätstheorie*. 4. Auflage. Elsevier—Spektrum Akademischer Verlag, Amsterdam.
- [26] Rosenblueth, A., Wiener, N. and Bigelow, J. (1943) *Philosophy of Science*, **10**, 18-24.
<https://doi.org/10.1086/286788>
- [27] Tributsch, H. (2019) *Time Arrow as Trace of Energy. Logical Key to a Spiritual Universe*, MyMorawa, Vienna.
- [28] Gravity Probe B. https://en.wikipedia.org/wiki/Gravity_Probe_B
- [29] <https://www.mccdaq.com/TechTips/TechTip-1.aspx>
- [30] Compère, G. (2019) *Advanced Lectures on General Relativity*. Springer, Berlin.
<https://doi.org/10.1007/978-3-030-04260-8>

- [31] Dick, R. (2019) Special and General Relativity: An Introduction to Spacetime and Gravitation. IOP Publishing, Bristol. <https://doi.org/10.1088/2053-2571/aaf173ch1>
- [32] Guidry, M. (2019) Modern Relativity Theory, Black Holes, Gravitational Waves and Cosmology. Cambridge University Press, Cambridge.
- [33] Deruelle, N. and Uzan, J.-P. (2018) Relativity in Modern Physics. Oxford Graduate Texts, Oxford. <https://doi.org/10.1093/oso/9780198786399.001.0001>
- [34] Luscombe, J.H. (2018) Core Principles of Special and General Relativity. CRC Press, Boca Raton. <https://doi.org/10.1201/9780429023835>
- [35] Popper, K.R. (1979) Die beiden Grundprobleme der Erkenntnistheorie. J.C.B. Mohr (Paul Siebeck), Tübingen, 426-427.



Call for Papers

Journal of Modern Physics

ISSN: 2153-1196 (Print) ISSN: 2153-120X (Online)
<http://www.scirp.org/journal/jmp>

Journal of Modern Physics (JMP) is an international journal dedicated to the latest advancement of modern physics. The goal of this journal is to provide a platform for scientists and academicians all over the world to promote, share, and discuss various new issues and developments in different areas of modern physics.

Editor-in-Chief

Prof. Yang-Hui He

City University, UK

Subject Coverage

Journal of Modern Physics publishes original papers including but not limited to the following fields:

Biophysics and Medical Physics	New Materials: Micro and Nano-Mechanics and Homogeneization
Complex Systems Physics	Non-Equilibrium Thermodynamics and Statistical Mechanics
Computational Physics	Nuclear Science and Engineering
Condensed Matter Physics	Optics
Cosmology and Early Universe	Physics of Nanostructures
Earth and Planetary Sciences	Plasma Physics
General Relativity	Quantum Mechanical Developments
High Energy Astrophysics	Quantum Theory
High Energy/Accelerator Physics	Relativistic Astrophysics
Instrumentation and Measurement	String Theory
Interdisciplinary Physics	Superconducting Physics
Materials Sciences and Technology	Theoretical High Energy Physics
Mathematical Physics	Thermology
Mechanical Response of Solids and Structures	

We are also interested in: 1) Short Reports—2-5 page papers where an author can either present an idea with theoretical background but has not yet completed the research needed for a complete paper or preliminary data; 2) Book Reviews—Comments and critiques.

Notes for Intending Authors

Submitted papers should not have been previously published nor be currently under consideration for publication elsewhere. Paper submission will be handled electronically through the website. All papers are refereed through a peer review process. For more details about the submissions, please access the website.

Website and E-Mail

<http://www.scirp.org/journal/jmp>

E-mail: jmp@scirp.org

What is SCIRP?

Scientific Research Publishing (SCIRP) is one of the largest Open Access journal publishers. It is currently publishing more than 200 open access, online, peer-reviewed journals covering a wide range of academic disciplines. SCIRP serves the worldwide academic communities and contributes to the progress and application of science with its publication.

What is Open Access?

All original research papers published by SCIRP are made freely and permanently accessible online immediately upon publication. To be able to provide open access journals, SCIRP defrays operation costs from authors and subscription charges only for its printed version. Open access publishing allows an immediate, worldwide, barrier-free, open access to the full text of research papers, which is in the best interests of the scientific community.

- High visibility for maximum global exposure with open access publishing model
- Rigorous peer review of research papers
- Prompt faster publication with less cost
- Guaranteed targeted, multidisciplinary audience



**Scientific
Research
Publishing**

Website: <http://www.scirp.org>

Subscription: sub@scirp.org

Advertisement: service@scirp.org